Pharmacometric approaches to assess hydrocortisone therapy in paediatric patients with adrenal insufficiency

Inaugural-Dissertation

to obtain the academic degree
Doctor rerum naturalium (Dr. rer. nat.)

submitted to the Department of Biology, Chemistry and Pharmacy
of Freie Universität Berlin

by

Johanna Stina Elisabet Melin

from Kungsbacka, Sweden

Berlin 2017

This dissertation was done from 2013 to 2017 with the supervision of Prof. Dr. Charlotte Kloft at the Institute of Pharmacy, Freie Universitaet Berlin.

1. Reviewer:	Prof. Dr. Charlotte Kloft
2. Reviewer:	APL Prof. Dr. Georg Hempel
Dissertation on:	01. December 2017

If we knew what it was we were doing,

it wouldn't be called research, would it?

Albert Einstein

Till Lilleman och MoP

Abstract

Pharmacometric approaches are commonly applied to increase the understanding of pharmacokinetics, pharmacodynamics, disease of a system and their interactions. These approaches are often used both in academia, industry and in the clinical setting to contribute to a more rational use of medicines. In the current thesis, pharmacometric approaches were used to assess the current dosing strategies in paediatric patients with adrenal insufficiency. Congenital adrenal hyperplasia (CAH) is a common kind of adrenal insufficiency resulting from a deficiency in 21-hydroxylase, which is an important enzyme in the cortisol synthesis pathway. This patient population represents a very vulnerable population with no/low endogenous synthesis of cortisol, thereby requiring lifelong substitution therapy with glucocorticoids from birth. Hydrocortisone is the recommended glucocorticoid in growing paediatric patients, since longer-acting glucocorticoids are associated with more reduction in final height. The aim of the treatment is to mimic the physiological circadian cortisol concentrations. Hydrocortisone is therefore administered two-four times daily, due to its relatively short terminal half-life (1.5 h). Monitoring treatment in CAH patients is important, since overtreatment (too high cortisol concentrations) may lead to Cushing's syndrome and reduced final height, whereas undertreatment (too low cortisol concentrations) may lead to disease progression, virilisation in girls, electrolyte imbalances and increased risk for adrenal crisis. An increased mechanism-based understanding of the pharmacokinetics and pharmacokinetics/pharmacodynamics of hydrocortisone in this population may contribute to a more rational use of hydrocortisone in patients with adrenal insufficiency.

Firstly, rich phase 1 data from healthy adults administered a novel hydrocortisone formulation suitable for newborns (Infacort®), allowed for quantifying the pharmacokinetics in a semi-mechanistic way accounting for: i) constant cortisol baseline after dexamethasone suppression, ii) nonlinear plasma protein binding to CBG and linear binding (to e.g. albumin/erythrocytes) and iii) a saturable absorption process. This was the first semi-mechanistic PK model of hydrocortisone, which successfully could very well predict the observed data in paediatric patients with adrenal insufficiency (neonates to 6 years) administered Infacort.

Secondly, a reduced paediatric pharmacokinetic model was established on sparse phase 3 data from paediatric patients (neonates to 6 years), from which a slightly lower and higher clearance was observed in neonates and infants, respectively.

In a third step, data from a more clinical situation was used to further reduce the paediatric PK model to better describe the data in paediatric patients (7-17 years) with CAH administered licenced hydrocortisone tablets and intravenous hydrocortisone. In addition, concentrations from a clinically-

relevant biomarker 17-hydroxyprogesterone (17-OHP), a precursor to cortisol which is elevated in patients with CAH, was used to establish a pharmacokinetic/pharmacodynamic model considering the cortisol-mediated inhibition of the 17-OHP synthesis and the circadian rhythm of 17-OHP. The established pharmacokinetic/pharmacodynamic model was also used to simulate cortisol and 17-OHP concentration-time profiles after three and four times daily administration of hydrocortisone tablets. None of the studied dosing regimens could well mimic the rhythm, but a four times daily dosing regimen was superior to a three times daily dosing regimen and resulted in higher cortisol concentrations in the morning. This analysis visualised the difficulties associated with mimicking the physiological cortisol concentrations after three or four times daily dosing. Since outcome measures, such as final height and disease progression are of primary interest, prospective studies should be performed to evaluate the impact of changing dosing regimen on these outcomes.

To conclude: treatment optimisation in patients with adrenal insufficiency is challenging especially in paediatrics but important to perform in order to possibly avoid disease progression, adrenal crisis or Cushing's syndrome. An increased understanding regarding the pharmacokinetics of hydrocortisone in the studied population may contribute to a better understanding regarding how to administer hydrocortisone and help to inform galenic development. The results in the current thesis therefore represent a first step towards individualising hydrocortisone therapy, which may in the long run contribute to a more rational decision-making in the substitution therapy with hydrocortisone in paediatric patients with adrenal insufficiency.

Zusammenfassung

Pharmakometrische Ansätze werden häufig eingesetzt, um neue Erkenntnisse über die Pharmakokinetik, Pharmakodynamik und/oder Erkrankung eines Systems und ihre Verknüpfung zu gewinnen. Diese Ansätze werden oft sowohl in der akademischen Forschung und pharmazeutischen Industrie als auch in der Klinik verwendet, um zu einem rationaleren Arzneimitteleinsatz beizutragen. In der vorliegenden Arbeit wurden pharmakometrische Ansätze genutzt, um gegenwärtige Dosierungsstrategien bei pädiatrischen Patienten mit Nebennierenrindeninsuffizienz zu beurteilen. Das Adrenogenitale Syndrom (AGS) ist eine häufige Form der Nebennierenrindeninsuffizienz als Folge einer Störung des Enzyms 21-Hydroxylase, welches eine wichtige Rolle im Syntheseweg von Cortisol einnimmt. Die betroffene Patientenpopulation weist keine oder nur geringe endogene Produktion von Cortisol auf und muss sich daher einer lebenslangen Substitutionstherapie mit Glucocorticoiden unterziehen. Das Glucocorticoid der Wahl für sich noch im Wachstum befindende pädiatrische Patienten ist Hydrocortison, da länger wirksame Glucocorticoide mit einer Reduktion der endgültigen Körpergröße assoziiert sind. Ziel der Behandlung ist, die physiologischen zirkadianen Cortisolkonzentrationen nachzuahmen; Hydrocortison wird daher und aufgrund der relativ kurzen terminalen Halbwertszeit (1.5 h) zwei- bis viermal täglich verabreicht. Die Therapie gestaltet sich insofern schwierig und bedarf Überwachung, als dass zu hohe Dosen (und damit zu hohe Cortisolkonzentrationen) das Risiko eines Cushing Syndroms bergen, zu niedrige Dosen (und damit zu niedrige Konzentrationen) jedoch das Fortschreiten der Erkrankung, die Vermännlichung von Patientinnen, Elektrolytstörungen oder eine Addison-Krise begünstigen. Ein besseres und Mechanismus-basiertes Verständnis der Pharmakokinetik bzw. von pharmakokinetisch/pharmakodynamischen Beziehungen von Hydrocortison in dieser besonders vulnerablen Population könnte zu einem rationaleren Gebrauch von Hydrocortison in AGS-Patienten beitragen.

Im ersten Schritt erlaubte eine datenreiche Phase 1-Studie mit gesunden Erwachsenen, denen eine neue für Neugeborene geeignete Hydrocortison-Formulierung (Infacort®) verabreicht wurde, die Quantifizierung der Pharmakokinetik mit Hilfe eines semi-mechanistischen Ansatzes. Dieser berücksichtigte i) konstante Cortisol-Basislinienwerte nach Dexamethason-Suppression, ii) nichtlineare Plasmaproteinbindung an CBG sowie lineare Bindung (z.B. an Albumin/Erythrozyten) und iii) einen sättigbaren Absorptionsprozess. Das entwickelte Modell war das erste semi-mechanistische pharmakokinetische Modell für Hydrocortison, das erfolgreich beobachtete Daten bei Kindern mit Nebenniereninsuffizienz (Neugeborene-6 Jahre) nach Gabe von Infacort® vorhersagen konnte.

Im nächste wurde aus nur spärlichen Daten einer Phase 3-Studie mit pädiatrischen Patienten (Neugeborene-6 Jahre) ein reduziertes pädiatrisches pharmakokinetisches Modell etabliert, das eine leicht reduzierte Clearance bei Neugeborenen und höhere Clearance bei Kleinkindern zeigte.

Im dritten Schritt wurden Daten aus einer klinischen Studie eines Krankenhauses genutzt, um das pädiatrische pharmakokinetische Modell weiter zu reduzieren und Daten von pädiatrischen Patienten mit AGS (7-17 Jahre) nach Gabe von zugelassenen Hydrocortison-Tabletten und intravenösen Infusionen besser zu beschreiben. Außerdem wurden Konzentrationen des klinisch relevanten Biomarkers 17-Hydroxyprogesteron (17-OHP), eines bei Patienten mit AGS erhöhten Vorläufers von Cortisol, verwendet, um ein pharmakokinetisch/pharmakodynamisches Modell zu entwickeln, das die durch Cortisol vermittelte Inhibition der 17-OHP Synthese und den zirkadianen Rhythmus von 17-OHP berücksichtigt. Das etablierte Modell wurde außerdem verwendet, um Konzentrations-Zeitprofile von Cortisol und 17-OHP nach drei- und viermal täglicher Gabe von Hydrocortison-Tabletten zu simulieren. Obwohl keines der untersuchten Dosierungsschemata den zirkadianen Rhythmus sehr gut abbilden konnte, war eine viermal tägliche Gabe der dreimal täglichen Gabe überlegen und führte zu höheren morgendlichen Cortisolkonzentrationen. Die Analyse zeigte die Schwierigkeit auf, physiologische Cortisolkonzentrationen nach der dritten von vier täglichen Gaben zu erreichen. Da Zielgrößen wie endgültige Körpergröße oder das Fortschreiten der Erkrankung von primärem Interesse sind, sollten prospektive Studien durchgeführt werden, um den Einfluss von sich ändernden Dosierungsschemata auf die genannten Zielgrößen zu evaluieren.

Zusammenfassend kann gesagt werden, dass die Optimierung der Behandlung von AGS-Patienten vor allem in der Pädiatrie herausfordernd aber zugleich sehr bedeutend ist, um das Fortschreiten der Erkrankung sowie das Auftreten einer Addison-Krise oder des Cushing-Syndroms zu vermeiden. Ein besseres Verständnis der Pharmakokinetik von Hydrocortison in der untersuchten Population könnte zu einem besseren Verständnis hinsichtlich des Einsatzes von Hydrocortison und zur Verbesserung der Arzneiform beitragen. Die Ergebnisse dieser Dissertation stellen deshalb einen ersten Schritt in Richtung Individualisierung der Hydrocortisontherapie dar, welche langfristig gesehen zu einer rationaleren Substitutionstherapie mit Hydrocortison bei pädiatrischen Patienten mit Nebenniereninsuffizienz beitragen kann.

Table of contents

Abbreviations

Notation in italics refers to parameters or pharmacokinetic variables

-2LL	Minus two times the log likelihood
*11*β-HSD1	11β-hydroxysteroid dehydrogenase type 1
*11*β-HSD2	11β-hydroxysteroid dehydrogenase type 2
17-OHP	17-hydroxyprogesterone
A_c	Amount in central compartment
ACTH	Adrenocorticotropic hormone
A_{depot}	Amount in depot compartment
AIC	Akaike information criterion
AMP24	Amplitude of cosine function for 24 h
AMP12	Amplitude of cosine function for 12 h
A_p	Amount in peripheral compartment
A_u	Amount unbound
AUC	Area under the concentration-time profile
$AUC_{0\text{-}8h}$	Area under the concentration-time profile over 8 h
$AUC_{0\text{-}24h}$	Area under the concentration-time profile over 24 h
$Baseline_{17\text{-}OHP}$	17-OHP baseline
$Baseline_{cort}$	Cortisol baseline
BID	Twice daily dosing
B_{max}	Maximum binding capacity
BSA	Body surface area
BW	Body weight
CAH	Congenital adrenal hyperplasia
CDD	Case deletion diagnostics
CBG	Corticosteroid-binding globulin

CIRC	Circadian function
CL	Total clearance
CL_u	Unbound clearance
C_{max}	Maximum concentration
C_{min}	Minimum concentration
CMT	Compartment
CRH	Corticotropin releasing hormone
C_{tot}	Total cortisol concentration
C_u	Unbound cortisol concentration
CV	Coefficient of variation
CWRES	Conditional weighted residuals
DEX	Dexamethasone
ELS	Extended least squares
F	Bioavailability
FOCE I	First-order condition estimation method with interaction
f_u	Fraction unbound
γ	Gamma factor accounting for steepness in concentration-effect or maturation model
GOF	Goodness of fit
HC	Hydrocortisone
HT	Height
I	Inhibitory effect
IC_{50}	Concentration at 50% of I_{max}
I_{max}	Maximum inhibitory effect
IMP	Importance sampling
IIV	Interindividual variability
k_a	First-order absorption rate constant
k_d	Unbound cortisol concentration at 50% of B_{max}

K_m	Amount in depot compartment at 50% of V_{max}
k_{in}	Zero-order synthesis rate constant
k_{out}	First-order elimination rate constant
LLOQ	Lower limit of quantification
LLP	Log likelihood profiling
LRT	Likelihood ratio test
NCA	Noncompartmental analysis
N_{CBG}	Number of binding sites at CBG
NLME	Nonlinear mixed-effects modelling
NONMEM	Nonlinear mixed-effects modelling software
ODE	Ordinary differential equation
OFV	Objective function value
OLS	Ordinary least squares
Q	Intercompartmental clearance
QID	Four times daily
PD	Pharmacodynamic(s)
PK	Pharmacokinetic(s)
PsN	Perl speaks NONMEM
RSE	Relative standard error
RUV	Residual unexplained variability
SAEM	Stochastic approximation expectation maximisation
SD	Standard deviation
SHFT24	Time shift for cosine function for 24 h
SHFT12	Time shift for cosine function for 12 h
TID	Three times daily dosing
t_{max}	Time of C_{max}
t_{min}	Time of C_{min}

V_c	Central volume of distribution
V_{max}	Maximum absorption rate
V_p	Peripheral volume of distribution
VPC	Visual predictive check

Symbols

ε	Random-effect parameter, residual variability
$P_{k,i}$	k^{th} model parameter for the i^{th} individual
σ^2	Variance of ε
σ	Standard deviation of ε
θ	Typical population parameter estimate
$t_{1/2}$	Half-life
η	Random-effects parameter
η_i	Individual random-effect
ω^2	Variance of η

1 Introduction

When prescribing a drug, it is important to select a rational dosing regimen for the patient to receive the desired beneficial effect while avoiding adverse effects. A rational dosing regimen is related to how a drug is having its effect, how large the effect is and for how long the effect stays. It is, therefore, first important to understand the pharmacokinetics of the drug (PK), i.e. "how the body handles the drug". PK comprise how the drug is absorbed, distributed, metabolised and excreted (ADME properties) and generates an understanding about how the drug concentrations in the body change over time [1]. The pharmacodynamics (PD), on the other hand, refer to "how the drug affects the body" and gives an understanding of which concentrations of drug are efficacious or of safety concerns based on a biomarker or the clinical outcome of interest [1]. When combining the two; the PK/PD relationship describes how the effect (biomarker or clinical outcome) changes over time. These types of analyses are of uttermost importance for understanding which dose may be efficacious and safe, since they consider both the time course of the drug concentrations and the effect [2]. Sometimes, it is also of importance to consider how the underlying disease system is changing, which can be done with disease models.

In the present thesis, pharmacometric approaches were used to explore the underlying physiological system and to characterise the pharmacokinetics of hydrocortisone in paediatric patients with adrenal insufficiency and healthy volunteers. In addition the pharmacokinetic/pharmacodynamic relationship of hydrocortisone was evaluated in paediatric patients with congenital adrenal hyperplasia by using a disease-specific biomarker. The introduction will outline the concept of pharmacometrics, the importance of studying pharmacokinetics in paediatric patients, cortisol regulation, adrenal insufficiency (e.g. congenital adrenal hyperplasia), and the pharmacokinetics/pharmacodynamics of hydrocortisone.

1.1 Pharmacometric approaches

Pharmacometric approaches involve using mathematical and statistical methods to assess the physiological system, PK and PD of different drugs [3]. PK can be evaluated using empirical/semi-mechanistic approaches ("top-down"), which uses measured data (e.g. clinically observed concentrations) to learn about the system [4]. One example of empirical approaches is the use of compartmental models which will be described below. The parameters in empirical models do not have a physiological interpretation, and the ability to extrapolate knowledge when the physiology is

changing is therefore limited [5]. On the other hand, semi-mechanistic PK or PD models relates some parameters to physiological processes, such as plasma protein binding [6] or different sources of elimination routes (e.g. hepatic or renal) [7], which improves the ability for extrapolation [5]. "Bottom-up" approaches, such as physiologically based PK (PBPK), consider the physiological properties of the target population, as well as properties of the drug/drugs, to simulate concentration-time profiles [4]. These profiles can later be compared to measured concentration-time profiles to evaluate if the PBPK model can describe the observed data or whether there is a mechanistic component that is still not captured. PBPK can incorporate e.g. age-dependent changes in physiology, and is therefore commonly used to predict PK in children [8]. In recent years, top-down and bottom-up approaches have been combined to "middle-out" approaches. These models are informed by both *in vitro* and clinical data and are therefore both mechanistically accurate and clinically relevant [9]. In addition, disease models may be useful to increase the understanding of the underlying disease physiology and its impact on drug efficacy.

1.1.1 Compartmental models

In PK, PD and disease modelling analyses, it is common to assume a compartmental model structure. In the case of a PK model this could refer to a two-compartmental disposition model after intravenous (iv) drug administration (Figure 1.1). Compartments are assumed to be a kinetically homogenous space [10], and several compartments (e.g. one-, two- or three- compartments) are commonly connected with first-order rate constants to describe the concentration-time profiles. Commonly the drug concentrations are measured in plasma/blood and are therefore related to the amounts in the central compartment (A_c, Figure 1.1).

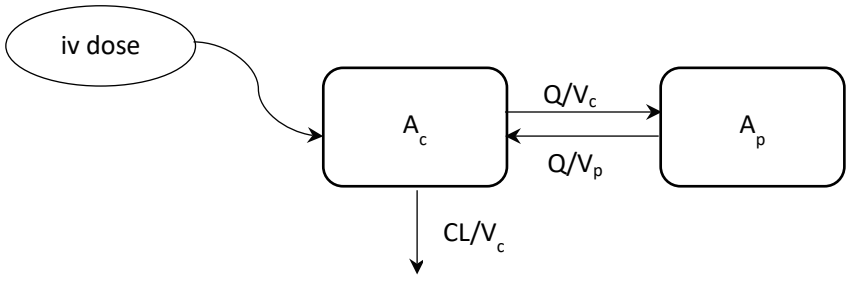

Figure 1.1 Schematic representation of a two-compartmental pharmacokinetic model after intravenous (iv) administration. Amount in central compartment (A_c), amount in peripheral compartment (A_p), clearance (CL), central volume of distribution (V_c), intercompartmental clearance (Q), peripheral volume of distribution (V_p).

Other measurements, such as microdialysis concentrations in e.g. interstitial space fluid or adipose tissue, could potentially be attributed to e.g. the amounts in the peripheral compartment (A_p, Figure 1.1). Parameter estimates, such as clearance (*CL)*, central volume of distribution (V_c), intercompartmental clearance (*Q*) and peripheral volume of distribution (V_p), are commonly estimated. If a drug is administered orally or via inhalation different parameters such as: first- or zero-order absorption as well as sequential/simultaneous zero- and first-order absorption may be used to describe the absorption into the central compartment. The compartmental modelling may be applied using a population approach.

1.1.2 Population modelling approaches

In the current thesis, a population method was applied to increase the understanding regarding the physiological/disease system, PK and PD in different populations by estimating mean population estimates, as well as the variability between individuals (interindividual variability) and within individuals (residual variability) [11]. There are different population methods available such as naïve pooling and the two-stage approach. The naïve pooling approach is less affected by sparse data, since the data is analysed as though it originates from one patient. On the other hand this approach only describes the central tendency of the data and does not assess the variability between individuals, which limits our understanding of the system [11,12]. In the two-stage approach every individual is analysed sequentially and the individual model parameters are statistically summarised to get an understanding regarding the average parameters (e.g. mean) and their distribution (e.g. standard deviation) of the population. The two-stage approach is therefore highly dependent on rich data from every individual. The nonlinear mixed-effects (NLME) modelling approach is more complex but generates a less biased estimation and precision than naïve pooling or two-stage approach [11]. This approach was applied throughout this thesis and will thus be explained further in the next section.

1.1.2.1 Nonlinear mixed-effects modelling

NLME modelling involves analysing all individuals simultaneously rather than sequentially. This allows for describing the individual as well as population behaviour simultaneously, and for individuals with fewer samples to borrow information from the population [13]. NLME is therefore suitable for both rich, sparse and unbalanced data. As the name “mixed-effects” implies, the population structural parameters and covariate effects (i.e. the fixed-effects) are estimated simultaneously with the variability (i.e. random-effects) [12]. The variability can be divided further into interindividual (IIV) and residual unexplained variability (RUV), and IIV can thereafter be explained by addition of

different covariates (i.e. patient characteristics). The identification of covariates explaining variability of PK is important since it may allow for individualising therapy. This is very useful since "one dose fits all" rarely applies to commonly used drugs. In special patient populations with high variability, such as critically ill, elderly or paediatric patients, NLME has also proven very efficient [12]. Disadvantages with NLME includes the complexity of the applied mathematical methods, the computational resources needed for the analysis and the time it takes to perform an analysis [14].

1.1.3 Simulations

In a next step, a validated NLME PK model can be used to simulate new concentration-time profiles, i.e. the model parameters and sometimes the variability between patients are used to obtain concentration measurements at different times for virtual patients. By changing e.g. covariates for the virtual patient population and/or dosing regimens, concentration-time profiles for different scenarios can be generated and evaluated. If using paediatric covariates (e.g. paediatric body weight) simulations can be useful to extrapolate PK knowledge from adults to children to get an understanding of expected concentrations in this population before the trial has been conducted. After the trial has been conducted in paediatric patients and the PK (and potentially PK/PD) has been characterised, simulations can sequentially be used to assess which dosing regimens are likely to result in therapeutic concentrations with a beneficial treatment effect. Simulations are commonly applied in e.g. the anti-infectives area to identify patients at risk for undertreatment or adverse effects. An example is described in Minichmayr *et al*., in which a simulation-based analysis helped to identify patients with sepsis receiving the standard dosing regimen at risk of not attaining the pre-specified PD target [15]. In addition to dosing evaluation/optimisation, simulations are commonly applied to evaluate different clinical trial designs and to assess which impact different design variables (e.g. number of individuals, number of doses) may have on the study outcome [16]. Simulations are also commonly used to evaluate pharmacometrics models, which will be outlined more in section 2.1.5. Simulations are a key component in pharmacometrics and are commonly applied by scientists in academia, industry and regulatory to address different questions, which will be discussed in the next section.

1.1.4 Role and benefit from pharmacometrics in drug development and therapeutic use

Pharmacometrics is nowadays a key component in academic research and model-informed drug development. Pharmacometric approaches are used frequently in drug development, and has shown to reduce costs by making development more efficient and terminating compounds earlier in the

development [17]. Pharmacometrics is also used by scientists in the regulatory agencies, to assess the data and support approval and labelling of new drugs [18]. The field of pharmacometrics has enabled model-informed decisions throughout different phases of clinical drug development [19], which will be exemplified below.

Pharmacometric approaches can be used to optimise the study design (both *in vitro* and *in vivo*) to maximise the information obtained in the study [20]. In Kretsos *et al*., an optimal design approach was applied which resulted in the study meeting its endpoints after recruiting 50% of the planned patients, thereby improving efficiency and reducing costs [21].

Pharmacometric approaches can also be used to identify patients with increased exposure or learn about the importance of elimination pathways. In van der Walt *et al.*, a semi-mechanistic model for dapagliflozin separating hepatic and renal clearance was developed. By including covariates for renal function (creatinine CL) and hepatic function (Child-Pugh score) the model could be used to evaluate the impact of renal and hepatic impairment on systemic exposure of dapagliflozin [7]. Patients with moderate to severe renal impairment had higher exposure, indicating that renal elimination/metabolism was of high importance for dapagliflozin.

Pharmacometric approaches may also be useful to support dose selection and therapy optimisation both in the industry and the clinics. Tarjinder and Della Pasqua compared simulated exposures of pyrazinamide in tuberculosis patients after a fixed dosing regimen and the standard weight-banded regimen. Their analysis identified patients with body weight between 45 and 55 kg at risk for undertreatment, if applying a weight-banded regimen. Hence a fixed dosing regimen was proposed [22]. Another example of dose optimisation is provided by Höglund *et al*., in which a model-based meta-analysis was undertaken to characterise the PK of piperaquine in adults and children with malaria as well as healthy volunteers (n=728). The analysis identified lower exposure of piperaquine in paediatric patients below 25 kg and heavier adults. By using simulations new dosing regimens resulting in improved exposure were suggested, which were later adopted by the WHO [23].

In addition to previous possibilities, pharmacometrics is also useful to bridge information between different populations, such as obese, elderly or paediatric patients [19]. A recent example of how efficacy was extrapolated from adults to paediatrics for esomeprazole is given in Mehrota *et al.* [24]. In this analysis, a developed paediatric PK model was used to simulate steady state exposures following esomeprazole dosing. Sequentially, new weight-based paediatric dosing regimens, resulting in similar exposure as adults, were proposed and approved by the FDA. This example shows how pharmacometric approaches can be used to extrapolate knowledge from adults, in order to avoid

performing studies in a paediatric population. However, paediatric patients should not be considered only to be “small adults”, which is why it is also important to study the PK also in paediatric populations. The next sections will therefore outline the importance of studying PK in paediatric patients and which consequences there are if no studies are available in this population.

1.2 Pharmacokinetics and off-label treatment in paediatric patients

Paediatric patients refer to patients below 18 years of age and can be further divided into sub-groups depending on which nomenclature is used [25]. For the purpose of this thesis, age will be grouped as follows: neonate (<28 days), infant (≥28 days-2 years), young child (2-6 years), child (6-12 years) and adolescents (12-18 years). When analysing data from neonates or infants, the chronological age might not be informative enough and instead e.g. postmenstrual age (PMA) can be used. PMA is the chronological age plus the time from the last menstrual period to birth (gestational age, [26]). In addition to chronological age and PMA, older paediatric patients can be divided based on pubertal status judged by e.g. Tanner staging. The different Tanner stages (stage 1 (pre-pubertal)-stage 5 (post-pubertal)) are given by the development of pubic hair, height, external male genitalia (only boys) and breasts (only girls) [27,28].

It is commonly debated whether children are small adults or not (i.e. if body size adjusted adult doses are appropriate for children) in the PK community. Anderson and Holford have proposed that from a PK point of view “Children are small adults, neonates are immature children” [29]. By this, they imply that differences in PK between adults and children are related to differences in body size, since the maturation and organ function are similar in these two populations. A body size adjusted dosing regimen should therefore result in similar exposure in adults and children older than two years. This is not the case for infants or neonates, in which maturation processes of e.g. immature hepatic enzymes or renal function may also have an impact on the PK. In addition, the PD between children and adults may vary due to different expression of target receptors [30]. As a consequence, just extrapolating body size adjusted dosing regimens without taking the maturation into consideration may result in an increased risk of over- or underdosing, since the maturation processes are commonly nonlinear [30]. Potential maturation factors that could have an impact on the PK of hydrocortisone will be discussed in sections 1.4.1-1.4.3.

Studies in paediatric populations are needed in order to better understand PK differences between paediatric and adults, to allow for a rational therapy in paediatric populations. Performing studies in a paediatric population are, however, challenging due to ethical considerations and restrictions

regarding number of blood samples and sample volume [31,32]. Few studies were therefore earlier performed in these groups, resulting in missing documentation about the use of many drugs in paediatric patients. The situation is now improving since the paediatric regulation in Europe and Pediatric research Equity Act in the US require studies in paediatric patients (in Europe: Paediatric investigation plan, in US: Pediatric Study Plan) [33,34].

However, drugs that have not been studied in paediatric patients are still commonly administered to this population. This is called off-label use, i.e. use of drug not corresponding to the Product Summary Characteristics. Example of off-label use could be use of approved drugs in an age or a body weight for which the drug is not approved or use of approved drugs for an alternative indication [25]. The off-label use is common both in outpatient care and in hospitals [35,36], and has been related to an increased incidence of adverse drug reactions [37]. Use of non-marketed drugs or extemporaneously produced (compounded e.g. in a community pharmacy) products are also common in paediatric patients, due to lack of documentation or suitable formulation. A previous study showed that 49% of all drugs administered to paediatric patients in Swedish hospitals (during two days in 2008) were either off-label, non-marketed drugs or extemporaneously produced drugs [36]. The excessive use of off-label, nonmarketed drugs or extemporaneously produced drugs results in an unnecessary risk of adverse events for the paediatric patients [38]. In addition, one may expect an increased risk for inadequate disease control.

For hydrocortisone, which was studied in the current thesis, there is currently no licensed formulation for patients below six years in Europe or the US. Off-label use is common in these patients, and they are commonly administered low doses (0.5-5 mg) as crushed tablets suspended in water [39,40]. The accuracy associated with dividing a licensed tablet (e.g. 10 mg in Europe) to generate a low dose is poor and may impact treatment outcomes [40]. Indeed, a large variability in dose was observed in a study on extemporaneously compounded HC capsules provided by patients in Germany [41]. Administering a HC suspension is also a common option, but has been associated with inadequate disease control, due to inhomogeneous distribution of HC in the suspension and short shelf-life [42]. As a result of this, hydrocortisone was on the EMA priority list for off-patent medicines to be studied in children 2010 [43]. The TAIN (Treatment of adrenal insufficiency in neonates and infants) project was therefore initiated after receiving funding by the Seventh Framework Programme of the European union [44]. Within this initiative Infacort® (hydrocortisone granules with taste masking) was developed [40]. Data from administration of this formulation has been characterised in this thesis (project 1 and 2).

To summarise, increased understanding regarding the PK, efficacy and safety in paediatric patients are needed to shed light on how to give the right dose, in the right dosing regimen to the right patient (i.e. rational dosing). In the current thesis, data from paediatric patients with congenital adrenal hyperplasia was used, and this patient population will be described in the next sections.

1.3 Adrenal insufficiency: Congenital adrenal hyperplasia

Patients with adrenal insufficiency have a deficient cortisol synthesis, which may be present at birth (congenital) or acquired. The insufficiency can be related to dysfunction of the adrenal gland (primary adrenal insufficiency) or the pituitary gland (secondary adrenal insufficiency). Congenital primary adrenal insufficiency is either related to an enlarged (hyperplasia) or reduced (hypoplasia) adrenal gland [40]. Congenital adrenal hyperplasia (CAH) is the most common etiology for primary adrenal insufficiency in paediatric patients [45]. In order to understand the pathophysiology for CAH, the regulation of cortisol and 17-hydroxyprogesterone (17-OHP) in a healthy population will be addressed first.

1.3.1 Physiological regulation and circadian rhythm of cortisol and 17-hydroxyprogesterone in a healthy population

Cortisol is synthesised in the adrenal glands, and is important for maintaining homeostasis by modulating metabolism, growth and the immune system. Stress is referred to the state when the homeostasis is challenged, and cortisol is an important mediator of the stress system [46]. Cortisol is therefore sometimes called the “stress-hormone”. Cortisol synthesis is regulated centrally via the hypothalamus-pituitary-adrenal (HPA) axis according to Figure 1.2. The suprachiasmatic nuclei of the molecular circadian clock activates the release of corticotropin releasing hormone (CRH) from hypothalamus upon light/dark stimuli during the night [47,48]. CRH promotes the release of adrenocorticotropic hormone (ACTH) from the pituitary and ACTH stimulates the conversion of cholesterol to glucocorticoids, mineralocorticoids and androgens in the adrenal glands (Figure 1.3). Cortisol is the major glucocorticoid and exerts a negative feedback on CRH and ACTH release, thereby inhibiting the HPA axis (Figure 1.2) [49].

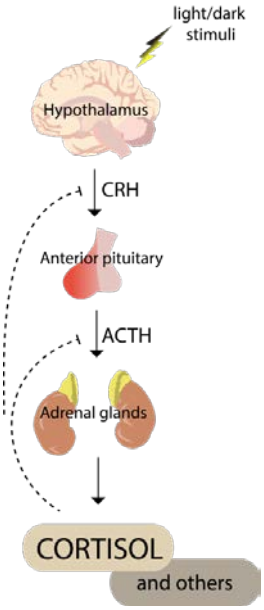

Figure 1.2. Cortisol regulation via the hypothalamic-pituitary-axis in a healthy population. Corticotropin releasing hormone (CRH), adenocorticotropin hormone (ACTH).

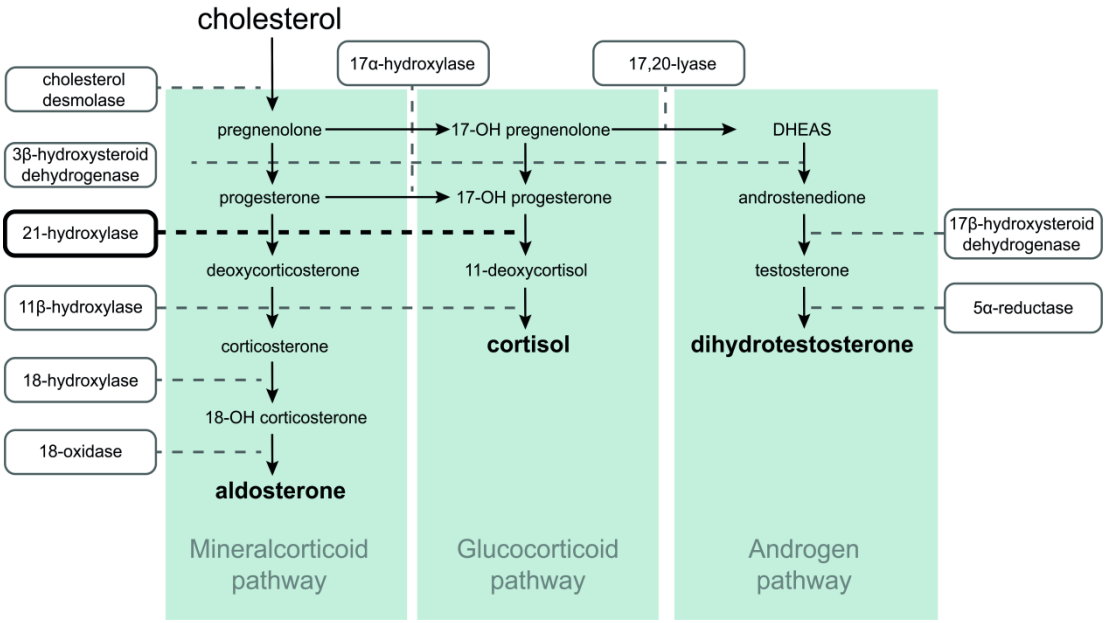

Figure 1.3 Steroid synthesis of mineralocorticoids, glucocorticoids and androgens in a healthy population. Enzymes and steroids are shown in boxes and without boxes, respectively.

The HPA-axis has a circadian rhythm, leading to circadian concentrations of cortisol (Figure 1.4). The highest cortisol concentrations are commonly observed directly after wakening whereas the nadir (lowest concentrations) are observed around midnight [48]. The circadian rhythm of cortisol is established two or three months after birth [50,51], even though some papers suggest an even earlier appearance [52]. A study performed in 235 healthy Swedish children in the ages of 2.2-18.5

years found no impact of age or gender on cortisol concentrations but observed a large variability between individuals [53]. 17-OHP is a cortisol precursor of importance for CAH, which also has a circadian variation in saliva in healthy children older than 12 months [54].

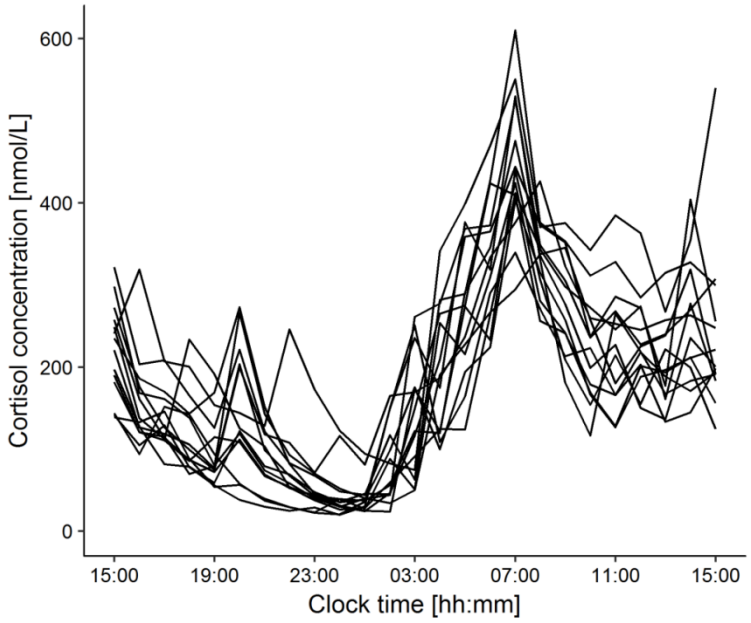

Figure 1.4. Circadian rhythm of cortisol in 14 healthy volunteers from the data described in section 2.2.2 and 3.1.2.3.

1.3.2 Pathophysiology and classification of congenital adrenal hyperplasia

Patients with CAH is a vulnerable patient group with adrenal insufficiency due to mutations in enzymes involved with the cortisol synthesis pathway. The prevalence of CAH is in general 1:15000-16000 in Europe and the USA [55]. Many countries in Europe screen neonates for CAH, since it could be lethal if untreated [55]. Deficiency in 21-hydroxylase is the most prevalent one (>90%) followed by deficiency in 11β–hydroxylase [56]. 21-hydroxylase is responsible for converting 17-OHP and progesterone to 11-deoxycortisol and deoxycortisone, respectively (Figure 1.3). A deficiency in 21-hydroxylase therefore leads to low concentrations of cortisol and accumulation of cortisol precursors, such as 17-OHP (Figure 1.5). 17-OHP is therefore commonly assessed using filter papers for sampling in the neonatal screening process [55]. The increasing concentrations of 17-OHP shift the synthesis to androgens via several pathways that normally are of minor importance [39]. Since 21-hydroxylase is also involved in the synthesis of mineralocorticoids, the synthesis of aldosterone may also be affected.

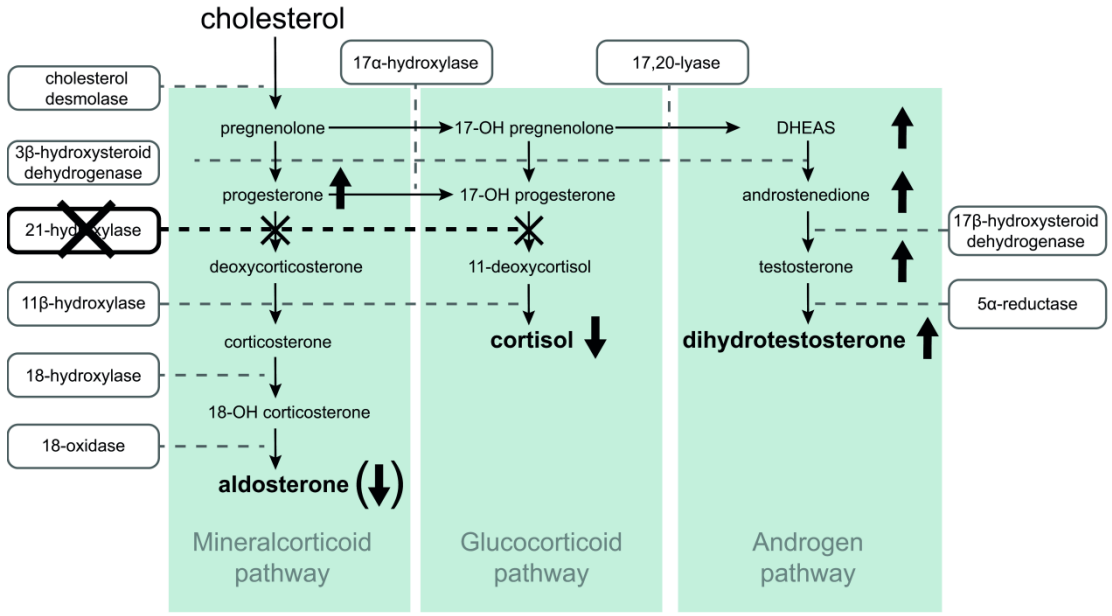

Figure 1.5 Steroid synthesis of mineralocorticoids, glucocorticoids and androgens in patients with congenital adrenal hyperplasia. Enzymes and steroids are shown in boxes and without boxes, respectively. Hydroxy (OH).

The low/no synthesis of cortisol leads to a diminished negative feedback on the HPA axis [57], which leads to a more active HPA axis and a less synchronized circadian rhythm of cortisol as seen in Figure 1.6 (left, digitalised data from [58,59]). In addition, the variability in cortisol and 17-OHP concentrations is very high between patients and 17-OHP also seems to have a circadian variation (Figure 1.6).

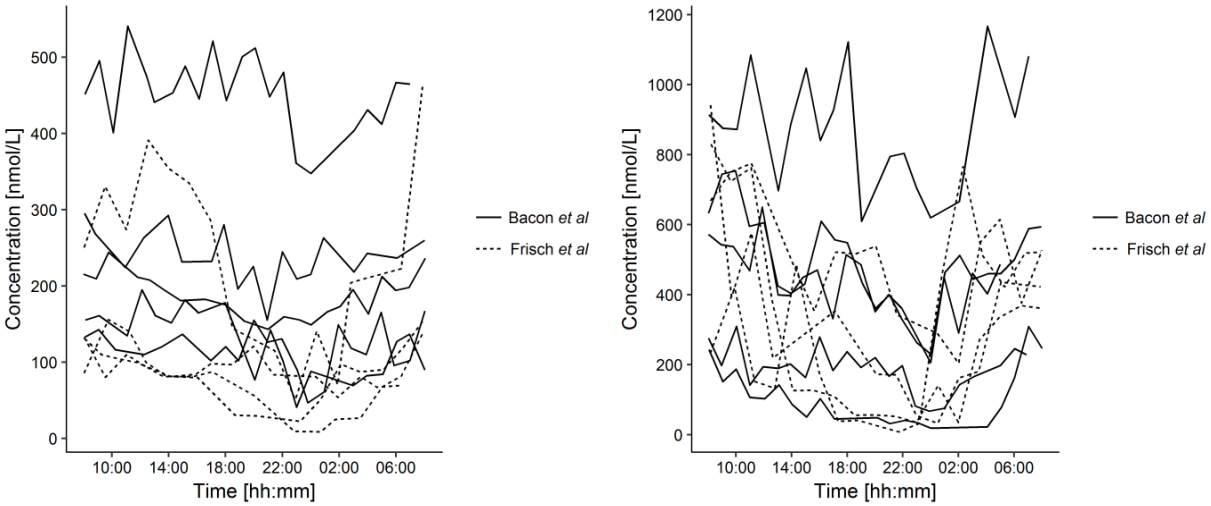

Figure 1.6 Cortisol (left) and 17-hydroxyprogesterone (17-OHP, right) concentrations over 24 h in untreated paediatric patients with CAH. The data was digitalised from Bacon *et al.* (solid lines) and Frisch *et al.* (dashed lines) [58,59].

The symptoms of patients with CAH are to a large extent related to the hormone disturbances depicted in Figure 1.5, and to the class of CAH. The classic form is more severe than the non- classic form of CAH. Patients with the non-classic form present physiological cortisol and aldosterone concentrations, but may have slightly elevated androgen concentrations [56]. The clinical manifestation is hence less severe than the classic one.

The classic form can be further divided into salt wasters or simple virilisers. Salt wasters is the most common one (75%), and refers to a deficiency also in the aldosterone synthesis [60]. Aldosterone regulates the sodium/potassium balance, and aldosterone deficiency may therefore lead to hyperkalemia, hyperreninemia and hypovolemia [56]. The decrease in cortisol disturbs the cardiac function, vascular response to catecholamines and reduces the glomerular filtration rate. The effects of a combined aldosterone and cortisol deficiency therefore increase the risk for hyponatremic dehydration and shock if untreated [56].

The elevated concentrations of androgens, leads to signs of androgen excess manifested as virilisation (masculinisation, enlargement of clitoris and hirsutism [56]) in females, precocious (too early) puberty and short final height due to early closure of the epiphyseal plate. Appropriate treatment of CAH patients is needed to reduce androgen excess and decrease the risk for reduced final height, which will be discussed in the next section.

1.3.3 Treatment of paediatric patients with adrenal insufficiency

Since cortisol is important for maintaining homeostasis, patients with adrenal insufficiency require life-long substitution therapy with glucocorticoids in order to prevent adrenal crisis, which is lethal if untreated. In addition to maintenance therapy with hydrocortisone, patients need additional hydrocortisone doses to cope with stressful situations such as trauma, surgery or febrile illness. This is referred to as stress dosing [61]. Since only maintenance therapy with hydrocortisone was assessed in the current thesis, the stress dosing will not be discussed further. Patients with aldosterone deficiency also need replacement therapy with fludrocortisone and addition of sodium chloride supplements [39], which will also not be further addressed in the current thesis.

The substitution therapy with hydrocortisone aims to suppress the androgen excess, and to mimic the circadian rhythm of cortisol [48]. As described previously in section 1.2, off-label treatment is common in CAH patients below six years due to lack of licensed formulation for this population. Substitution therapy in this age group is therefore particularly challenging.

The recommended glucocorticoid for growing children is hydrocortisone (HC, i.e. synthetic cortisol), which is commonly dosed based on body weight (BW) or body surface area (BSA), to reduce the variability in cortisol exposure compared to using a fixed dose [62]. The recommended starting dose for children who have not reached their final height (i.e. still growing) with adrenal insufficiency consists of 8 mg/m^2/day divided in three to four doses [63]. A more specific recommendation to patients with CAH of 10-15 mg/m^2 hydrocortisone divided into three daily doses has also been proposed [39]. Although four doses daily has also been suggested [64], due to the relatively short half-life of HC (1.5 h [65]). The current regimen often results in peaks with supraphysiological cortisol concentrations followed by periods with subphysiological cortisol concentrations [48]. Many doses per day would be required to accurately mimic the circadian rhythm, which would be challenging from an adherence point of view. Use of longer-acting glucocorticoids, a modified release HC formulation or subcutaneous HC infusion would improve adherence issues and result in fewer fluctuations in cortisol concentrations. Using longer-acting glucocorticoids is however not recommended for growing patients, since it increases the risk of reduced final height and other side-effects [39]. Use of modified release formulations, such as Plenadren or Chronocort, are available for adults but have not been approved for use in paediatric patients [48]. In addition, the use of modified release formulations would be difficult for the youngest children who cannot swallow whole tablets. Administering hydrocortisone subcutaneously via insulin pumps resulted in appropriate circadian cortisol profile and improved 17-OHP concentrations [66]. Use of these pumps is however associated with problems with pump failure and are not commonly used since they are very expensive and require intensive training [48].

Monitoring the treatment is challenging, since there are currently no validated target cortisol concentrations or target concentration-time profiles available for CAH patients. Since, 17-OHP concentrations are elevated in patients with CAH, 17-OHP is currently used to evaluate therapy. A target 17-OHP concentration range of 12-36 nmol/L has previously been suggested by Merke *et al.* [61]. Androstenedione and testosterone concentrations are also commonly elevated in CAH patients, and are therefore commonly measured to monitor hydrocortisone treatment. The aim of the treatment is not to fully normalise the steroid concentrations, since this is rather seen as a sign of overtreatment [39]. The possibility to quantify steroids by using dried blood spot techniques or from saliva samples have improved the ability to monitor the treatment from the patients home. In addition to laboratory values, the height and signs of adrenal excess are assessed to monitor treatment. This is however challenging, since it is difficult to separate signs of overtreatment with signs of disease progression [48]. Monitoring the treatment in paediatric patients is however

important, since undertreatment increases the risk of weakness, hypotension, disturbance in the electrolytes, disease progression and adrenal failure. Overtreatment of hydrocortisone may on the other hand lead to hypertension, dyslipidaemia, obesity, decreased glucose tolerance, osteoporosis and reduced final height [67,68]. An increased understanding of the PK of hydrocortisone may contribute to a better understanding of how to administer this drug to avoid under/overdosing.

1.4 Pharmacokinetics of hydrocortisone

The PK of hydrocortisone has been extensively characterised in healthy adult volunteers [65,69–73], and in adult [62,74–76] and paediatric [77–80] patients with adrenal insufficiency. Out of these studies, only two studies applied a pharmacometric approach [74,81]. The following sections will outline the pharmacokinetic properties of hydrocortisone administered as an immediate release formulation, and summarise potential developmental factors during childhood that may have an impact on the absorption, distribution, metabolism and excretion of hydrocortisone.

1.4.1 Absorption and its maturational aspects

Hydrocortisone is a lipophilic substance classified as a class II drug according to the biopharmaceutical classification system (BCS) [82]. This indicates that hydrocortisone has a low dissolution rate and high intestinal permeability [83]. The dissolution is hence the rate-limiting step, which is not affected by changes in pH [84]. Hydrocortisone is absorbed mainly via passive diffusion and is a poor substrate for the efflux protein P-glycoprotein [83]. The absorption is relatively quick, with the maximal concentration (C_{max}) appearing approximately (mean/median t_{max}) 1-1.7 h or 0.7-1 h after administration of tablet [65,69,72,73,76] or solution [71,72] to adults, respectively. A study including several oral dose levels (tablets: 10, 30 and 50 mg), observed a delayed t_{max} for the highest dose (t_{max} (mean (SD)), 10 mg: 1 h (0.5), 30 mg: 1 h (0.5), 50 mg: 1.7 h (0.3)). This was however less apparent for studies administering hydrocortisone suspensions [69,71], potentially due to a dissolution-rate limited absorption for the tablets. Studies performed in paediatric patients with adrenal insufficiency showed median/mean t_{max} of 0.33-3 h [78,85]. No obvious difference in t_{max} could be observed between studies with paediatric and adult patients/healthy volunteers, even though the t_{max} was very low for the morning dose (t_{max}: 0.33 h) compared to the evening (t_{max}: 3 h) dose in Charmandari *et al.* [78]. The absorption half-life ($t_{1/2,abs}$) of hydrocortisone increased three-fold after administration together with food ($t_{1/2,abs,\ fasting}$: 15 min, $t_{1/2,abs,\ fed}$: 43 min) [62], which was

potentially explained by the gastric emptying. The absorption of hydrocortisone in Simon *et al.* was described by a zero-order absorption with duration of approximately 30 min [74].

The extent of absorption, for drugs in BCS class II, is expected to increase when co-administered with food [86]. A small trend towards higher AUC of hydrocortisone when taken with food was observed in Mah *et al.* [62], probably due to the increased time for hydrocortisone to dissolve [83]. Bioavailability after administration of maximum 20 mg was close to 100% in paediatric patients and healthy adults [65,78]. A lower bioavailability of 54% was however derived in patients with adrenal insufficiency after administration of 50 mg hydrocortisone [76]. A dose-dependent C_{max} and *AUC*, with less than dose-proportional increase, was observed after oral administration in Toothaker *et al.* [69]. After performing further studies with intravenous administration the authors concluded that this was probably attributed to dose-dependent changes in bioavailability [70].

A slightly delayed t_{max} of hydrocortisone could be expected in neonates, since the rate of absorption was lower in neonates for six different compounds. This was explained by the reduced intestinal motility in neonates [87]. The rate of absorption in infants were, however, similar to adult values [88]. In addition, absorption of hydrocortisone may be delayed due to the prolonged gastric emptying (especially after breast feeding) in neonates, which reaches adult values at 6-8 months [88]. Since neonates and infants need feeding more often than adults, this could have an impact on the hydrocortisone absorption. The bioavailability of drugs is in general lower in infants and neonates than in adults [89], hence a slightly lower bioavailability of hydrocortisone could be expected in this population.

1.4.2 Distribution, plasma protein binding and its maturational aspects

Hydrocortisone has a rather small central volume of distribution (V_c) in healthy adult volunteers with mean/median V_c ranging from 7 to 23.9 L [65,70] after intravenous administration. The V_c is also independent of dose (5 mg (mean (SD)): 8.5 L (2.1), 40 mg: 8.8 L (1.8)) [70]. Studies in patients with adrenal insufficiency showed a slightly higher V_c (28.4 L) after administration of 50 mg hydrocortisone [76]. Mean relative volume of distribution (V_c/F) was 38.7-52.3 L in patients with adrenal insufficiency [74–76]. The mean V_c/F for paediatric patients was slightly lower than adults but was associated with a high uncertainty (mean (SD): 17.5 L (10.5) [80]). Charmandari *et al.* indicated higher V_c/F for pubertal patients (prepubertal (Mean (SD): 27.1 L (8.4); pubertal: 49.5 L (12.2); postpubertal: 40.8 L (16.0)). On the contrary to V_c, volume of distribution at steady state (V_{ss}) was increasing with increasing doses (5 mg: 20.7 L (7.3), 40 mg: 37.5 L (5.8))) [70], indicating increased distribution to tissue. The authors hypothesised that these changes may result from the

saturable plasma protein binding of cortisol occurring at high cortisol concentrations [70]. This is very likely, since cortisol is highly bound with high affinity to corticosteroid-binding globulin (CBG,) and to a lesser extent to albumin and erythrocytes (low affinity) [90]. The high affinity to CBG and the relatively low CBG concentrations compared to albumin (CBG (range): 14.9-67.1 mg/L [91], albumin: 35-50 g/L [92]) contribute to a low fraction unbound (approximately 5%), and CBG being saturated in the therapeutic range. When CBG has been saturated at total cortisol concentrations (C_{tot}) above 200 ng/mL (550 nmol/L) [70], the unbound cortisol concentration (C_u) increases disproportionally with respect to C_{tot}. Since only C_u can be distributed to tissue or be eliminated, this subsequently leads to an increased distribution and elimination (i.e. increased V_{ss} and CL).

Changes in CBG concentration may therefore have an impact on the PK of cortisol. No differences in CBG concentrations were observed between sex or between pre- and postpubertal patients in Tsai *et al.* [93]. Elevated CBG concentrations have been measured in pregnant women and women on oestrogen therapy, whereas lower CBG concentrations were observed in patients on glucocorticoid treatment or with Cushing's syndrome [94,95]. Two previous studies identified a circadian rhythm of CBG [96,97], whereas another study with measurements during daytime (08:00-19:00) did not. It has previously been hypothesised that the circadian rhythm of CBG could have an impact on the exposure of HC, dependent on when the dose is administered [78,98].

Overall, maturational factors affecting distribution of hydrocortisone are related to the amount of body water and maturation of plasma proteins. The fraction of total body water is 80%-90% in young infants and decreases to 55%-60% in adults. Conversely, the fat content is low at birth (10%-15%). A smaller volume of distribution was observed in neonates for hydrophobic drugs [99], which may also be expected for hydrocortisone. Measured CBG concentrations were lower in neonates, whereas infants had reached adult values [100]. Lower CBG concentrations may lead to an increased distribution to tissues, which is less likely due to the low lipid content. The affinity of cortisol to CBG has to our knowledge not been studied in neonates, but a lower affinity has been observed for albumin in this age group [99].

1.4.3 Metabolism, excretion and its maturational aspects

Cortisol is metabolised in different tissues by different enzymes, and the main metabolic pathways are shown in Figure 1.7. 11β-hydroxysteroid dehydrogenase is a bidirectional enzyme available in two sub types; type 1 (11β-HSD1) and type 2 (11-βHSD2). The latter one is responsible for converting cortisol to cortisone especially in the kidney, to ensure less cortisol-mediated activation of the

mineralocorticoid receptors in the kidneys. 11-βHSD1, on the other hand, predominantly activates cortisone to cortisol in liver and adipose tissue among many [101].

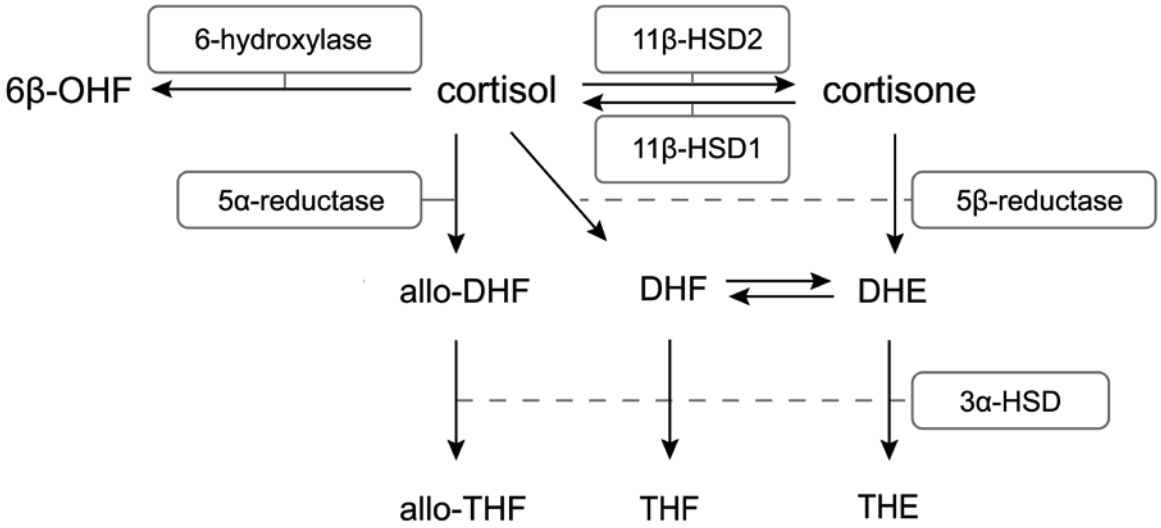

Figure 1.7 Main metabolic pathways for cortisol modified from Hoshiro *et al.* [102]. Responsible enzymes are shown in boxes and metabolites renally excreted are in italics. Hydroxysteroid dehydrogenase (HSD), dihydrocortisol (DHF), dihydrocortisone (DHE), tetrahydrocortisol (THF), tetrahydrocortisone (THE), hydroxycortisol (OHF).

In addition to the reversible processes mediated by 11-βHSD, cortisol and cortisone may also be subject to unidirectional metabolism. Cortisol and cortisone may be metabolised via 5α-reductase and 5β-reductase to dihydrocortisol (DHF), dihydrocortisone (DHE) and allo-DHF, respectively. These metabolites are further metabolised by 3α-hydroxysteroid dehydrogenase (3α-HSD) to tetrahydrocortisol (THF), tetrahydrocortisone (THE) and allo-tetrahydrocortisol (allo-THF), which are excreted renally [102]. In addition, approximately 1% of cortisol is metabolised by 6β-hydroxylase (CYP3A4) to 6β-hydroxycortisol, which is excreted renally. Small amounts of cortisol and cortisone is also excreted unchanged [102].

Hydrocortisone is a low extraction drug with mean/median *CL* ranging from 12.5 to 20.2 L/h in adults after iv administration of 5 to 50 mg hydrocortisone [65,70,75,76]. *CL* increased from 12.5 L/h after 5 mg to 17.6 L/h after 40 mg in Toothaker *et al.* [70]. The potential dose-dependency could be related to the saturable plasma protein binding previously discussed in section 1.4.2. Saturation of CBG leads to C_u increasing disproportionally with respect to C_{tot}. Since only C_u can be eliminated, this

subsequently leads to an increased elimination (i.e. CL) and dose-dependent CL. Unbound *CL* (CL_u) however remains constant, since it is independent of f_u.

The median/mean relative *CL* (*CL/F*) after administration of 10-20 mg was similar to after iv administration (19.1 L/h [75]), indicating a bioavailability close to 1. CL/F was higher after intake of 50 mg (27.3 L/h[76]) in adult patients with adrenal insufficiency and variable (12.4-25.6 L/h) in paediatric patients with adrenal insufficiency [79,80]. The highest value was observed for pubertal patients.

The area under the cortisol concentration-time profile (*AUC*) increases less than dose-proportional to increasing doses similarly to C_{max}. This indicates that nonlinear processes (such as e.g. saturable plasma protein binding or saturable absorption) are influencing the PK of hydrocortisone, such as changes in CL or F with higher doses [69,71].

Relevant maturational changes for the metabolism and excretion include maturation of plasma protein binding and metabolising enzymes. Maturation of CBG has previously been discussed in section 1.4.2. The lower concentrations of CBG in neonates may potentially lead to an increased CL, due to increased C_u. When it comes to metabolising enzymes, 11-βHSD1 (converting cortisone to cortisol) had undetectable activity until 3 months and stabilised approximately at 12 months. 11-βHSD2 activity increased from birth up to 52 weeks, when activity similar to adults was achieved [103]. 5α-reductase activity was low in newborns and reached the highest activity after 3 months. The activity then declined until 52 weeks and was similar between 3.5-17.5 years [103,104]. A lower CL may therefore be expected in neonates due to low activity of 11-βHSD2 and 5α-reductase. An increased CL may be expected for infants at least up to 1 year of age due to the increased activity of 5α-reductase.

1.5 Pharmacodynamics of hydrocortisone

As previously discussed, cortisol affects multiple physiological features. Administration of hydrocortisone may, therefore, also result in a large range of different effects, since hydrocortisone is equivalent to endogenous cortisol. Hydrocortisone may e.g. have an effect on the endogenous cortisol synthesis and on T cell dynamics, which has previously been quantified [105].

In the current thesis, the pharmacodynamic effects on 17-OHP synthesis were of interest. A previous analysis by Charmandari *et al.*, used a cross-correlation approach to evaluate the time shift of 17-OHP in relation to cortisol decrease. The study identified that the cortisol concentration at time of hydrocortisone administration correlated most with 17-OHP concentration 1 h post dose, indicating a

delayed inhibitory effect on 17-OHP concentrations (r=-0.302) [77]. Another study evaluated the correlation between AUC for cortisol and 17-OHP, for which no correlation was found [80].

1.6 Objectives

Adrenal insufficiency is a complex pathophysiological condition requiring life-long substitution therapy with glucocorticoids from birth in order to avoid adrenal crisis. Selecting appropriate dosing regimens is important to possibly avoid disease progression or effects related to over- and undertreatment. The overall aim of the current thesis was to assess the substitution therapy with hydrocortisone in paediatric patients with adrenal insufficiency, with the ultimate aim of contributing to a more rational dosing in this population. To accomplish this, pharmacometric approaches were applied to explore the underlying physiological system in healthy adults and paediatric patients with adrenal insufficiency, as well as PK and PK/PD in different populations. The physiological system in adults considered e.g. the impact of dexamethasone-suppression on the HPA-axis resulting in "disease-mimicking" adults, whereas the pathophysiological system in the paediatric patients considered the low/no endogenous cortisol synthesis. The physiological system was linked to drug treatment to allow for a more appropriate characterisation of the PK and PK/PD in the different populations studied. The combined system was used to simulate expected drug exposure, which was compared with physiological cortisol concentrations. The objectives were sought to be met in the following projects:

Project 1: As a part of clinical drug development, the PK of hydrocortisone administered as a novel hydrocortisone formulation (Infacort) was studied in a phase 1 trial in healthy adult volunteers in whom the disease was mimicked. The objective was to characterise the PK of hydrocortisone, while considering the underlying physiology of the system. In order to enable a more appropriate extrapolation of PK knowledge to paediatric patients with adrenal insufficiency, a semi-mechanistic approach considering plasma protein binding was pursued. This project also aimed to evaluate the impact of body weight on predicted cortisol exposure in patients in a wide body weight range including the paediatric weight range. In addition, this project aimed to characterise the circadian behaviour of CBG, and to assess its potential impact on the exposure of cortisol.

Project 2: Sequential to the studies in adults, a PK study in paediatric patients with adrenal insufficiency was undertaken. The semi-mechanistic PK model from project 1 was extrapolated to the sparse phase 3 data by applying a range of different approaches with

diminishing impact of adult data. The objectives of project 2 were to characterise the PK of hydrocortisone administered as the novel formulation in paediatric patients with adrenal insufficiency, and to assess the potential impact of maturational factors affecting the PK.

Project 3: In project 3, rich data from paediatric patients with CAH from a clinical investigator initiated study was characterised. Since both cortisol and 17-OHP concentrations were available, the objective was to characterise the PK/PD relationship using 17-OHP as a biomarker. The previously developed PK model from project 2 was refined and used when characterising the PK/PD in paediatric patients with CAH. In addition, simulated exposure after recommended dosing regimens for growing paediatric patients with CAH were assessed and compared to physiological cortisol profiles from the literature.

2 Methods and studies

2.1 Nonlinear mixed-effects modelling

As previously described in section 1.1.2.1, nonlinear mixed-effects (NLME) modelling involves analysing the population and individual level simultaneously. The name mixed-effects modelling refers to the use of fixed-effects (i.e. parameters constant in a population) and random-effects (i.e. stochastic parameters) to evaluate the general tendency and variability of the data, respectively. The following sections will outline the different model components of a NLME model used in the current thesis.

2.1.1 Model components

A NLME model is built up by several submodels; The structural model, pharmacostatistical model and covariate model (Figure 2.1), which will be described hereafter.

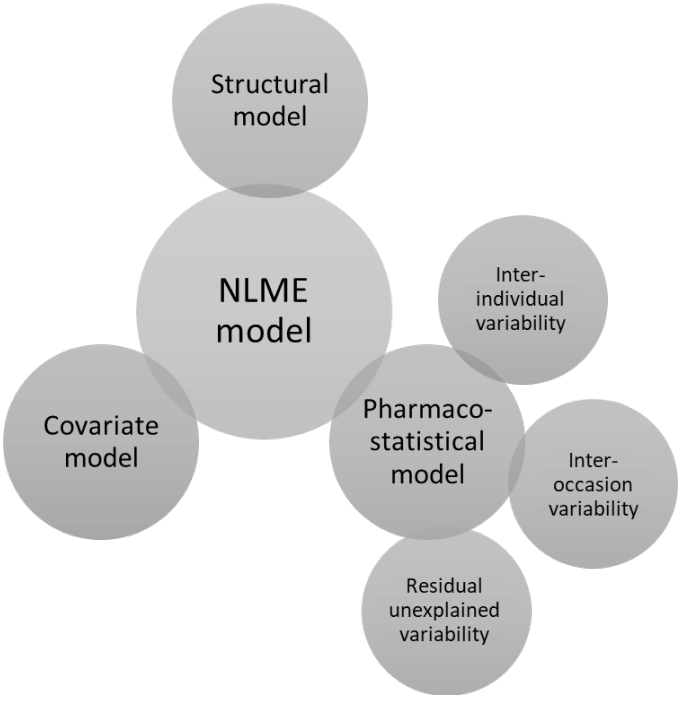

Figure 2.1 Schematic illustration of the different submodels of a population model.

2.1.1.1 Structural model

The structural model describes the central tendency in the data. In the case of a PK model in the current thesis, this could refer to e.g. the central tendency of the cortisol concentration-time profiles after administration of hydrocortisone. In the initial phase of model development, the population PK models to be evaluated was chosen based on the exploratory graphical analysis, in which the appearance of the concentration-time profile (e.g. mono-, multi-phasic decline) gives an understanding regarding which compartmental model (number of compartments, kinetics of transfers) could be appropriate. The aim of a pharmacometric analysis is to develop the simplest model, which still describes the data accurately. A simple one compartment model is therefore commonly applied initially, which also enables an easier computational estimation process. Assuming negligible residual error, the structural model is described by Eq. 2.1, which determines the vector of the observed dependent variable (e.g. drug or biomarker concentrations) for the i^{th} individual at the j^{th} timepoint (y_{ij}). *f is* a nonlinear function (i.e. pharmacokinetic model) relating y_{ij} to the vector of model parameters (ϕ_i, e.g. *CL* or V_c) and study design variables (x_{ij}) such as covariates, dose and sampling times [14].

$$y_{ij} = f(\phi_i, x_{ij}) \quad \text{(Eq. 2.1)}$$

2.1.1.2 Pharmacostatistical model

There are several hierarchical levels of pharmacostatistical models one may consider; e.g. interindividual variability (IIV), interoccasion variability (IOV) and residual unexplained variability (RUV).

Interindividual variability

Interindividual variability acknowledges the difference between individuals and allows for the individual parameter estimate to differ from the population estimate. IIV is however not describing the reason for the different parameter estimate. In this thesis, three different IIV models were assessed. The additive IIV model is described in Eq. 2.2, in which the individual model parameters (ϕ_i) are related to the population parameter estimates (θ) and the covariates (z_i) via a nonlinear function *g*. The discrepancy between the population estimate and individual model parameter (Empirical bayes estimates, EBE) is denoted η_i. η_i is assumed to be independent of each other and normally distributed around zero with a variance of ω^2. η_i is the same within an individual unless IOV is applied. IIV can also be applied as a proportional (Eq. 2.3) or exponential model (Eq. 2.4). The exponential model is most commonly applied in PK analyses, since the PK parameters tend to be log-

normally distributed and this prevents estimation of negative EBEs. On a logarithmic scale, the coefficient of variation (CV%) is commonly approximated from ω^2 (Eq. 2.5).

$$\phi_i = g(\theta, z_i) + \eta_i \quad \text{(Eq. 2.2)}$$

$$\phi_i = g(\theta, z_i) \cdot (1 + \eta_i) \quad \text{(Eq. 2.3)}$$

$$\phi_i = g(\theta, z_i) \cdot e^{\eta_i} \quad \text{(Eq. 2.4)}$$

$$\text{CV\%} = 100 \cdot \sqrt{(e^{\omega^2} - 1)} \quad \text{(Eq. 2.5)}$$

Interoccasion variability

Interoccasion variability acknowledges the variability between different occasions, and allows for the individual estimate to differ between occasions. Occasions can be defined as different doses, different days, or different study periods depending on the study design. When implementing IOV, the variability in parameters between occasions (κ_i) is assessed in addition to IIV (Eq. 2.6). κ_i is assumed to be normally distributed around 0 with variance π^2 and independent of each other. [106]. IOV does not describe the reason for the variability between occasions, and should only be used if the model parameters change randomly between occasions. IOV between doses was assessed in project 3 (section 2.4.3.5)

$$\phi_i = g(\theta, z_i) \cdot e^{\eta_i + \kappa_i} \quad \text{(Eq. 2.6)}$$

Residual unexplained variability

RUV refers to the unexplained variability resulting from e.g. measurement error, model misspecification and errors in dosing. RUV, describes the discrepancy between the observed (y_{ij}) and individually predicted ($f(\phi_i, x_{ij})$) concentration. The difference is denoted ε_{ij} and is assumed to be normally distributed around 0 with variance σ^2. In the current thesis, RUV was assessed using an additive (Eq. 2.7), proportional (Eq. 2.8) or combined (Eq. 2.9) model. If estimating parameters using log-transformed data an additive model is commonly applied, since it approximates an exponential or a proportional RUV model on a linear scale.

$$y_{ij} = f(\phi_i, x_{ij}) + \varepsilon_{add,ij} \quad \text{(Eq. 2.7)}$$

$$y_{ij} = f(\phi_i, x_{ij}) \cdot (1 + \varepsilon_{prop,ij}) \quad \text{(Eq. 2.8)}$$

$$y_{ij} = f(\phi_i, x_{ij}) \cdot (1 + \varepsilon_{prop,ij}) + \varepsilon_{add,ij} \quad \text{(Eq. 2.9)}$$

2.1.1.3 Covariate model

When the structural and pharmacostatistical models have been established, covariates influencing the PK, PD or disease parameters can be identified. This is often an important aim for clinical studies, and may provide insight into whether there are any dose adjustments needed in specific populations. After a graphical evaluation, relationships between covariates and PK parameters can be quantified and included into the model thereby potentially reducing some unexplained IIV [12]. Commonly used covariates include body size related covariates or creatinine clearance for drugs with renal elimination. Covariates are commonly assumed to be constant during the study period, but models for time-varying covariates have also been suggested [107]. In project 1 of the current thesis (section 2.2.3.2), a linear covariate relationship was assessed, in which the individual parameter estimate (ϕ_i) was derived from the population parameter (θ) and a covariate effect (θ_{cov}) with respect to the individual covariate value (z_i, Eq. 2.10). The median value of the covariate (z_{median}) was used to normalise z_i, and θ therefore corresponds to the parameter estimate with covariate value equal to z_{median}.

$$\phi_i = \theta + \theta_{cov} \cdot (z_i - z_{median}) \quad \text{(Eq. 2.10)}$$

2.1.2 Parameter estimation and estimation methods

In NLME modelling, the aim is to generate parameter estimates that describe the observed data most appropriately. This is achieved by using maximum likelihood estimation, which iteratively selects the parameters maximising the probability of observing the data. In the software NONMEM, the objective function value (OFV) is a single value indicating how well the model can describe the data. The OFV of the maximum likelihood estimation is proportional to minus 2 times the log likelihood (-2LL), corresponding to the extended least squares objective function (OFV_{ELS}, Eq. 2.11) [108]. y_i refers to the vector of observations, $\hat{y}_i$ to the vector of expected y_i, and var(y_i) to the expected variance of y_i.

$$OFV_{ELS} = \sum_{i=1}^{n} \left[\frac{(y_i - \hat{y}_i)^2}{var(y_i)} + \ln(var(y_i)) \right] \quad \text{(Eq. 2.11)}$$

PK models are in general nonlinear and the OFV can most commonly not be solved analytically. The OFV estimation of parameters is therefore dependent on numerical approximations, which can be done by e.g. gradient-based algorithms. Gradient-based algorithms commonly use Taylor series approximations for numerical solution of the likelihood function. The first-order expansion is used in

the frequently applied first-order conditional estimation (FOCE) algorithm, which is linearised by conditioning on the individual etas [109,110]. A similar approach considering the interaction between ε and η is available in the FOCE with interaction (FOCEI) [109]. FOCEI was applied in project 1 for the plasma protein binding model (section 2.2.3.2), CBG model (section 2.2.3.3), as well as initially for the semi-mechanistic PK model (section 2.2.3.5) in project 1, and for the pharmacokinetic model (2.3.3) and pharmacokinetic/pharmacodynamic model (section 2.4.4) in project 3. LAPLACE is a second-order approximation and is the only gradient-based estimation method that can be used for categorical data [110]. This algorithm was applied in project 3 (section 2.4.3.3) when using likelihood-based approaches to consider observations below LLOQ, which will be described in section 2.1.4.

If a more complex model is applied, the first-order conditional methods may not be stable or very inefficient. For these models, expectation-maximisation algorithms such as stochastic approximation expectation maximisation (SAEM) or importance sampling (IMP) algorithms can be applied [111]. These algorithms first include an expectation step (E), which evaluates the expected likelihood with respect to the conditional distribution of η_i based on the current parameter estimates and the observed data. Step E can be performed by stochastic approximation (e.g. SAEM) or Monte-Carlo integration (e.g. IMP). After step E, the maximisation (M) step maximises the expected likelihood (from step E) to generate new parameter estimates [110]. Both steps are thereafter repeated until minor changes are observed. In IMP, Monte-Carlo sampling is used in step E to assess the conditional mean and variance of η_i. The SAEM includes one burn-in and one accumulation phase. In the burn-in phase, approximation is done on few samples per individual, and maximised and the process is repeated until the estimates have stabilised. Thereafter, the individual random-effects are sampled and averaged together [112]. The objective function is commonly generated by few iterations of IMP for the final parameter estimates. This was performed in project 1 (section 2.2.3.5) and 2 (section 2.3.3), for which SAEM followed by IMP were used.

2.1.3 Endogenous baseline models

Baseline models are commonly applied in pharmacodynamic analyses to consider the baseline values observed before and after treatment. In this thesis, these models were applied in project 1 (section 2.2.3.1), 2 (section 2.3.3.1) and 3 (section 2.4.3.1) to consider the underlying endogenous synthesis of cortisol. In addition, baseline models were evaluated to consider the endogenous biomarker (17-OHP) in project 3 (2.3.3.1).

Dansirikul *et al.*, described four different baseline models (B1 – B4) [113], out of which two were evaluated in the current thesis (B1 and B2). Using the B1 method, the individual baseline ($baseline_i$)

was derived considering IIV (η_i) and the population baseline (*baseline,* Eq. 2.12). An exponential IIV model was assessed, thereby assuming a log-normal distribution of the baseline. This method does not require pre-dose measurements, and is commonly seen as the gold standard [113].

In the second baseline method (B2 method), the estimated $baseline_i$ is informed by the individually observed initial concentration ($baseline_{obs,i}$) and the interindividual variability corresponding to the residual variability (η_i,*RV,* Eq. 2.13). $Baseline_i$ is commonly used as the starting point for the analysis, by e.g. initialising the compartment of interest [113].

$$baseline_i = baseline \cdot e^{\eta_i} \quad \text{(Eq. 2.12)}$$

$$baseline_i = baseline_{obs,i} \cdot e^{\eta_i,RV} \quad \text{(Eq. 2.13)}$$

2.1.4 Handling data below lower limit of quantification

Concentrations below LLOQ are common in PK data., The best solution to avoid concentrations below LLOQ would be to improve the LLOQ of the bioanalytical assays, which may not always be possible [114]. By ignoring data below LLOQ, predicted data near or below LLOQ will be biased and slightly overpredicted [115]. This may result in biased parameter estimates [114], and Byon *et al.* therefore suggested that BLQ observations should be considered if the fraction BLQ is larger than 10% [116]. On the other hand, censoring BLQ in data with a low fraction BLQ (10%) had minor impact for a one-compartmental model, whereas an impact on the two-compartmental model was observed [117].

Different approaches to handle concentrations below LLOQ have previously been described by Beal [115], and sequentially described and evaluated extensively [114–116,118]. Censoring observations below LLOQ (M1) method was evaluated in all three projects. In addition, a second approach (M3) was considered in project 3 (section 2.4.3.3). In the M3 method, the likelihood for the observations below LLOQ is assessed. The maximum likelihood estimation is performed considering all observations (i.e. the ones above and below LLOQ). The predicted data in the lower concentration range (near or below LLOQ) is therefore more appropriate than for the M1 method. Since continuous (concentrations above LLOQ) and categorical (whether the concentration is above or below LLOQ) data is modelled simultaneously, the LAPLACE estimation method is used. This estimation method is more unstable than e.g. FOCE, and the M3 method may therefore not be possible for more complex models. Choosing M3 over M1 generally provides more accurate parameter estimates [114,118], but

the improvement depends on model complexity and fraction of observations below LLOQ, and the pattern of missingness [115].

2.1.5 Model selection and evaluation for all models

Model development is an iterative process in which models are evaluated, selected and updated before the process starts over again. Model evaluation is an important step considering many different factors, such as plausibility of parameter estimates, stability of parameter estimation and model convergence. In addition, numerical/statistical and graphical methods are used to evaluate the models and ease the selection process. These different criteria will be further outlined below.

2.1.5.1 Numerical and statistical evaluation of model performance

Objective function value

Model selection in NLME modelling is to a large extent guided by the OFV. As previously stated, parameters are estimated by minimising the -2LL, which corresponds to the OFV. A lower OFV indicates a better description of the data. For nested models (complex models which can be collapsed to the simpler one), the likelihood ratio test (LRT) can be used to compare the OFV between two models. The LRT assumes a χ^2 distribution of the OFV difference between the models, and the distribution is defined by the degrees of freedom (number of additional parameters) in the more complex model. The resulting test statistic can then be seen as the probability of observing the difference between the models, given that the null hypothesis assumes no difference [109]. The significance level (α) is usually pre-specified and a value of 0.01 was selected in the current thesis. If considering an increase of 2 parameters (degrees of freedom=2) this significance level would correspond to a difference if OFV of 9.21.

Akaike Information Criterion

If models are not nested, other criteria such as the Akaike Information Criterion (AIC) can be used. AIC also considers the number of parameters (p, Eq. 2.14) [119]. The lower AIC indicates the better description of the data.

$$\mathrm{AIC} = -2LL + 2 \cdot p \qquad \text{(Eq. 2.14)}$$

2.1.5.2 Graphical evaluation of model performance

In addition to statistical methods, graphical evaluation tools are useful to identify trends in the model prediction or model misspecifications. In the current thesis two kinds of graphical evaluation were applied: Standard goodness of fit (GOF) graphics and visual predictive checks (VPCs).

Standard Goodness of fit graphics

GOF graphics are an important tool for fast initial evaluation of the model, and was used in all projects of the current thesis. GOF graphics commonly include comparison of the predicted versus the observed concentrations, in which observations should be scattered evenly around the line of identity. The plot including population or individual predictions is informative for evaluating the appropriateness of the structural model or the stochastic model, respectively. In addition, residual-type diagnostics are useful to detect trends or model misspecification. Since the residuals (difference between observed and predicted concentration) are dependent on the magnitude of the prediction, conditional weighted residuals (CWRES) are a better alternative. CWRES are residuals which have been adjusted based on the FOCE approximation, and are therefore appropriate for graphical evaluation if the FOCE algorithm has been used [120]. CWRES versus population predictions are valuable for identifying concentration-dependencies in the data (assuming that the dependent variable is a concentration), and to assess appropriateness of the RUV model. CWRES versus time is also helpful graphic to find time-dependent trends, which may provide information if the model specification appears in the absorption or the elimination phase. For both plots, The CWRES should be close to zero (± 2 SD) and randomly scattered around zero [121].

Visual predictive checks

Visual predictive check is a commonly used simulation-based graphical evaluation tool to evaluate predictive performance of a model, and was used in all projects in the current thesis. The principle behind the VPC is to graphically evaluate the ability of a model to reproduce the observed data (i.e. predictive performance). This is done by simulating a large number of datasets (e.g. 1000) using the model to be evaluated. The percentiles of interest (commonly 5^{th},50^{th} and 95^{th}) and the confidence interval of respective percentiles for the simulated concentrations are derived and then compared graphically with the same percentiles of the observed concentrations [122]. Commonly, the percentiles of the simulated and observed concentrations are derived for selected time ranges (bins) instead for at every time to ease the comparison. In a structured sampling design, the bins could refer to the time interval around the planned sampling times. The percentiles of the simulated and observed data are thereafter compared graphically [123]. Since the VPC is displayed on the normal time-scale, it is easy to identify which part of the PK profile which is sub-optimally described (e.g. absorption or elimination phase). If the PK (or PK/PD) is not dependent on clock time, time after dose is a commonly used time scale to use for VPCs after multiple dosing. For categorical data, such as

when using a model to consider concentrations below LLOQ, categorical VPC is a useful tool to evaluate performance [118]

2.1.5.3 Evaluation of uncertainty in parameter estimates

The precision of a model parameter can be derived by different methods. If the variance-covariance matrix is generated in NONMEM, the standard errors of the parameter estimates can be derived from taking the square root of the diagonal elements in variance-covariance matrix. The relative standard error (%RSE) is commonly computed to evaluate parameter precision for fixed-effects, which is derived from the final population parameter (θ) and the standard error of the population parameter (SE(θ), Eq. 2.15). Usually fixed-effects estimates with %RSE below 30% are considered to be precisely estimated [109].

The %RSE for random-effects parameters on a standard deviation scale can be derived similarly from the final variance (ω^2) and the standard error of this variance (SE(ω^2), Eq. 2.16). Random-effects are commonly less precisely estimated and %RSE of 40%-50% is acceptable [109]. In addition to the standard error from the covariance step, there are other approaches available for generating the parameter precision, such as bootstrap and log-likelihood profiling.

$$\%\mathrm{RSE}(\theta) = 100 \cdot \frac{SE(\theta)}{\theta} \qquad \text{(Eq. 2.15)}$$

$$\%\mathrm{RSE}(\omega^2) = 100 \cdot \frac{SE(\omega^2)}{2 \cdot \omega^2} \qquad \text{(Eq. 2.16)}$$

Bootstrap method

Using the bootstrap method, a pre-specified number of new datasets are first generated from the original dataset by sampling individuals with replacement. The established model is then estimated using the new datasets to generate new parameter estimates, from which the confidence interval (e.g. 95% confidence interval (95% CI)) can be derived. The confidence interval and the median estimate of the parameter estimates can thereafter be compared to the estimates of the original data [124], to provide information regarding the generalisability of the model (i.e. if the model is too specific to the data or if the model can be applied to other populations). The number of bootstrap simulations needed depends on the aim of the bootstrap. 200 datasets may be needed for generating the standard errors [124]. In the current thesis, 1000 new datasets were sampled in all projects and the bootstrap were generated using the software PsN [124].

Log-Likelihood profiling

Log-likelihood profiling is first-most a method to assess the surface of the likelihood to see if the OFV from the final model refers to the global minimum. This approach may however also be used to generate confidence intervals for the parameter estimates which does not assume a specific distribution. The analysis is performed individually for the respective parameter estimate of interest, and the final model is initially estimated with the final parameter estimate. The model is thereafter re-estimated by fixing the respective parameter to a slightly different estimate (e.g. ±5% or ±20%) until the selected significant difference in likelihood (e.g. ΔOFV: 3.84, df=1, α=0.05) between the full and reduced model is achieved. When this difference has been attained, the lower and upper boarder of the 95% confidence interval for the parameter has been reached [109,125]. In the current thesis, log-likelihood profiling was applied using PsN to generate the confidence interval in project 2 (section 2.3.4) [124].

2.1.5.4 Identification of influential individuals

Influential individuals may have a large impact on model selection or on parameter estimates [126]. Influential individuals can be identified by comparing individual OFV in the NONMEM output. Another approach is to use case-deletion diagnostics.

Case-deletion diagnostics

In case-deletion diagnostics, new datasets are created from the original dataset, in which one individual/dataset has been removed. The developed model is estimated with the new datasets, and the difference in OFV, % change in parameter estimates or precision of the parameter estimates are assessed [124]. An individual, which generates a relative change in parameter estimates of ±20% after removal is considered an influential individual [127]. Case-deletion diagnostics was applied using PsN on the plasma protein binding model and CBG model in project 1 (section 2.2.4), as well as PK and PK/PD model in project 3 (section 2.4.5) of this thesis.

2.1.5.5 External model evaluation

An external model evaluation is a useful tool to evaluate the ability of a developed model to predict external data not used for model development. In the current thesis, external model evaluations were performed similarly to VPCs (section 2.1.5.2); the covariates (i.e. dose, body weight etc.) of the external data and the model to be assessed were used to simulate 1000 new datasets with new concentration-time profiles. The percentiles of the observed and simulated concentrations were derived and sequentially compared graphically. An external model evaluation was performed for the

plasma protein binding model in project 1 (2.2.4) and for the full adult semi-mechanistic PK model in project 2 (2.3.3).

2.1.6 Deterministic and stochastic simulations

As previously described in section 1.1.3, simulations provide a useful tool to evaluate scenarios which are difficult to study clinically. Commonly, two different types of simulations are carried out: deterministic and stochastic simulations. Deterministic simulations do not consider the random-effects parameters of the model, thereby only generating the typical concentration-time profile for a given set of covariates. Deterministic simulations are useful to visualise and assess which impact changes in dose will have on e.g. exposure, which was performed to predict exposure in paediatric patients (section 2.2.5.2) in project 1. Stochastic simulations, on the other hand consider the random-effects parameters, which is commonly used when generating VPCs. Stochastic simulations require appropriate precision of all parameters (fixed- and random-effects parameters). Stochastic simulations can be informative to guide dose selection or to compare different dosing scenarios, which was performed in project 3 (section 2.4.6). In addition, stochastic simulations were applied in project 1 (section 2.2.5.3), to assess the potential impact of circadian CBG on the cortisol exposure after treatment with Infacort.

2.1.7 Software

NLME modelling can be performed using several different software programs such as NONMEM and Monolix, from which the first is still the most commonly used one. Perl speaks NONMEM (PsN) is a commonly used tool to ease the model development [124]. Pirana is a graphical user interface which enables an easier documentation of models and the modelling process [128].

All modelling and simulation related activities in the current thesis were performed in NONMEM 7.2-7.3 [112] together with Perl speaks NONMEM (4.3.3-4.40) [124] and the user interface Pirana ([128]), if not stated otherwise. Some modelling activities in all three projects were performed on the high performance computing cluster of Freie Universitaet Berlin [129]. All dataset preparation have been performed in the software R (3.3.0 [130]). Graphical evaluation have been performed using the R-package ggplot2 [131] and Xpose4 ([128]). The VPCs were generated using the R-package VPC [132]. Bootstrap, log-likelihood profiling and case-deletion diagnostics were performed in PsN.

2.2 Project 1: Pharmacokinetic characterisation of a novel hydrocortisone formulation in healthy adults

2.2.1 Objectives

There is currently no licensed hydrocortisone formulation for paediatric patients below six years of age in Europe or the US. Infacort®(Diurnal Ltd), hydrocortisone granules with taste masking, was therefore developed to provide a formulation suitable from birth. The PK of Infacort in adults has previously been analysed with a NCA, which provides a simple description, but does not account for known nonlinearities of cortisol [40]. Consequently, an NCA cannot be used to extrapolate information to paediatric patients. This analysis aimed to provide a quantitative and mechanistic understanding of the complex PK of HC after administration of Infacort in healthy adult volunteers using a NLME approach and to use the established model to predict HC exposure in paediatric patients.

2.2.2 Study design

Project 1 is based on data from two clinical cross-over trials (ClinialTrials.gov Identifier: NCT02777268, NCT01960530, EudraCT number: 2013-000260-28; 2013-000259-42 [40,97]) in healthy male volunteers with four and five study periods, respectively. Both studies were performed at Simbec Research Ltd (Merthyr Tydfil, UK) according to the Helsinki declaration [133], association of the British Pharmaceutical Industry Guidelines for Phase 1 Trials (2012 [134]), International Conference on Harmonisation (ICH) Harmonised Tripartite Guideline for Good clinical practice (GCP) [135] and the Medicines for Human Use (Clinical Trials) regulations 2004 (Statutory Instrument 2004 No. 1031) [136] and applicable amendments. Healthy males (18-60 years) not working shifts with no clinically significant sensitivity to hydrocortisone and/or dexamethasone (DEX) or infection were included into the studies.

DEX was administered in several study periods to suppress the hypothalamic-pituitary-adrenal (HPA) axis activity. Volunteers not sufficiently suppressed, as judged by elevated ACTH concentrations in the morning, were excluded from the analysis. Participants in both studies received standardised meals after administration of HC (08:00 and 13:00) to not interfere with the absorption process. In both studies, body weight (BW), height (HT) and age were recorded.

Study 1 included four study periods, in which the volunteers received single morning oral (po) doses of 0.5, 2, 5 and 10 mg Infacort (n=16 [5]) in a random order with a washout period of at least 1 week

between periods. Total plasma cortisol concentrations (C_{tot}) were sampled predose and 0.5, 1, 1.5, 2.5, 3, 3.5, 4, 4.5, 5, 5.5, 6, 6.5, 7, 7.5, 8, 9, 10, 11 and 12 h post dose in study 1. DEX (1 mg) was administered in each study period, according to (Figure 2.2), to suppress the endogenous cortisol synthesis.

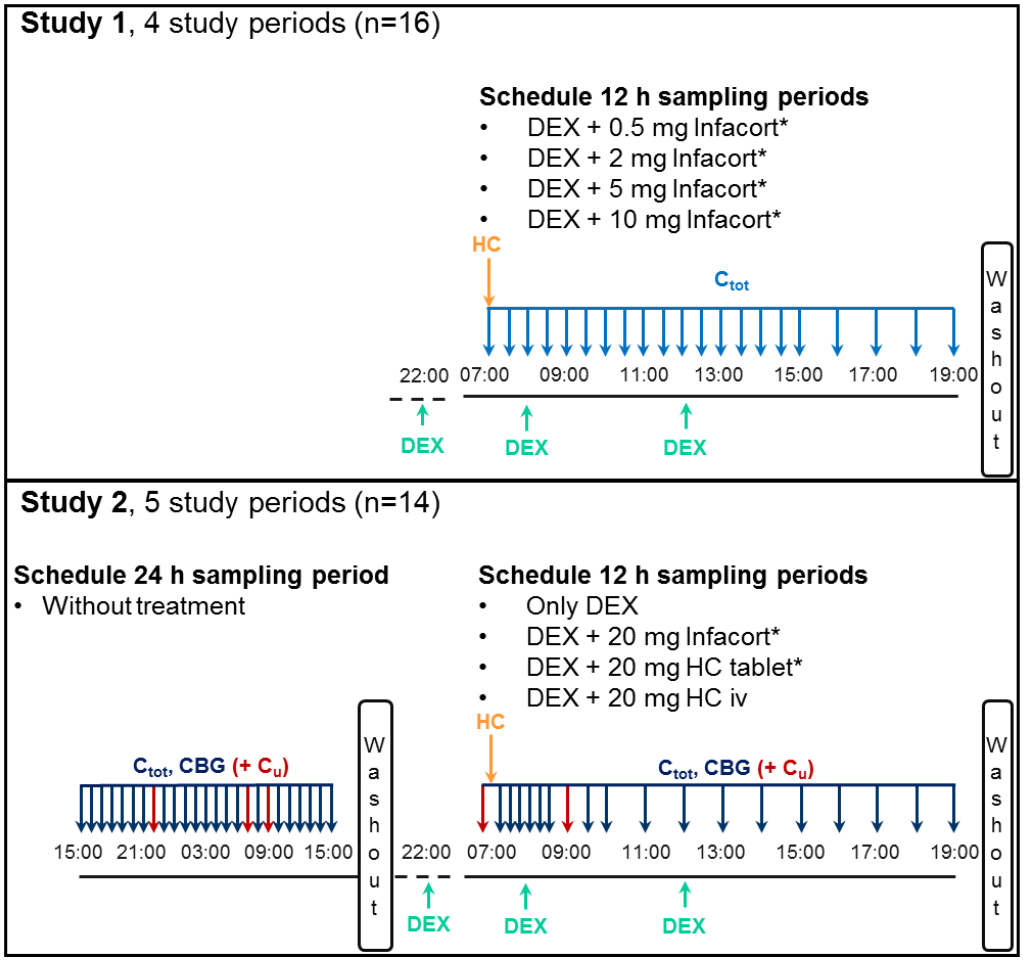

Figure 2.2 Schematic representation of the hydrocortisone (HC) and dexamethasone (DEX) administrations and sampling schedule for the two cross-over studies; study 1 (upper panel) and study 2 (lower panel). Study 1 consisted of 4 sampling periods of 12 h, in which total cortisol concentrations (C_{tot}: light blue arrows) were measured after DEX suppression (turquoise arrows) and administration of single doses of 0.5, 2, 5 and 10 mg of Infacort (orange arrows) with a washout period of at least one week between periods.

In study 2, C_{tot}, corticosteroid-binding globulin (CBG, CBG+C_{tot}: dark blue arrows) and unbound cortisol concentrations (C_u, CBG+C_{tot}+C_u: red arrows) were measured, first over 24 h in the absence of DEX, followed by 12 h sampling periods (n=4) with DEX suppression and no HC, 20 mg Infacort, 20 mg licensed HC tablet and HC intravenously (iv). The washout period between study periods was at least one week. *Randomised study periods. Adapted by permission from Springer Nature Terms and Conditions for RightsLink Permissions Springer Customer Service Centre GmbH: Springer, Clinical Pharmacokinetics [137] © 2018.

Study 2 included an additional evaluation of the endogenous cortisol synthesis/concentrations in absence of DEX over 24 h at the beginning of the study, in which C_{tot} and CBG were collected once every hour for 24 h (15:00-15:00, Figure 2.2). Subsequently, in four periods the volunteers (n=14) received only DEX (1 mg), DEX and single doses of 20 mg Infacort or 20 mg licensed oral HC tablet (Auden Mackenzie Ltd) in a random order followed by intravenous (iv) bolus HC administration (hydrocortisone succinate) with a washout period of at least one week. In these periods C_{tot} and CBG were sampled predose, and 0.25, 0.5, 0.75, 1, 1.25, 1.5, 2, 2.5, 3, 4, 5, 6, 8, 10 and 12 h post HC dose/period start. In addition, unbound concentrations (C_u) were obtained at 22:00, 07:00 and 09:00 in absence of DEX and pre dose and 2 h post dose after administration of DEX with/without HC (Figure 2.2).

2.2.2.1 Bioanalytical quantification of total cortisol concentrations

Samples were stored at -20°C prior to analysis. C_{tot} was quantified by liquid chromatography with tandem mass spectrometry detection (LC-MS/MS) at Simbec Research Ltd (Merthyr Tydfil, UK). The system consisted of an Applied Biosystems MDS Sciex API 365 triple quadrupole atmospheric pressure ionisation mass spectrometer. The column was a Phenomenex Luna C18 column with the respective Phenomenex C18 guard column, and separation was achieved with a mobile phase consisting of water/acetronile (55/45 (v/v)) and 1% (v/v) formic acid. The LLOQ was 1.38 nmol/L for C_{tot}. Intra-assay and interassay variability (CV) was 9.6% and 3.7% for 4.14 and 553 nmol/L. Accuracy was <5% between 0.5 and 300 nmol/L [40].

2.2.2.2 Bioanalytical quantification of unbound cortisol concentrations

Samples were stored at approximately -80°C prior to analysis. C_u were obtained using temperature-controlled ultrafiltration at 37°C and quantified with LC/MS-MS at the University of Manchester (Manchester, UK). The sample volume was not corrected after ultrafiltration, as cortisol was measured in the protein-depleted ultrafiltrate. Collection of ultrafiltrate was kept to a minimum, i.e. 10%-20% of the total plasma volume. Adsorption to the ultrafiltration device was assessed and was found to be negligible. The chromatography was done using a gradient method with mobile phase A: 0.1% (v/v) formic acid in water, and mobile phase B: 0.1% (v/v) formic acid in methanol) The system consisted of a Waters Xevo TQ-MS in electrospray positive mode, and a Waters AcquityTM LCsystem. The assay had a LLOQ of 0.80 nmol/L and intra- and interassay variability <8.0% and <9.5%, respectively. Accuracy was <10.4% for concentrations between 2.7 and 72.0 nmol/L [97,138].

2.2.2.3 Bioanalytical quantification of corticosteroid-binding globulin concentrations

CBG samples were stored at approximately -70°C prior to analysis. The CBG samples were diluted and quantified using ELISA (Biovendor, Czech republic, Brno) with an LLOQ of 3.13 ng/mL, intra- and inter-assay variability <3.0% and <8.0%, respectively [91]. The bioanalysis was performed at Simbec Research Ltd (Merthyr Tydfil, UK).

2.2.3 Development of a semi-mechanistic pharmacokinetic model of hydrocortisone

The semi-mechanistic PK model was built from four different structural submodels; i) disease model, ii) plasma protein binding model (cortisol to plasma proteins), iii) CBG model (and its relation to the plasma protein binding model), and iv) pharmacokinetic model as depicted in Figure 2.3. These structural submodels will be described separately below, as well as pharmacostatistical model (2.2.3.6).

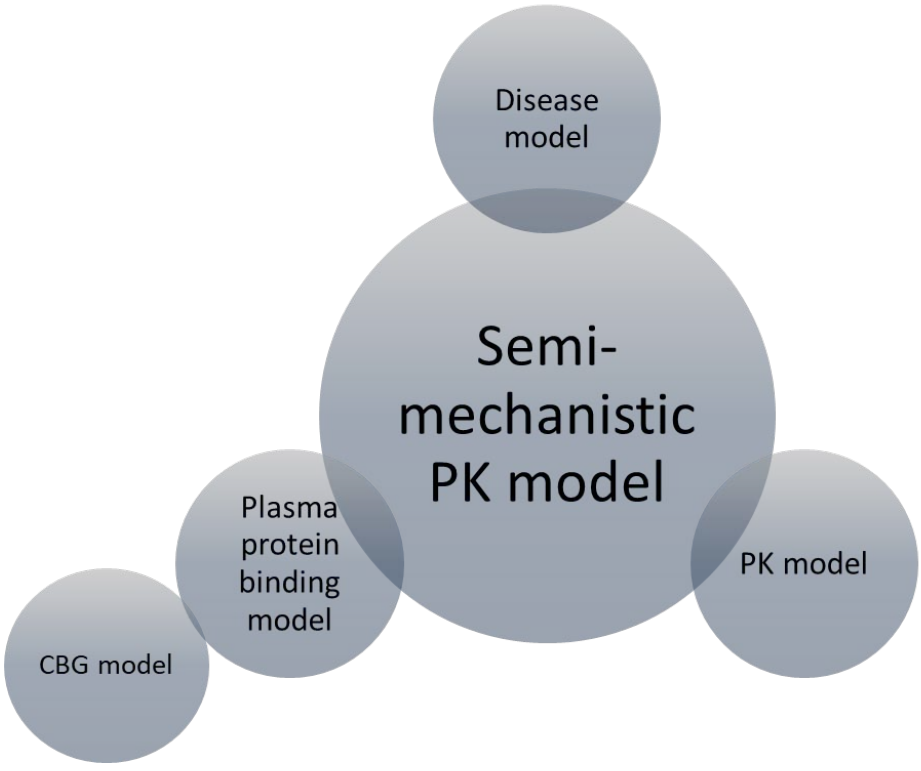

Figure 2.3 Schematic representation of the different submodels (i.e. disease model, plasma protein binding model, corticosteroid-binding globulin (CBG) model and pharmacokinetic (PK) model) building up the full semi-mechanistic PK model

2.2.3.1 Disease model

To suppress the endogenous cortisol synthesis, in order to measure the cortisol from the HC administration and to mimic the disease, the healthy volunteers were administered DEX prior to Infacort administration. To consider the measurable cortisol concentrations prior to dose, a baseline was estimated ($Baseline_{cort}$, Eq. 2.12) [113], as previously described in section 2.1.3. Since the cortisol concentrations before dosing were similar to the concentrations twelve hours after dose, a constant underlying baseline (disease model) was assumed. No other baseline models were considered in this project.

2.2.3.2 Plasma protein binding model of cortisol

C_{tot} and C_u from study 2 were used to characterise the plasma protein binding of cortisol. Linear (Eq. 2.17), nonlinear (Eq. 2.18) and combined linear and nonlinear (Eq. 2.19) plasma protein binding models were investigated. In these equations, the bound cortisol concentration (C_b) was derived by estimating the maximal binding capacity (B_{max}), the equilibrium dissociation constant (K_d) and/or the linear nonspecific binding *(NS*) parameter. The combined model assumes parallel linear and nonlinear binding in rapid equilibrium. Parameter estimation was done using FOCEI on log-transformed data due to the large cortisol concentration ranges evaluated. The fraction of post-dose C_u was low (4%). No likelihood-based methods to account for concentrations below LLOQ were therefore assessed.

$$C_b = NS \cdot C_u \quad \text{(Eq. 2.17)}$$

$$C_b = \frac{B_{max} \cdot C_u}{K_d + C_u} \quad \text{(Eq. 2.18)}$$

$$C_b = \frac{B_{max} \cdot C_u}{K_d + C_u} + NS \cdot C_u \quad \text{(Eq. 2.19)}$$

It is reasonable to assume that B_{max} (i.e. the maximum binding capacity) is dependent on the concentration of corticosteroid-binding globulin (CBG), and the number of binding sites at CBG (N_{CBG}). Using the *measured* CBG and N_{CBG} to derive B_{max} was evaluated according to Eq. 2.20. In addition, CBG was also evaluated as a covariate on B_{max} (Eq. 2.21), in which θ_{Bmax_CBG} corresponded to the linear increase in B_{max} with increasing CBG concentrations, which was centralised around the median of CBG (CBG_{median}). Further covariate modelling was pursued when relations between the individual parameter estimates and collected covariates were identified. The covariates were evaluated in the plasma protein binding model using a linear relationship as seen in Eq. 2.21.

$$B_{max} = CBG \cdot N_{CBG} \quad \text{(Eq. 2.20)}$$

$$B_{max,cov} = B_{max} + \theta_{Bmax\_CBG} \cdot (CBG - CBG_{median}) \quad \text{(Eq. 2.21)}$$

2.2.3.3 Model of corticosteroid-binding globulin

Since no CBG concentration measurements were available in study 1, CBG concentrations from the different time periods in study 2 were used to develop two different CBG models. The first model described the CBG concentrations during the day (07:00-19:00, periods with DEX), and was used to impute CBG concentrations for study 1. The second model considered the circadian CBG concentrations over 24 h (periods without DEX). The CBG models were estimated using FOCEI on non-transformed data, for which all measurements were above LLOQ. In the first model, a constant CBG baseline (Eq. 2.22) was implemented estimating the typical CBG ($baseline_{CBG}$) and the associated variability to generate the individual CBG baseline ($baseline_{CBG,i}$). For the second model, circadian CBG baselines including one to three cosine functions with different periodicity (24, 12 and 8 h) on the baseline were considered. Two cosine functions exemplified in (Eq. 2.23-Eq. 2.25), in which the proportional increase in amplitude (amp_{24}, amp_{12}) and the time shift of the cosine function ($shift_{24}$, $shift_{12}$) were estimated.

$$baseline_{CBG,i} = baseline_{CBG} \cdot e^{\eta i} \quad \text{(Eq. 2.22)}$$

$$CIRC_{24} = amp_{24} \cdot \cos(\frac{2 \cdot \pi \cdot (time - shift_{24})}{24}) \quad \text{(Eq. 2.23)}$$

$$CIRC_{12} = amp_{12} \cdot \cos(\frac{2 \cdot \pi \cdot (time - shift_{12})}{12}) \quad \text{(Eq. 2.24)}$$

$$CBG_{circ} = baseline_{CBG,i} \cdot (1 + CIRC_{24} + CIRC_{12}) \quad \text{(Eq. 2.25)}$$

Potential covariates such as HT and BW were evaluated as linear covariates for the baseline for CBG, similar to Eq. 2.21. Additional, covariate modelling was only pursued if the graphical evaluation implied relation between EBEs and the individual covariate value.

2.2.3.4 Pharmacokinetic model of hydrocortisone

Different PK disposition models (one-, two- and three-compartmental models) were evaluated simultaneously for the iv data and the different oral doses. Absorption was assessed as a zero-order absorption, zero-order absorption into the depot compartment (A_{depot}) followed by first-order absorption, first-order absorption or saturable absorption (Michaelis-Menten process, Eq. 2.26). The latter included estimation of the maximum absorption rate (V_{max}) and A_{depot} resulting in half of V_{max}

(K_m). Different PK disposition models (one-, two- and three-compartmental models) were evaluated simultaneously for the iv data and the different oral doses.

$$\frac{dA_{depot}}{dt} = \frac{-V_{max} \cdot A_{depot}}{K_m + A_{depot}} \quad \text{(Eq. 2.26)}$$

2.2.3.5 Structural semi-mechanistic pharmacokinetic model of hydrocortisone

The different structural submodels were merged together as described below. The disease model consisting of a constant baseline estimated according to Eq. 2.27, in which the predicted total cortisol concentration in the central compartment (C_{tot}) was derived from the total amount in central compartment (A_c), the central volume of distribution (V_c) and the individual cortisol baseline ($baseline_{cort,i}$).

The time course of A_c was described according to Eq. 2.28, thereby acknowledging that only the unbound amount in the central compartment (A_u) could be distributed to the peripheral compartment (V_p) with intercompartmental clearance (Q) and eliminated by CL. The peripheral amount (A_p) was assumed to be distributed back to the central compartment with Q (Eq. 2.29). A_u was obtained by solving Eq. 2.19 (Eq. 2.30), which described the relation between bound and unbound cortisol concentrations. The parameters of the plasma protein binding model were fixed and added to the PK model. The missing CBG concentrations in Study 1 were imputed with the typical value of the CBG model (section 2.2.3.3) and used to derive B_{max}. The ODE solver LSODA (ADVAN 13 in NONMEM) is useful for both stiff and non-stiff equations and was used when estimating the full PK model. The PK analysis was performed using log-transformed data, and FOCEI and SAEM with interaction followed by IMP were used during model development. The fraction of concentrations below LLOQ was zero for C_{tot}, hence models to account for concentrations below LLOQ were not implemented.

$$C_{tot} = \frac{A_c}{V_c} + baseline_{cort} \quad \text{(Eq. 2.27)}$$

$$\frac{dA_c}{dt} = \frac{V_{max} \cdot A_{depot}}{K_m + A_{depot}} - \frac{CL}{V_c} \cdot A_u - \frac{Q}{V_c} \cdot A_u + \frac{Q}{V_p} \cdot A_p \quad \text{(Eq. 2.28)}$$

$$\frac{dA_p}{dt} = \frac{Q}{V_c} \cdot A_u - \frac{Q}{V_p} \cdot A_p \quad \text{(Eq. 2.29)}$$

$$A_u = \frac{A_c - K \cdot (1 + NS) - A_{max} + \sqrt{(A_c - K \cdot (1 + NS) - A_{max})^2 + 4 \cdot K \cdot A_c \cdot (1 + NS)}}{2 \cdot (1 + NS)} \quad \text{(Eq. 2.30)}$$

Allometric scaling with BW using an exponent of 0.75 and 1 for clearance and distribution parameters, respectively was applied, since the aim was to extrapolate the developed model into paediatric patients with adrenal insufficiency. No other covariates were evaluated in the structural PK model.

The estimated CL corresponded to the unbound CL, since only the unbound amount could be eliminated and distributed. To enable comparison of PK parameters with references in the literature, the total CL was derived in R using the individual estimate of unbound CL and the predicted fraction unbound (f_u, Eq. 2.31). The predicted f_u was derived according to Eq. 2.32, in which the C_{tot} was derived from A_c and V_c according to Eq. 2.27, C_u was derived from the full binding equation (Eq. 2.30), using concentrations instead of amounts (C_{tot}, K_d, B_{max}).

$$Total\ CL = unbound\ CL \cdot f_u \quad \text{(Eq. 2.31)}$$

$$f_u = \frac{C_u}{C_{tot}} \quad \text{(Eq. 2.32)}$$

2.2.3.6 Pharmacostatistical model

IIV was implemented as an exponential model as previously described (Eq. 2.4), thereby assuming a log-normal distribution of the structural parameters. Residual unexplained variability was modelled as an additive error (Eq. 2.7), corresponding to an exponential error on linear scale for the binding and PK model. A proportional error was applied for the CBG models.

2.2.4 Model selection and evaluation of pharmacokinetic models

Model performance was judged by plausibility, OFV (section 2.1.5.1), GOF plots (section 2.1.5.2), parameter precision (section 2.1.5.3) and model stability. LRT was used to compare nested models, for which a reduction in the OFV of 6.63 points was considered statistically significant assuming a χ^2-distribution (p-value: 0.01, degrees of freedom: 1). AIC (section 2.1.5.1) was used for non-nested models. Precision of parameter estimates was assessed by bootstrap (section 2.1.5.3) in PsN 4.4.0 [124]. Case-deletion diagnostics (section 2.1.5.4) was performed for the plasma protein binding model and CBG model to identify potential influential individuals.

Predictive performance was evaluated by generating VPCs in which the percentiles (in this study: 5th, 50th and 95th) of observed and simulated data (using the model to be evaluated, n=1000) were compared. In addition, an external model evaluation was performed to evaluate the ability of the plasma protein binding model to predict external data. For this purpose, previously published binding

data from Lentjes an Romijn were digitalised using WebPlotDigitizer [139] and used for the evaluation. The data contained C_{tot} in the range range of 300-850 nmol [90].

2.2.5 Simulation-based analyses

2.2.5.1 Predicted concentrations (unbound, specific binding and non-specific binding) of cortisol

The different concentrations of cortisol (unbound, bound with specific binding, bound with non-specific binding) were simulated in R 3.3.0 [130] deterministically (i.e. not considering random-effects parameters) using the combined plasma protein binding model (Eq. 2.19) over a range of C_{tot} from 23.7 (corresponding to C_u of 0.5 nmol/L) to 492 nmol/L (the 75th percentile of observed C_{max} from Knutsson *et al.*[53]. When deriving B_{max} from *measured* N_{CBG} and binding sites (Eq. 2.20), the typical CBG baseline value (22.4 µg/mL, section 3.1.4) was used.

2.2.5.2 Predicting cortisol exposure in paediatric patients

To explore the dose-exposure relationship of Infacort (0.5-20 mg), C_{max} and *AUC* in individuals with different BW (5-100 kg) and the typical CBG concentration were simulated (n=96) using the semi-mechanistic PK model in NONMEM. No random-effects were considered for the simulations to firstly explore the typical behaviour (i.e. deterministic simulations, section 2.1.6). The simulated C_{max} and *AUC* were compared to C_{max} and *AUC* extracted from Knutsson *et al.*[53]. from healthy paediatric volunteers (2.2 – 18.5 years) [24]: The C_{max} comparison range, consisting of the 25th-75th percentiles of the C_{max} for the morning peak in children was extracted digitally using WebPlotDigitizer [25]. The *AUC* comparison range (95% confidence interval) was derived as 1/3 of the reported *AUC* over 24 h for children, assuming a recommended three times daily dosing regimen with equal doses.

2.2.5.3 Impact of circadian corticosteroid-binding globulin concentrations on cortisol exposure

Previously, it has previously been hypothesised that the potential circadian rhythm of CBG may have an impact on the clearance and distribution of cortisol and, sequentially, also the exposure of hydrocortisone. If so, this could indicate the need to adjust the dose dependent on when during the day it is administered. To evaluate this further, the semi-mechanistic PK model previously described (section 2.2.3.5) was used to simulate exposure (in terms of C_{max} and *AUC*) in a structured trial setting (scenario 1) and in a clinical use setting (scenario 2).

Scenario 1: Impact of circadian CBG concentrations on HC exposure after single dose administration at different times (structured trial setting)

The simulations were done in a stepwise manner, in which the established circadian CBG model was first used to simulate individual CBG concentration-time profiles over 24 h in a virtual population considering variability between individuals (n=100). A body weight of 70 kg was assumed for all virtual individuals, to exclude impact of changing body weight on cortisol exposure. In the second step, exposure (*AUC*, C_{max}) in the virtual population was simulated (considering random-effects parameters) after administration of single Infacort doses (0.5, 2, 5, 10 and 20 mg) at every hour of the day (= 5 doses · 24 administration times = 120 different scenarios), to assess impact of dosing Infacort at different clock times. The lowest and highest *AUC* ($AUC_{\downarrow}$, $AUC_{\uparrow}$) and C_{max} ($C_{max\downarrow}$, $C_{max\uparrow}$) were identified and compared according to Eq. 2.33 and Eq. 2.34, to derive the % increase from the lowest to highest exposure *(% difference* $AUC_{\uparrow}$ and *% difference* $C_{max\uparrow}$).

$$\%\ difference\ AUC_{\uparrow} = \frac{AUC_{\uparrow} - AUC_{\downarrow}}{AUC_{\downarrow}} \qquad \text{(Eq. 2.33)}$$

$$\%\ difference\ C_{max\uparrow} = \frac{C_{max\uparrow} - C_{max\downarrow}}{C_{max\downarrow}} \qquad \text{(Eq. 2.34)}$$

Scenario 2: Impact of circadian CBG concentrations on HC exposure after a recommended dosing regimen (clinical use setting)

In scenario 2, one population with individual *circadian* profiles of CBG (n=100), and one with individual *constant* CBG profiles (n=100) were first simulated using the established circadian and constant CBG model, respectively. All virtual patients in both populations had the same body weight (70 kg) to only evaluate impact of changing CBG on cortisol exposure. *AUC* from dose to 8 h ($AUC_{0\text{-}8h}$) post-dose and C_{max} were simulated in the population with circadian (AUC_{circ}, $C_{max,circ}$) and constant (AUC_{const}, $C_{max,\ const}$) CBG concentrations using a recommended thrice daily dosing (10 mg at 06:00, 5 mg at 14:00 and 5 mg at 22:00) of 20 mg daily HC dose to adult patients with adrenal insufficiency [63]. The % difference in *AUC* and C_{max} by assuming circadian instead of constant CBG concentrations (*% difference* AUC_{circ} and *% difference* $C_{max,circ}$) was derived according to Eq. 2.35 and Eq. 2.36.

$$\%\ difference\ AUC_{circ} = \frac{AUC_{circ} - AUC_{const}}{AUC_{const}} \qquad \text{(Eq. 2.35)}$$

$$\%\ difference\ C_{max,circ} = \frac{C_{max,circ} - C_{max,const}}{C_{max,const}} \qquad \text{(Eq. 2.36)}$$

Simulations were performed in NONMEM 7.3 and the graphical evaluation and comparisons were done in R for both scenarios.

2.3 Project 2: Pharmacokinetic characterisation of a novel hydrocortisone formulation in paediatric patients with adrenal insufficiency

2.3.1 Objectives

As previously described, there is no available hydrocortisone formulation for paediatric patients below six years of age. The new formulation Infacort was therefore developed. As a part of clinical drug development, the PK of hydrocortisone administered as Infacort was studied in healthy adult volunteers (data for project 1). It is of course also important to study the PK in the target population, which was done for project 2. Project 2 therefore aimed to characterise the PK of hydrocortisone administered as the novel formulation Infacort in paediatric patients with adrenal insufficiency using clinical trial data. The paediatric PK model was informed by the semi-mechanistic PK model from project 1. Since only sparse data was available from this population, different approaches with diminishing impact of the adult data were employed to generate reliable paediatric PK parameter estimates.

2.3.2 Study design

Project 2 was based on a phase 3, open label and single centre clinical trial conducted at the Institute of Experimental Paediatric Endocrinology at Charité-Universitätsmedizin Berlin, CVK, Berlin (EudraCT number: 2014-002265-30). The study was performed according to Helsinki declaration [133], ICH Harmonised Tripartite Guideline for Good clinical practice (GCP) [135], and requirements from Research Ethics Committees and the Federal Institute for Drugs and Medical devices in Germany (BfArM). A written informed consent from parents/carer was received before inclusion of the children in the study. Paediatric patients in three different age groups were included; Cohort 1: 2-6 years (young children, n=12 patients), Cohort 2: 28 days-2 years (infants, n=6) and cohort 3: birth-28 days (neonates, n=6). The children in cohort 1 were studied first, followed by cohort 2 and lastly cohort 3 with safety interim analyses between every cohort.

One dose of individualised Infacort, corresponding to the individual standard morning dose (1-4 mg) was administered in the morning upon arrival to the clinic. Dosing was done after at least 2 h fasting, and patients were not allowed to eat before 60 min post-dose (30 min for children below 1 year). The Infacort capsule was opened and the granules were administered with a spoon onto the tongue of the child and washed down with fluid (milk, juice, water). An intravenous cannula was inserted prior to Infacort administration to enable easier blood sampling. All patients underwent plasma

sampling prior to dose, 1 and 4 h post-dose. Three additional samples were retrieved in cohort 1 according to Table 2.1**.**, in which every individual was randomised into one of the four groups (n=3). Total cortisol concentrations were quantified at all these times. In addition, CBG and albumin concentrations were quantified in the pre-dose sample in all patients.

Table 2.1 Additional sampling times for patients in cohort 1.

Group	Sampling time points (time sampling window, min post dose)						
	30 min (25-35)	45 min (40-50)	90 min (80-100)	120 min (110-130)	150 min (140-160)	180 min (170-190)	t_{min} (300-t_{min})
1	X		X				X
2		X		X			X
3			X		X		X
4				X		X	X

2.3.2.1 Bioanalytical quantification of total cortisol and corticosteroid-binding globulin concentrations

The bioanalytical analyses of total cortisol and corticosteroid-binding globulin concentrations were performed at Simbec Research Ltd (Merthyr Tydfil, UK) according to the methods previously described in section 2.1.2.1. and section 2.2.2.3.

2.3.3 Development of a pharmacokinetic model of novel hydrocortisone formulation in paediatric patients with adrenal insufficiency

Since only sparse data was available in project 2, different approaches were assessed to use the knowledge from the semi-mechanistic PK model based on rich data in project 1 in the healthy adults. Initially the predictive performance of the adult semi-mechanistic model (section 3.1.5) was evaluated: This external model evaluation compared simulated cortisol concentration-time profiles (n=1000) using the paediatric covariates (dose, body weight and CBG concentration) with the observed paediatric cortisol concentrations. The evaluation indicated the need to re-evaluate the baseline model for the paediatric data, which was undertaken in the first step. The ODE solver of ADVAN 13 (LSODA), which is useful for both stiff and non-stiff equations, was used throughout model development. The PK analysis was performed using log-transformed data and SAEM with interaction followed by IMP. The fraction of concentrations below LLOQ post-dose was low (5.6%). Hence no models to consider the concentrations below LLOQ values were deemed necessary.

2.3.3.1 Baseline model

According to the external model evaluation of the semi-mechanistic adult PK model, the baseline model needed to be re-assessed. Different baseline models (section 2.1.3) were evaluated to consider the measurable pre-dose concentrations of cortisol: i) The B1 method, which estimates a typical baseline and the associated variability, according to Eq. 2.12. ii) The B2 method, which uses the measured pre-dose concentration to inform the model of the initial concentration (Eq. 2.13) [113].

2.3.3.2 Modelling approaches based on paediatric data exploring use of adult information

Once the baseline model had been assessed, a stepwise strategy sequentially diminishing the influence of adult data was undertaken. The approaches ranged from re-estimating only key parameters (*CL* and V_c) based on paediatric data, via using the adult PK model as a frequentist prior, to a PK model estimated based on only paediatric data. Since the adult studies included data after iv administration, all the previous adult PK parameters in project 1 were absolute rather than relative. To enable comparison with the paediatric relative parameters (no iv data), adult relative PK parameters were also estimated by only using the po data. Since the estimated CL corresponded to unbound CL, total CL and fraction unbound were derived as in project 1 (Eq. 2.31 and Eq. 2.32). Allometric scaling with an exponent of 0.75 and 1 was applied for clearance and disposition parameters, respectively. The following steps were evaluated:

i) Re-estimating *only* key parameters (*CL*, V_c, $baseline_{cort}$) and IIV for the key parameters (ω*CL*, ωV_c, ω$baseline_{cort}$), while fixing the remaining parameters to the adult estimate of the semi-mechanistic adult PK model (section 3.1.5) based on *only* paediatric data.

ii) Re-estimating *all* fixed- and random-effects parameters of the semi-mechanistic adult PK model based on *both* adult and paediatric data.

iii) Re-estimating *all* fixed- and random-effects parameters of the semi-mechanistic adult PK model using the adult PK parameters as prior information for *all* parameters, and based on *only* paediatric data.

The prior approach (i.e. maximum a posteriori estimation, in pharmacometrics also known as "frequentist prior") is commonly used for sparse data, and involves stabilising parameter estimation with additional information from a previous model established on rich data [140]. This approach is more flexible than fixing the parameter estimates (step i), since the estimated parameters are allowed to deviate from prior estimates. In this approach, the parameter estimation using sparse data is performed by minimising not only the OFV of the sparse data

(OFV_S), but also the OFV for prior information (OFV^P). OFV^P approximates the OFV of the original rich data by assuming an appropriate prior distribution of the parameters. If the estimated parameters deviate from the prior parameters during the minimisation process, the OFV^P increases (i.e. worse model fit). This prevents the parameters from changing from the prior value, hence the OFV^P is commonly referred to as a penalty term [140].

The prior distribution combination in the current analysis was the normal-inverseWishart (NWPRI), assuming a normal distribution and inverseWishart distribution of the fixed-effect and random-effects parameters, respectively. The degrees of freedom (df) was needed to define the inverseWishart distribution, and df was highly influencing the impact of the prior. A higher value for df indicated a more informative prior, and sequentially a higher impact of the prior. Degrees of freedom were derived according to Eq. 2.37 from the variance of interindividual variability (ω^2) and the corresponding standard error (se_ω) [112]. The df was assessed for all ω^2, and the lowest was used in the analysis.

$$df = 2\left(\frac{\omega^2}{se_{\omega^2}}\right)^2 + 1 \qquad \text{(Eq. 2.37)}$$

iv) Re-estimating *all* parameters using the adult model as prior information for *non-key* parameters, and based on *only* paediatric data

The adult relative PK parameters were used to inform the parameter estimation using the frequentists prior previously described.

v) Re-estimating all parameters based on *only* paediatric data

i. Reduce paediatric model

If the parameter precision for the full semi-mechanistic PK model was poor, the model was reduced. Since the aim of the analysis was to generate reliable paediatric PK parameter estimates, we aimed to use an approach with as much influence from the paediatric data as possible.

2.3.3.3 Evaluating maturation models for clearance

Maturation models are commonly applied in paediatric PK analyses to consider maturation-dependent differences after considering size-dependent differences using allometric scaling. The individual CL (CL_i) is derived from the product of CL in a standard size adult (CL_{std}), the factors for the size (F_{size}), the maturation processes (F_{mat}) and the organ function (F_{organ}, Eq. 2.38) [141]. The F_{size} is then derived as the fraction between the individual (BW_i) and standard BW (BW_{std}), and using an exponent of 0.75 (Eq. 2.39), as in allometric scaling.

In the current analysis, maturation models were evaluated after selecting the most appropriate approach (step i-v), as described in section 2.3.3.2. F_{mat} was derived according to Eq. 2.40 by using the individual post-menstrual age (PMA), and estimating the gamma factor (γ) and the maturation half-life (TM_{50}).

$$CL_i = CL_{std} \cdot F_{size} \cdot F_{mat} \cdot F_{organ} \quad \text{(Eq. 2.38)}$$

$$F_{size} = \left(\frac{BW_i}{BW_{std}}\right)^{0.75} \quad \text{(Eq. 2.39)}$$

$$F_{mat} = \frac{PMA^{\gamma}}{PMA^{\gamma} + TM_{50}^{\gamma}} \quad \text{(Eq. 2.40)}$$

2.3.3.4 Pharmacostatistical model

IIV was implemented as an exponential model as previously described for the baseline (Eq. 2.4), thereby assuming a log-normal distribution of the individual parameters. Residual variability was modelled as an additive error (Eq. 2.7), corresponding to an exponential error on linear scale.

2.3.4 Model selection and evaluation of the pharmacokinetic model

Model performance was judged by plausibility, GOF plots (section 2.1.5.2), parameter precision (section 2.1.5.3), predictive performance and model stability. If possible, the LRT was used to compare nested models, for which a reduction in the OFV of 6.63 points was considered statistically significant assuming a χ^2-distribution (p-value: 0.01, degrees of freedom: 1). AIC was used for non-nested models. Precision of parameter estimates was assessed by bootstrap and/or log-likelihood profiling in PsN 4.4.0 [124] (section 2.1.5.3). Predictive performance was evaluated by generating VPCs, in which the percentiles (in this study: 5th, 50th and 95th) of observed and simulated data (using the model to be evaluated, n=1000) were compared (section 2.1.5.2).

2.4 Project 3: Pharmacokinetic/pharmacodynamic characterisation of a licensed hydrocortisone formulation in paediatric patients with congenital adrenal hyperplasia

2.4.1 Objectives

The objectives of project 3 were to characterise the PK and PK/PD of hydrocortisone in paediatric patients with adrenal insufficiency using data from a less structured observational study rather than a structured clinical trial. Data from a clinically relevant biomarker (17-OHP) was used for the pharmacodynamic analysis.

2.4.2 Study design

A subset of patients from a study previously described was used for the analysis [77,78]. 42 patients were admitted to the study at the London Centre for Paediatric Endocrinology, and the study was approved by the University College London Hospitals Committee on the Ethics of human research. Patients with classical 21-hydroxylase deficiency in the age of 7-17 years with an adequate HPA axis suppression (ACTH concentrations at 08:00 <71 pg/mL and 17-OHP concentrations <20 nmol/L) were included. Patients with signs of precocious puberty or other signs of endocrine disorder were excluded from the study. Tanner staging and an anthropometric examination was performed one day prior to first drug administration. Only patients with sufficient dosing history were included in our analysis. Patients received standard treatment of fludrocortisone (median (range): 123.8 µg/m^2 (54.0-160.0) [77]) once daily in the morning. The regular two (n=17) or three (n=13) times daily regimen of oral HC (Hydrocortone, Merck Sharp & Dohme Ltd) were given at 08:00, 15:00 and 22:00 or 09:00 and 21: 00 respectively. Two venous catheters, one for sampling and one for administration of drugs in the case of iv HC administration, were inserted at least 12 hours prior to administration start. Intensive blood sampling was performed every 20 min up to 24 h after po administration. In addition, 16 of the patients received a single iv bolus administration of an individualised HC dose (Solu-Cortef, Pharmacia & Upjohn) corresponding to 15 mg/m^2. Blood sampling after iv was performed every 10 min up to 6 h post dose. Total cortisol concentrations were quantified in all samples after iv and po administration, whereas 17-OHP concentrations were quantified in all samples after po administration only.

2.4.2.1 Bioanalytical quantification of total cortisol and 17-hydroxyprogesterone concentrations

Plasma samples were stored at -20 °C prior to analysis. Cortisol concentrations were quantified with solid phase radioimmune assay (Coat-A-Count, DPC, Los Angeles, CA, USA). The lower limit of quantification (LLOQ) was 28 nmol/L for cortisol, which gradually decreased during the study to 21 nmol/L. Between-assay variability (CV) was 6.3% and 4.5% at 138 and 276 nmol, respectively [78].

17-OHP concentrations were quantified with solid phase radioimmune assay (Coat-A-Count, DPC, Los Angeles, CA, USA). LLOQ for 17-OHP was 0.3 nmol/L with a between assay variability (CV) of 11% and 8.5% at 1.06 and 18.5 nmol/L [77].

2.4.3 Development of pharmacokinetic model for hydrocortisone in paediatric patients with congenital adrenal hyperplasia

Initially the developed semi-mechanistic PK model with two disposition compartments developed on adult data from project 1 was evaluated. Using the full semi-mechanistic PK model resulted in poor precision of V_c and Q. This model was, therefore, judged as too complex for this data. Simplifying the absorption model, removing the plasma protein binding or reducing the number of disposition compartments all resulted in poor precision and/or implausible parameter estimates. The reduced semi-mechanistic model (from project 2) was therefore applied, which also resulted in implausible parameter estimates. This could be due to the different formulations, different dose ranges, different age ranges, different assays used for cortisol concentration quantification, and/or different study setting in the two paediatric studies. CBG concentrations were not measured in project 3. Based on this, the model from project 2 was used as the starting point when evaluating the PK of hydrocortisone in project 3 in different steps that will hereafter be described. The ODE solver of ADVAN 13 (LSODA), useful for stiff and and non-stiff equations, was used when estimating the PK model. The PK analysis was performed using log-transformed data and FOCEI.

2.4.3.1 Baseline model for cortisol

To consider the measurable cortisol concentrations prior to administration of HC, different baseline models (section 2.1.3) were evaluated: i) The B1 method estimates a typical baseline and the associated variability, according to Eq. 2.12. ii) The B2 method uses the measured pre-dose concentration to inform the model (Eq. 2.13). The B1 method is seen as the “gold standard” method, since it is independent of the data. This method is therefore superior to the B2 method if the model should be used for simulations [113]. On the other hand one may consider sampling pre-dose concentrations from the empirical distribution, if using the B2 to perform simulations. Since the

cortisol concentrations in several individuals stabilised to a relatively constant baseline similar to pre-dose concentrations after the elimination phase, a constant underlying baseline was also evaluated.

2.4.3.2 Pharmacokinetic model

One-, two- and three-compartmental disposition models with linear elimination were evaluated. The absorption process was described with first-, zero-order absorption, sequential zero- followed by first-order absorption, saturable absorption or first-order absorption with lagtime. The differential equations for a one-compartmental disposition model with first-order absorption are exemplified in Eq. 2.41 and Eq. 2.42, in which the amount in the depot compartment (A_{depot}) was absorbed into the central compartment with a first-order absorption rate contant (k_a). The elimination rate constant for amount in the central compartment (A_c) was given by the ratio of clearance (CL) to volume of distribution (V_c). Since it is known that the plasma protein binding of cortisol may be saturated in the physiological range, a plasma protein binding model was included allowing for only the unbound amount to be eliminated and distributed, similar to the approach used in project 1 (Eq. 2.30 and Eq. 2.28). Covariates, such as pubertal status, age and dosing occasion, were evaluated if strong relation between individual parameters and respective covariate was identified.

$$\frac{dA_{depot}}{dt} = -k_a \cdot A_{depot} \qquad \text{(Eq. 2.41)}$$

$$\frac{dA_c}{dt} = -\frac{CL}{V_c} \cdot A_c - k_a \cdot A_{depot} \qquad \text{(Eq. 2.42)}$$

2.4.3.3 Approaches to handle concentrations below lower limit of quantification

The overall percentage of concentrations below LLOQ after po and iv administration was 7.7% and 0%, respectively. The fraction of values concentrations below LLOQ at the last time in the dosing interval after po administration was however high, and slightly higher in the group receiving two times daily dosing (BID) compared to thrice daily dosing (TID) regimen (BID, morning: 70.6%, evening: 100%; TID, morning: 23.1%, afternoon: 46.2%, evening: 63.6%). Since the fraction of concentrations below LLOQ after po administration exceeded 10% at certain times, this implied the need to evaluate approaches to handle the concentrations below LLOQ. The concentrations below LLOQ were censored (M1) during model development, whereas the use of a likelihood-based approach to model the concentrations below LLOQ (M3) was also considered for the final model [115]. This method has been described more in detail in section 2.1.4.

2.4.3.4 Impact of inaccurate dose- or sampling times

During the exploratory graphical analysis it became obvious that there were discrepancies between the planned and actual dose- and sampling times. As seen in Figure 7.1 (Appendix), these cortisol concentrations were increasing fast prior to the planned dose (vertical lines in the example before 2nd and 3rd dose). These inaccuracies may have a large impact on residual variability and parameter estimates, especially for absorption parameters and volume of distribution. The current model was developed using the confirmed dosing times, and a sensitivity analysis was performed for the final model to evaluate impact of different approaches to consider the inaccurate times. The following approaches were applied:

- Keeping the confirmed dosing regimen only
- Adjusting the dose to the sampling time just before the increase in cortisol concentrations, which was identified graphically by the analyst.
- Adjusting all doses to an earlier time (e.g. 3 h), and fixing the lagtime to the same value (in this case 3 h). By allowing for variability of the lagtime, the most appropriate dose time should be chosen by the software rather than by the analyst.
- Applying a separate RUV for implausible observations.

2.4.3.5 Pharmacostatistical model

IIV was implemented as an exponential model (Eq. 2.4), thereby assuming a lognormal distribution of the individual parameters. Use of IOV to account for differences in k_a, CL and V_c between different dosing occasions (i.e. morning, afternoon and evening dosing) was also assessed (section 2.1.1.2, Eq. 2.6), since differences in absorption was observed in the previous analysis with the current data [78]. Residual variability was modelled as an additive error (Eq. 2.7) on log-transformed data, corresponding to an exponential error on linear scale. Since data from two routes of administration were used in the study, use of different RUV for the different routes of administration was assessed. As previously described in section 2.4.3.4, a different RUV was evaluated for times with suspected inaccurate dose- or sampling times.

2.4.4 Development of a pharmacokinetic/pharmacodynamic model for hydrocortisone in paediatric patients with congenital adrenal hyperplasia

The PK/PD model was established using fixed empirical Bayes estimates from the developed PK model described in section 2.4.3 and 3.3.4. The PK/PD model included the biomarker 17-OHP, which is a cortisol precursor commonly elevated in paediatric patients with CAH (Section 1.3.2). Model

development included consideration of different submodels, such as a baseline model for 17-OHP, selection of a model for delayed concentration-effect, circadian functions for synthesis of 17-OHP and use of mixture models, which will be outlined in the following sections. The ODE solver of ADVAN 13 was used when estimating the PK/PD model using log-transformed data and FOCEI.

2.4.4.1 Baseline model for 17-hydroxyprogesterone

Baseline models are commonly used in PD models to account for measurable concentrations at study start. Two different baseline models (section 2.1.3) were considered for 17-OHP; estimating one typical baseline (*Baseline*$_{17\text{-}OHP}$) and the associated variability (B1 model, Eq. 2.12) or using the measured pre-dose concentrations of 17-OHP to inform the model, while considering measurement error corresponding to the residual variability (B2 model, Eq. 2.13). The use of constant baseline models was also evaluated.

2.4.4.2 Effect models to account for the delayed effect

As described in section 1.3.1, cortisol mediates a negative feedback on the HPA axis, thereby inhibiting the synthesis of 17-OHP and other steroids. The negative feedback is not instantaneous, why a delay in the inhibition of 17-OHP in relation to the increase in cortisol concentrations was expected. A clockwise hysteresis was also observed when plotting 17-OHP concentrations versus cortisol concentrations (Figure 2.4), confirming the delayed inhibition of the 17-OHP concentrations in relation to increase in cortisol concentrations. This is expected for compounds activating endogenous negative feedback mechanisms [142],

Different approaches could be applied to consider the delay/endogenous negative feedback, such as indirect response models with either stimulation of the first-order elimination rate constant of 17-OHP (k_{out}) or with inhibition of the zero-order synthesis rate of 17-OHP (k_{in}). Since it was mechanistically known that cortisol mediates a negative feedback on the synthesis of 17-OHP, the use of an indirect response model with inhibition of k_{in} rather than stimulation of k_{out} was chosen. The change in 17-OHP over time was thus described by Eq. 2.43., in which cortisol is mediating an inhibitory effect (I) on k_{in}, and 17-OHP was eliminated with the first-order rate constant k_{out}. k_{in} was parameterised as the product of k_{out} and the estimated 17-OHP baseline (*Baseline*$_{17\text{-}OHP,}$ Eq. 2.44).

$$\frac{d17\text{-}OHP}{dt} = k_{in} \cdot I - k_{out} \cdot 17\text{-}OHP \qquad \text{(Eq. 2.43)}$$

$$k_{in} = k_{out} \cdot 17\text{-}OHP_{baseline} \qquad \text{(Eq. 2.44)}$$

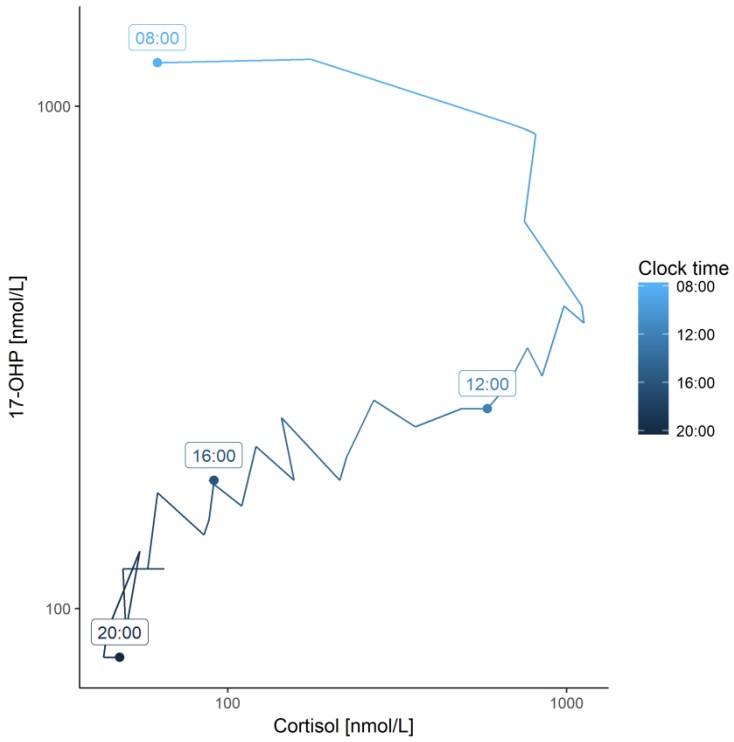

Figure 2.4 17-hydroxyprogesterone (17-OHP) versus cortisol concentrations for one dosing interval of hydrocortisone in one patient.

The inhibitory effect model described the relationship between cortisol and 17-OHP after considering the delay. Different inhibitory effect models such as the linear model, I_{max} and sigmoidal I_{max} models were assessed. The linear slope model derived the inhibitory effect, *I*, by estimating the linear concentration-effect parameter (*slope*, Eq. 2.45). In the nonlinear I_{max} model (Eq. 2.46), the maximum inhibitory effect (I_{max}) and cortisol concentration at 50% of the I_{max} (IC_{50}) were estimated. The sigmoidal I_{max} model (Eq. 2.47) resembled the I_{max} model, but included the additional gamma factor (γ). γ shapes the effect relationship: A high or a low γ indicates a steep or flat concentration-effect relationship, respectively.

$$I = 1 - slope \cdot cortisol \quad \text{(Eq. 2.45)}$$

$$I = 1 - \frac{I_{max} \cdot cortisol}{IC_{50} + cortisol} \quad \text{(Eq. 2.46)}$$

$$I = 1 - \frac{I_{max} \cdot cortisol^{\gamma}}{IC_{50}{}^{\gamma} + cortisol^{\gamma}} \quad \text{(Eq. 2.47)}$$

2.4.4.3 Circadian 17-hydroxyprogesterone synthesis

Since a systematic underprediction was observed for the steep morning 17-OHP increase, addition of a circadian rhythm on k_{in} was evaluated. By using a cosinor analysis, which is commonly applied to consider periodicity [143], addition of different numbers of cosine functions (1-3) with different periodicity (24, 12 and 8 h) were evaluated. The derivation of the two cosine functions for functions with periodicity of 24 h ($CIRC_{24}$) and 12 h ($CIRC_{12}$) is exemplified in Eq. 2.48 and Eq. 2.49, in which the amplitude (amp_{24}, amp_{12}) as well as the time shift ($shift_{24}$, $shift_{12}$) were estimated. The cosine functions were added to k_{in} proportionally according to Eq. 2.50 to derive the circadian k_{in} ($k_{in,circ}$). The full ordinary differential equation for 17-OHP including $k_{in,circ}$ and the I_{max} effect model is exemplified in Eq. 2.51. In addition to time-dependent rebound effects, also concentration-dependent rebound effects using an indirect-response model with a pool compartment were assessed [144].

$$CIRC_{24}(t) = amp_{24} \cdot \cos\left(\frac{2 \cdot \pi \cdot (t - shift_{24})}{24}\right) \quad \text{(Eq. 2.48)}$$

$$CIRC_{12}(t) = amp_{12} \cdot \cos\left(\frac{2 \cdot \pi \cdot (t - shift_{12})}{12}\right) \quad \text{(Eq. 2.49)}$$

$$k_{in,circ}(t) = k_{in} \cdot (1 + CIRC_{24} + CIRC_{12}) \quad \text{(Eq. 2.50)}$$

$$\frac{d17\text{-}OHP}{dt} = k_{in,circ} \cdot \left(1 - \frac{I_{max} \cdot cortisol}{IC_{50} + cortisol}\right) - k_{out} \cdot 17\text{-}OHP \quad \text{(Eq. 2.51)}$$

2.4.4.4 Mixture model to consider different baselines for 17-hydroxyprogesterone concentrations

Since a high variability and potential bimodality in the baseline concentrations of 17-OHP was observed, a mixture model for the baseline estimate was assessed. Mixture models allow for estimating different typical parameter estimates for different subpopulations and assign individuals to the subpopulation with the highest individual probability. With NLME, the number of subpopulations are selected and the proportions of the respective subpopulations are estimated [145]. In the present analysis, use of two subpopulations was evaluated to allow for estimation of two different typical $Baseline_{17\text{-}OHP}$.

2.4.5 Model evaluation of pharmacokinetic and pharmacokinetic/pharmacodynamic model

Model selection and evaluation of intermediate models were based on plausibility, reduction in OFV (section 2.1.5.1), parameter precision (section 2.1.5.3), model stability and goodness of fit plots (2.1.5.2). In addition, VPCs (n=1000, 2.1.5.2) were performed to discriminate between models based on predictive performance during model development, and to evaluate key models in the final steps

of model development. Bootstrap (n=1000, 2.1.5.3) were performed to generate confidence intervals for parameter precision.

To support the use of the circadian synthesis of 17-OHP in the PK/PD model, the physiological soundness of the circadian synthesis of 17-OHP was evaluated. Predicted 17-OHP concentrations in absence of hydrocortisone treatment were compared with observed 17-OHP concentrations in non-treated CAH patients digitalised from Bacon *et al.* and Frisch *et al.* using WebPlotDigitizer [58,59,139]. Since the 17-OHP baseline is highly variable and had a large impact on the predicted 17-OHP concentrations, baseline values consisting of the typical baseline from the established PK/PD model (section 3.3.5) and the median value from the literature data (633 nmol/L) were assessed.

2.4.6 Evaluating dosing regimens of hydrocortisone in paediatric patients with congenital adrenal hyperplasia

A simulation-based analysis was performed to evaluate performance of different dosing regimens in the typical pre-pubertal (BW: 37.0 kg, BSA: 1.18 m^2) and pubertal (BW: 62.2 kg, 1.67 m^2) patient from the present study. Dosing regimens were chosen according to the recommended treatment of 10-15 mg/m^2/day to patients with CAH (prepubertal: 12-18 mg/day, pubertal: 17-25 mg/day) [39]. The selected daily doses were in the low (12 mg) or high (18 mg) recommended range for prepubertal. Since similar results were expected in the pubertal patients, a daily dose in the middle range was selected for this population (20 mg).

The simulation scenario comprised a structured comparison between administration of four (QID) and three times daily dosing regimen administered at fixed times (QID= 06:00, 12:00, 18:00, 24:00; TID= 07:00, 14:00, 21:00). The amount administered was either same/similar during all occasions or higher in the morning and the evening (Table 2.2). The higher morning dose was evaluated to potentially mimic the circadian cortisol concentrations. In addition, the higher evening dose was evaluated to ensure higher C_{min} concentrations the morning after.

Table 2.2 Design of structured simulation scenarios

	Prepubertal	Pubertal
Median BW [kg]	37	62.2
Median BSA [m2]	1.18	1.67
Recommended daily dose [mg]	12-18 mg (11.8-17.7 mg)	17-25 mg (16.7-25.05 mg)
QID, same low doses *	(3, 3, 3, 3) Tot: 12 mg	(5, 5, 5, 5) Tot: 20 mg
QID, different low doses*	(4, 2, 2, 4) Tot: 12 mg	(6, 4, 4, 6) Tot: 20 mg
TID, same low doses*	(4, 4, 4) Tot: 12 mg	(7, 6.5, 6.5) Tot: 20 mg
TID, different low doses*	(5, 2, 5) Tot: 12 mg	(7.5, 5, 7.5) Tot: 20 mg
QID, same high doses	(4.5, 4.5, 4.5, 4.5) Tot: 18 mg	
QID, different high doses	(6, 3, 3, 6) Tot: 18 mg	
TID, same high doses	(6, 6, 6) Tot: 18 mg	
TID, different high doses	(7, 4, 7) Tot: 18 mg	

Body weight (BW), body surface area (BSA), four times daily dosing (QID), three times daily dosing (TID), total daily dose (Tot).*Corresponds to daily dose in the medium range for pubertal patients.

There were no cortisol concentration targets reported in the literature for CAH, to enable comparison of performance between different dosing regimens. For this purpose, cortisol concentration-time data from healthy paediatric volunteers (n=28) sampled every 20 min were used to derive fixed concentration targets to evaluate the different dosing regimens [146]. Since the median physiological cortisol concentrations were never below 50 or above 500 nmol/L, the efficacious and safe cortisol concentration interval was set from 50 to 500 nmol/L. The 17-OHP concentration target for efficacy was set to the previously proposed target range (12-36 nmol/L [61]). The individual fraction of time within the targets over 24 h were derived (fraction of time with cortisol concentrations between 50 to 500 nmol/L ($\%T_{cort}$ 50-500), and fraction of time with 17-OHP concentrations between 12 to 36 nmol/L ($\%T_{17\text{-}OHP}$ 12-36)). In addition, the simulated concentration-time profiles were thereafter graphically compared with the physiological data, to see how well the proposed dosing regimens could mimic the circadian concentrations of cortisol qualitatively.

3 Results

3.1 Project 1: Pharmacokinetic characterisation of a novel hydrocortisone formulation in healthy adults

3.1.1 Population characteristics

16 healthy volunteers, evaluated over 4 study periods, were included in study 1 (Figure 2.2). Data from one and three study periods for two volunteers (6.25% of all observations) were excluded, due to insufficient suppression of the HPA axis. All 14 healthy volunteers in study 2 completed the study and presented no signs of insufficient suppression of the HPA axis.

The median BW and HT were similar and representative for healthy volunteers in both studies, whereas the median age was slightly lower in study 2 (28.5 years) compared to study 1 (43.5 years). The ranges were however overlapping, and no influence in PK parameters between studies were therefore expected (Table 3.1). A relatively high correlation (Pearson correlation coefficient>0.7) was observed between BW and HT, as well as HT and CBG (Figure 3.1).

Table 3.1 Covariates (median (range)) for all healthy volunteers (Total population, n=30), and separately for study 1 (n=16) and 2 (n=14), respectively.

Covariates	Units	Total population	Study 1	Study 2
Body weight	[kg]	81.8 (63.6-102.7)	81.6 (64.7-96.0)	82.9 (63.6-102.7)
Body height	[m]	1.79 (1.64-1.96)	1.77 (1.64-1.95)	1.83 (1.68-1.96)
Age	[years]	31.5 (21.0-60.0)	43.5 (21.0-59.0)	28.5 (22.0-60.0)

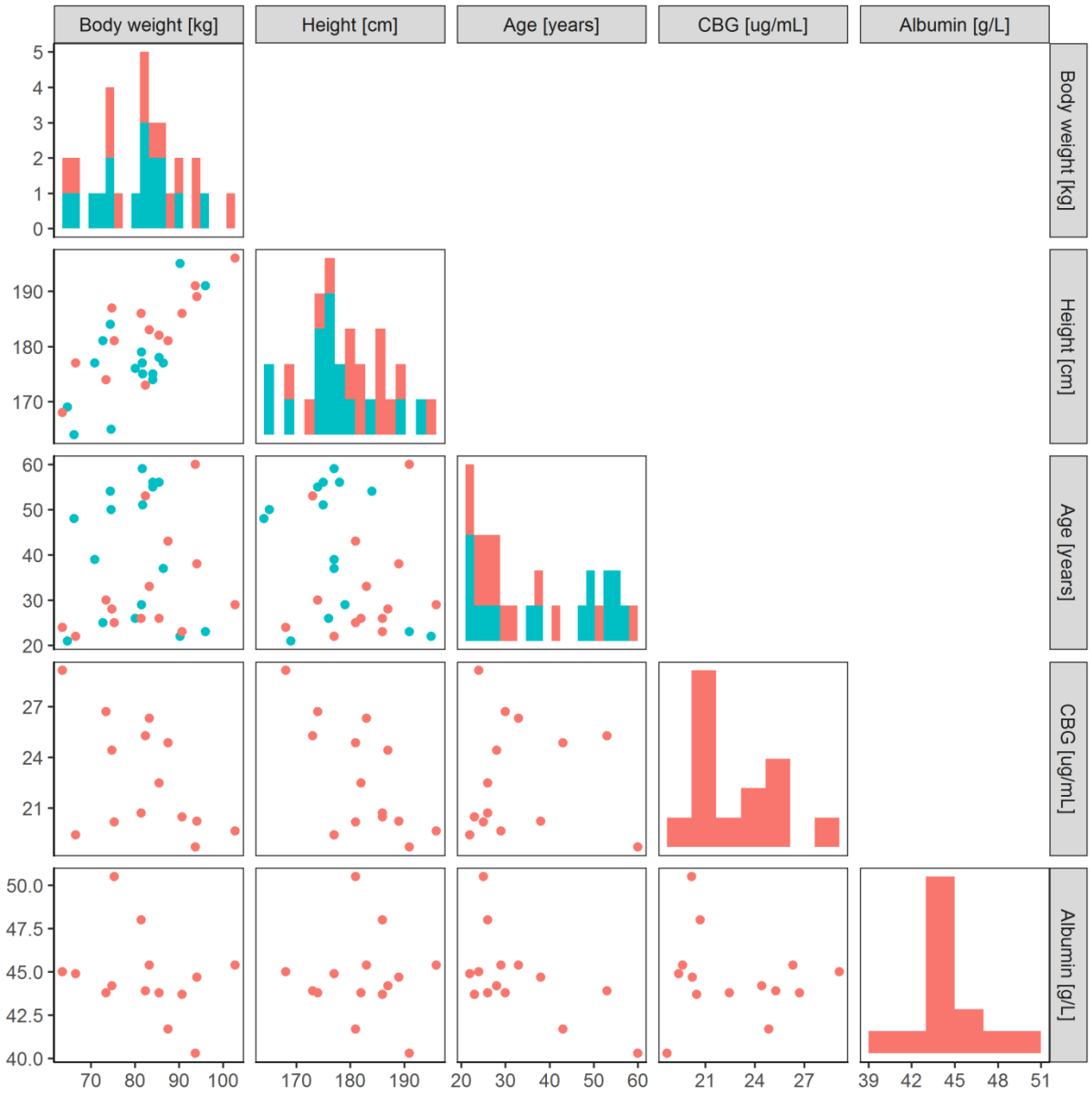

Figure 3.1 Correlation between covariates (lower triangle) and histogram of covariate distribution (diagonal elements, y-axis corresponding to the number of patients (0-5)) with the turquoise and pink colours corresponding to covariates in study 1 and study 2, respectively.

3.1.2 Graphical evaluation of pharmacokinetic data

3.1.2.1 Binding data

C_{tot} and C_u were used to assess the binding kinetics of cortisol. A total number of 121 C_{tot} and C_u were measured, of which 59 C_u (48.7%) were below LLOQ. The majority of the unbound concentrations below LLOQ (95%) were measured pre-dose or post-dose in the presence of only DEX. One C_{tot} was considered as an extreme outlier (>12-fold lower than other C_{tot}) and was therefore omitted from the analysis. The model and plots were therefore generated using the remaining 61 C_{tot} and corresponding C_u.

As seen in Figure 3.2, the increase in C_{tot} was proportional to C_u at low concentrations (C_u<20 nmol/L). At higher concentrations, however, the increase in C_{tot} was less than proportional to C_u, indicating saturation of the specific plasma protein binding.

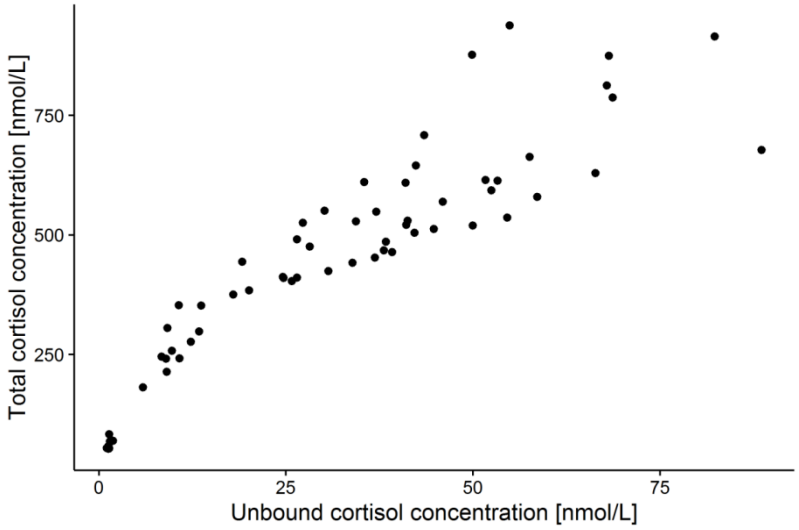

Figure 3.2 Total cortisol concentrations versus unbound cortisol concentrations. Reprinted by permission from Springer Nature Terms and Conditions for RightsLink Permissions Springer Customer Service Centre GmbH: Springer, Clinical Pharmacokinetics [137] © 2018.

3.1.2.2 Corticosteroid-binding globulin data

The CBG concentrations were measured in the five study periods in study 2, according to Figure 2.2. Although a high variability was detected, the 895 CBG concentrations from 14 individuals measured between 07:00-19:00 after administration of DEX were approximately constant (Median (range)): 22.1 µg/mL (13.7-32.4) (Figure 3.3, left). The lower panel, showing the % change in CBG

concentrations from baseline, also indicated that CBG was approximately constant during this time interval. No differences in the range or pattern of CBG were seen between periods when individuals received DEX in absence or presence of hydrocortisone. None of the measured CBG concentrations were below LLOQ.

A circadian rhythm of CBG was, however, apparent when observing the 350 CBG concentrations from 14 individuals measured during 24 h in absence of DEX (Figure 3.3, right). The maximum CBG concentrations ($C_{max,CBG}$, median (range)) were 24.3 µg/mL (20.0-29.5), representing a 32.0% difference between the lowest and the highest $C_{max,CBG}$. $C_{max,CBG}$ was observed at (median (interquartile range)): 18:00 (18:00-19:00) and the CBG concentrations decreased until reaching the minimum CBG concentrations ($C_{min,CBG}$) at 03:30 (03:00-08:45). $C_{min,CBG}$ was 20.4 µg/mL (15.9-23.5), with a difference between the highest and lowest $C_{min,CBG}$ comparable to $C_{max,CBG}$ (32.2%). The relative change in CBG concentrations during 24 h ($C_{max,CBG}/C_{min,CBG}$) was 23.0% (16.4%-38.8%), indicating that the variability within an individual is approximately equal to the variability between individuals.

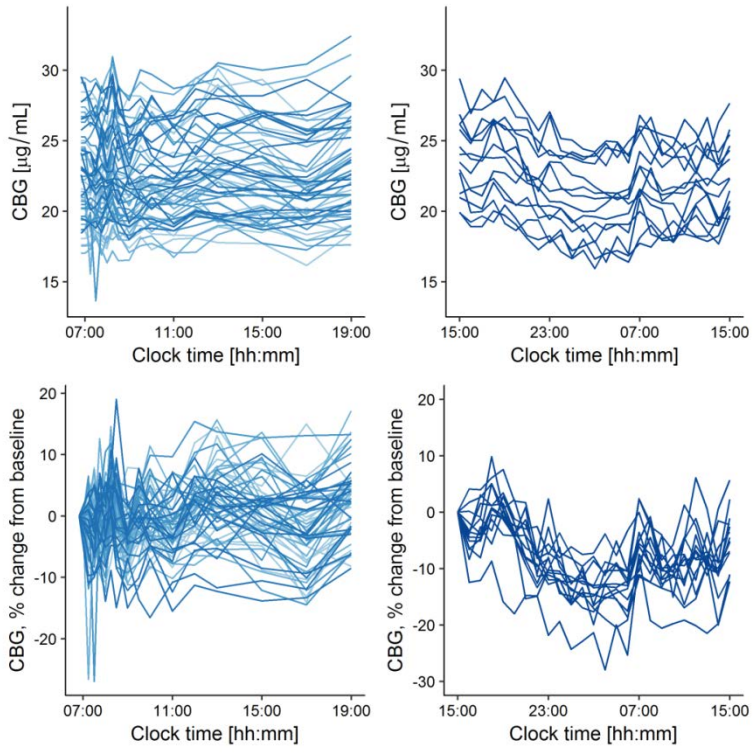

Figure 3.3 Corticosteroid-binding globulin (CBG) concentration-time profiles (upper panel) and change in CBG concentrations from baseline over time (lower panel), during daytime after administration of dexamethasone (left) and during 24 h in absence of dexamethasone (right). Adapted by permission from Springer Nature Terms and Conditions for RightsLink Permissions Springer Customer Service Centre GmbH: Springer, Clinical Pharmacokinetics [137] © 2018.

3.1.2.3 Cortisol concentrations in absence of hydrocortisone

Similarly to CBG, the cortisol concentrations in absence and presence of DEX were evaluated in study 2. As expected, a circadian rhythm of cortisol was observed in absence of DEX (Figure 3.4, left). The C_{max} (median (range): 453 nmol/L (339-610)) and C_{min} (32.0 nmol/L (20.1-74.4)) were observed approximately at (median (interquartile range)) 00:00 (23:00-03:00) and 07:00 (06:00-09:00), respectively. Administration of DEX to inhibit the HPA axis, resulted in a diminished circadian rhythm and lower approximately constant cortisol concentrations ((median (range)): 16.8 nmol/L (9.04-26.4), Figure 3.4, right). Small peaks were observed initially for few volunteers, potentially due to low endogenous cortisol production despite the suppression with DEX.

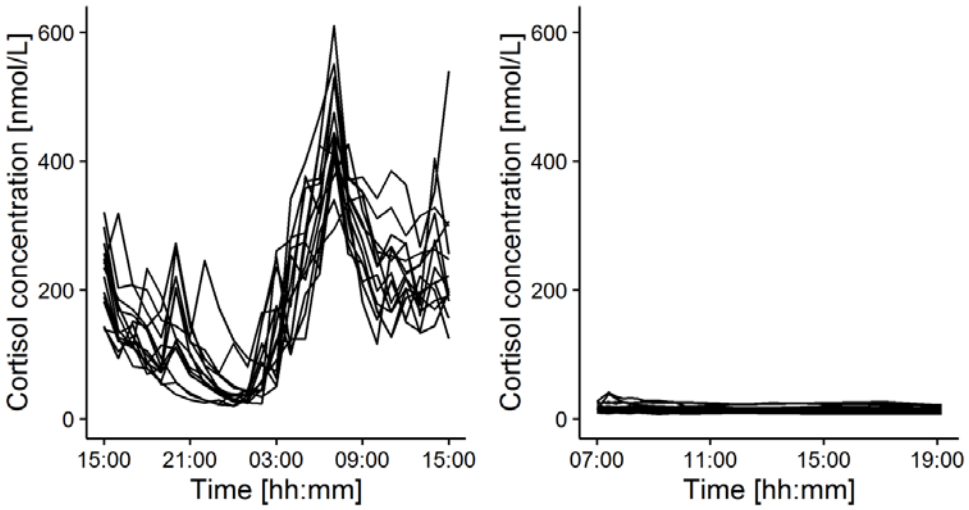

Figure 3.4 Cortisol concentration-time profiles in absence (left) and in presence of dexamethasone (right).

3.1.2.4 Pharmacokinetic data

Overall, 1789 total cortisol concentrations from 30 individuals were available from both studies. Concentrations from participants not sufficiently suppressed (n=84, 4.69%) were excluded, and hence 1705 total cortisol concentrations were used for the analysis. Hydrocortisone displayed a bi-phasic decline after iv and po administration as seen in the semi-logarithmic concentration-time profile (Figure 3.5). The bi-phasic decline was, however, more pronounced for the lower doses. A large variability was observed in the data, especially after iv administration; differences in the highest concentration after iv between volunteers was almost 3-fold (range: 966-2800 nmol/L), whereas differences in C_{max} were 1.5-2.6 fold after po administration. All concentration-time profiles after iv and po administration were approaching and stabilising at approximately 10-20 nmol/L (Figure 3.5, left), which is approximately the same concentration range observed after treatment with DEX only

(Figure 3.4). The highest dose-normalised maximum concentration (C_{max}/D) was observed for the lowest dose (Figure 3.5, right, 0.5 mg: purple lines), whereas the lowest C_{max}/D was observed for the highest dose (Figure 3.5, right, 20 mg, red and light blue lines), as seen in Figure 3.5. The median time of C_{max} (t_{max}) was also slightly delayed for the higher doses (10 and 20 mg: 0.75 h) compared to the lower doses (0.5, 2 and 5 mg: 0.5 h), but the range in t_{max} was similar for 2-20 mg.

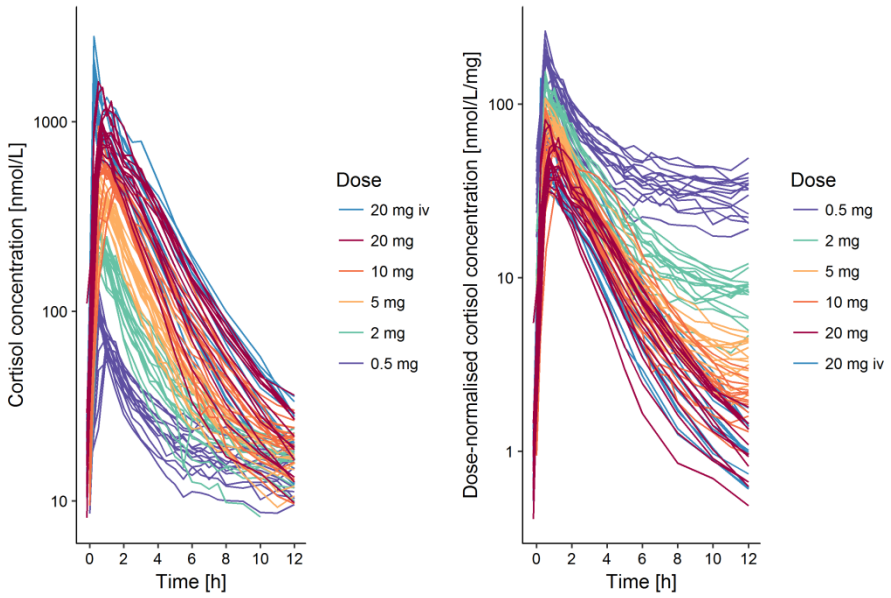

Figure 3.5 Absolute total cortisol concentration-time profiles (left) and dose-normalised cortisol concentration-time profiles (right) after oral administration of Infacort 0.5 mg (n=15), 2 mg (n=16), 5 mg (n=15), 10 mg (n=14) and 20 mg (n=14) and intravenous administration of hydrocortisone succinate (n=14). Reprinted by permission from Springer Nature Terms and Conditions for RightsLink Permissions Springer Customer Service Centre GmbH: Springer, Clinical Pharmacokinetics [137] © 2018.

3.1.3 Plasma protein binding model

3.1.3.1 Base model development

61 C_{tot} and the respective C_u from 11 volunteers in study 2 were used to establish the plasma protein binding model of cortisol to plasma proteins. Linear, nonlinear and combined linear and nonlinear plasma protein binding models were evaluated sequentially, and key models are summarised in Table 7.1 (Appendix). A model including nonlinear and linear binding described the plasma protein binding most adequately as judged by reduction in OFV (Table 7.1, Appendix), parameter precision, GOF plots (Figure 7.2, Appendix) and performance of VPCs (Figure 3.6, upper left). IIV was evaluated

on B_{max}, K_d and *NS*, and addition of IIV on B_{max} resulted in a larger drop in OFV (ΔOFV: -48.2) compared to NS and K_d and was hence retained in the model. The data did not support estimation of more than one IIV, based on the poor precision in variance parameters and small reduction in OFV. Parameter estimates for the base model are summarised in Table 3.2.

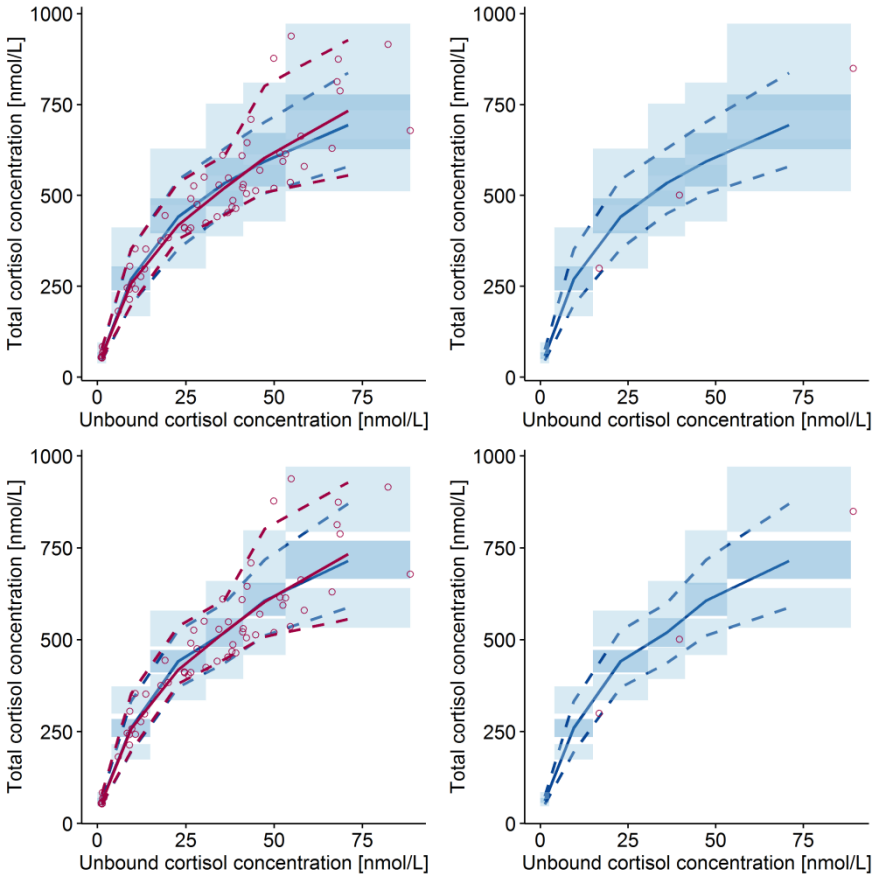

Figure 3.6 Visual predictive check (n=1000) for the plasma protein binding model including both a nonlinear and linear component (upper panel), including a substituted B_{max} (lower panel), and external model evaluation using observed concentrations from Lentjes et al. [90] (right). Lines: the 5th, 50th and 95th percentiles of observed (red) and simulated (blue) data; corresponding areas: 95% confidence interval around the simulated percentiles; circles: observations. Adapted by permission from Springer Nature Terms and Conditions for RightsLink Permissions Springer Customer Service Centre GmbH: Springer, Clinical Pharmacokinetics [137] © 2018.

Table 3.2 Population parameter estimates for base model and final model substituting maximum binding capacity (B_{max}) to the product of CBG and number of binding sites (N_{CBG}).

		Base model		Final model	
Parameter	Unit	Estimate	95% CI	Estimate	95% CI
Fixed-effects					
B_{max}	[nmol/L]	495	420, 579	-	-
K_d	[nmol/L]	11.8	9.50, 14.5	9.71	8.89, 10.4
NS	[-]	3.12	1.89, 4.70	4.15	3.72, 4.70
N_{CBG}	[-]	-	-	1 FIX	-
Interindividual variability					
ωB_{max}	[CV%]	16.0	8.07, 20.7	-	-
ωN_{CBG}	[CV%]	-	-	7.00	1.56, 10.4
Residual variability					
σexp^*	[CV%]	7.21	4.80, 8.63	7.25	5.13, 8.56

95% confidence interval (95% CI), maximum binding capacity (B_{max}), equilibrium dissociation constant (K_d), linear nonspecific binding component (NS), number of CBG binding sites for cortisol (N_{CBG}), variance of exponential residual variability (σexp). *estimated as additive on log scale. Adapted by permission from Springer Nature Terms and Conditions for RightsLink Permissions Springer Customer Service Centre GmbH: Springer, Clinical Pharmacokinetics [137] © 2018.

3.1.3.2 Covariate model development

The ability of covariates to explain parts of the IIV of B_{max} was assessed only if relations were observed between the covariates and individual estimates of B_{max}. Based on this, CBG, BW and HT were evaluated as potential covariates on B_{max}. CBG was seen as the most promising covariate, since B_{max} potentially corresponds to the binding capacity of cortisol to CBG. Subsituting B_{max} by the measured CBG and N_{CBG} (number of binding sites on CBG) according to Eq. 2.20, explained more than half of the variability in B_{max} (IIV_B_{max}: 17%, IIV_N_{CBG}: 7%) and decreased OFV (ΔOFV: -16.2). The estimated N_{CBG} was close to 1 (1.09), and fixing it to 1 (assuming that 1 molecule of cortisol binds to 1 molecule of CBG) did not worsen model performance, and was therefore kept. Substituting CBG in B_{max} resulted in a similar OFV (Table 7.1, Appendix) and GOF plots as using CBG as a linear covariate on B_{max}, and the former was selected given model plausibility and the lower number of estimated fixed-effect parameters. Addition of other covariates (BW, HT) was not supported by the data.

The plasma protein binding model including linear and nonlinear binding substituting CBG in B_{max} described the data well, as judged by GOF plots (Figure 7.3, Appendix) and VPCs (Figure 3.6, lower panels).

3.1.3.3 Final plasma protein binding model

The final model included linear and nonlinear binding and substitution of B_{max}. The pharmacostatistical model was re-evaluated after inclusion of the covariate and IIV for N_{CBG} was kept in the model. Estimation of other IIVs was not supported by the data. Parameter estimates for the final model are summarised in Table 3.2 (right column). The derived B_{max} (median (range): 414 nmol/L (312-632)) agreed well with observation indicating saturable plasma protein binding at total cortisol concentrations above 500 nmol/L. The equilibrium dissociation constant (K_d) was 9.71 nmol/L and the non-specific binding component (*NS*) was 4.15. The GOF plots indicated a good description of the data, as judged by observations versus individual predictions being close to the line of identity, and randomly scattered CWRES (Figure 7.3). In addition, the GOF plots were slightly improved compared to model without CBG as a covariate (Figure 7.2). The predictive performance of the model was also good, as seen in the internal (VPC) and external model evaluation (Figure 3.6, lower panels). The latter was performed using binding data from Lentjes and Romijn [3], for which the data could be well predicted. A small overprediction was observed, but the observations were, however, within the 95% confidence interval. The bootstrap method was performed to assess the 95% confidence intervals of the parameter estimates: The typical parameter estimates were all within the 95% confidence interval of the bootstrap, indicating that the parameters were well estimated (Table 3.2, right). The case-deletion diagnostics identified one influential individual, which had an impact on the IIV for N_{CBG}. Removal of this individual resulted in a lower ωN_{CBG} (3.03%CV). Since ωN_{CBG} including this individual was low (7.00%CV), and removal of this individual did not have a major impact on any structural parameters, this individual was kept in the final model.

3.1.4 Corticosteroid-binding globulin models

3.1.4.1 Base model development

Two different CBG models were developed for two different time intervals: i) during daytime (07:00-19:00) and ii) during 24 h (15:00-15:00). The CBG concentrations during the daytime were accurately described by estimating a constant baseline, as seen in the GOF plots (Figure 7.4, Appendix). Addition of one cosine function to consider potential rhythmicity did not decrease the OFV significantly (ΔOFV= -0.19, Table 7.2 in Appendix). Addition of IOV to account for variability between study

periods resulted in a large drop in OFV, but did not have an impact on the parameter estimates. The estimated IOV was also minor (5.6%CV) and was hence excluded from the final model.

Assuming a constant CBG model for the CBG concentrations measured over 24 h resulted in underprediction of CBG concentrations from study start (15:00) to approximately 21:00, followed by overpredictions until approximately 08:00 (Figure 7.5, Appendix). Cosine functions were therefore added to consider the rhythmicity of CBG. A circadian CBG model containing two cosine functions described the CBG sampled over 24 h most accurately, as seen in the GOF plots (Figure 7.6, Appendix). Addition of a third cosine function improved the model prediction even further (ΔOFV: -12.9, Table 7.2 in Appendix), but was rejected due to the poor precision of the amplitude for the 8 h cosine function. The parameter estimates for the constant and circadian CBG models are available in Table 3.3. A relation was found between CBG baseline and HT in the constant CBG model. Using HT as a covariate was however not supported by the data.

Table 3.3 Parameter estimates for corticosteroid-binding globulin (CBG) models developed on CBG concentrations observed during the day (left) and during 24 h (right).

	CBG model during the day		CBG model during 24 h	
Parameter	**Estimate**	**95% CI**	**Estimate**	**95% CI**
Fixed-effects				
Baseline [µg/mL]	22.4	20.8, 24.1	21.8	20.3, 23.3
amp_{24} [%]			5.53	4.80, 6.20
$shift_{24}$ [h]			1.77	1.33, 2.27
amp_{12} [%]			2.87	2.21, 3.42
$shift_{12}$ [h]			15.7	15.4, 16.0
Interindividual variability				
ωBaseline [CV%]	12.9	8.43, 15.5	11.9	7.76, 14.0
Residual variability				
σprop [CV%]	6.44	5.86, 7.01	3.90	3.46, 4.32

95% confidence interval (95% CI), amplitude for 24 h cosine function (amp_{24}), time shift for 24 h cosine function ($shift_{24}$), amplitude for 12 h cosine function (amp_{12}), time shift for 12 h cosine function ($shift_{12}$), variance or proportional residual variability (σprop). Adapted by permission from Springer Nature Terms and Conditions for RightsLink Permissions Springer Customer Service Centre GmbH: Springer, Clinical Pharmacokinetics [137] © 2018.

3.1.4.2 Final corticosteroid-binding globulin models

The final models were the same as the baseline models previously described. The constant CBG baseline was estimated to 22.4 µg/mL and the associated IIV was relatively low (12.9%, Table 3.3). The observations versus individual predictions were close to line of identity and CWRES were scattered evenly as seen in the GOF plots (Figure 7.4, Appendix). The constant CBG model could appropriately predict the CBG concentrations during daytime, as shown in the VPC (Figure 3.7, left).

In the circadian CBG model, the estimated baseline for CBG was 21.8 µg/mL and the associated interindividual variability was minor (11.9%), both in well agreement with those from the constant CBG model. The amplitude for the 24 and 12 h cosine function were relatively small (24 h: 5.53%, 12 h: 2.87%). The predicted C_{maxCBG} (18:00) and C_{minCBG} (02:00) were in well agreement with the observed values (section 3.1.2.2). As seen in the VPC (Figure 3.7, right), comparing the percentiles of the observed data (red) and the simulated data using the final CBG model (blue), the model could well predict the observed CBG concentrations. The 95% confidence intervals generated from the bootstrap included the final parameter estimates from the respective model, indicating that the model can potentially be generalised to other populations (Table 3.3). The case deletion diagnostics did not identify any influential individuals.

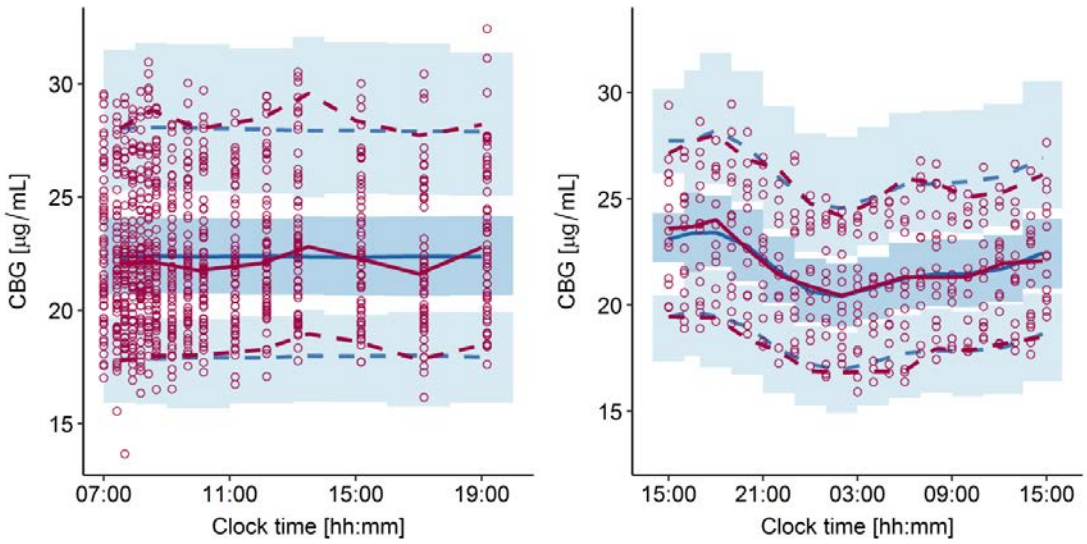

Figure 3.7 Visual predictive check (n=1000) for the constant corticosteroid-binding globulin (CBG) model during daytime (07:00-19:00, left) and circadian CBG model during 24 h (15:00-15:00, right). Lines: the 5th, 50th and 95th percentiles of observed (red) and simulated (blue) data; corresponding areas: 95% confidence interval around the simulated percentiles; circles: observations. Adapted by permission from Springer Nature Terms and Conditions for RightsLink Permissions Springer Customer Service Centre GmbH: Springer, Clinical Pharmacokinetics [137] © 2018.

3.1.5 Semi-mechanistic pharmacokinetic model

3.1.5.1 Base model development

The disposition model was developed on 1705 total cortisol concentrations from 30 patients from study 1 and 2. A two-compartmental disposition model was superior to a one- or three-compartmental model, as seen in Table 7.3 (Appendix). Since the aim was to extrapolate the model to paediatric patients, allometric scaling was applied for the base model. This had minor impact on model performance (ΔOFV:-1.3), but was retained to allow for a more appropriate extrapolation.

The absorption process was evaluated as first-order absorption, zero-order absorption, zero-order absorption into the depot compartment followed by first-order absorption or saturable absorption. Zero-order absorption into the depot compartment followed by first-order absorption or saturable absorption resulted in a large reductions in OFV compared to first- or zero-order absorption (Table 7.3, Appendix). Although OFV was lower for the sequential absorption model, the saturable absorption was kept based on predictive performance in the VPC. Inclusion of a saturable absorption, improved the description of the absorption phase across doses, allowing also for a slightly delayed t_{max} for higher doses.

Since cortisol pre-dose concentrations and concentrations 12 h post-dose were similar, a constant underlying cortisol baseline ($Baseline_{cort}$) of approximately 15.5 nmol/L was estimated [113]. This was considered the disease model of the system. The associated variability for the baseline [%CV] was 30%. Estimation of a constant baseline was also supported by the low and approximately constant cortisol concentrations observed after DEX suppression in absence of HC therapy (Figure 3.4, right).

Use of linear PK models not considering the plasma protein binding or dose-dependent bioavailability resulted in underprediction and overprediction of cortisol concentrations in the VPCs for the lower and the higher hydrocortisone doses, respectively (Figure 7.7, Appendix). Addition of the plasma protein binding model, and imputing CBG for study 1 from the constant CBG model (22.4 µg/mL, section 3.1.4) improved model performance especially for the higher concentrations. No further covariate analysis was pursued, since no relation was apparent between the covariates and parameter estimates.

3.1.5.2 Final model

The final model was a two-compartmental disposition model, including a plasma protein binding model to consider the linear and nonlinear plasma protein binding of cortisol (Figure 3.8, Table 3.4). The estimated *CL,* corresponding to the unbound *CL,* was high (131 L/h). The predicted fraction unbound (1.54%-15.1%) was used to derive total CL, which ranged from 1.42 to 26.2 L/h and was increasing with the higher doses (Figure 3.9).

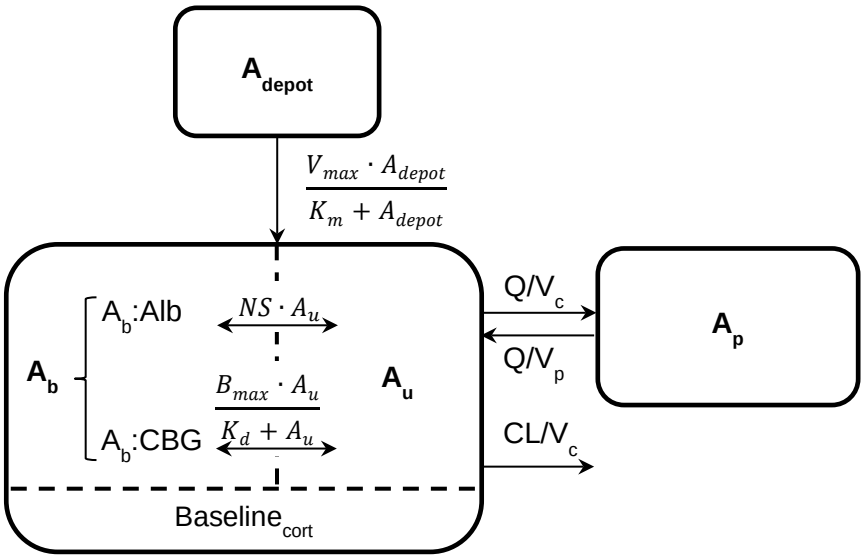

Figure 3.8 Schematic representation of the final semi-mechanistic pharmacokinetic hydrocortisone model considering the endogenous cortisol baseline ($Baseline_{cort}$) after suppression with dexamethasone, and plasma protein binding. Amount in depot compartment (A_{depot}), maximum absorption rate (V_{max}), amount in depot compartment resulting in half of V_{max} (K_m), amount bound (A_b), amount bound to albumin (A_b:Alb), amount bound to corticosteroid-binding globulin (A_b:CBG), unbound amount (A_u), linear non-specific binding, parameter (NS), maximum binding capacity (B_{max}), equilibrium dissociation constant (K_d), intercompartmental clearance (Q), central volume of distribution (V_c), peripheral volume of distribution (V_p), amount in peripheral compartment (A_p), clearance (CL). Vertical and horizontal dashed lines divides the central compartment into A_b, A_u and $Baseline_{cort}$ subcompartments, respectively. Adapted by permission from Springer Nature Terms and Conditions for RightsLink Permissions Springer Customer Service Centre GmbH: Springer, Clinical Pharmacokinetics [137] © 2018.

A saturable absorption was used and the amount at 50% of the maximal absorption rate (K_m) was 2230 nmol, indicating a nonlinear absorption for doses >5 mg. The GOF plots in Figure 7.8 (Appendix) indicated no major model misspecification, despite a slight underprediction for higher concentrations

in the plot displaying CWRES vs population predictions. The model could well predict the observed data, as judged by the VPCs (Figure 3.10). A slight underprediction was however observed at early time points for the 20 mg dose. The data for the doses relevant for neonates/infants and young children below six years (0.5-5 mg) were well predicted, supporting the extrapolation of PK knowledge to this population.

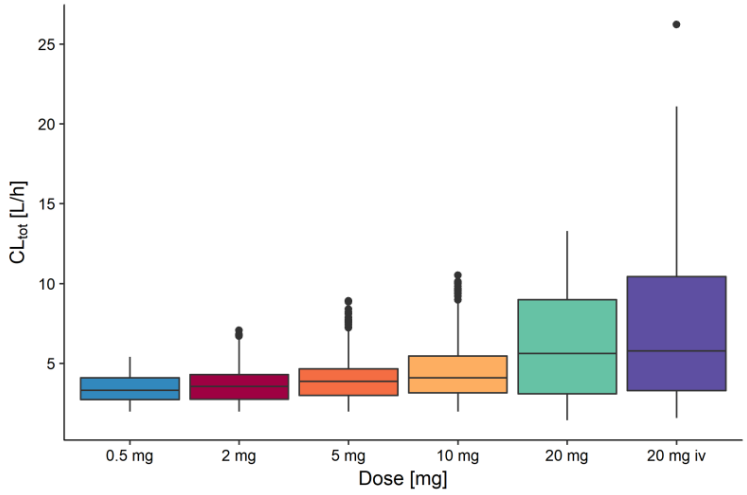

Figure 3.9 Derived total clearance (CL_{tot}) in adults for the different doses. Intravenous administration (iv).

IIV was supported for *CL*, V_c and $Baseline_{cort}$, which were moderate (25.6%-30.8%CV). A positive correlation between *CL* and V_c was identified, and RUV was minor (14.3%CV). The bootstrap method was used to derive the 95% confidence interval for the final parameter estimates, which were all reasonable and including the final parameter estimates, thus supporting identifiability of all model components and model adequacy.

Table 3.4 Population pharmacokinetic parameters and parameter precision for the final semi-mechanistic pharmacokinetic model of hydrocortisone, including fixed parameters for the binding model and constant corticosteroid-binding globulin model

Parameter	Estimate	95% CI
Fixed-effects		
CL [L/h]	131	111, 148
V_c [L]	3.3	2.73, 3.78
Q [L/h]	94.9	75.6, 118
V_p[L]	60	50.1, 69.5
$Baseline_{cort}$ [nmol/L]	15.5	14.0, 17.3
V_{max} [nmol/h]	10100	7620, 12200
K_m [nmol]	2230	1410, 3090
F [-]	0.369	0.302, 0.423
Interindividual variability		
ωCL [CV%]	25.6	13.8, 32.2
$Corr\ (CL,V_c)$	1	1, 1
ωV_c [CV%]	29.7	15.7, 37.8
$\omega Baseline_{cort}$ [CV%]	30.8	21.1, 39.4
Residual variability		
$\sigma exp*$ [CV%]	14.3	12.2, 16.3

95% confidence interval (95 CI), clearance (CL), central volume of distribution (V_c), intercompartmental clearance (Q), peripheral volume of distribution (V_p), endogenous cortisol baseline ($Baseline_{cort}$), maximum absorption rate (V_{max}), amount in depot compartment resulting in half of V_{max} (K_m), scaling factor of amount in depot (F), correlation between CL and V_c (Corr (CL, V_c)). *Estimated as additive error on a logarithmic scale. Adapted by permission from Springer Nature Terms and Conditions for RightsLink Permissions Springer Customer Service Centre GmbH: Springer, Clinical Pharmacokinetics [137] © 2018.

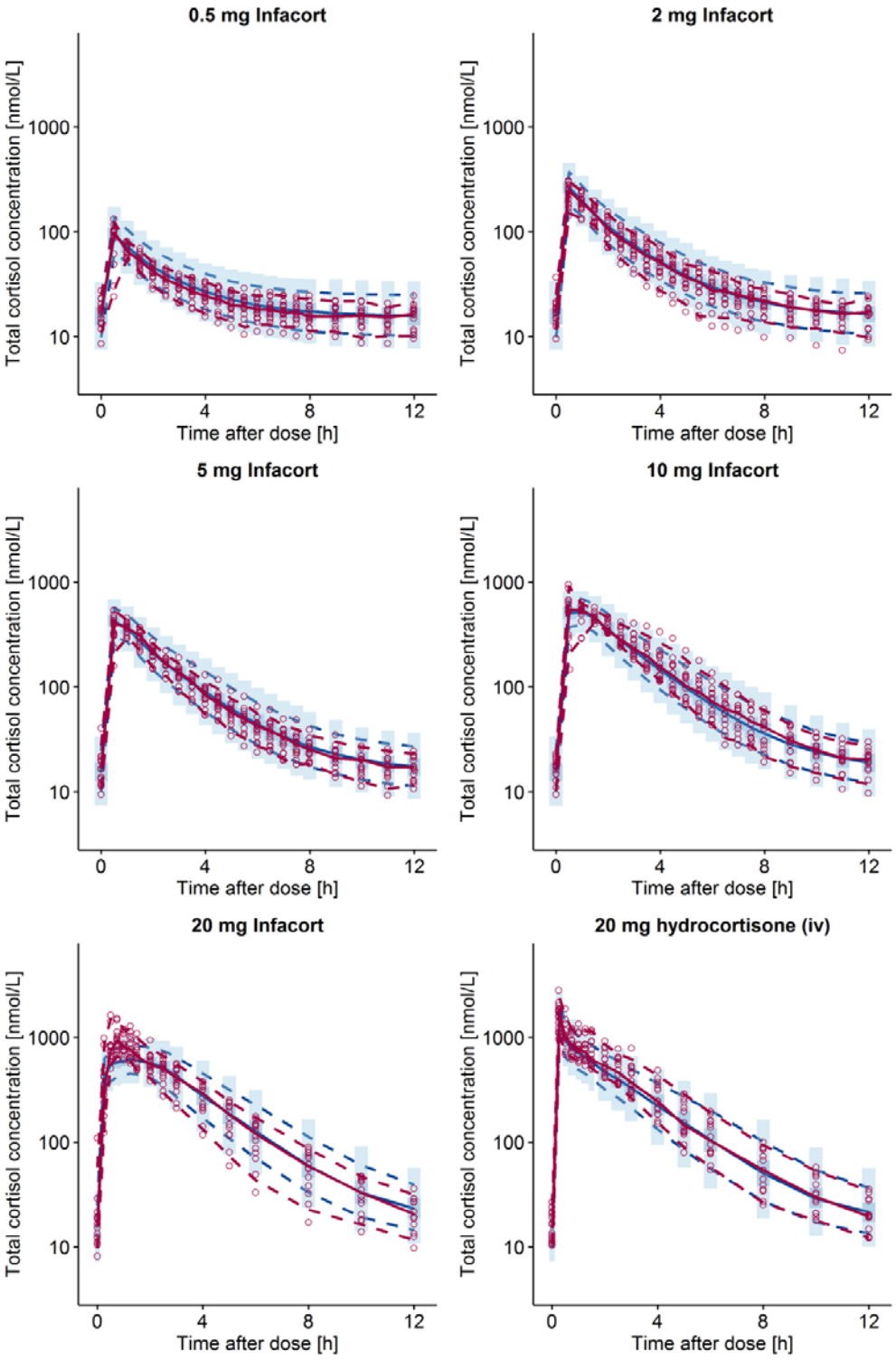

Figure 3.10 Visual predictive check (n=1000) for final semi-mechanistic pharmacokinetic model including saturable absorption and the plasma protein binding model. Lines: the 5th, 50th and 95th percentiles of observed (red) and simulated (blue) data; corresponding areas: 95% confidence interval around the simulated percentiles; circles: observations. Reprinted by permission from Springer Nature Terms and Conditions for RightsLink Permissions Springer Customer Service Centre GmbH: Springer, Clinical Pharmacokinetics [137] © 2018.

3.1.6 Simulation-based analyses

3.1.6.1 Predicted concentrations (unbound, specific binding and non-specific binding) of cortisol

The plasma protein binding model was used to simulate the unbound and bound cortisol concentrations (with specific or non-specific binding) for concentrations including the target C_{max} in children derived from Knutsson *et al*. The dominating specific binding (i.e. binding to CBG, dark blue area) was higher for lower (89%) compared to higher (70%) concentrations (Figure 3.11). The fraction of cortisol bound with non-specific binding (i.e. albumin and erythrocytes, middle blue area) increased from 8.7% at low concentrations to 24% at higher concentrations. In the evaluated C_{tot} range (23.7-492 nmol/L), the fraction of unbound cortisol (light blue area) increased considerably from 2.1 to 6.4% translating to C_u ranging from 0.5 to 31.5 nmol/L.

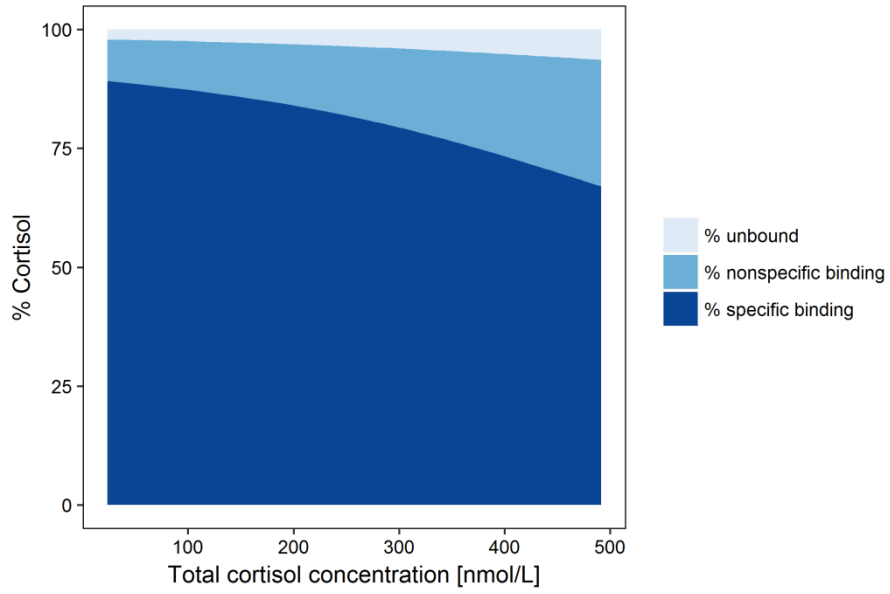

Figure 3.11 Simulated cortisol concentrations (%) as unbound, with nonspecific binding (linear) or specific binding (nonlinear) based on final plasma protein binding model. The total concentration ranges from 22.3 nmol/L (corresponding to C_u of 0.5 nmol/L) to the 75th percentile of observed maximum physiological cortisol concentration (492 nmol/L) observed in Knutsson *et al*. [53]. Reprinted by permission from Springer Nature Terms and Conditions for RightsLink Permissions Springer Customer Service Centre GmbH: Springer, Clinical Pharmacokinetics [137] © 2018.

3.1.6.2 Predicting cortisol exposure in paediatric patients

Simulations were performed to illustrate the impact of the nonlinearities in the semi-mechanistic model on cortisol exposure, and to evaluate the predicted exposure after the administration of different doses to virtual patients with different BW (5-100 kg). As expected, dose-normalised C_{max} and *AUC* were higher and varied more for low compared to high doses (Figure 3.12, top). Both C_{max}

and *AUC* decreased with increasing BW in the virtual population (Figure 3.12, bottom). The exposure varied considerably for a given BW for patients with low BW (<20 kg), and stabilised at adult BW (>55 kg). As paediatric reference ranges, *AUC* and C_{max} from physiological cortisol concentrations in healthy paediatric volunteers were extracted from Knutsson *et al.* Large discrepancies in the dose selected for each BW range was observed for the *AUC* and C_{max} comparison ranges, and C_{max} overall suggested lower doses than the *AUC* range. The largest difference in appropriate dose selection was observed for lower BW of e.g. 20 kg, for which a three- to fourfold difference in doses was observed (C_{max}: 1 mg; *AUC*: 3-4 mg).

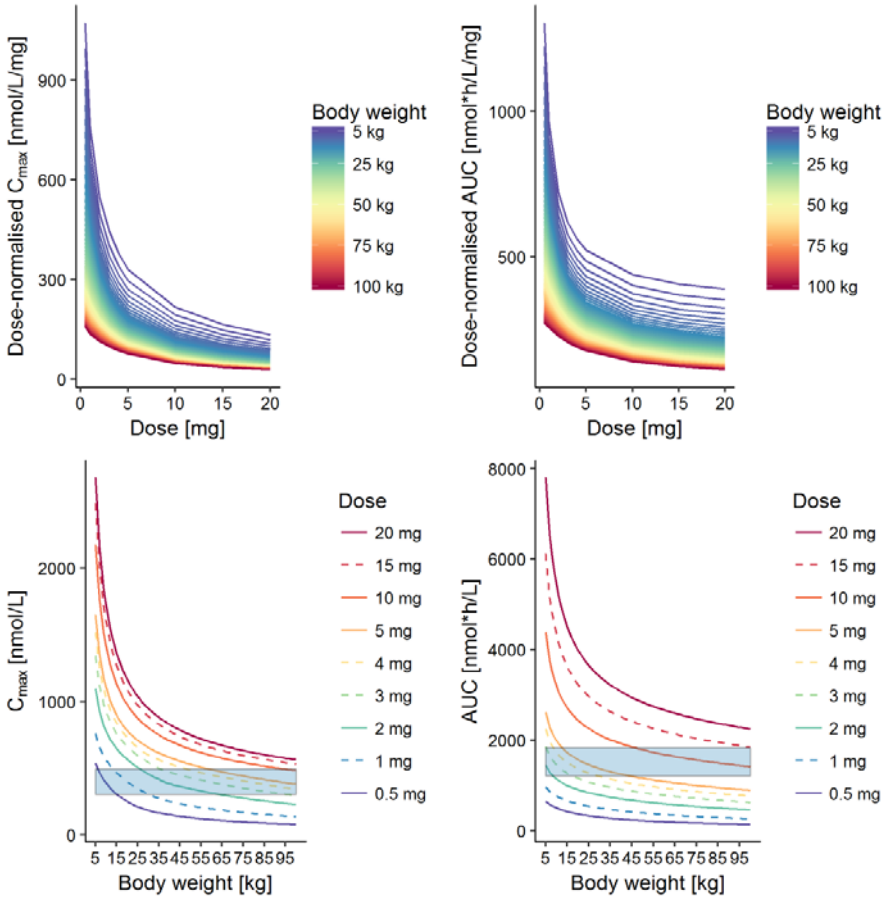

Figure 3.12 Simulated maximum concentration (C_{max}, left) and area under the total cortisol concentration-time curve (AUC, right) for administration of 0.5-20 mg Infacort to a virtual population with body weights ranging from 5-100 kg. The upper panel displays the dose-normalised C_{max} and AUC versus dose for each body weight. The lower panels display the C_{max} and AUC versus body weight, for which solid and dashed lines correspond to the doses included and not included in the study protocol, respectively. The blue area for C_{max} corresponds the 25^{th}-75^{th} percentiles of the peak cortisol concentration in healthy paediatric volunteers in absence of dexamethasone from Knutsson et al. [53]. The blue area for AUC corresponds to a third of the observed AUC over 24 h in healthy paediatric volunteers in absence of dexamethasone from Knutsson et al. Reprinted by permission from Springer Nature Terms and Conditions for RightsLink Permissions Springer Customer Service Centre GmbH: Springer, Clinical Pharmacokinetics [137] © 2018.

3.1.6.3 Impact of circadian CBG on exposure

Scenario 1: Impact of circadian CBG concentrations on HC exposure after single dose administration at different times (structured trial setting)

In scenario 1, the impact of dosing time across 24 h of the day on *AUC* and C_{max} for cortisol was simulated by combining the circadian CBG model (section 3.1.4) with the semi-mechanistic PK model for hydrocortisone (section 3.1.5). Across all doses (0.5-20 mg), the lowest and highest median *AUC* ($AUC_{\uparrow}$, $AUC_{\downarrow}$) and median C_{max} ($C_{max\downarrow}$, $C_{max\uparrow}$) for the different simulated dose levels are summarised in Table 7.4 (Appendix). As seen in Figure 3.13 (upper panels), $AUC_{\downarrow}$ was observed for doses administered between 23:00-01:00, whereas $AUC_{\uparrow}$ was observed for doses administered in the afternoon (15:00-16:00). Time for $C_{max\downarrow}$ (01:00-02:00) and $C_{max\uparrow}$ (17:00-18:00) were slightly delayed compared to time for $AUC_{\downarrow}$ and $AUC_{\uparrow}$. The difference between $AUC_{\uparrow}$ and $AUC_{\downarrow}$ (*% difference* $AUC_{\uparrow}$) was, however, relatively small (9.48%-12.2%), with the largest difference observed for the lower doses. The *% difference* $C_{max\uparrow}$ ranged from 4.20% to 9.01%.

Scenario 2: Impact of circadian CBG concentrations on HC exposure after a recommended dosing regimen (clinical setting)

In scenario 2, the impact of assuming circadian or constant CBG concentrations on HC exposure ($AUC_{0\text{-}8h}$, C_{max}) in the clinical setting was simulated using the semi-mechanistic PK model for hydrocortisone (section 3.1.5). As seen in Figure 3.13 (lower panels), the simulated $AUC_{0\text{-}8h}$ was slightly lower when assuming circadian CBG profiles (green, AUC_{circ}) compared to constant CBG profiles (purple, AUC_{const}) for the doses in the morning (*% difference* AUC_{circ}: -8.29%) and evening (*% difference* AUC_{circ}: -10.4%). *% difference* AUC_{circ} for the afternoon dose was low (-2.79%), indicating no impact of assuming circadian or constant CBG concentrations when dosing in the afternoon. The impact of considering the circadian rhythm of CBG was small for C_{max} for all doses, for which *% difference* $C_{max,circ}$ were ranging from -4.57% to -7.31% (Table 7.4, Appendix).

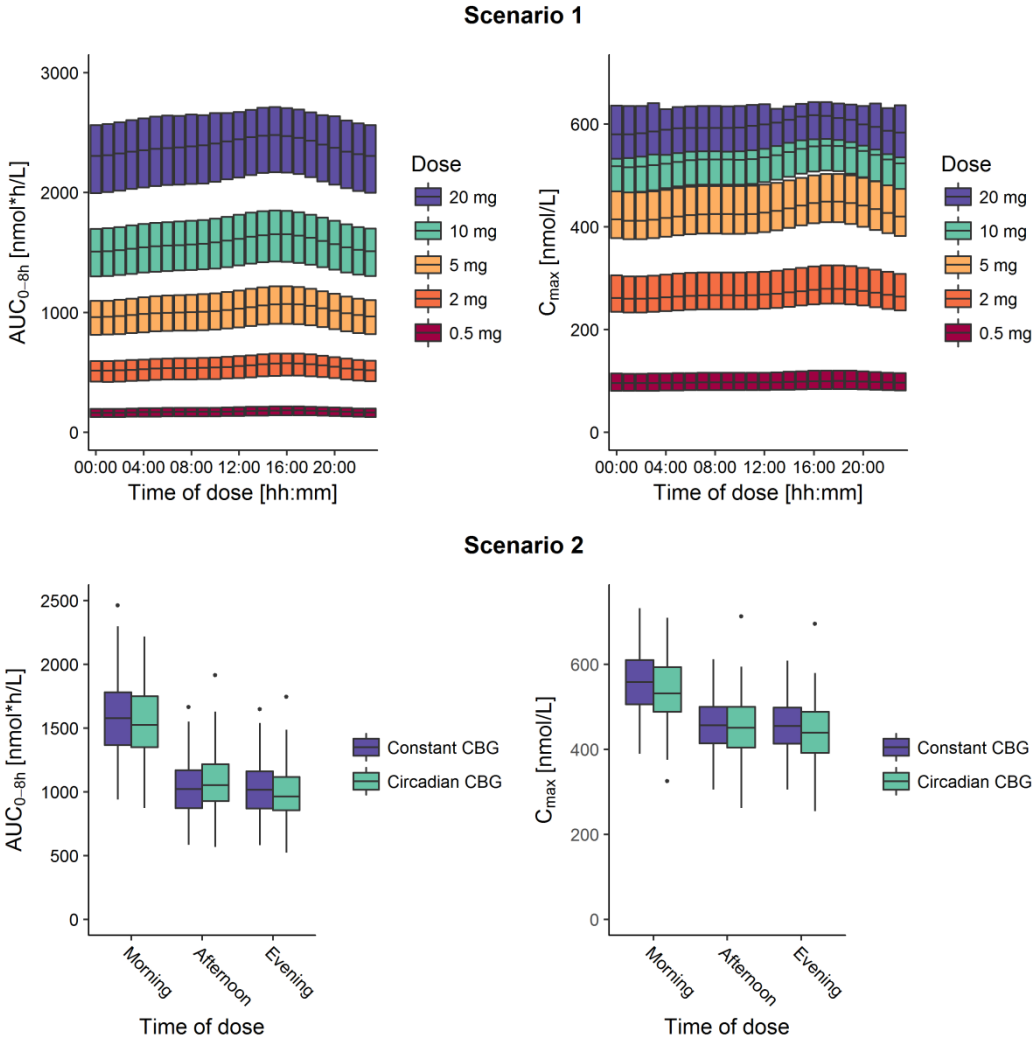

Figure 3.13 Simulation scenario 1 (top): Simulated area under cortisol concentration-time curve (*AUC*) and maximum cortisol concentration (C_{max}) after single oral administration of Infacort every hour during 24 h to 100 individuals with different circadian corticosteroid-binding globulin (CBG) profiles. The box corresponds to the interquartile range.

Scenario 2 (bottom): Simulated AUC from dose to 8 h post-dose ($AUC_{0\text{-}8h}$) and C_{max} after administration of Infacort; 10 mg in the morning (06:00), 5 mg in the afternoon (14:00) and 5 mg in the evening (22:00) for virtual patients with constant (purple, n=100) or circadian (green, n=100) CBG profiles, respectively.

3.2 Project 2: Pharmacokinetic characterisation of a novel hydrocortisone formulation in paediatric patients with adrenal insufficiency

3.2.1 Population characteristics

24 paediatric patients with adrenal insufficiency were included into the study. As expected, the median BW and HT were the highest in cohort 1 (young children) and lowest in cohort 3 (neonates). The ranges for HT were not overlapping, whereas the range for BW was barely overlapping for cohort 1 and 2 (Table 3.5). In addition, the distribution of CBG and albumin concentrations were overlapping between the three different cohorts, indicating no age-dependency for the CBG or albumin concentrations. A very strong correlation (Pearson correlation coefficient >0.9) was observed between BW, HT and age (Figure 3.14).

Table 3.5 Covariates (median (range)) for paediatric patients with adrenal insufficiency (Total population, n=24).

Patient characteristics	Units	Cohort 1 Children (n=12)	Cohort 2 Infants (n=6)	Cohort 3 Neonates (n=6)
Female	[-]	5	2	4
Male	[-]	7	4	2
Body weight	[kg]	16.2 (12.2-21.0)	11.1 (6.70-12.5)	3.65 (2.80-4.90)
Height	[cm]	93.5 (84.0-108)	79.5 (62.0-83.0)	53.5 (49.0-57.0)
Age	[months]	39.9 (24.8-56.9)	16.6 (4.13-22.1)	0.767 (0.533-0.867)
PMA	[months]	48.2 (33.9-64.3)	28.6 (12.7-30.9)	9.87 (9.46-10.1)
CBG concentrations	[µg/mL]	29.0 (23.8-38.7)	27.0 (22.9-29.6)	27.6 (16.8-29.6)
Albumin	[g/L]	43.4 (41.9-48.0)	42.8 (33.4-46.8)	44.6 (41.4-50.9)
Po dose	[mg]	2.5 (2.0-4.0)	2.0 (2.0-2.5)	2.0 (1.0-2.0)

Postmenstrual age (PMA), corticosteroid-binding globulin (CBG), oral (po)

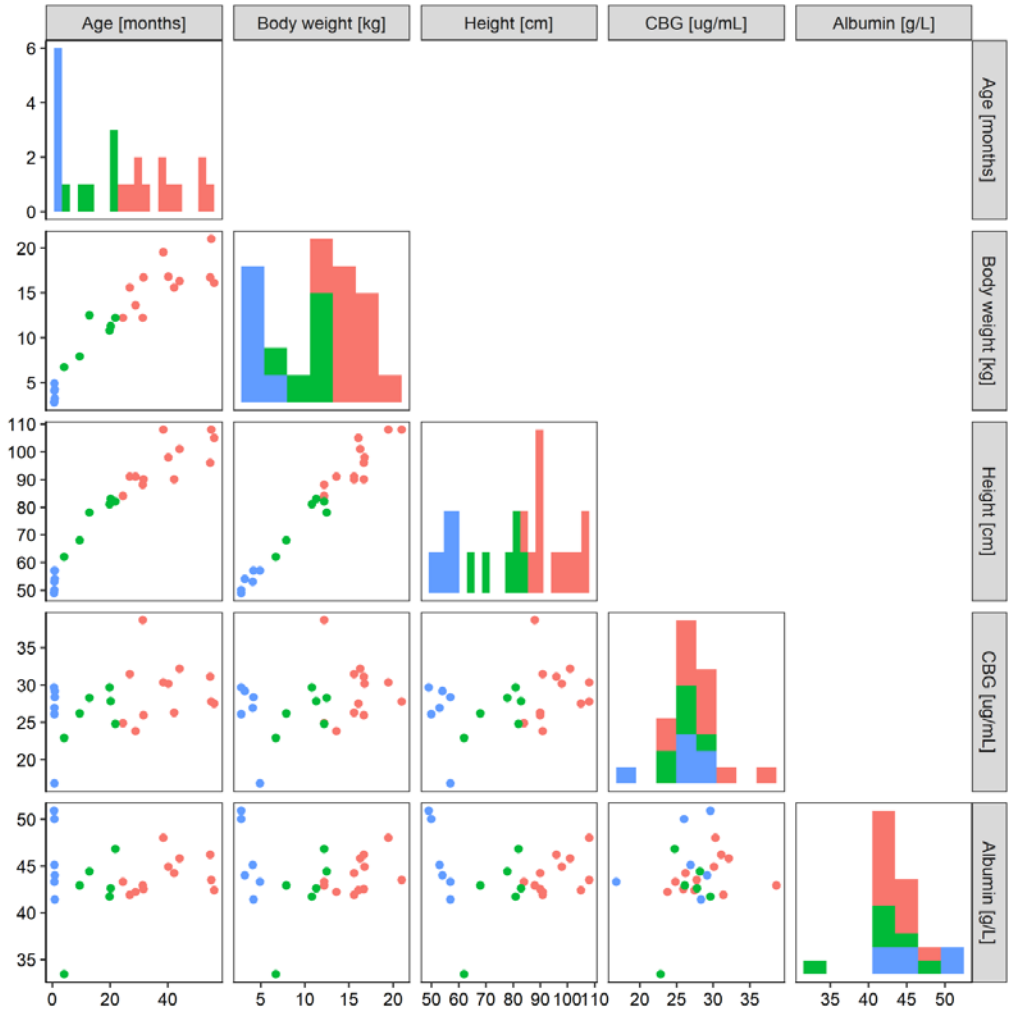

Figure 3.14 Scatterplot of covariates (lower triangle) and histogram of covariate distribution (diagonal elements, y-axis corresponding to the number of patients (0-6)) for neonates (blue), infants (green) and young children (pink). Corticosteroid-binding globulin (CBG).

3.2.2 Graphical evaluation of pharmacokinetic data

A total number of 106 observations were retrieved from the paediatric patients. 2 samples were discarded due to a too small sample volume. 6 post-dose concentrations were below LLOQ (5.6%). 54% of the pre-dose concentrations were below LLOQ, and none of the pre-dose concentrations in the neonates were quantifiable. For the infants and young children, 50% and 25% of the pre-dose concentrations were below LLOQ. The measurable pre-dose concentrations ranged from 19.0 to 105 nmol/L and from 25.2 to 47.6 nmol/L in infants and young children, respectively. In total, 87 total cortisol concentrations were used for model development. The cortisol concentration-time profiles showed a mono-phasic decline (Figure 3.15). Three very high C_{max} were observed in cohort 3 (neonates).

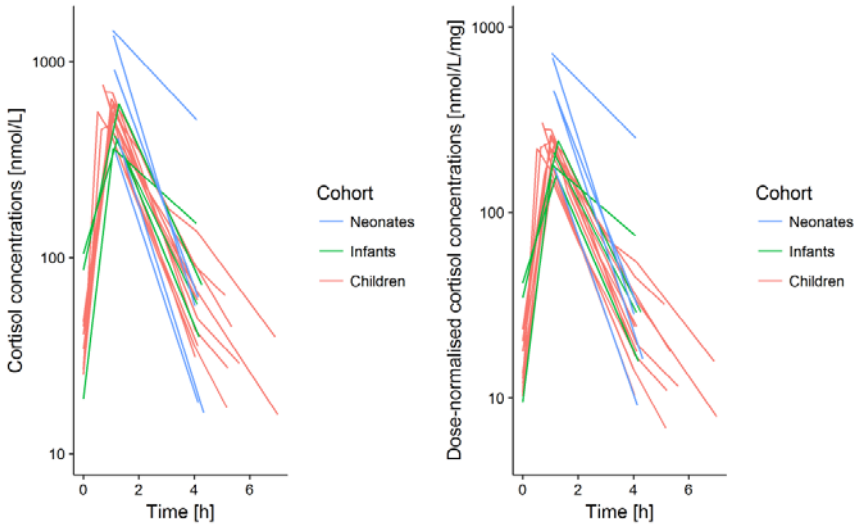

Figure 3.15 Absolute (left) and dose-normalised (right) cortisol concentration-time profiles after single oral administration of Infacort to paediatric patients with adrenal insufficiency.

3.2.3 External model evaluation using adult semi-mechanistic PK model

An external model evaluation was performed to evaluate the predictive performance of the semi-mechanistic adult PK model. By using the covariates (dose, BW, CBG) from the paediatric patients in project 2, the cortisol concentrations were simulated (1000 simulations) and compared to the observed paediatric cortisol concentrations. The model could overall very well predict the observed paediatric data (Figure 3.16). The C_{max} was especially well described, whereas two areas with slight discrepancies were identified: the pre-dose concentrations and concentrations after 4 h.

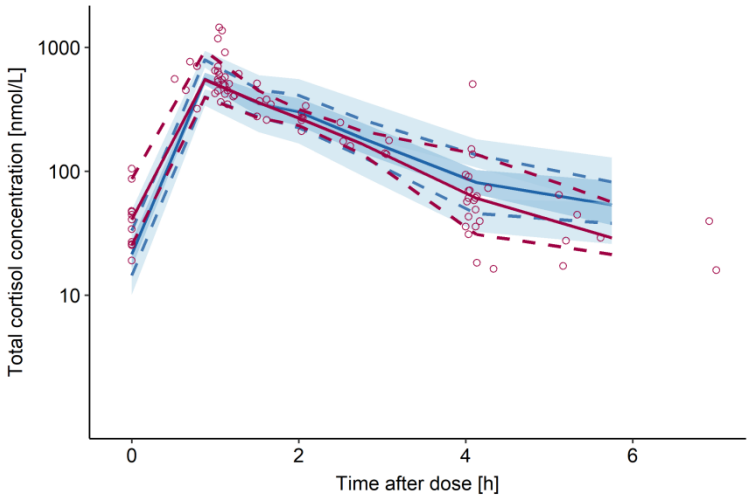

Figure 3.16 External model evaluation of semi-mechanistic adult PK model from project 1. Lines: the 5th, 50th and 95th percentiles of observed paediatric (red) and simulated paediatric (blue) data; corresponding areas: 95% confidence interval around the simulated percentiles; circles: observations

3.2.4 Pharmacokinetic model for hydrocortisone in paediatric patients with adrenal insufficiency

3.2.4.1 Base model development

The overall good predictive performance of the semi-mechanistic PK model gave us confidence that this model was a good starting point for the paediatric analysis and model refinement.

A constant underlying cortisol baseline ($Baseline_{cort}$: 15.5 nmol/L) was estimated in the dexamethasone-suppressed healthy volunteers. The suboptimal description of the pre-dose concentrations for the paediatric data indicated that the baseline needed to be re-evaluated. The first approach in the stepwise assessment (step i: Re-estimating *only* key parameters based on *only* paediatric data) was used when re-assessing the baseline model. Using the constant baseline estimated in adults resulted in trends in CWRES plots (Figure 7.9, Appendix), which were improved when using the *measured* pre-dose concentration to inform the model (Figure 7.10, Appendix). This baseline model was therefore used further during model development.

3.2.4.2 Modelling approaches based on paediatric data exploring use of adult information

Since the aim of the current analysis was to establish reliable paediatric PK parameters, different approaches with diminishing impact of adult data were applied and have been summarised in Table 7.5 and Table 7.6 (Appendix). Estimating key parameters based on only paediatric data (step i) resulted in precise fixed-effects parameters but poor precision in IIV. Re-estimating all parameters based on adult and paediatric data (step ii) generated precise fixed-effects and random-effects parameters, which very similar to the adult PK model (Table 7.5, Appendix). Most probably due to the very low number of paediatric observations (n=87) in comparison to adult observations (n=1705). Use of the frequentist prior approach for all parameters (step iii) resulted in parameters very similar to the adult parameters estimates, except for higher IIV for *CL* and V_c (Table 7.6, Appendix). The precision of the parameter estimates were all acceptable (RSE%<25.1), indicating that this model can appropriately be used for stochastic simulations. Using prior information for all non-key parameters also resulted in similar *CL* and V_c (Table 7.6, Appendix). The precision of the fixed-effects parameters were good, whereas the precision for IIV was poor (95% CI, ωCL: 0, 63.2%CV, ωVc: 0, 56.0%CV). This model should therefore not be used for stochastic simulations.

The model estimating all PK parameters based on only paediatric data was highly sensitive to initial estimates, and was therefore deemed too complex for the sparse data. These sensitive estimates could therefore not be compared to the parameter estimates of other approaches. Since a model based on only paediatric data was the ultimate aim, the model was reduced. Reducing the saturable

absorption to a first-order absorption process and removing the peripheral compartment resulted in a small decrease in OFV (ΔOFV: -4.22), a more stable estimation of the parameters and appropriate precision of the fixed-effects parameters (RSE%<16). The precision for the covariance of *CL* and V_c was however poor (95% CI for correlation: -1, 1). Removing the covariance increased OFV only slightly (ΔOFV: +3.09). The parameter precision of the reduced model was assessed by bootstrap and log-likelihood profiling. The precision for IIV was poor as judged by bootstrap (95% CI, ωCL: 0, 54.0%CV, ωVc: 0, 95.6%CV), probably due to the large variability of the sparse data. The log-likelihood profiling indicated that the parameters were identifiable, as judged by an appropriate 95% confidence interval (95% CI, ωCL: 21.1, 60.7%CV, ωVc: 31.2, 91.5%CV).

To evaluate whether a maturation model should be implemented, the individual CL (empirical Bayes estimates) from the reduced PK model were normalised to a CL corresponding to a BW of 70 kg and graphically visualised with respect to cohort. As seen in Figure 3.17, a slightly lower CL was estimated for neonates, whereas infants tended to have a slightly higher CL than adults. As expected, the CL for young children (2-6 years) and adults were overlapping.

Addition of a sigmoidal maturation function (Eq. 2.40) to describe potential age-dependency was evaluated since slightly lower CL was seen for neonates. Implementing a maturation function decreased OFV (ΔOFV: -12.4) and improved the VPC slightly (Figure 7.11, Appendix). The gamma factor, responsible for shaping the steepness of the maturation function, was very large (17.8) and had a high uncertainty (%, RSE: 143.3). The estimated maturation half-life (TM_{50}) was 0.816 years (PMA: 42.4 weeks). CL was fully matured at PMA of 62.4 weeks, corresponding to a chronological age of 22 weeks (assuming full term pregnancy of 40 weeks). The PMA was an important predictor for CL at PMA less than 1.2 years, whereas BW was an important predictor at PMA more than 1.2 years (Figure 3.18). In addition, both the predicted CL for the allometric scaling (purple) and model including the maturation function (green) were well in agreement with the individual estimates from the respective models. As seen in Figure 3.19, the shift from immature CL to mature CL happens when PMA is approaching $TM_{50.}$ Even though inclusion of the maturation function improved model performance slightly, it was not kept due to the poor precision of the gamma factor.

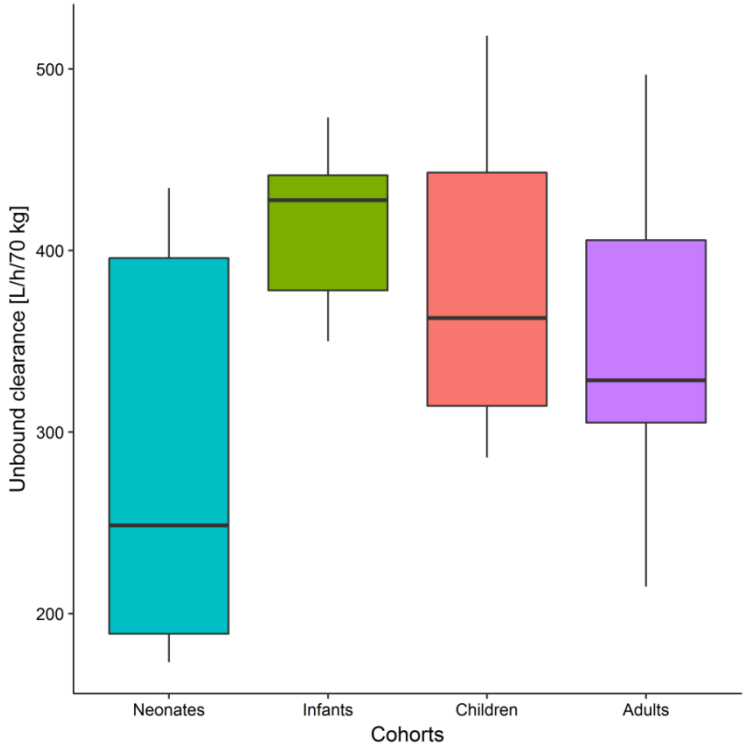

Figure 3.17 Derived individual clearance estimates scaled to a body weight of 70 kg for neonates, infants, children and adults.

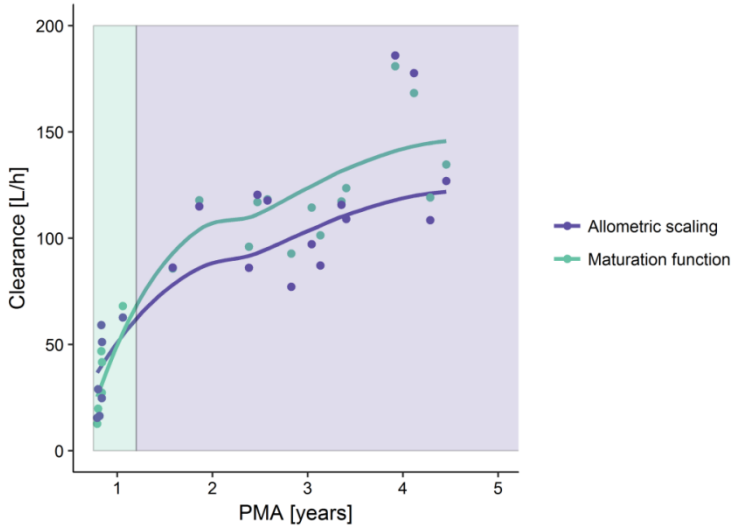

Figure 3.18 Lines correspond to the predicted clearance using maturation function (green) or allometric scaling (pruple). Areas show age range in which the postmenstrual age (PMA, green) or body weight (purple) has most importance in the maturation function. Dots correspond to the individually estimated CL using the maturation function (purple) or allometric scaling (green).

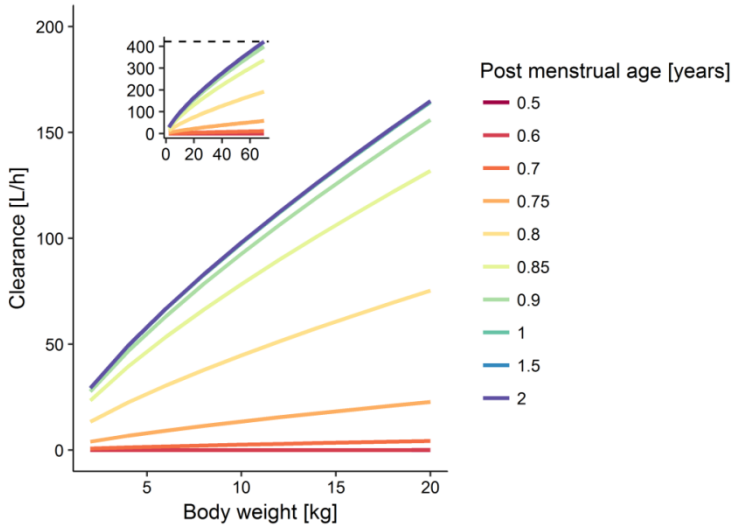

Figure 3.19 Predicted clearance versus body weight for different post menstrual age for reduced paediatric pharmacokinetic model including the maturation function.

3.2.4.3 Final models

In the current analysis a range of approaches were applied to generate reliable paediatric estimates. Hence, different models may be used depending on the aim of the analysis. The reduced (and more empiric) model consisting of a one-compartmental disposition model with first-order absorption (Figure 3.20) predicted the observed data well for the three different cohorts (Figure 3.21, left and Figure 7.12, Appendix). In addition, this model had minor impact of the adult data, except for the plasma protein binding model which was developed on adult data (section 3.1.3). If an empirical model is deemed inappropriate, the semi-mechanistic model using prior information for all parameters (step iii) had an appropriate parameter precision and predictive performance (Figure 3.21, right). This model could therefore be used for stochastic simulations. The parameter estimates were larger for IIV, but very similar to previous adult estimates (Table 7.6, Appendix). Due to the large influence of adult data on these PK parameter estimates, the focus will hereafter be on the reduced paediatric model.

For the reduced paediatric PK model, the V_c was 16.3 L and the IIV for V_c was high (59.0%CV). The k_a was 2.12 h^{-1}, corresponding to an absorption half-life of approximately 20 min. The *CL,* corresponding to the unbound relative *CL* for a patient with body weight of 70 kg, was 353 L/h and the IIV was intermediate (38.2%CV). This translated to an estimated individual unbound CL of (median (range)); cohort 1: 121 L/h (77.2-186), cohort 2: 101 L/h (62.7-121), cohort 3: 26.9 L/h (15.5-59.1).

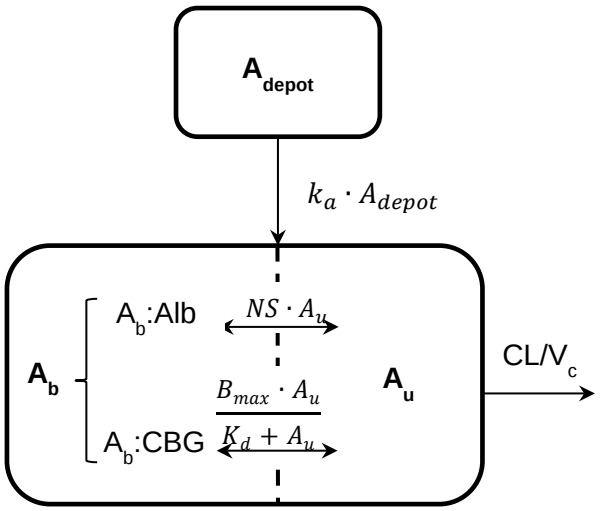

Figure 3.20 Schematic representation of the reduced paediatric pharmacokinetic model. Amount in depot compartment (A_{depot}), amount bound (A_b), amount bound to albumin (A_b:Alb), unbound amount (A_u), amount bound to corticosteroid-binding globulin (A_b:CBG), linear non-specific binding parameter (NS), maximum binding capacity (B_{max}), equilibrium dissociation constant (K_d), central volume of distribution (V_c), clearance (CL). The dashed line divides the central compartment into the A_b and A_u subcompartments, respectively.

The predicted unbound fraction (f_u) was derived using the individual CBG concentrations and the individually predicted concentrations in the central compartment. The predicted f_u was (range): 1.31-7.66% and 1.77-6.52% for cohort 1 (young children)and cohort 2 (infants) and slightly larger for cohort 3 (1.80%-11.3%). f_u and body weight were used to derive the ranges of relative total *CL* for a 70 kg person, which were similar between the different cohorts; cohort 1: 4.72-32.1 L/h, cohort 2: 18.2 6.18-23.8 L/h, cohort 3: 3.94-32.4 L/h. Total CL was dependent on the predicted concentration, meaning that CL was increasing with increasing concentrations.

The model could very well predict the observed cortisol concentrations in paediatric patients as seen in the VPC (Figure 3.21, left). As described previously the 95% confidence intervals for IIV for *CL* and V_c generated by bootstrap were large (Table 3.6) whereas the confidence intervals from log-likelihood profiling were appropriate. This indicated that the model cannot reliably be generalised to other paediatric populations, but that the parameters estimated are identifiable based on the data available. This model is therefore deemed sufficient to be used for deterministic simulations based on the suboptimal precision of IIV for CL and V_c.

Table 3.6 Population parameters and the respective 95% confidence interval for the reduced paediatric PK model

Disposition model	Population parameter estimate	95% Confidence interval, bootstrap	95% Confidence interval, llp
Fixed-effects			
k_a [h^{-1}]	2.12	1.82, 2.54	1.80, 2.85
CL [L/h]	353	271, 437	275, 424
V_c [L]	16.3	11.8, 21.5	12.6, 21.7
Interindividual variability			
ωCL [CV%]	38.2	0, 54.0	21.1, 60.7
ωV_c [CV%]	59.0	0, 95.6	31.2, 91.5
Residual variability			
σexp* [CV%]	13.5	7.74, 23.9	10.3, 19.1

Log-likelihood profiling (llp), first-order absorption rate (k_a), clearance (*CL*), central volume of distribution (V_c), interindividual variability (ω), residual variability (σ). *Estimated as additive error on a log scale.

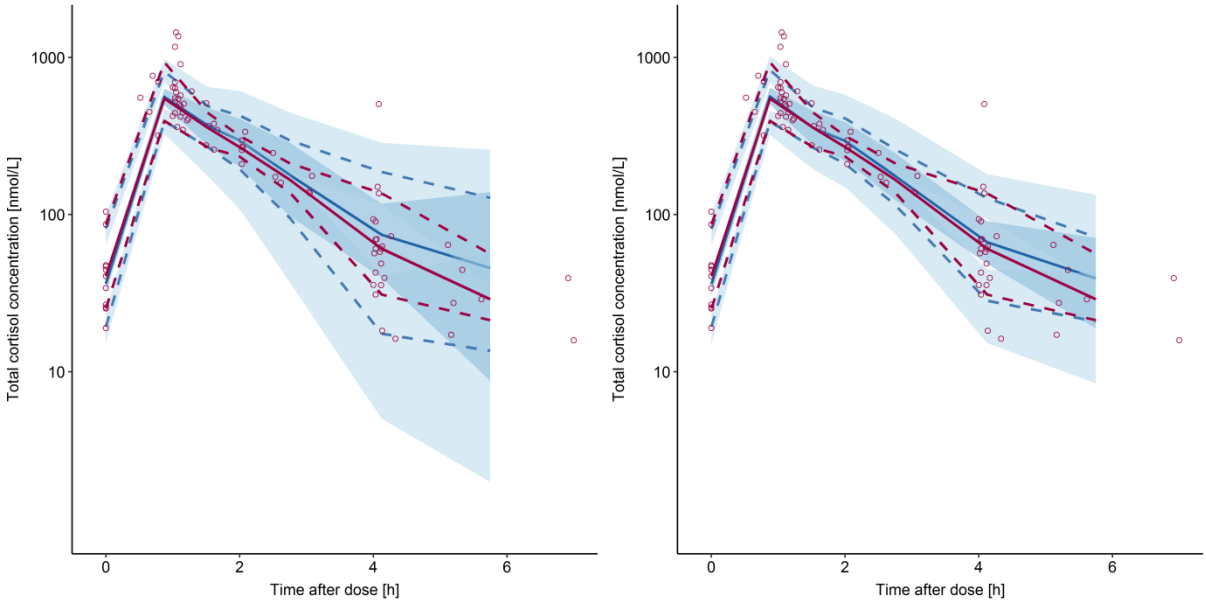

Figure 3.21 Visual predictive check (n=1000) for the reduced paediatric pharmacokinetic model (left) and semi-mechanistic pharmacokinetic model using the adult PK parameters as prior information (right). Lines: the 10th, 50th and 90th percentiles of observed (red) and simulated (blue) data; corresponding areas: 95% confidence interval around the simulated percentiles; circles: observations.

3.3 Project 3: Pharmacokinetic/pharmacodynamic characterisation of a licensed hydrocortisone formulation in paediatric patients with congenital adrenal hyperplasia

3.3.1 Population characteristics

42 patients were included into the clinical study. 12 patients (28.6%) had insufficient dosing history and were therefore excluded from the analysis. 46.7% and 53.3% of the remaining patients were prepubertal or pubertal/postpubertal, respectively. Since there were only two postpubertal patients, they have been included in the group with pubertal patients. According to the patient characteristics displayed in Table 3.7, the median age was slightly higher in the pubertal group (14 years) compared to the prepubertal group (9.20 years). The age range for the pubertal group did however almost cover the whole range for the prepubertal group (pubertal: 8-17.4, prepubertal: 7-14). Similar results were observed for HT and BW, for which the medians were slightly higher in the pubertal group, but the ranges were overlapping (Table 3.7).

Table 3.7 Covariates for prepubertal and pubertal/postpubertal paediatric patients with congenital adrenal hyperplasia

		Prepubertal, n=14		Pubertal/postpubertal, n=16	
	Units	Median	Range	Median	Range
Female/Male	[-]	9/5	-	12/4	-
Body weight	[kg]	37.0	32.0-63.0	62.4	38.1-103.7
Height	[m]	1.42	1.26-1.77	1.59	1.37-1.77
Age	[years]	9.20	7.00-14.0	14	8.00-17.4
BID	[-]	9*	-	8*	-
Daily dose po, BID	[mg]	17.5	15-25	27.5	12.5-35
TID	[-]	5*	-	8*	-
Daily dose po, TID	[mg]	25	17.5-32.5	30	20-40
Morning po dose	[mg]	10	10-15	15	7.5-20
Afternoon po dose	[mg]	2.5	2.5-7.5	8.75	5-10
Evening po dose	[mg]	7.5	5-15	10	5-15
Morning iv dose	[mg]	15.7	11.6-20.6	25.4	21.9-30.2

Two times daily dosing (BID), three times daily dosing (TID), oral administration (po), intreavenous administration (iv). *Number of patients

More pubertal/postpubertal patients had a TID regimen compared to for prepubertal patients (Table 3.7). In addition, the daily dose ranges was slightly higher in the pubertal/postpubertal group (median (range): 30 mg (20-40)) but almost overlapping with the prepubertal group (25 mg (17.5-32.5)). As expected, a high correlation (Pearson correlation coefficient >0.6) was observed between BW, HT and age (Figure 3.22).

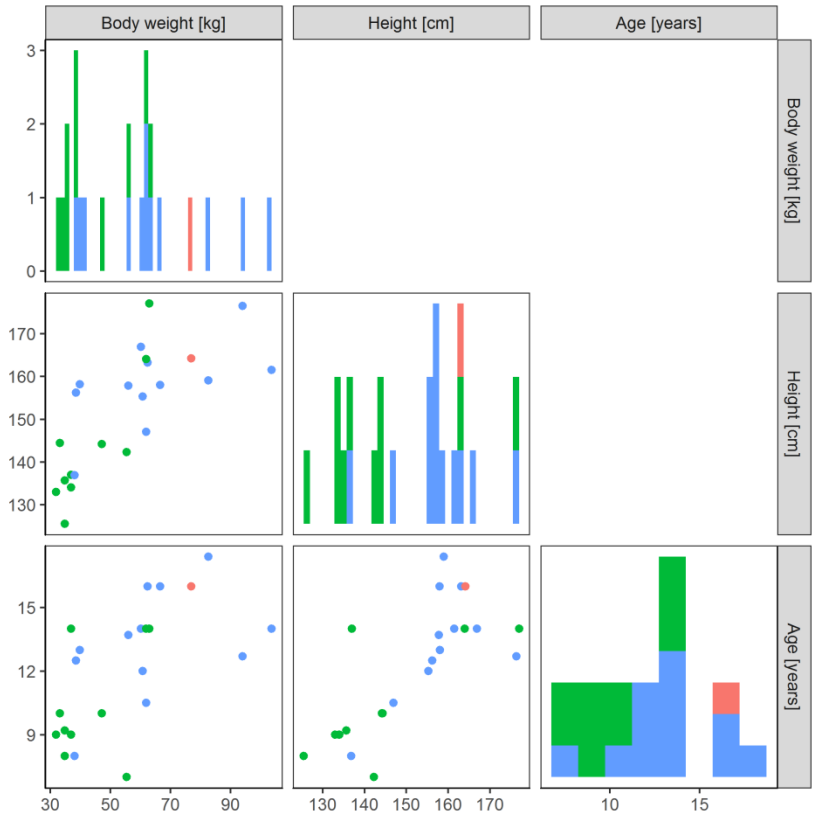

Figure 3.22 Correlation between covariates (lower triangle) and histogram of covariate distribution (diagonal elements, y-axis corresponding to the number of patients (0-3)) with the green, blue and pink colours correspond to covariates in prepubertal, pubertal and postpubertal, respectively.

3.3.2 Dataset

2502 total cortisol concentration measurements from 30 patients were used for the PK analysis. The first observation for one patient after iv administration was 5.4-fold higher than the observation 10 min later (9702 vs 1800 nmol/L), and was considered an outlier. The concentrations were sometimes increasing spontaneously, probably due to endogenous synthesis rather than exogenous hydrocortisone. Four individuals with spontaneous bursts of endogenous cortisol synthesis were identified and are shown in the Appendix (Figure 7.13). The outlier and times with spontaneous

cortisol bursts were excluded during model development and reintroduced to the dataset at a later stage to evaluate their impact on parameter estimates.

As previously discussed, some individuals had a high increase in cortisol concentrations prior to dose, indicating inaccurate recording of time of dose/plasma sample (Figure 7.14, Appendix). The impact of these inaccurate times was evaluated using different approaches (section 2.4.3.4 and 3.3.4.1).

3.3.3 Graphical evaluation of data

3.3.3.1 Pharmacokinetic data

A monophasic decline with a high variability between patients was seen in the concentration-time profiles (Figure 3.23) after po administration of hydrocortisone. Some patients reached a plateau after the rapid elimination of hydrocortisone, in the same range as pre-dose concentrations. A large variability was observed in the absorption phase, which was expected due to the issue with inaccurate dosing or sampling times previously described in section 2.4.3.4.

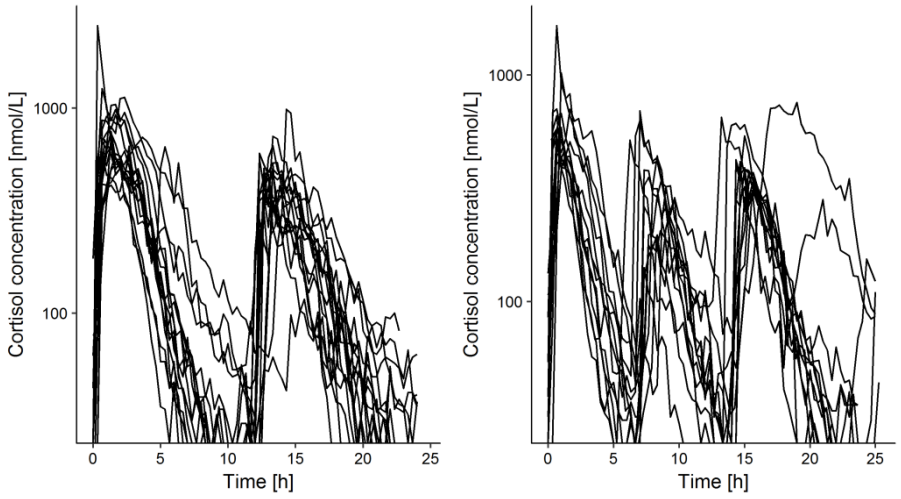

Figure 3.23 Individual cortisol concentration-time profiles in paediatric patients with congenital adrenal hyperplasia after two (left, n=17) and three (right, n=13) times daily oral dosingof hydrocortisone.

A large variability was also observed in the pre-dose concentrations: 15 patients had pre-dose concentrations below LLOQ, 13 patients had measurable concentrations ranging from 24 to 184 nmol/L. 5 and 13 patients were in the prepubertal and pubertal group, respectively. The highest concentrations were observed in patients potentially dosed too early. A mono-phasic decline was also observed for the iv data (Figure 3.24).

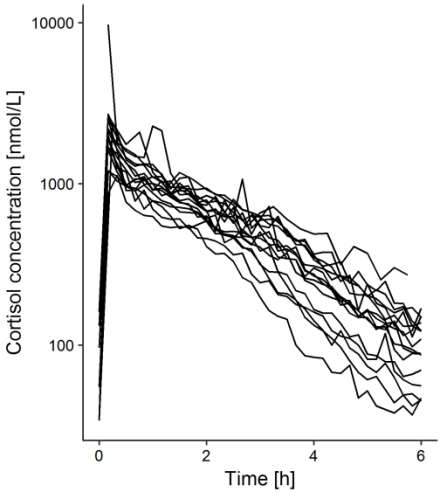

Figure 3.24 Individual cortisol concentration-time profiles after administration of a single intravenous dose (n=16) to paediatric patients with congenital adrenal hyperplasia.

3.3.3.2 Pharmacokinetic/pharmacodynamic data

Overall, 1642 17-OHP concentration measurements from 30 patients administered oral hydrocortisone were used for the PK/PD analysis. 17-OHP concentrations for 7 patients (22.0%) were all below LLOQ. A large variability was observed in the pre-dose 17-OHP concentrations (median (range): 38.0 nmol/L (below LLOQ-1490)). Overall, a large variability in 17-OHP concentration-time profiles was observed after BID and TID in patients with measurable 17-OHP concentrations (Figure 3.25). A hysteresis was also observed for 17-OHP versus cortisol concentrations (Figure 7.15 and Figure 7.16 in Appendix), indicating a delay/endogenous negative feedback in the inhibitory effect of 17-OHP in relation to cortisol increase.

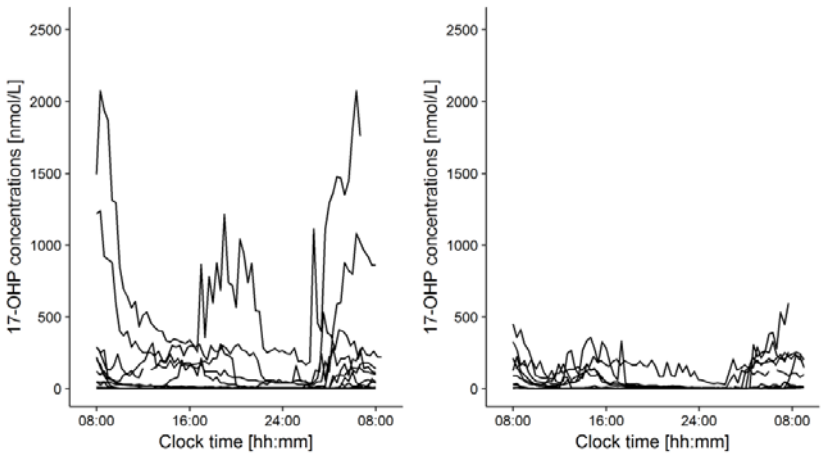

Figure 3.25 17-hydroxyprogesterone (17-OHP) concentration-time profiles after two (left, n=12) and three (right, n=11) times daily oral dosing regimen of hydrocortisone to paediatric patients with congenital adrenal hyperplasia.

3.3.4 Pharmacokinetic model for hydrocortisone in paediatric patients with congenital adrenal hyperplasia

3.3.4.1 Base and covariate model development

Initially different baseline models were evaluated using a one-compartmental disposition model with first-order absorption. Since some patients reached a plateau with concentrations similar to the pre-dose concentrations after the elimination phase, use of a constant underlying baseline was also evaluated. Estimating a constant underlying baseline ($Baseline_{cort}$) and the associated IIV was superior to using the pre-dose concentration as a covariate, resulting in improved GOF plots (Figure 7.17, Appendix) and large reduction in AIC (ΔAIC: -819). Use of a constant baseline also resulted in less trends in the CWRES.

The PK model was evaluated after the appropriate baseline model had been selected. Addition of a second compartment resulted in a non-significant reduction in OFV (ΔOFV: -3.2), and was therefore rejected. The one-compartmental model was therefore used when assessing the different absorption models. Applying a sequential zero-order absorption followed by first-order absorption or first-order absorption and adding a lagtime resulted in a significant reduction in OFV (Table 7.7 in Appendix). These models were however rejected due to parsimony, since no improvement in the absorption process was observed in the VPCs and GOF plots. Use of saturable absorption or zero-order absorption did not change OFV or resulted in a higher OFV, respectively, and were hence also rejected. Approaches to consider the saturable plasma protein binding resulted in unstable models with implausible estimates, and were therefore not pursued further. Since the variability in general was higher for the po data compared to the iv data, use of different RUV for po and iv data was assessed. Estimating two RUV resulted in a large reduction in OFV (ΔOFV: -424) and was therefore kept in the final model. Allometric scaling was also included, due to the large BW range in the studied population. No additional covariates were evaluated since no strong relations between the different parameter estimates and the respective covariates were identified. Allowing for variability between occasions for k_a, CL or V_c resulted in large drops in OFV, but was rejected due to no improvement in GOF plots and poor parameter precision. The concentrations below LLOQ was censored (M1 method) throughout model development. Use of a likelihood based approach (M3 method) to consider the concentrations below LLOQ was thereafter assessed for the key models. Use of the M3 method changed the parameter estimates but did not improve predictive performance of the VPC. The M1 method was hence also used for the final model.

The different approaches to consider the inaccurate dose- or sampling times were assessed using the one-compartmental model with first-order absorption. Adjusting the dose to the sampling time just before the increase in cortisol concentrations had minor impact on most parameters (<4%), but resulted in slight changes in k_a (-14.6%), ωk_a (-20.8%), $\omega Baseline_{cort}$ (14.4%) and $baseline_{cort}$ (-21.9%). Estimating a different residual variability for inappropriate dose times resulted in a decrease in $\omega Baseline_{cort}$ (-8.75%) and had low impact on other parameter estimates (<4%). Using the "lagtime" approach resulted in an unstable model sensitive to initial estimates. The sensitive estimates from this model could therefore not be compared to the other approaches.

3.3.4.2 Final pharmacokinetic model

The final model was a one-compartmental model with first-order absorption and estimating a constant underlying baseline (Figure 3.26). The final parameter estimates are presented in Table 3.8. Re-introduction of the identified outliers (Figure 7.13, Appendix) resulted in minor impact on parameter estimates and was therefore kept in the dataset. The typical k_a was 1.12 h^{-1} and the associated IIV was high (68%CV). *CL* and V_c were 22.4 L/h and 39.3 L, respectively. The IIV for *CL* and V_c, and the correlation between the two parameters were moderate (CV%: ωCL: 33.4, ωV_c: 31, Corr(CL, V_c): 0.605).

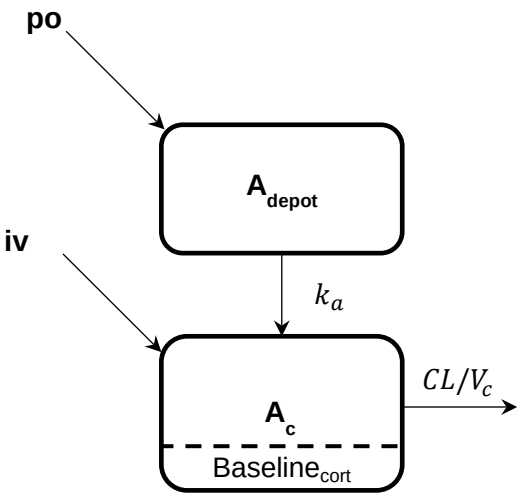

Figure 3.26 Schematic representation of pharmacokinetic model of hydrocortisone in paediatric patients with congenital adrenal hyperplasia after oral (po) and intravenous (iv) bolus administration. Amount in depot compartment (A_{depot}), first-order absorption rate constant (k_a), amount in central compartment (A_c), cortisol baseline ($Baseline_{cort}$), clearance (CL), central volume of distribution (V_c).

A constant underlying baseline (*Baseline$_{cort}$*) of 26.5 nmol/L was estimated to consider the measurable cortisol concentrations after the elimination phase. The IIV for *Baseline$_{cort}$* was considerable (58.1%), which was expected due to the high variability seen in the pre-dose concentrations and post-elimination phase concentrations. The RUV was moderate after iv (CV%: 18.6%) and high after po (CV%: 49.8%) administration, respectively.

Table 3.8 Final parameter estimates for pharmacokinetic model of hydrocortisone in paediatric patients with congenital adrenal hyperplasia

Pharmacokinetic model	Typical parameter estimate	95% Confidence interval
Fixed-effects		
k_a [h^{-1}]	1.12	0.892, 1.50
CL* [L/h]	22.4	19.6, 25.6
V_c* [L]	39.3	33.1, 45.0
F [-]	0.826	0.676, 0.950
$Baseline_{cort}$ [nmol/L]	26.5	20.2, 34.2
Interindividual variability		
ωk_a [%CV]	68.6	44.2, 67.6
ωCL [%CV]	33.4	23.2, 42.6
Corr (CL, V_c)	60.5	
ωV_c [%CV]	31.0	22.5, 38.6
ω$Baseline_{cort}$ [%CV]	58.1	39.5, 77.4
Residual variability		
σexp, po** [%CV]	49.8	40.2, 60.8
σexp, iv**[%CV]	18.6	15.3, 22.1

First-order absorption rate constant (k_a), clearance (CL), central volume of distribution (V_c), bioavailability (F), endogenous cortisol baseline ($Baseline_{cort}$). *Allometrically scaled to a body weight of 70 kg. **Estimated as additive error on a log scale.

The developed model described the data accurately as seen in the GOF plots (Figure 7.18, Appendix). Slight trends in the conditional weighted residuals were observed for the iv data. The magnitude of this trend was, however, small. As seen in the VPCs in Figure 3.27, the model could predict the observed data after iv and po administration very well. The case-deletion diagnostics identified one individual which influenced the typical parameter estimate *k_a*. Removal of this individual resulted in a

21.5% lower k_a (k_a: 1.04 h^{-1}), which was expected due to the inaccurate dose/sampling times for this individual. This individual was kept in the final analysis, due to the relatively small number of patients.

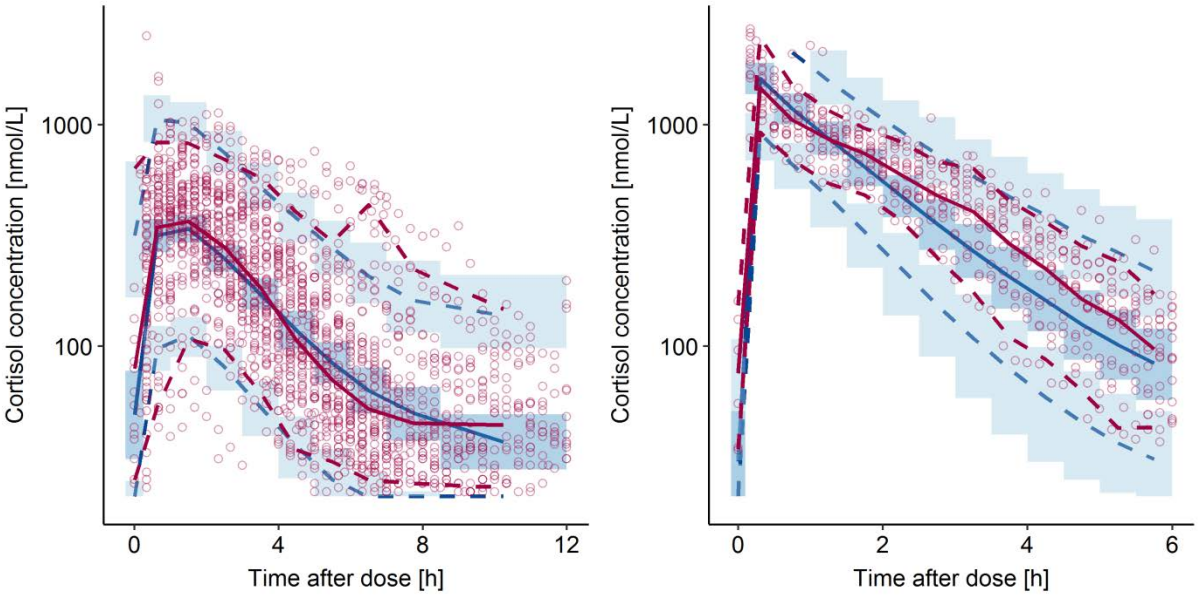

Figure 3.27 Visual predictive check (n=1000) for pharmacokinetic model for hydrocortisone in paediatric patients with congenital adrenal hyperplasia following oral (left) and intravenous (right) administration. Lines: the 5th, 50th and 95th percentiles of observed (red) and simulated (blue) data; corresponding areas: 95% confidence interval around the simulated percentiles; circles: observations.

3.3.5 Pharmacokinetic/pharmacodynamic model for hydrocortisone in paediatric patients with congenital adrenal hyperplasia

3.3.5.1 Base model development

The base model was established in different steps as outlined below and in Table 7.8 (Appendix).

Different baseline models were evaluated to consider the baseline concentrations of 17-OHP. Estimating a constant typical baseline ($Baseline_{17\text{-}OHP}$) and the associated variability according to the B1 method was the most appropriate baseline model. Using the measured initial concentration as a covariate to inform the model (B2 method) resulted in an unstable model sensitive to initial estimates and was therefore rejected.

Since cortisol is mediating a delayed inhibition of the synthesis of 17-OHP, an indirect response model with inhibition of the 17-OHP synthesis was used. Different concentration-effect models were applied to consider the inhibitory relationship between cortisol and 17-OHP. The I_{max} model

described the data better than the slope model (ΔOFV: -304). Addition of a shaping factor (γ=1.24) in the sigmoidal I_{max} model resulted in a minor reduction in OFV (ΔOFV: -5.61). The effect model therefore consisted of an indirect response model with a cortisol-mediated non-sigmoidal I_{max} inhibition of the 17-OHP synthesis.

Systematic trends in CWRES and underprediction of the steep morning increase in 17-OHP was observed (Figure 7.19, Appendix). For this purpose, time- and concentration-dependent models were applied to capture the rebound. Addition of one cosine function with a 24 h periodicity reduced OFV considerably (ΔOFV: -332) and improved trends in GOF plots (Figure 7.20, Appendix). The estimated time shift for the 24 h cosine function was close to 0, and was therefore fixed to 0. Addition of a second cosine function (12 h periodicity) reduced OFV (ΔOFV: -63.4) and improved trends especially in conditional weighted residuals further (Figure 7.21, Appendix). Addition of a third cosine function (8 h periodicity) reduced OFV even further (ΔOFV: -45.8) but did not improve GOF plots. In addition, the precision was poor for the amplitude of the 8 h cosine function and the third cosine function was hence rejected. Use of concentration-dependent feedback models resulted in a less stable model with inferior GOF plots (Figure 7.22, Appendix). The time-dependent cosinor approach using two cosine functions were therefore kept and applied in the base model.

As previously discussed in section 1.3.2, 17-OHP has a circadian pattern in healthy individuals and CAH patients in absence of hydrocortisone treatment. To support the assumption of a circadian 17-OHP synthesis, the predicted 17-OHP concentrations in absence of treatment were compared to digitalised concentrations from non-treated patients in Bacon *et al.* and Frisch *et al*. As seen in Figure 3.28, assigning $Baseline_{17\text{-}OHP}$ to the population estimate (39.2 nmol/L) from the established PK/PD model resulted in 17-OHP concentrations (red solid lines) much lower than the observed literature data. This was expected based on the high IIV for baseline17-OHP in the current model and the high variability in the literature data. On the other hand, using the median of the initial concentrations from the observed data from Bacon *et al.* and Frisch *et al.* (633 nmol/L) to inform the $Baseline_{17\text{-}OHP,}$ resulted in predicted 17-OHP concentrations (red dashed lines) agreeing well with the tendencies of their observed data. This was a strong indicator that the circadian rhythm inferred from the treated population could be generalised to a non-treated population and supported the assumption of a circadian 17-OHP synthesis.

A mixture model was evaluated to allow estimation of different typical 17-OHP baselines and the associated IIV, due to the high variability in the initial 17-OHP concentrations. Although use of a

mixture component improved GOF plots, it had minor impact on OFV (ΔOFV: -7.73), and was therefore rejected.

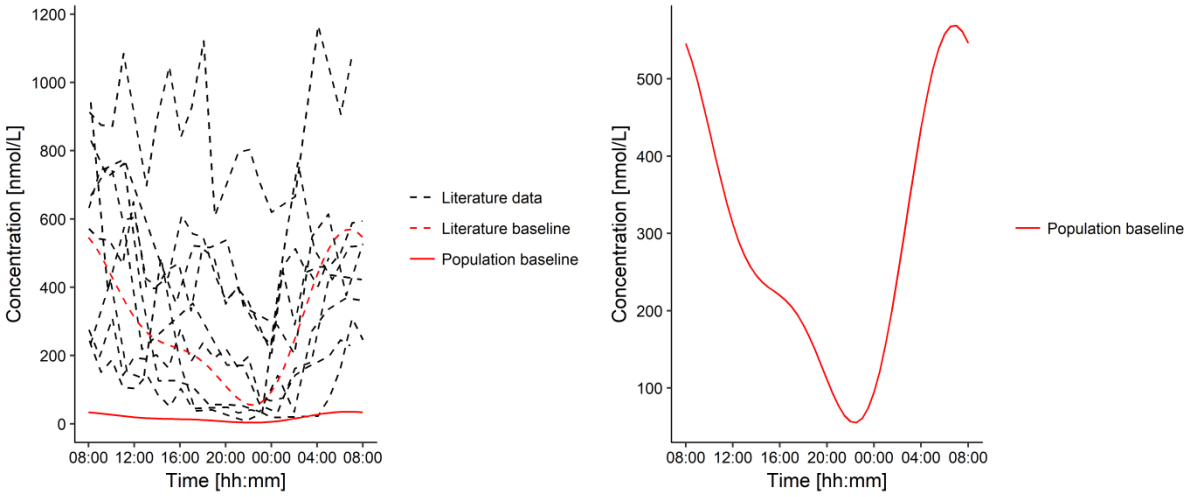

Figure 3.28 Comparison of 17-hydroxyprogesterone (17-OHP) concentrations in absence of hydrocortisone treatment. Black lines correspond to individual 17-OHP concentrations from Bacon *et al.* and Frisch et al. (dashed black lines [58,59]). Red lines correspond to the predicted 17-OHP concentrations by assigning the 17-OHP baseline to the median initial concentration from the literature data (dashed line, baseline: 633 nmol/L) or the population baseline estimate (solid line, baseline: 39.2 nmol/L).

3.3.5.2 Final pharmacokinetic/pharmacodynamic model

The final model consisted of an indirect response model with a cortisol-mediated inhibition of the circadian 17-OHP synthesis. A schematic representation of the model is available in Figure 3.29. The typical $Baseline_{17\text{-}OHP}$ was 39.2 nmol/L, which is similar to the observed pre-dose concentrations (median (range)): 38.0 (below LLOQ-1490) nmol/L. The IIV for $Baseline_{17\text{-}OHP}$ was very large (Table 3.9), which was expected due to the very large variability observed in the data. IC_{50} was low (47.2 nmol/L), indicating that cortisol is inhibiting the responsible enzyme already at low concentrations.

The impact of the cosine functions with relatively large amplitudes for the 24 (0.759) and 12 h (0.29) functions on the otherwise constant k_{in}, is visualied in Figure 3.28 (right part). The model described the data accurately as seen in the GOF plots (Figure 7.21) and VPC (Figure 3.30). A case-deletion diagnostics was performed to identify influential individuals. One individual was seen as influencing the precision of the parameter estimates, but did not have a major impact on the parameter estimates and was hence kept in the dataset.

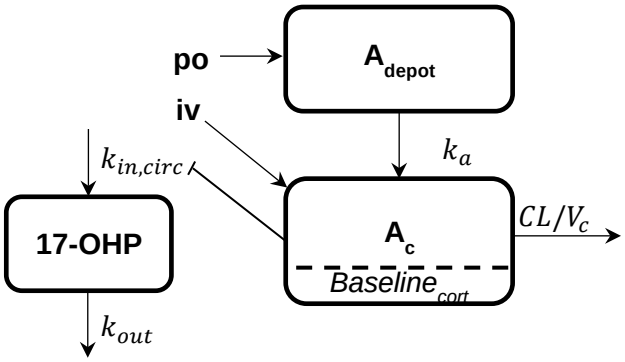

Figure 3.29 Schematic representation of pharmacokinetic/pharmacodynamic model of hydrocortisone in paediatric patients with congenital adrenal hyperplasia after oral (po) and intravenous (iv) administration. Amount in depot compartment (A_{depot}), first-order absorption rate constant (k_a), amount in central compartment (A_c), cortisol baseline ($Baseline_{cort}$), clearance (CL), central volume of distribution (V_c), 17-hydroxyprogesterone concentrations ($17\text{-}OHP$), circadian synthesis rate constant of 17-OHP ($k_{in,circ}$, Eq. 2.44), first-order elimination rate constant of 17-OHP (k_{out}).

Table 3.9 Final parameter estimates for pharmacokinetic/pharmacodynamic model of hydrocortisone in paediatric patients with congenital adrenal hyperplasia

PK/PD model	Typical parameter estimate	95% Confidence interval
Fixed-effects		
$Baseline_{17\text{-}OHP}$ [nmol/L]	39.2	17.2, 83.0
k_{out} [h^{-1}]	0.453	0.312, 0.604
k_{in} [nmol/L h]	17.8	-
I_{max} [-]	1 *fixed*	
IC_{50} [nmol/L]	47.2	29.3, 104
amp_{24} [-]	0.759	0.560, 1.00
$shift_{24}$ [h]	0 *fixed*	-
amp_{12} [-]	0.290	0.180, 0.450
$shift_{12}$ [h]	10.0	8.84, 11.4
Interindividual variability		
ω$Baseline_{17\text{-}OHP}$ [CV%]	505.7	227, 1063
Residual variability		
σexp* [CV%]	93.7	76.7, 114

Baseline for 17-hydroxyprogesterone concentrations ($Baseline_{17\text{-}OHP}$), first-order elimination rate constant (k_{out}), maximum inhibitory effect (I_{max}), cortisol concentration inhibiting 50% of I_{max} (IC_{50}), amplitude for cosine functions (amp_{24}, amp_{12}), time shift for cosine functions ($shift_{24}$, $shift_{12}$).*Estimated as additive error on a log scale.

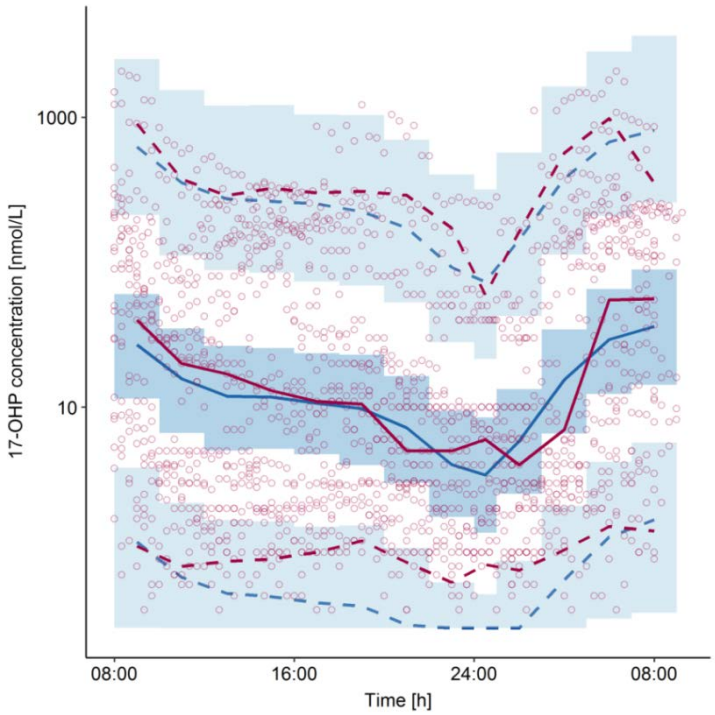

Figure 3.30 Visual predictive check (n=1000) for pharmacokinetic/pharmacodynamic model for hydrocortisone in paediatric patients with congenital adrenal hyperplasia. Lines: the 5th, 50th and 95th percentiles of observed (red) and simulated (blue) data; corresponding areas: 95% confidence interval around the simulated percentiles; circles: observations.

3.3.6 Evaluating dosing regimens of hydrocortisone in paediatric patients with congenital adrenal hyperplasia

A simulation-based analysis was employed to evaluate the performance of QID and TID, with lower (e.g. 3, 3, 3, 3 mg) or higher doses (e.g. 4.5, 4.5, 4.5, 4.5 mg) either with the similar (e.g. 3, 3, 3, 3 mg) or higher doses in the morning and evening (e.g. 4, 2, 2, 4 mg) throughout the day in the typical prepubertal and pubertal patient (Table 2.2). The evaluation was done comparing the percentage of time (during 24 h) with cortisol and 17-OHP concentrations within the cortisol and 17-OHP target concentration range (%T_{cort} 50-500 and %$T_{17\text{-}OHP}$ 12-36) for each virtual patient, respectively. %T_{cort} 50-500 in pre-pubertal patients (Figure 3.31, upper left) was in general higher after QID compared to TID, and more than 75% of the population (the lower quartile of the box to the upper whisker) were at least 75% of time between 50 to 500 nmol/L (%T_{cort} 50-500≥75) after QID. Similar results were seen for the pubertal patients (Figure 3.31, lower left), for which approximately 60% and 80% were at least 75% of time within the cortisol target range in the TID and QID groups respectively. %$T_{17\text{-}OHP}$ 12-36 was comparable for all dosing regimens in both populations (Figure 3.31, right), and 75% of the

population (the upper quartile of the box to the lower whisker) were at least 50% of the time within the 17-OHP target ($\%T_{17\text{-}OHP}$ 12-36≤50). None of the studied regimens had patients always being within the 17-OHP target.

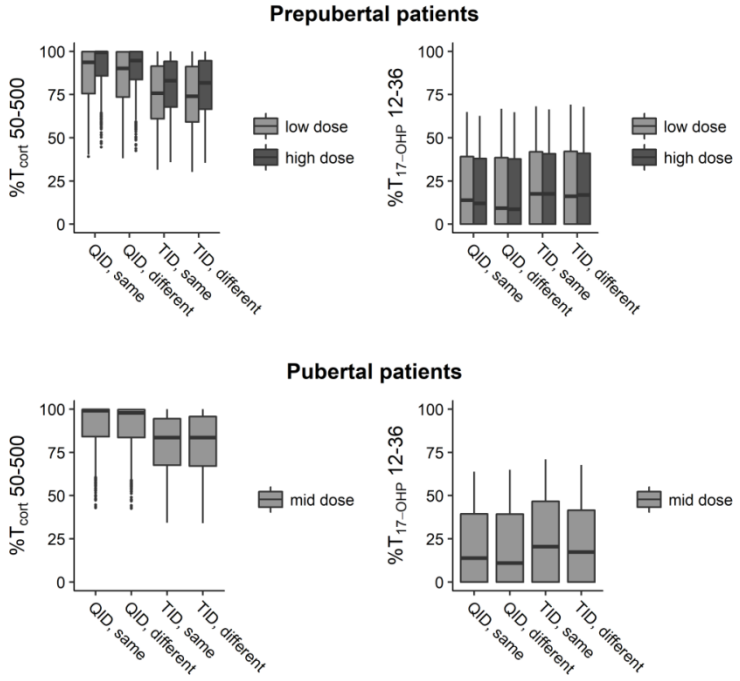

Figure 3.31 % of time with cortisol concentrations between 50 and 500 nmol/L ($\%T_{cort}$50-500, left) % of time with 17-hydroxyprogesterone (17-OHP) concentrations between 12 and 36 nmol/L ($\%T_{17\text{-}OHP}$ 12-36) in prepubertal (upper panel) and pubertal (lower panel) patients.

To further evaluate the impact of the different evaluated scenarios, a graphical analysis was done to compare the simulated cortisol concentration-time profiles with the physiological cortisol concentrations from Peters *et al.* [146], and the cortisol target concentrations (50-500 nmol/L, dotted lines). As seen in Figure 3.32, mimicking the circadian rhythm is challenging with administration of immediate release formulations of hydrocortisone three or four times daily. The simulated morning cortisol concentrations were in general lower than the observed physiological cortisol concentrations for all evaluated dosing regimens. The simulated peaks around lunch (12:00-13:00) were in accurate agreement with the physiological concentrations, for all dosing regimens except for the lowest doses (2-3 mg). The time between 18:00 and 00:00 were best captured in the QID dosing regimen with a 3 mg dose. Overall the increase in cortisol concentrations during the night was poorly captured by all dosing regimens, but slightly better captured by the QID, which had a later night dose. The minimum concentrations (C_{min}) just before next dose were overall slightly higher for the higher doses, as expected. As expected, a similar pattern was observed also for pubertal patients

(Figure 3.33). Based on a visual evaluation of Figure 3.32, an improved QID dosing regimen for the typical pre-pubertal patient consisting of 7, 4, 3 and 4 mg was suggested (Figure 3.34).

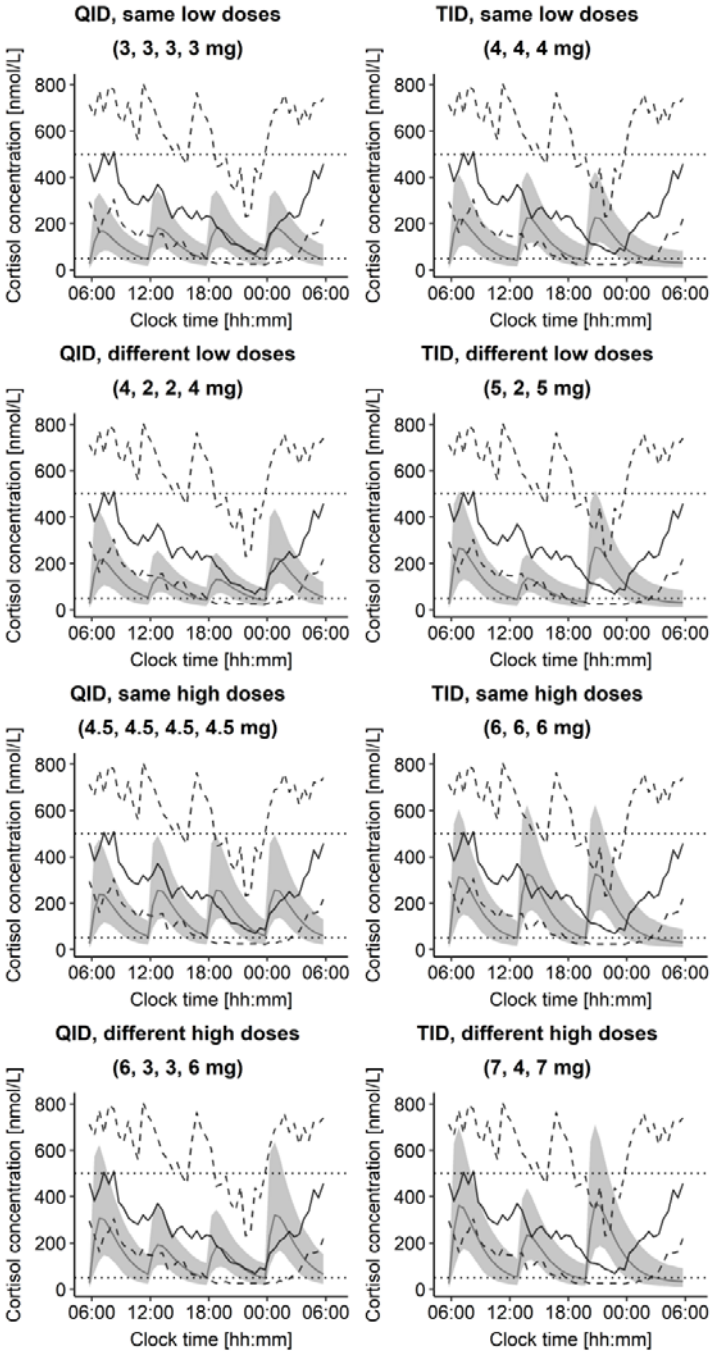

Figure 3.32 Median (solid black line) and 95% confidence interval (dashed black lines) for reported cortisol concentrations in healthy children (n=28, [146]). Grey lines correspond to the simulated typical cortisol concentration-time profiles, associated with the 95% confidence interval (grey areas, n=1000) in the typical prepubertal patient. Four times daily dosing (QID), three times daily dosing (TID). Dotted lines correspond to the cortisol target range between 50 and 500 nmol/L.

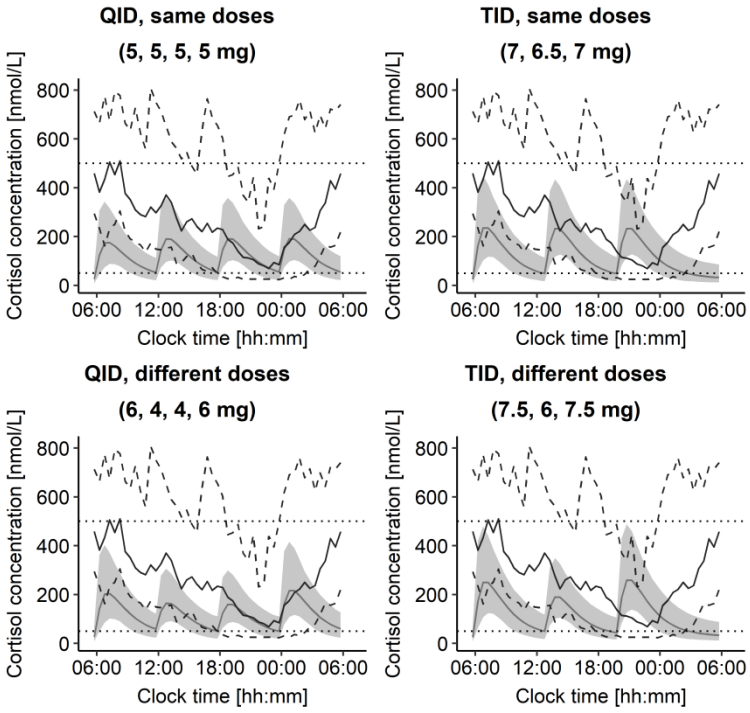

Figure 3.33 Median (solid black line) and 95% confidence interval (dashed black lines) for observed cortisol concentrations in healthy children (n=28, [146]). Grey lines correspond to the simulated typical cortisol concentration-time profiles, associated with the 95% confidence interval (grey areas, n=1000) in the typical pubertal patient. Four times daily dosing (QID), three times daily dosing (TID)

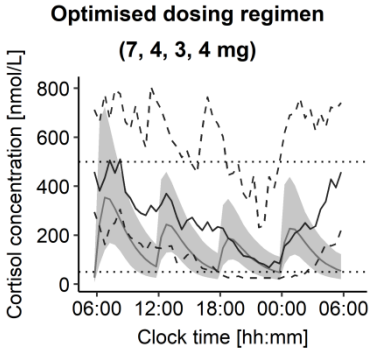

Figure 3.34 Median (solid black line) and 95% confidence interval (dashed black lines) for observed cortisol concentrations in healthy children (n=28, [146]). Grey lines correspond to the simulated typical cortisol concentration-time profiles, associated with the 95% confidence interval (grey areas, n=1000) for the improved treatment regimen (7, 4, 3, 4 mg) in the typical pre-pubertal patient.

4 Discussion

4.1 Project 1: Pharmacokinetic characterisation of a novel hydrocortisone formulation in healthy adults

Project 1 aimed to characterise the PK of hydrocortisone administered as the novel formulation (Infacort) using rich phase 1 data. Infacort was developed to supply a HC formulation suitable from birth, since there is currently no licensed HC formulation for patients below 6 years in Europe. This phase 1 data has previously been analysed using NCA [40], which does not allow for considering the nonlinear PK and extrapolation to paediatric patients. In this project a population PK model was established to describe the complex PK of HC in a semi-mechanistic way. Model complexity could be supported since doses in a large range (0.5-20 mg), with information after po and iv administration (20 mg) were available from two clinical trials in adults. The semi-mechanistic model formed the basis for extrapolation to paediatric patients, and consisted of different structural sub-models which will be outlined below.

4.1.1 Disease model and consideration of endogenous cortisol

PK knowledge generated from healthy volunteers is sometimes difficult to extrapolate to patients, since these populations are commonly very different. In the current analysis, it was therefore important to justify the use of PK data from dexamethasone-suppressed healthy participants to extrapolate PK knowledge to paediatric patients with adrenal insufficiency (no or low endogenous synthesis). The first step was hence to assure appropriate estimation of PK parameter estimates by considering the endogenous and exogenous cortisol concentrations.

In both studies, healthy participants received DEX prior to HC treatment to suppress the HPA axis to better purely quantify the exogenous hydrocortisone and to better mimic the disease (low/no endogenous cortisol synthesis and diminished negative feedback of the HPA-axis). After administration of DEX and Infacort, the cortisol concentrations in all dose groups were cleared relatively fast from C_{max} until approaching the pre-dose concentrations. A constant baseline (15.5 nmol/L) was hence estimated. The use of a constant cortisol baseline was further supported by the very low and approximately constant median cortisol concentrations (median (range)): 16.8 nmol/L (9.04-26.4) (Figure 3.4) after DEX suppression only. In addition the CV% for the median cortisol after

DEX only (33.1%) was similar to IIV for $Baseline_{cort}$ (30.8%). The similar baselines for periods with DEX and in absence/presence of HC, indicated that HC did not affect the cortisol baseline.

The physiological mechanism behind the approximately constant underlying cortisol baseline is to our knowledge unknown. One may hypothesise that it is resulting from the cortisol-cortisone equilibrium. Studies characterising the cortisol and cortisone simultaneously may provide useful information about the physiology of the system and the plausibility of this hypothesis. Another explanation for the approximately constant cortisol concentrations may be the CBG acting as a reservoir and releasing cortisol as the cortisol concentrations are decreasing.

There are different ways to analyse the PK for compounds which are endogenous. The present analysis used the actually measured cortisol concentrations, and estimated an endogenous baseline to enable appropriate parameter estimation, thereby allowing for possible random error in the baseline [147]. Another commonly used approach is to subtract the baseline concentrations from the subsequent measurements. This approach may result in negative concentrations, which are then imputed by a selected value (e.g. 0), contributing to potential bias in the AUC calculation [147]. The chosen methodology in the present thesis was judged as superior to generate unbiased parameter estimates, thereby allowing for potential extrapolation to other populations.

4.1.2 Plasma protein binding model and simulated cortisol fractions

Previous studies have identified that cortisol has a high plasma protein binding contributing to a nonlinear PK [69,70,90]. The available C_u and corresponding C_{tot} measurements allowed us to explore the binding kinetics of cortisol, and to establish a plasma protein binding model that was integrated in the PK model. Both nonlinear (specific) and linear (non-specific) processes were identified, potentially corresponding to binding to CBG (high affinity, limited capacity) and albumin/erythrocytes (low affinity, high capacity), respectively. To provide a more physiological interpretation of the model, B_{max} was derived using CBG concentration and a parameter (N_{CBG}) representing the number of binding sites of CBG to cortisol. This approach explained more than 50% of the IIV of B_{max}. The IIV of N_{CBG} can therefore rather be regarded as RUV for the CBG *measurements*, with 7%CV potentially corresponding to imprecision of the bioanalytical assay. Fixing N_{CBG} to 1, i.e., one binding site for cortisol per CBG molecule, was in line with previous findings [148]. Furthermore, the derived B_{max} using CBG concentrations was well in agreement with previous observations, suggesting a saturable binding at C_{tot} above 550 nmol/L [2]. The equilibrium dissociation constant (K_d, 11.8 nmol/L) and

linear nonspecific binding component *(NS*, 3.12) were in similar range as previous estimates (K_d: 33 nmol/L [149], *NS*: 1.75 [94]).

Since the plasma protein binding model was established on C_{tot} and C_u from a range of concentrations smaller than those observed for the high doses, an external model evaluation was performed to increase model reliability. The plasma protein binding model could adequately predict the observed data from Lentjes *et al.*, with C_{tot} ranging from 300 to 850 nmol/L. A slight overprediction, was however observed, which could potentially be due to a different analytical assay used in Lentjes *et al*.

To visualise the impact of the different binding processes, the concentrations (unbound, specific binding and non-specific binding) of cortisol were simulated using C_{tot} in a 20-fold range (23.7-492 nmol/L, Figure 3.11). A three-fold increase was observed in fraction unbound, which together with C_{tot} translated to a large range (~60-fold) in C_u (0.5-31.5 nmol/L) [53], illustrating the importance of the specific and non-specific binding for lower (i.e. in paediatric patients) and higher concentrations, respectively.

The established plasma protein binding model does not consider other steroids (e.g. corticosterone, deoxycortisol, 17-OHP, progesterone [150]) with high affinity to CBG that may compete with the binding of cortisol to CBG. Future studies characterising the binding in patients with CAH may shed light on whether changes in plasma protein binding occur and needs to be considered clinically.

4.1.3 Corticosteroid-binding globulin model

B_{max} was derived using CBG, which was not quantified in study 1. A constant CBG model was established on periods with DEX to enable imputation of CBG in study 1. The CBG concentrations measured in our study were in the lower end of reported reference ranges (e.g. reference range 14.9-67.1 µg/mL [91]), which is rather large indicating a large variability between individuals. Previous studies have indicated that CBG has a circadian rhythm [96,97], whereas other studies have contradicted this [98]. We found that CBG concentrations were approximately constant from 07:00 to 19:00, which is why a constant CBG baseline with associated variability was sufficient to describe the CBG concentrations during this time span. The CBG measurements from every hour during 24 h showed, however, a clear circadian rhythm. The circadian rhythm of CBG was well described by adding two cosine functions to the CBG baseline. The parameter precision was good and the CBG_{max} at 18:00 and CBG_{min} at 03:30 were well captured by the model, as seen in the VPC (Figure 3.10). The circadian rhythm of CBG is somewhat contradictory to the rhythm of cortisol: The CBG concentrations are high 18:00 when the cortisol are declining, and the CBG concentrations are low

during the night when the cortisol concentrations are increasing. This may have a biological implication to e.g. decrease free (biologically active) cortisol concentrations in the afternoon [96].

4.1.4 Semi-mechanistic pharmacokinetic model

Previous PK analyses used a one- or two-compartmental disposition model depending on route of administration and study design [65,74]. Our data was most accurately described by a two-compartmental model, although a trend of a mono-phasic decline could be observed for higher doses. This may be due to the slight time delay in absorption, masking the first disposition phase for the higher doses in our data. The absorption process was most accurately described by saturable absorption (Michaelis-Menten kinetics). The amount resulting in half of the maximum absorption rate was 2300 nmol, indicating a saturated absorption for the three highest doses (5, 10 and 20 mg). The lower doses were below K_m, for which a first-order absorption rate constant (V_{max}/K_m) of 4.53 h^{-1}, and short absorption half-life of approximately 10 min can be assumed. The nonlinear absorption process could be due to poor solubility at higher doses, which has been observed in experiments performed *in vitro* [83]. In addition, allometric scaling was applied to enable a more appropriate extrapolation to paediatric patients.

Few previous PK models have considered the plasma protein binding of cortisol. It should be acknowledged, that changes in plasma protein binding rarely are clinically relevant after oral administration and may have little impact of unbound exposure. The plasma protein binding may however have an impact on the PK parameter estimates and sequentially the description of the total concentrations [151]. In our model, the inclusion of the plasma protein binding model significantly improved model performance especially for the highest dose (20 mg), which had many total cortisol concentrations above B_{max}. Addition of the plasma protein binding model related *CL*, *Q*, *V3 and F* to unbound concentrations, preventing a direct comparison to previous parameters. Total CL was therefore derived using fraction unbound, to enable a comparison with estimates from the literature. Maximal total CL was observed for the higher doses (Figure 3.9), which was expected due to the higher fraction unbound in these doses. The range of total CL (1.42-26.2 L/h) included the mean/median CL from the literature (12.5-20.2 L/h, [65,70,75,76]) following iv administration of hydrocortisone. The previous NCA indicated a dose-dependency in *AUC*, which can be explained either by F decreasing or *CL* increasing with higher doses. The latter scenario is compatible with our modelling approach, in which CL increases with the fraction unbound, resulting in an increased *CL* after saturation of CBG.

In the current thesis, estimation of PK parameters was performed only considering data after hydrocortisone treatment. In a future analysis, data from study periods without any treatment and only in presence of dexamethasone could be used to establish a physiological "placebo" model. Re-estimating the PK parameters simultaneously with the physiological placebo model may further increase the understanding of the physiological system and its interplay with the treatment effect. A model also considering the previously mentioned conversion between cortisol and cortisone would improve the understanding even further.

In summary, we have applied a nonlinear mixed-effects modelling approach to evaluate the PK after rich sampling in healthy adult volunteers. Rich data allowed for the parameter estimation of a semi-mechanistic model that more mechanistically quantified known aspects of HC PK, such as its saturable binding to plasma proteins. Each of the features implemented was supported by an improvement in the model fit, considerable reduction in the OFV/AIC, and acceptable precision of parameters. The semi-mechanistic model was built on doses in a wide range, including doses used in the paediatric population, and mechanistic understanding, why we were confident to extrapolate this model to paediatric patients, as done in project 2. The developed semi-mechanistic model represents a first step towards a better understanding of HC PK, extrapolation to paediatric patients, and can potentially be used to evaluate hydrocortisone therapy in this population.

4.1.5 Predicting cortisol exposure in paediatric patients

One of the powerful applications of a validated pharmacometric model is to explore new therapeutic scenarios and guide dose selection. The ultimate aim of the model here presented would be to extrapolate to paediatric population and guide dose selection. That is why in this work we have explored how C_{max} and *AUC* varied with different BW (within the range expected in a paediatric population). There is currently no validated target for the HC therapy in this population. We have thus hypothesised that it could be beneficial to mimic the physiological cortisol rhythm. One aspect to be monitored could then be the cortisol concentrations in the morning (highest cortisol concentrations), which is why the average C_{max} and *AUC* of cortisol in healthy paediatric volunteers were derived from Knutsson *et al*. and used as a reference. By using deterministic simulations, we visualised how the C_{max} and *AUC* differed with different BW and compared them with proposed PK comparison ranges derived from Knutsson *et al*. The model predicted a much larger variation in C_{max} and *AUC* within a small BW range in individuals <20kg. This implies that defining an accurate dose to replicate physiological concentrations becomes very important for children <20kg. These simulations represent an extrapolation of the semi-mechanistic model to a special population with different body

weight range. It should be noted that the simulations does not consider age-relevant factors, such as maturation of CBG for neonates [100] or the slightly lower and higher 5α-reductase activity in neonates and infants [103], respectively. The clinical interpretation of the results should therefore be done with caution for patients below two years of age (body weight ≤ 15 kg [152]), and be verified with prospective clinical trials.

4.1.6 Impact of circadian CBG on exposure

It has previously been hypothesised that the PK of cortisol is not constant during 24 h but is rather changing (i.e. chronopharmacokinetics), due to the circadian rhythm of CBG [78]. Changes in e.g. CL of cortisol due to changes in CBG could imply the potential need to adjust the hydrocortisone dose, dependent on when during the day it is administered.

In this analysis, a simulation approach was employed to evaluate the potential impact of circadian CBG on cortisol exposure after administration of hydrocortisone. By combining the previously established semi-mechanistic model together with the presented circadian CBG model, the impact of changes in CBG on hydrocortisone exposure could be evaluated. For this purpose we evaluated two different scenarios; scenario 1 represented a systematic evaluation of exposure after single dose administration every hour, and scenario 2 represented evaluation of exposure after multiple administrations according to a clinically used dosing regimen.

Even though CBG has a circadian rhythm, the prediction intervals for the lowest and highest simulated *AUC* and C_{max} in scenario 1 were overlapping for all doses. The differences between the lowest and highest median *AUC* and C_{max} in the respective dose group were also minor (*% difference* $AUC_{\uparrow}$: 9.48%-12.2%, *% difference* $C_{max\uparrow}$: 4.20%-9.01%). These results indicate that the circadian rhythm of CBG does not translate into a major difference in the exposure of cortisol. This is potentially due to the relatively small difference (~23%) between the lowest and highest CBG concentrations, which also resulted in relatively small amplitudes in the circadian variation.

In scenario 2, the exposure after administration of a clinically relevant TID dosing regimen was assessed in two virtual populations with constant or circadian CBG concentrations, respectively. Median exposure assuming circadian CBG was in general slightly lower compared to assuming constant CBG. Assuming circadian instead of a constant CBG concentrations resulted in the largest difference in *AUC* for the morning and the evening dose (*% difference* AUC_{circ}: 9%-11%). Probably since the circadian CBG was slightly lower than the constant CBG during these times. The prediction intervals for *AUC* and C_{max} were however overlapping similarly to scenario 1.

To evaluate the clinical relevance of the differences in exposure, one may hypothesise how a difference in *AUC* or C_{max} may translate into difference in pharmacodynamic effect. Assuming that the pharmacodynamic effect mediated by cortisol upon binding to the glucocorticoid-receptor is linear, this may indicate a maximum of 10% difference in effect depending on timing of dose. A 10% difference is relatively small compared to the variability in PK parameters (~25%-30%CV) and variability associated with other sources. The impact of the circadian CBG rhythm on hydrocortisone exposure is, therefore, likely not clinically relevant. Dose adjustments based on when the dose is administered are probably not needed.

4.2 Project 2: Pharmacokinetic characterisation of a novel hydrocortisone formulation in paediatric patients with adrenal insufficiency

Project 2 aimed to characterise the PK of hydrocortisone administered as Infacort in paediatric patients with adrenal insufficiency using clinical trial data. Since only sparse phase II data was available, the semi-mechanistic PK model from project 1 was used to inform the paediatric PK model during model development.

4.2.1 Pharmacokinetic model

Initially, the external model evaluation showed that the semi-mechanistic PK model established on only adult data could well predict the observed paediatric observations based on BW and CBG. This supported that PK models with semi-mechanistic features increase the predictive performance of models. The external model evaluation, however, indicated that the concentrations pre-dose and four hours post-dose were sub optimally described. The PK assessment therefore started with improving the baseline model.

A constant underlying cortisol baseline allowed for an accurate description/separation of the endogenous and exogenous cortisol in the adult data (project 1). For the paediatric data, several post-dose concentrations were lower than the pre-dose concentrations. Assuming a constant underlying baseline hence forced the predictions to always be above the estimated baseline, which resulted in large trends in the residuals (Figure 7.9). This indicated that the constant underlying baseline might not be supported for the evaluated age group.

The observed pre-dose cortisol concentrations could either result from the previous hydrocortisone dose or from residual cortisol synthesis. No pre-dose concentrations were observed for neonates; hence no endogenous synthesis was likely in this group. This was expected, since the circadian

rhythm of cortisol is evident first after an age of 2-3 months [50,51]. For the infants and children, 50% and 75% of the pre-dose concentrations were quantifiable, indicating potential endogenous synthesis. Larger studies may be able to evaluate the degree of endogenous synthesis in this age group, and identify potential age differences. The source of the measurable cortisol is unknown, unless studies with labelled cortisol would be performed. Labelling cortisol may on the other hand affect the affinity to the plasma protein binding and yield unwanted results, which was shown for tritium and ^{14}C labelled cortisol [153].

The aim of project 2 was to generate reliable paediatric PK parameter estimates with as little influence from the adult data as possible. For this purpose a stepwise assessment including several different approaches with diminishing impact of adult data and increasing impact of paediatric data was applied. The selection between models was therefore not based on OFV but rather on predictive performance, model stability, GOF plots and parameter precision. Approaches including a large impact of adult data, such as re-estimating using both adult and paediatric data, as well as use of prior approaches, resulted in parameter estimates very similar to the adult data. This was probably due to the relatively sparse paediatric data.

Overall, approaches based on paediatric data only resulted in precisely estimated fixed-effects parameters, whereas the IIV was not precisely estimated. Parameter precision was assessed by bootstrap, in which the model is estimated using new datasets created by resampling with replacement from the original dataset. The imprecision in IIV generated with bootstrap were potentially due to resampling from a dataset with few individuals with relatively high variability. The imprecision for models based on only paediatric PK data indicated that the PK parameters are probably not generalisable to larger populations, and should therefore not be used for stochastic simulations. For the final reduced model parameter precision from the log-likelihood profiling was appropriate. This indicates that the model parameters were identifiable in the studied population. Informing the model with more data for all cohorts may result in an IIV which could be better generalised to other populations.

Applying the full semi-mechanistic PK model on paediatric data only resulted in a very unstable model sensitive to initial estimates. Reducing the model to a one-compartmental disposition model with first-order absorption resulted in a stable model with good parameter precision for fixed-effect parameters. The model could also well describe the observed data, as seen in the VPC (Figure 3.21). The reduced model had some influence by the previous data, since the included plasma protein binding model was established using data from adult healthy volunteers. The plasma protein binding

do not consider potential binding competitors, which is applicable for healthy volunteers who have a stable HPA axis and no elevated hormones. In contrast, patients with CAH may have a hyperactive HPA axis and potential accumulation of e.g. 17-OHP that can compete with cortisol for the CBG binding sites. Extrapolation of the plasma protein binding model may therefore not be appropriate in patients with CAH with very active disease. In the current analysis, no obvious trends were seen in the GOF plots, supporting that the plasma protein binding model could be applied to the current age range. Further studies on the plasma protein binding in CAH patients measuring relevant binding competitors with high affinity to CBG (e.g. corticosterone, deoxycortisol, 17-OHP, progesterone [150]), may be able to quantify the plasma protein binding in CAH patients.

By using the reduced model, slightly different CL normalised to a body weight of 70 kg were observed for the different populations. Neonates had slightly lower CL than young children and adults, which could potentially be explained by the lower activity of 11-βHSD2 (converting cortisol to cortisone) and 5α-reductase (irreversible metabolism of cortisol to allo-DHF) in this age group. Conversely, CL in infants was slightly higher than in children and adults, potentially due to the high activity of 5α-reductase in infants. Use of a maturation function to describe this improved model performance slightly. The maturation model was however rejected due to poor precision and implausible value of the gamma factor. As previously stated in section 1.4.3, there are several developmental processes relevant for the metabolism of cortisol. The use of a maturation function should therefore be evaluated again once the model has been informed with more data.

The PK of hydrocortisone has previously been characterised in older patients with CAH and in critically ill pre-term neonates [78–81]. These studies were however performed using licensed formulations in age groups not covered in this study or in a different patient population. The estimated unbound CL for cohort 1 (median (range): 121 L/h (77.2-186) agreed well with previous unbound CL in a slightly older prepubertal cohort (mean (SD): 149 L/h (59) [79]). A previous study characterised the PK of cortisol using unbound concentrations in critically ill preterm and full-term neonates [81]. The unbound CL estimated for a 70 kg body weight in that study (population estimate (95% confidence interval): 20.2 L/h (15.9-24.5)) was much lower than the population estimate in our study (353 L/h (275-424)). The reason for the large discrepancy is not well understood but could partly be related to the critical condition of that population, which is known to cause changes in PK for e.g. antibiotics [154].

The overall range of predicted f_u (cohort 1: 1.31%-7.66%, cohort 2: 1.77%-6.52%, cohort 3: 1.80%-11.3%) was similar between the different cohorts and corresponded well with f_u of 5% [90] or 10%

[94] for cortisol from the literature. A similar f_u was expected based on the comparable CBG concentrations in the different populations, even though a previous study observed slightly lower CBG concentrations in neonates [100]. The reason for this discrepancy may be due to the relatively low number of patients in the current study. The higher maximum f_u in the neonates was observed for the three patients with the higher C_{max}. The higher C_{max} could potentially be explained by the smaller volume of distribution, which was observed for hydrophobic compounds in neonates [99]. Total CL for a 70 kg person, derived by using the individual body weight and predicted f_u, was similar between the different cohorts. The ranges of total CL (cohort 1: 4.72-32.1 L/h, cohort 2: 18.2 6.18-23.8 L/h, cohort 3: 17.4 3.94-32.4 L/h) were also in the same range as previous estimates of CL slightly older pre-pubertal CAH patients (mean (SD): 14.9 L/h (6.04) [79]) and CAH patients between 1.4 and 18.1 years (mean (SD): 12.4 L/h (7.99) [80]). The estimated volume of distribution (16.3 L) was similar in the CAH patients between 1.4 and 18.1 years (mean (SD): 17.5 L (10.5) [80]) but lower than the pre-pubertal patients in Charmandari *et al.* (mean (SD): 27.1 L (8.4) [79]). Overall, the observed results in the current study were similar to previous results from the literature, except for the data from Vezina *et al.* in critically ill preterm neonates [81].

To summarise, a reduced paediatric PK model considering the plasma protein binding of cortisol to CBG has been established. The model describes the data accurately for the different cohorts, and could in the future be used to explore cortisol exposure following different dosing regimens. When the model has been informed by more data, the IIV may be more precisely estimated, allowing for optimising amount, as well as time of the different hydrocortisone doses. More data may also allow for identifying age-dependent factors affecting the PK of hydrocortisone, thereby contributing to a more rational dosing in these vulnerable paediatric patients with adrenal insufficiency.

4.3 Project 3: Pharmacokinetic/pharmacodynamic characterisation of a licensed hydrocortisone formulation in paediatric patients with congenital adrenal hyperplasia

Project 3 aimed to characterise the PK and PK/PD of hydrocortisone in paediatric patients with adrenal insufficiency in the clinical setting. For this purpose we used data from observational studies that were less structured than clinical trials. Data from a clinically relevant disease biomarker (17-OHP) was used for the PK/PD analysis.

4.3.1 Pharmacokinetic model for hydrocortisone in paediatric patients with congenital adrenal hyperplasia

As previously discussed, the PK model describing the data from a clinical setting was developed in a sequential manner. An appropriate baseline model was deemed necessary to distinguish between the endogenous and exogenous cortisol. A constant underlying baseline model described the data most accurately and improved GOF plots to a large degree. This assumption was supported by the approximately constant concentrations after the rapid elimination phase, which was in the same range as pre-dose concentrations. This strong assumption may not hold true for all paediatric patients in the studied age range (7-17.4 years), since the cortisol concentrations are related to disease severity, as well as previous treatment history. A recent analysis was able to identify different cortisol synthesis rates between groups of CAH patients (salt wasters, simple virilisers, non-classic CAH) [155], indicating that this is important to evaluate in future trials. The cortisol baseline was quite low (26.5 nmol/L), but the associated variability was high (58.1%CV). Previous studies measuring cortisol concentrations in untreated paediatric patients with CAH, indicated higher cortisol concentrations with a large variability (41.2-541 nmol/L [58], 8.64-461 nmol/L [59]). The reason for higher concentrations in the literature data is not well understood, but could be related to differences between treated and non-treated patients. Further studies in paediatric patients with CAH are needed to fully understand if the constant underlying baseline is an appropriate assumption.

Initially, the previously established semi-mechanistic model (project 1) was applied on the current data. Use of the full semi-mechanistic model or the reduced paediatric PK model from project 2 resulted in unreliable estimates. This could be due to the different formulations, different assays used for quantification, and different study setting in the two paediatric studies. In addition, CBG was not measured in the current study. Based on this, the model from project 2 (one compartmental model with first-order absorption using allometric scaling and including the plasma protein binding model) was used as the starting point when evaluating the PK of hydrocortisone in project 3.

As previously described in section 4.1.4, previous models for HC in the literature have applied one- or two-compartmental models depending on the route of administration and study schedule. In the present analysis, a one-compartmental model with first-order absorption described the data appropriately, even though data after po and iv administration with very rich sampling schedule was available. This was supported by the approximately mono-phasic decline in the cortisol concentration-time profiles (Figure 3.23 and Figure 3.24).

Different absorption models were applied, out of which the first-order absorption was kept for the final model. Other absorption models (sequential first- followed by zero-order absorption or use of lagtime) allowing for more flexibility in the absorption phase reduced OFV significantly, potentially due to the better description of the inappropriate dose/sampling. Use of these models therefore made the model more specific to the present data and less useful for extrapolation. In addition these models did not improve model performance according to GOF plots and VPCs, and were therefore rejected.

The *CL* (22.4 L/h) and *F* (82.6%) was similar, whereas V_c (39.3 L) was larger than previous results from Derendorf *et al.* (*CL*: 18 L/h, V_c*:* 23.9 L, *F*: 96% [65]). Higher *CL* and V_c were expected in pubertal patients , due to alterations in the endocrine pattern in sex steroids and growth hormone in the this patient group[79]. Since no large obvious differences in parameter estimates for the different pubertal status were identified, use of pubertal status was not evaluated, even though this has previously been described [78]. Larger studies might be able to identify the impact of pubertal status on PK parameters and help to individualise treatment regimens

Different methods to handle concentrations below LLOQ were applied to key models, since high fractions of concentrations below LLOQ were observed in the late time interval. Use of the M3 method did not improve model performance according to the VPCs. Censoring the concentrations below LLOQ (M1 method) was therefore kept, although there is a risk for biased parameter estimates. The risk for biased estimates was deemed very low, given the very rich data situation and the simple disposition model.

An appropriate recording of the dose and sampling times is a prerequisite for generating reliable data and thereby reliable parameter estimates. When failing to do so, the pharmacometrician is challenged with generating parameters as reliable as possible, and can only assess the potential bias/uncertainty in the estimated parameters. In the present study, inappropriate sampling/dose times (Figure 7.14, Appendix) were identified during the exploratory graphical analysis. Since it would be inappropriate to shift the actual doses administered in the dataset, a sensitivity analysis was performed to evaluate the potential impact of the inappropriate doses on PK parameter estimates (section 2.4.3.4). As expected, adjusting the dose to the first time before the increase in cortisol concentration decreased k_a (-14.6%) and ωk_a (-20.8%), since the absorption can be slower if the dosing time is later than the actual cortisol increase. This indicates that the k_a might be slightly lower than if the appropriate times were available. In addition, $Baseline_{cort}$ (-21.9%) and $\omega Baseline_{cort}$ (14.4%) were slightly changed. Since these parameters decide the initial concentrations of the

cortisol in the central compartment, they might be changed to adjust for the improved description of the absorption. Using a different residual variability for inappropriate times also had a small impact on $\omega Baseline_{cort}$ (-8.75%), further supported that the $\omega Baseline_{cort}$ might be influenced by the inappropriate times. Use of the lagtime approach was very appealing since it allows for the software (i.e. NONMEM) to select the most appropriate dosing time. This approach unfortunately resulted in a highly unstable model, which could not reliably be evaluated. This was potentially due to the difficulties associated with distinguishing the random-effects for lagtime and absorption.

To summarise, a population model describing the PK of hydrocortisone in paediatric patients with CAH has been established. The model describes the data accurately for the different times of the day and after different routes of administration. The sensitivity analysis implied that the parameters of especially k_a and $Baseline_{cort}$, might be slightly biased due to the potentially inaccurate dose/sampling times. Addition of more reliable data may help to inform and improve model performance and reliability.

4.3.2 Pharmacokinetic/pharmacodynamic model for hydrocortisone in paediatric patients with congenital adrenal hyperplasia

After the PK model had been established, a PK/PD model was developed sequentially to describe the cortisol-mediated inhibition of the 17-OHP synthesis. The individual PK parameters were fixed during model development. It is known that potential bias in the PK model can be carried over to the PD model when doing so. An attempt to re-estimate the PK and PD parameters simultaneously was therefore carried out, which unfortunately resulted in a highly unstable model.

The baseline model was first selected to assure an appropriate description of the 17-OHP concentrations. Use of its initial concentration to inform the model resulted in an unstable model sensitive to initial estimates and was hence rejected. A constant 17-OHP baseline resulted in a good description of the data and was kept in the final model. The $Baseline_{17\text{-}OHP}$ the associated IIV were high. A recent study identified disease status as a covariate on the 17-OHP synthesis, and was able to estimate different synthesis rates for salt wasters, simple virilisers and nonclassic CAH [155]. In the present analysis all patients were salt wasters, which is why we could not estimate different baselines based on the different disease types. Differences in residual cortisol synthesis may also contribute to the high variability, and would be an interesting covariate to look further into.

The delay in the cortisol-mediated inhibition of 17-OHP synthesis was described using an indirect response model with inhibition of the synthesis rate (k_{in}). Other approaches, such as use of an effect

compartment or an indirect response model with stimulation of the elimination rate constant (k_{out}) could also have been applied. The first option was unreasonable since the delay in an effect compartment model is then assumed to relate to the distribution process of the lipophilic cortisol rather than the time of the actual inhibition. The second option was not supported by the known physiology of cortisol and was therefore less logical than the model with inhibition of the k_{in}.

Different inhibitory effect models were then evaluated and the I_{max} model was found to describe the data most accurately. The IC_{50} of 47.2 nmol/L indicated inhibition of the responsible enzyme already at very low cortisol concentrations, since cortisol concentrations were ranging from LLOQ (21 or 28 nmol/L) to ~2500 nmol/L. The IC_{50} value was similar to the IC_{50} (56.0 nmol/L) from a recent analysis investigating the PK/PD relationship between cortisol and 17-OHP in a similar way as in the current analysis [155], whereas k_{out} was lower (current: 0.453 h^{-1}, Ahmed *et al*: 1.02 h^{-1}).

The model prediction for the steep morning increase was systematically too low prior to adding circadian functions to k_{in}. In the final model, two cosine functions were applied to the k_{in}, which improved model performance especially for the steep morning increase. In addition to cosine functions, use of concentrations rebound models, commonly applied to other endogenous substances were applied to capture the steep morning increase. This did however not result in a better description of the data. The use of a time-dependent feedback was therefore selected and was also supported by the known circadian rhythm of cortisol and 17-OHP.

To support the assumption of a circadian 17-OHP synthesis, the predicted 17-OHP concentrations in absence of treatment were compared to concentrations digitalised from Bacon *et al.* and Frisch *et al.* [58,59]. Assigning $baseline_{17\text{-}OHP}$ to the median initial 17-OHP concentrations from the literature data resulted in predicted 17-OHP concentrations agreeing very well with the observed concentrations. This gave us further confidence that the predicted time course of circadian synthesis is physiologically plausible, and that the circadian synthesis potentially can be generalised to other patient populations, if informed by the individual 17-OHP baseline.

Mixture models were evaluated to enable estimation of two different typical $baseline_{17\text{-}OHP}$. Use of mixture models were not supported in the current analysis based on OFV and overall model stability. To capture a better description of the baseline it would be better to try to identify covariates, such as disease status, to potentially explain the variability in the data.

All 17-OHP concentrations were below LLOQ in 7 well/over-suppressed patients. Censoring this data may result in slightly different parameter estimates (especially the baseline), since the very well/overtreated patients are removed, whereas data from poorly treated patients are kept.

Improving the sensitivity of bioanalytical assay for 17-OHP may allow for quantifying these very low concentrations in the future. This would allow for an improved overall understanding of potential differences between the PK/PD relationship in patients with well- or poorly suppressed disease.

4.3.3 Evaluating dosing regimens of hydrocortisone in paediatric patients with congenital adrenal hyperplasia

Modelling and simulation approaches have previously been used to evaluate dosing regimen in patients with adrenal insufficiency [62,74]. Simon *et al.*, evaluated the cortisol concentrations after substitution therapy in adolescents and adults and compared it to the physiological circadian rhythm of cortisol. A new optimised treatment regimen for adults with adrenal insufficiency of 10 mg (07:30), 5 mg (12:00) and 5 mg (16:30) was suggested [74]. Mah *et al.*, applied modelling and simulation techniques to construct a nomogram with adult dose recommendations based on BW for a three times daily dosing regimen (06:00, 12:00 and 18:00). Both these analyses have an uneven distribution of the doses throughout the day (i.e. patients were not dosed every 8 h), which might lead to too low minimum concentrations. In addition, the last dose was administered very early (16:30 and 18:00), which does not ensure appropriate HPA-axis suppression during the night. In addition both these analyses were applied on data in adults/adolescents.

Based on these shortcomings, we explored the impact of different dosing regimens on cortisol and 17-OHP based targets by using the established PK/PD model. As expected, a QID regimen resulted in a higher fraction of time within the cortisol concentration range compared to a TID dosing regimen. In our analysis, 50 nmol/L was selected as the minimum target concentration, based on the minimum median cortisol concentration of the physiological data [146]. This minimum target cortisol concentration was also supported by the IC_{50} value, which indicated inhibition of 17-OHP synthesis corresponding to 50% of the maximum inhibitory effect for cortisol concentrations of approximately 50 nmol/L. Hence, in order to avoid accumulation of 17-OHP concentrations cortisol concentrations above 50 nmol/L are recommended, which is easier achieved with a QID rather than TID dosing regimen. $\%T_{cort}$ 50-500 was overall high, but as expected slightly higher for the higher doses. $\%T_{17\text{-}OHP}$ 12-36 were in general low, and did not differ between the different dosing regimens. Based on the evaluation using fixed concentration targets, a more frequent dosing (QID) with evenly distributed dosing times is preferred in order to avoid too low minimum concentrations. This evaluation could not evaluate whether it was better to administer similar doses throughout the day or whether higher doses in the morning and evening were better. For this purpose a qualitative graphical evaluation

was performed to compare the evaluated dosing regimens with the physiological cortisol concentrations.

The graphical evaluation indicated that none of the evaluated dosing regimens could successfully mimic the circadian cortisol concentrations (Figure 3.32). The QID administration resulted in slightly better performance between 18:00-00:00 and slightly higher minimum concentrations in the morning the day after. A slightly improved dosing regimen was suggested in order to try to mimic the physiological concentrations better, which used a higher morning dose (7 mg), followed by lower doses at lunch time (4 mg), in the evening (3 mg) and in the night (4 mg). This dosing pattern (higher dose in the morning, followed by lower doses during the day) is commonly applied in clinical practise and seems to be supported by the physiological rhythm of cortisol. Our analysis shows the importance of establishing circadian concentration targets, which could be used to optimise the hydrocortisone substitution therapy, and is the first step towards optimising treatment regimens in paediatric patients with CAH. Future projects should aim to optimise time of dose, as well as amount administered, once the PK/PD model has been informed with more data.

To summarise: the established PK/PD model was used to evaluate different dosing regimens for hydrocortisone in paediatric patients with CAH. Based on our evaluation, QID dosing regimen should be better than TID with respect to i) avoiding too low cortisol minimum concentrations, ii) enabling a better resemblance to the physiological cortisol concentrations and iii) a higher fraction of the population being most of the time within the suggested cortisol target range. Prospective clinical trials are of course needed to confirm if there is a clinical benefit with respect to improvement in disease status, growth velocity, and lower androgen concentrations of administering hydrocortisone four times daily. These trials will also be useful to evaluate potential issues with adherence associated with the QID dosing regimen.

4.4 Hydrocortisone pharmacokinetics in different age ranges

In the current thesis, the pharmacokinetics of hydrocortisone was characterised in different populations with varying ages spanning from adults to vulnerable newborns, and for different purposes. Studies in vulnerable paediatric patients are challenging both from a practical and ethical point of view. The most complex model, i.e. the semi-mechanistic PK model based on rich adult data (project 1) was therefore established to gain mechanistic understanding to enable an appropriate extrapolation to paediatric patients. The purpose in project 2 was to generate reliable paediatric PK parameters from sparse clinical trial data. In project 3, the aim was to generate reliable paediatric

PK/PD parameter estimates from data from a less strict clinical study to sequentially evaluate different dosing regimens. Even though three different PK models were established in the three projects, the PK models were established based on different data and – most importantly- for different context of use, thus they all contribute to the overall understanding of the PK of hydrocortisone from neonates up to adults.

As described in section 1.4.1 the absorption of hydrocortisone is in general fast and may be slower for higher doses. Based on this prior knowledge, rich data in adults (project 1) following administration of a large range of doses was chosen and enabled to characterise a saturable absorption process. Due to the rather lipophilic nature of hydrocortisone, the absorption process of hydrocortisone is likely also saturable in paediatric patients (at high concentrations). Although saturable absorption could not be characterised for the paediatric data in project 2 or 3, this is most probable since only single/few different doses in a very small dose range were administered to every patient. In addition, project 2 had sparse sampling not allowing for characterisation of more complex absorption models. For these two paediatric projects, a simpler first-order absorption model was sufficient to accurately describe the data. Yet, to enable comparison of the paediatric with adult absorption parameter estimates, the first-order absorption rate constant (k_a) for the adult semi-mechanistic PK model was derived from the Michaelis-Menten equation (V_{max} /(K_m+A_{depot})), as follows: According to the saturable absorption model, lower doses/amounts in the depot compartment are absorbed with a first-order kinetics, i.e. characterised by the first-order absorption rate constant k_a (=V_{max}/K_m). The absorption of the higher doses/amounts in the depot compartment becomes more saturable and k_a is therefore derived from the whole Michaelis-Menten equation (V_{max}/(K_m+A_{depot})). k_a for adults ranged from 4.53 h^{-1} for small doses to 0.447 h^{-1} for the highest oral dose, which was overall in the range of paediatric patients, yet at smaller doses higher than the neonates/infants/young children in project 2 (k_a: 2.12 h^{-1} (1.80-2.85)) and children/adolescents in project 3 (k_a: 1.12 h^{-1} (0.892-1.50)). For smaller doses, this translates to absorption half-lives of ~10, ~20 and ~37 min for adults, neonates/infants/young children in project 2 and children/adolescents in project 3, respectively. As previous studies have indicated an absorption equivalent to adults already for infants [88], at first sight, a faster absorption for the adults was not expected. However, the largest k_a for adults corresponds to absorption of the lower doses, which are relatively much lower than in neonates/infants/young children. For high doses, the absorption half-life would be ~50-90 min, thus the k_a in adults is only higher for the lower doses. The absorption in project 2 was faster than in project 3. Assuming that the absorption is also saturable in paediatric patients, this may potentially be due to the slightly higher dose range administered in project 3 compared to project 2.

The novel formulation consists of hydrocortisone granules with taste masking, which may also potentially dissolve faster than the immediate release formulation. The estimated absorption rate constant in project 3 was also potentially affected by the inappropriate dosing/sampling times, which should also be considered when comparing this absorption rate constant. Overall, the description of the absorption process in all age populations was coherent; *in vitro* or dedicated clinical studies investigating the absorption more in detail may be useful to identify age-dependent factors affecting the absorption of hydrocortisone in neonates, infants and young children.

Several studies have previously evaluated the plasma protein binding of cortisol to CBG, which may have a major impact on both distribution and elimination (section 1.4.2 and 1.4.3). In project 1, a plasma protein binding model was established, which was informed by the individually measured CBG concentrations. The plasma protein binding model could successfully be included into the semi-mechanistic PK model to potentially enable a better extrapolation to paediatric patients. The plasma protein binding model was also successfully added to the reduced paediatric PK model in project 2. Inclusion of this plasma protein binding model was also pursued for project 3 by imputing the typical CBG concentration from the constant CBG model (section 3.1.4). Unfortunately, inclusion of the plasma protein binding model resulted in a very unstable model with implausible parameter estimates. Since glucocorticoid treatment has shown to reduce the CBG concentrations [95], model performance might be improved if individual CBG concentrations were available. In addition, the concentrations of steroids potentially competing with the binding site at CBG may be elevated in patients with CAH especially during puberty. Since the adult plasma protein binding model currently does not consider competitive binding of other steroids, this model may be inappropriate for this population of CAH patients. The plasma protein binding model was as previously stated, however, successfully included into a younger patient population with adrenal insufficiency (project 2). This could potentially be explained by the lower disease activity resulting in lower concentrations of steroids competing with the binding sites of CBG. Studies evaluating age-dependent changes affecting plasma protein binding to CBG (e.g. CBG concentrations, concentrations of steroids competing for the binding) in patients with CAH may help to characterise the plasma protein binding more properly and identify steroids which may a large impact on cortisol PK.

The range of fraction unbound for cortisol in adults (1.46%-10.8%) for the po model was overlapping with the ranges in neonates (1.80%-11.3%), infants (1.77%-6.52%) and young children (1.31%-7.66%). If only considering doses administered in project 2 (2 mg), the range of fraction unbound in adults was similar to the ranges in infants and young children (2.04%-4.86%). This was expected since

similar CBG concentrations were observed in infants and adults [100]. The slightly higher fraction unbound in the neonates was derived for individuals with very high C_{max}. The estimated CL in project 1 and 2 corresponded to the unbound CL, due to the inclusion of the plasma protein binding model. The total CL in neonates, infants, young children and adults corresponding to a BW of 70 kg was therefore derived using the individually predicted concentrations and the individual CBG concentration (typical constant CBG concentration was imputed for study 1 in project 1). The adult range of total relative CL for a BW of 70 was 3.56-40.0 L/h, of which the highest CL was observed for the higher doses (Figure 3.9). The range of total CL was comparable in young children (4.72-32.1 L/h), infants (6.18-23.8 L/h) and neonates (3.94-32.4 L/h). The CL range for the adult model including iv data was 1.42-26.2 L/h, which included the CL estimated on data from children/adolescents in project 3 (22.4 L/h).

Since cortisol and hydrocortisone are bioanalytically non-distinguishable, it was of uttermost importance to potentially separate the two substances in all projects of the current thesis. This was done by evaluating different approaches to consider the constant endogenous cortisol baseline/measurable pre-dose concentrations. In project 1, estimation of a constant underlying cortisol baseline (15.5 nmol/L) was used to consider the endogenous cortisol synthesis after dexamethasone suppression. The reason for this constant underlying cortisol baseline is to our knowledge unknown. One may hypothesise that it is resulting from the cortisol-cortisone equilibrium. Studies characterising the cortisol and cortisone simultaneously may provide useful information about the physiology of the entire HPA axis network and feedback system and whether this is a reasonable hypothesis. Another explanation for the approximately constant cortisol concentrations may be the CBG acting as a reservoir and releasing cortisol as the cortisol concentrations are decreasing.

A constant underlying cortisol baseline was also used in project 3, in which several cortisol concentration-time profiles reached a plateau after the elimination phase. 43% of the patients had measurable concentrations prior to po dose, corresponding to 57% of the pubertal and 36% of the prepubertal patients. In project 2, no cortisol concentration plateau was identified potentially due to the sparser sampling or the less activated HPA axis in this younger population. The non-quantifiable pre-dose concentrations in neonates and the slightly more quantifiable proportions in infants (50%) and young children (75%) support that the HPA axis may mature with age and that this may have an impact on the pre-dose measurements of cortisol. The measurable pre-dose cortisol concentrations or appearance of the cortisol concentration plateau may potentially reflect the HPA axis activity, and thereby disease status. Studies evaluating how the disease changes with age and how that affects

the endogenous cortisol synthesis may provide insight into the disease development and may sequentially be useful to optimise hydrocortisone treatment.

To summarise, this thesis laid the fundamentals for a coherent understanding of the underlying mechanism and processes of hydrocortisone substitution therapy across the different age populations generating new hypotheses to be studied in future.

5 Conclusions and perspectives

The aim of the present thesis was to assess hydrocortisone substitution therapy in paediatric patients with adrenal insufficiency using pharmacometric approaches. For this purpose, nonlinear mixed-effects modelling was used to increase the understanding of the underlying (patho)physiology linked to the pharmacokinetics and pharmacokinetics/pharmacodynamics of hydrocortisone administered as age-appropriate formulations to different populations. Since performing extensive clinical trials in paediatric patients is challenging and is typically avoided, the strategy was to first make use of clinical trial data in healthy adults to learn about the interaction between the "diseased" system (underlying physiology) and the pharmacokinetics of hydrocortisone. This approach successfully enabled an appropriate extrapolation of a semi-mechanistic PK model to paediatric patients, which confirmed the mechanistic features of the model. The paediatric model was further reduced and used to gain understanding about factors varying between healthy adults and paediatric patients. Finally, the established pharmacokinetic/pharmacodynamic model using a clinically relevant biomarker increased our understanding of the system and its impact of hydrocortisone further. The paediatric PK/PD model was sequentially used to assess the ability of the recommended hydrocortisone substitution therapy to mimic the physiological circadian cortisol concentrations in patients with CAH.

As previously discussed, rich data from healthy adults administered Infacort in project 1 allowed for quantifying the pharmacokinetics in a semi-mechanistic way accounting for: i) constant cortisol baseline after dexamethasone suppression, ii) nonlinear plasma protein binding to CBG and linear binding (e.g. to albumin/erythrocytes) and iii) a saturable absorption process. This was the first semi-mechanistic PK model of hydrocortisone model, which successfully could very well predict the observed data in paediatric patients (neonates-6 years) administered the same formulation (project 2).

The semi-mechanistic model was reduced to enable more reliable parameter estimates from the sparse phase II data in paediatric patients with adrenal insufficiency. Unfortunately, maturation effects could not be considered due to the sparse data situation, but slightly lower and higher CL was observed in neonates and infants, respectively. These findings were supported by the slightly lower and higher activity of 5α-reductase observed in neonates and infants [104]. In the future, the plasma protein binding model should also consider other steroids which also have a high affinity to CBG, such as deoxycortisol, corticosterone and 17-OHP [150]. This is of most importance to evaluate in

CAH patients, since this patient group has elevated 17-OHP concentrations which may compete with cortisol for the binding to CBG.

The paediatric PK model was further reduced to better describe the data in paediatric patients (7-17 years, project 3) with CAH administered hydrocortisone tablets. In addition, concentrations from a clinically-relevant biomarker (17-OHP) was used to establish a pharmacokinetic/pharmacodynamic model considering the cortisol-mediated inhibition of the 17-OHP synthesis and the circadian rhythm of 17-OHP. Since different baseline models for cortisol were used in the two paediatric studies, these results imply potential age dependent differences in HPA axis activity. Studies identifying age differences in HPA axis activity are needed to understand the level of endogenous synthesis in patients with CAH.

Overall, the present work advanced knowledge about the pharmacokinetics of hydrocortisone in paediatric patients in different age ranges as well as in healthy adults. Since our models represents simplified versions of the system, more mechanistic approaches such as quantitative systems pharmacology could be useful in the future. These approaches could be used to quantify the HPA axis (considering the respective hormones in the steroid synthesis) and the impact of disease on the HPA axis (i.e. disease model). These models could also be challenged with hydrocortisone and could potentially provide better understanding of cortisol concentrations than the models in the current thesis.

The pharmacokinetic and pharmacokinetic/pharmacodynamic knowledge gained in the current thesis was used for simulating exposure after different dosing regimens to assess the hydrocortisone therapy in paediatric patients with CAH.

In the first step, the semi-mechanistic PK model was used to predict exposure in a wide range of doses and for a wide range of BW. The simulations implied the need to define an exact dose to replicate physiological cortisol concentrations for paediatric individuals <20 kg.

In a second step, the established pharmacokinetic/pharmacodynamic model was used to evaluate treatment regimen given cortisol and 17-OHP based concentration targets. This analysis visualised the difficulties associated with mimicking the physiological cortisol concentrations, and also implied a slightly better performance by administering hydrocortisone four times daily dosing than three times daily dosing. In addition, a lower cortisol therapeutic concentration limit of 50 nmol/L was proposed based on physiological data and the cortisol concentration estimate resulting in 50% of the maximum inhibition of 17-OHP synthesis.

The current thesis supports the known difficulties with mimicking circadian cortisol concentrations by administering immediate release formulations. Use of modified release formulations of hydrocortisone may provide an appropriate solution for children who can swallow tablets. Available formulations of hydrocortisone suitable for neonates, infants and children not able to swallow tablets are, however, limited. Our results indicated a potential benefit of administering hydrocortisone four times daily. Studies in paediatric patients with adrenal insufficiency are of course needed to evaluate if a four times daily dosing regimen improves disease status. Prospective studies evaluating height gain, disease status, signs of androgen excess, electrolyte balance and other health aspects in the long term would also be useful to assess which dosing regimens are superior. Identification of covariates influencing the pharmacokinetics or pharmacodynamics and treatment outcome would further help to individualise therapy. This thesis represents a first step towards a more rational decision-making in the substitution therapy of hydrocortisone in paediatric patients with adrenal insufficiency, which was the ultimate aim of the current thesis.

6 Bibliography

[1] M. Rowland, T.N. Tozer. Clinical pharmacokinetics and pharmacodynamics: concepts and applications. Wolters Kluwer Health/Lippincott William & Wilkins, Philadelphia, 4th ed. (2011).

[2] H. Derendorf, B. Meibohm. Modeling of pharmacokinetic/pharmacodynamic (PKPD) relationships: concepts and perspectives. Pharm. Res., 16: 176–185 (1999).

[3] E.I. Ette, P.J. Williams, editors. Pharmacometrics: the science of quantitative pharmacology. John Wiley & Sone, Inc., Hoboken, New Jersey (2007).

[4] M. Jamei, G.L. Dickinson, A. Rostami-Hodjegan. A framework for assessing inter-individual variability in pharmacokinetics using virtual human populations and integrating general knowledge of physical chemistry, biology, anatomy, physiology and genetics: A tale of "bottom-up" vs "top-down" recognition. Drug Metab. Pharmacokinet., 24: 53–75 (2009).

[5] L. Aarons. Physiologically based pharmacokinetic modelling: A sound mechanistic basis is needed. Br. J. Clin. Pharmacol., 60: 581–583 (2005).

[6] Z.P. Parra-Guillen, J.M. Cendrós Carreras, C. Peraire, R. Obach, J. Prunynosa, E. Chetaille, I.F. Trocóniz. Population pharmacokinetic modelling of irosustat in postmenopausal women with oestrogen-receptor positive breast cancer incorporating non-linear red blood cell uptake. Pharm. Res., 32: 1493–1504 (2015).

[7] J.-S. van der Walt, Y. Hong, L. Zhang, M. Pfister, D.W. Boulton, M.O. Karlsson. A Nonlinear Mixed Effects Pharmacokinetic Model for Dapagliflozin and Dapagliflozin 3-O-glucuronide in Renal or Hepatic Impairment. CPT pharmacometrics Syst. Pharmacol., 2: 1–9 (2013).

[8] J.S. Barrett, O. Della Casa Alberighi, S. Läer, B. Meibohm. Physiologically based pharmacokinetic (PBPK) modeling in children. Clin Pharmacol Ther, 92: 40–9 (2012).

[9] N. Tsamandouras, A. Rostami-Hodjegan, L. Aarons. Combining the "bottom up" and "top down" approaches in pharmacokinetic modelling: Fitting PBPK models to observed clinical data. Br. J. Clin. Pharmacol., 79: 48–55 (2015).

[10] C. Cobelli, D. Foster, G. Toffolo. Tracer Kinetics in Biomedical Research: From data to model. Kluwer Academic/Plenum Publishers, New York (2000).

[11] L.B. Sheiner. The population approach to pharmacokinetic data analysis: rationale and

standard data analysis methods. Drug Metab. Rev., 15: 153–171 (1984).

[12] D.R. Mould, R.N. Upton. Basic concepts in population modeling, simulation, and model-based drug development. CPT pharmacometrics Syst. Pharmacol., 1: 1–14 (2012).

[13] S.B. Duffull, D.F.B. Wright, H.R. Winter. Interpreting population pharmacokinetic-pharmacodynamic analyses - a clinical viewpoint. Br. J. Clin. Pharmacol., 71: 807–14 (2011).

[14] E.I. Ette, P.J. Williams. Population pharmacokinetics I: Background, concepts, and models. Ann. Pharmacother., 38: 1702–1706 (2004).

[15] I.K. Minichmayr, A. Schaeftlein, J.L. Kuti, M. Zeitlinger, C. Kloft. Clinical Determinants of Target Non-Attainment of Linezolid in Plasma and Interstitial Space Fluid: A Pooled Population Pharmacokinetic Analysis with Focus on Critically Ill Patients. Clin. Pharmacokinet.,: 1–17 (2016).

[16] N. Holford, S.C. Ma, B. a Ploeger. Clinical Trial Simulation: A Review. Clin. Pharmacol. Ther., 88: 166–182 (2010).

[17] P.A. Milligan, M.J. Brown, B. Marchant, S.W. Martin, P.H. Van Der Graaf, N. Benson, G. Nucci, D.J. Nichols, R.A. Boyd, J.W. Mandema, S. Krishnaswami, S. Zwillich, D. Gruben, R.J. Anziano, T.C. Stock, R.L. Lalonde. Model Based Drug Development : a Rational Approach to Efficiently Accelerate Drug Development. Clin. Pharmacol. Ther., 93: 502–14 (2013).

[18] E. Manolis, R. Herold. Pharmacometrics for regulatory decision making: Status and perspective. Clin. Pharmacokinet., 50: 625–626 (2011).

[19] S. Marshall, R. Burghaus, V. Cosson, S. Cheung, M. Chenel, O. DellaPasqua, N. Frey, B. Hamrén, L. Harnisch, F. Ivanow, T. Kerbusch, J. Lippert, P. Milligan, S. Rohou, A. Staab, J. Steimer, C. Tornøe, S. Visser. Good Practices in Model-Informed Drug Discovery and Development: Practice, Application, and Documentation. CPT Pharmacometrics Syst. Pharmacol., 5: 93–122 (2016).

[20] L. Aarons, K. Ogungbenro. Optimal design of pharmacokinetic studies. Basic Clin. Pharmacol. Toxicol., 106: 250–255 (2010).

[21] K. Kretsos, A. Jullion, M. Zamacona, O. Harari, S. Shaw, B. Boulanger, R. Oliver. Model-Based Optimal Design and Execution of the First-Inpatient Trial of the Anti-IL-6, Olokizumab. CPT pharmacometrics Syst. Pharmacol., 3: 1–8 (2014).

[22] T. Sahota, O. Della Pasqua. Feasibility of a fixed-dose regimen of pyrazinamide and its impact

on systemic drug exposure and liver safety in patients with tuberculosis. Antimicrob. Agents Chemother., 56: 5442–5449 (2012).

[23] R.M. Hoglund, L. Workman, M.D. Edstein, N.X. Thanh, N.N. Quang, I. Zongo, J.B. Ouedraogo, S. Borrmann, L. Mwai, C. Nsanzabana, R.N. Price, P. Dahal, N.C. Sambol, S. Parikh, F. Nosten, E.A. Ashley, A.P. Phyo, K.M. Lwin, R. McGready, N.P.J. Day, P.J. Guerin, N.J. White, K.I. Barnes, J. Tarning. Population Pharmacokinetic Properties of Piperaquine in Falciparum Malaria: An Individual Participant Data Meta-Analysis. PLoS Med., 14: 1–23 (2017).

[24] N. Mehrotra, A. Bhattaram, J.C. Earp, J. Florian, K. Krudys, J.E. Lee, J.Y. Lee, J. Liu, Y. Mulugeta, J. Yu, P. Zhao, V. Sinha. Role of Quantitative Clinical Pharmacology in Pediatric Approval And Labeling. Drug Metab. Dispos., 44: 924–933 (2016).

[25] E. Kimland, V. Odlind. Off-label drug use in pediatric patients. Clin. Pharmacol. Ther., 91: 796–801 (2012).

[26] American academy of pediatrics. Age terminology during the perinatal period. Pediatrics, 114: 1362–4 (2004).

[27] W.A. Marshall, J.M. Tanner. Variations in the Pattern of Pubertal Changes in Boys. Arch. Dis. Child., 45: 13–23 (1970).

[28] W.A. Marshall, J.M. Tanner. Variations in the Pattern of Pubertal Changes in Girls. Arch. Dis. Child., 44: 291–303 (1969).

[29] B.J. Anderson, N.H.G. Holford. Understanding dosing: children are small adults, neonates are immature children. Arch. Dis. Child., 98: 737–44 (2013).

[30] R.F.W. De Cock, C. Piana, E.H.J. Krekels, M. Danhof, K. Allegaert, C.A.J. Knibbe. The role of population PK-PD modelling in paediatric clinical research. Eur. J. Clin. Pharmacol., 67: S5–S16 (2011).

[31] S.R.C. Howie. Blood sample volumes in child health research: review of safe limits. Bull. World Health Organ., 89: 46–53 (2011).

[32] L.C. Ku, P.B. Smith. Dosing in neonates: special considerations in physiology and trial design. Pediatr Res, 77: 2–9 (2015).

[33] European Medicines Agency. Paediatric Regulation [Internet]. [cited 2017 Mar 28]

[34] US Food and Drug administration. Pediatric Product Development [Internet]. [cited 2017 Mar 28]

[35] J. Olsson, E. Kimland, S. Pettersson, V. Odlind. Paediatric drug use with focus on off-label prescriptions in Swedish outpatient care - A nationwide study. Acta Paediatr. Int. J. Paediatr., 100: 1272–1275 (2011).

[36] E. Kimland, P. Nydert, V. Odlind, Y. Böttiger, S. Lindemalm. Paediatric drug use with focus on off-label prescriptions at Swedish hospitals - A nationwide study. Acta Paediatr. Int. J. Paediatr., 101: 772–778 (2012).

[37] B. Horen, J.L. Montastruc, M. Lapeyre-Mestre. Adverse drug reactions and off-label drug use in paediatric outpatients. Br. J. Clin. Pharmacol., 54: 665–670 (2002).

[38] L. Cuzzolin, A. Atzei, V. Fanos. Off-label and unlicensed prescribing for newborns and children in different settings: a review of the literature and a consideration about drug safety. Expert Opin. Drug Saf., 5: 703–18 (2006).

[39] P.W. Speiser, R. Azziz, L.S. Baskin, L. Ghizzoni, T.W. Hensle, D.P. Merke, H.F.L. Meyer-Bahlburg, W.L. Miller, V.M. Montori, S.E. Oberfield, M. Ritzen, P.C. White. Congenital adrenal hyperplasia due to steroid 21-hydroxylase deficiency: an Endocrine Society clinical practice guideline. J. Clin. Endocrinol. Metab., 95: 4133–60 (2010).

[40] M.J. Whitaker, S. Spielmann, D. Digweed, H. Huatan, D. Eckland, T.N. Johnson, G. Tucker, H. Krude, O. Blankenstein, R.J. Ross. Development and testing in healthy adults of oral hydrocortisone granules with taste masking for the treatment of neonates and infants with adrenal insufficiency. J. Clin. Endocrinol. Metab., 100: 1681–1688 (2015).

[41] U. Neumann, D. Burau, S. Spielmann, M.J. Whitaker, R.J. Ross, C. Kloft, O. Blankenstein. Quality of compounded hydrocortisone capsules used in the treatment of children. Eur. J. Endocrinol., 177: 239–242 (2017).

[42] D.P. Merke, D. Cho, K.A. Calis, M.F. Keil, G.P. Chrousos. Hydrocortisone Suspension and Hydrocortisone Tablets Are Not Bioequivalent In the Treatment of Children with Congenital Adrenal Hyperplasia. J. Clin. Endocrinol. Metab., 86: 441–445 (2001).

[43] E.M.A. Human Medicined Development and Evaluation. Revised priority list for studies on off-patent paediatric medicinal products [Internet]. EMA/PDCO/98717/2012 Rev. 2013/14. : 12 (2010).

[44] The TAIN project [Internet].

[45] R. Perry, O. Kecha, J. Paquette, C. Huot, G. Van Vliet, C. Deal. Primary adrenal insufficiency in

children: Twenty years experience at the Sainte-Justine Hospital, Montreal. J. Clin. Endocrinol. Metab., 90: 3243–3250 (2005).

[46] G.P. Chrousos. Stress and disorders of the stress system. Nat. Rev. Endocrinol., 5: 374–81 (2009).

[47] N. Nader, G.P. Chrousos, T. Kino. Interactions of the Circadian CLOCK System and the HPA Axis. Trends Endocrinol. Metab., 21: 277–286 (2010).

[48] J. Porter, J. Blair, R.J. Ross. Is physiological glucocorticoid replacement important in children? Arch. Dis. Child., 102: 199–205 (2017).

[49] C. Tsigos, G.P. Chrousos. Hypothalamic – pituitary – adrenal axis , neuroendocrine factors and stress. 53: 865–871 (2002).

[50] C. De Weerth, R.H. Zijl, J.K. Buitelaar. Development of cortisol circadian rhythm in infancy. Early Hum. Dev., 73: 39–52 (2003).

[51] D.A. Price, G.C. Close, B.A. Fielding. Age of appearance of circadian rhythm in salivary cortisol values in infancy. Arch. Dis. Child., 58: 454–6 (1983).

[52] K.W. Hindmarsh, L. Tan, K. Sankaran, V.A. Laxdal. Diurnal Rhythms of Cortisol, ACTH, and beta-Endorphin Levels in Neonates and Adults. West. J. Med., 151: 153–156 (1989).

[53] U. Knutsson, J. Dahlgren, C. Marcus, S. Rosberg, M. Brönnegård, P. Stierna, K. Albertsson-Wikland. Circadian cortisol rhythms in healthy boys and girls: relationship with age, growth, body composition, and pubertal development. J. Clin. Endocrinol. Metab., 82: 536–40 (1997).

[54] M. Gröschl, M. Rauh, H.-G. Dörr. Circadian rhythm of salivary cortisol, 17α-hydroxyprogesterone, and progesterone in healthy children. Clin. Chem., 49: 1688–1691 (2003).

[55] H.J. van der Kamp, J.M. Wit. Neonatal screening for congenital adrenal hyperplasia. Eur. J. Endocrinol., 151: U71–U75 (2004).

[56] P.W. Speiser, P.C. White. Congenital adrenal hyperplasia. N. Engl. J. Med., 349: 776–88 (2003).

[57] E.A. Webb, N. Krone. Current and novel approaches to children and young people with congenital adrenal hyperplasia and adrenal insufficiency. Best Pract. Res. Clin. Endocrinol. Metab., 29: 449–468 (2015).

[58] G.E. Bacon, M.L. Spencer, R.P. Kelch. Effect of cortisol treatment on hormonal relationships in

congenital adrenal hyperplasia. Clin. Endocrinol. (Oxf)., 6: 113–126 (1977).

[59] H. Frisch, K. Parth, E. Schober, W. Swoboda. Circadian patterns of plasma cortisol, 17-hydroxyprogesterone, and testosterone in congenital adrenal hyperplasia. Arch. Dis. Child., 56: 208–13 (1981).

[60] P.W. Speiser. Congenital adrenal hyperplasia owing to 21-hydroxylase deficiency. Endocr. Rev., 21: 245–291 (2000).

[61] D.P. Merke, S.R. Bornstein. Congenital adrenal hyperplasia. Lancet, 365: 2125–2136 (2005).

[62] P.M. Mah, R.C. Jenkins, A. Rostami-Hodjegan, J. Newell-Price, A. Doane, V. Ibbotson, G.T. Tucker, R.J. Ross. Weight-related dosing, timing and monitoring hydrocortisone replacement therapy in patients with adrenal insufficiency. Clin. Endocrinol. (Oxf)., 61: 367–75 (2004).

[63] S.R. Bornstein, B. Allolio, W. Arlt, A. Barthel, A. Don-Wauchope, G.D. Hammer, E.S. Husebye, D.P. Merke, M.H. Murad, C.A. Stratakis, D.J. Torpy. Diagnosis and treatment of primary adrenal insufficiency: An endocrine society clinical practice guideline. J. Clin. Endocrinol. Metab., 101: 364–389 (2016).

[64] P.C. Hindmarsh, E. Charmandari. Variation in absorption and half-life of hydrocortisone influence plasma cortisol concentrations. Clin. Endocrinol. (Oxf)., 82: 557–561 (2015).

[65] H. Derendorf, H. Mollmann, J. Barth, C. Mollmann, S. Tunn, M. Krieg. Pharmacokinetics and oral bioavailability of hydrocortisone. J Clin Pharm, 31: 473–476 (1991).

[66] P.C. Hindmarsh. The child with difficult to control Congenital Adrenal Hyperplasia: Is there a place for continuous subcutaneous hydrocortisone therapy. Clin. Endocrinol. (Oxf)., 81: 15–18 (2014).

[67] S.R. Peacey, C.Y. Guo, A.M. Robinson, A. Price, M.A. Giles, R. Eastell, A.P. Weetman. Glucocorticoid replacement therapy: are patients over treated and does it matter? Clin. Endocrinol. (Oxf)., 46: 255–61 (1997).

[68] G. Noppe, E.F.C. Van Rossum, J. Vliegenthart, J.W. Koper, E.L.T. Van Den Akker. Elevated hair cortisol concentrations in children with adrenal insufficiency on hydrocortisone replacement therapy. Clin. Endocrinol. (Oxf)., 81: 820–825 (2014).

[69] R.D. Toothaker, G.M. Sundaresan, J.P. Hunt, T.J. Goehl, K.S. Rotenberg, V.K. Prasad, W.A. Craig, P.G. Welling. Oral Hydrocortisone Pharmacokinetics: A comparison of Fluorescence and Ultraviolet High-pressure Liquid. J. Pharm. Sci., 71: 573–576 (1982).

[70] R.D. Toothaker, P.G. Welling. Effect of Dose Size on the Pharmacokinetics of Intravenous Hydrocortisone During Endogenous Hydrocortisone Suppression. J. Pharmacokinet. Biopharm., 10: 147–156 (1982).

[71] R.D. Toothaker, W.A. Craig, P.G. Welling. Effect of dose size on the pharmacokinetics of oral hydrocortisone suspension. J. Pharm. Sci., 71: 1182–5 (1982).

[72] R.B. Patel, M.C. Rogge, A. Selen, T.J. Goehl, V.P. Shah, V.K. Prasad, P.G. Welling. Bioavailability of hydrocortisone from commercial 20-mg tablets. J. Pharm. Sci., 73: 964–966 (1984).

[73] S. Tunn, H. Möllmann, J. Barth, H. Derendorf, M. Krieg. Simultaneous measurement of cortisol in serum and saliva after different forms of cortisol administration. Clin. Chem., 38: 1491–1494 (1992).

[74] N. Simon, F. Castinetti, F. Ouliac, N. Lesavre, T. Brue, C. Oliver. Pharmacokinetic evidence for suboptimal treatment of adrenal insufficiency with currently available hydrocortisone tablets. Clin. Pharmacokinet., 49: 455–63 (2010).

[75] A.H. Thomson, M.C. Devers, A.M. Wallace, D. Grant, K. Campbell, M. Freel, J.M.C. Connell. Variability in hydrocortisone plasma and saliva pharmacokinetics following intravenous and oral administration to Patients with adrenal insufficiency. Clin. Endocrinol. (Oxf)., 66: 789–796 (2007).

[76] V. Heazelwood, J. Galligan, G. Cannell, F. Bochner, R. Mortimer. Plasma cortisol delivery from oral cortisol and cortisone acetate: relative bioavailability. Br. J. Clin. Pharmacol., 17: 55–59 (1984).

[77] E. Charmandari, D.R. Matthews, A. Johnston, C.G. Brook, P.C. Hindmarsh. Serum cortisol and 17-hydroxyprogesterone interrelation in classic 21-hydroxylase deficiency: is current replacement therapy satisfactory? J. Clin. Endocrinol. Metab., 86: 4679–85 (2001).

[78] E. Charmandari, A. Johnston, C.G. Brook, P.C. Hindmarsh. Bioavailability of oral hydrocortisone in patients with congenital adrenal hyperplasia due to 21-hydroxylase deficiency. J. Endocrinol., 169: 65–70 (2001).

[79] E. Charmandari, P.C. Hindmarsh, A. Johnston, C.G. Brook. Congenital adrenal hyperplasia due to 21-hydroxylase deficiency: alterations in cortisol pharmacokinetics at puberty. J. Clin. Endocrinol. Metab., 86: 2701–8 (2001).

[80] K. Sarafoglou, C.L. Zimmerman, Þ.M.T. Gonzalez-bolanos, B.A. Willis, R. Brundage.

Interrelationships Among Cortisol , Exposures in the Management of Children With Congenital Adrenal Hyperplasia. 63: 35–41 (2015).

[81] H.E. Vezina, C.M. Ng, D.M. Vazquez, J.D. Barks, V. Bhatt-Mehta. Population pharmacokinetics of unbound hydrocortisone in critically ill neonates and infants with vasopressor-resistant hypotension. Pediatr. Crit. Care Med., 15: 546–53 (2014).

[82] G.L. Amidon, H. Lennernäs, V.P. Shah, J.R. Crison. A Theoretical Basis for a Biopharmaceutic Drug Classification: The Correlation of In Vitro Drug Product Dissolution and In Vivo Bioavailability. Pharm. Res., 12: 413–420 (1995).

[83] H. Lennernäs, S. Skrtic, G. Johannsson. Replacement therapy of oral hydrocortisone in adrenal insufficiency: the influence of gastrointestinal factors. Expert Opin. Drug Metab. Toxicol., 4: 749–758 (2008).

[84] B.L. Pedersen, H. Brøndsted, H. Lennernäs, F.N. Christensen, A. Müllertz, H.G. Kristensen. Dissolution of hydrocortisone in human and simulated intestinal fluids. Pharm. Res., 17: 183–189 (2000).

[85] K. Sarafoglou, J.H. Himes, J.M. Lacey, B.C. Netzel, R.J. Singh, D. Matern. Comparison of multiple steroid concentrations in serum and dried blood spots throughout the day of patients with congenital adrenal hyperplasia. Horm. Res. pædiatrics, 75: 19–25 (2011).

[86] J.M. Custodio, C.-Y. Wu, L.Z. Benet. Predicting drug disposition, absorption/elimination/transporter interplay and the role of food on drug absorption. Adv. Drug Deliv. Rev., 60: 717–733 (2008).

[87] G.L. Kearns. Impact of developmental pharmacology on pediatric study design: Overcoming the challenges. J. Allergy Clin. Immunol., 106: S128–S138 (2000).

[88] G. Heimann. Enteral absorption and bioavailability in children in relation to age. Eur. J. Clin. Pharmacol., 18: 43–50 (1980).

[89] I.H. Bartelink, C.M.A. Rademaker, A.F.A.M. Schobben, J.N. Van Den Anker. Guidelines on paediatric dosing on the basis of developmental physiology and pharmacokinetic considerations. Clin. Pharmacokinet., 45: 1077–1097 (2006).

[90] E.G.W.M. Lentjes, F.H.T.P.M. Romijn. Temperature-Dependent Cortisol Distribution among the Blood Compartments in Man. J. Clin. Endocrinol. Metab., 84: 682–687 (1999).

[91] J.G. Lewis, M.G. Lewis, P.A. Elder. An enzyme-linked immunosorbent assay for corticosteroid-

binding globulin using monoclonal and polyclonal antibodies: Decline in CBG following synthetic ACTH. Clin. Chim. Acta, 328: 121–128 (2003).

[92] T. Peters Jr. All about Albumin: Biochemistry, Genetics, and Medical Applications. Academic Press, Oxford, UK (1996).

[93] S.L. Tsai, K.J. Seiler, J. Jacobson. Morning cortisol levels affected by sex and pubertal status in children and young adults. J. Clin. Res. Pediatr. Endocrinol., 5: 85–89 (2013).

[94] J.-L. Coolens, H.V.A.N. Baelen, W. Heyns. Clinical use of unbound plasma cortisol as calculated from total cortisol and corticosteroid-binding globulin. J steroid Biochem, 26: 197–202 (1987).

[95] D.E. Henley, S.L. Lightman. New insights into corticosteroid-binding globulin and glucocorticoid delivery. Neuroscience, 180: 1–8 (2011).

[96] J.G. Lewis, B. Möpert, B.I. Shand, M.P. Doogue, S.G. Soule, C.M. Frampton, P.A. Elder. Plasma variation of corticosteroid-binding globulin and sex hormone-binding globulin. Horm. Metab. Res., 38: 241–245 (2006).

[97] M. Debono, R.F. Harrison, M.J. Whitaker, D. Eckland, W. Arlt, B.G. Keevil, R.J. Ross. Salivary cortisone reflects cortisol exposure under physiological conditions and after hydrocortisone. J. Clin. Endocrinol. Metab., (2016).

[98] T.T. Chung, K. Gunganah, J.P. Monson, W.M. Drake. Circadian variation in serum cortisol during hydrocortisone replacement is not attributable to changes in cortisol-binding globulin concentrations. Clin. Endocrinol. (Oxf)., 84: 496–500 (2016).

[99] M. Strolin Benedetti, R. Whomsley, E.L. Baltes. Differences in absorption, distribution, metabolism and excretion of xenobiotics between the paediatric and adult populations. Expert Opin. Drug Metab. Toxicol., 1: 447–71 (2005).

[100] A.J. Hadjian, M. Chedin, C. Cochet, E.M. Chambaz. Cortisol Binding to Proteins in Plasma in the Human Neonate and Infant. Pediatr. Res., 9: 40–45 (1975).

[101] J.W. Tomlinson, P.M. Stewart. Cortisol metabolism and the role of 11β-hydroxysteroid dehydrogenase. Best Pract. Res. Clin. Endocrinol. Metab., 15: 61–78 (2001).

[102] M. Hoshiro, Y. Ohno, H. Masaki, H. Iwase, N. Aoki. Comprehensive study of urinary cortisol metabolites in hyperthyroid and hypothyroid patients. Clin. Endocrinol. (Oxf)., 64: 37–45 (2006).

[103] S.L. Rogers, B. a Hughes, C. a Jones, L. Freedman, K. Smart, N. Taylor, P.M. Stewart, C.H.L.

Shackleton, N.P. Krone, J. Blissett, J.W. Tomlinson. Diminished 11β-hydroxysteroid dehydrogenase type 2 activity is associated with decreased weight and weight gain across the first year of life. J. Clin. Endocrinol. Metab., 99: E821–31 (2014).

[104] S.A. Wudy, M.F. Hartmann, T. Remer. Sexual dimorphism in cortisol secretion starts after age 10 in healthy children: urinary cortisol metabolite excretion rates during growth. Am. J. Physiol. Endocrinol. Metab., 293: E970–E976 (2007).

[105] D.E. Mager, S.X. Lin, R. a Blum, C.D. Lates, W.J. Jusko. Dose equivalency evaluation of major corticosteroids: pharmacokinetics and cell trafficking and cortisol dynamics. J. Clin. Pharmacol., 43: 1216–1227 (2003).

[106] M.O. Karlsson, L.B. Sheiner. The importance of modeling interoccasion variability in population pharmacokinetic analyses. J. Pharmacokinet. Biopharm., 21: 735–50 (1993).

[107] U. Wählby, A.H. Thomson, P.A. Milligan, M.O. Karlsson. Models for time-varying covariates in population pharmacokinetic-pharmacodynamic analysis. Br. J. Clin. Pharmacol., 58: 367–77 (2004).

[108] L.B. Sheiner, S.L. Beal. Evaluation of methods for estimating population pharmacokinetics parameters. I. Michaelis-Menten model: routine clinical pharmacokinetic data. J. Pharmacokinet. Biopharm., 8: 553–71 (1980).

[109] J.S. Owen, J. Fiedler-Kelly. Introduction to Population Pharmacokinetic/Pharmacodynamic Analysis with Nonlinear Mixed Effect Models. John Wiley & Sone, Inc., Hoboken, New Jersey (2014).

[110] Å.M. Johansson, S. Ueckert, E.L. Plan, A.C. Hooker, M.O. Karlsson. Evaluation of bias, precision, robustness and runtime for estimation methods in NONMEM 7. J. Pharmacokinet. Pharmacodyn., 41: 223–238 (2014).

[111] R.J. Bauer, S. Guzy, C. Ng. A survey of population analysis methods and software for complex pharmacokinetic and pharmacodynamic models with examples. AAPS J., 9: E60–83 (2007).

[112] S. Beal, L.B. Sheiner, A. Boeckmann, R.J. Bauer. NONMEM User's Guides. (1989-2009). Icon Development Solutions, Ellicott City, MD, USA (2009).

[113] C. Dansirikul, H.E. Silber, M.O. Karlsson. Approaches to handling pharmacodynamic baseline responses. J. Pharmacokinet. Pharmacodyn., 35: 269–83 (2008).

[114] J.E. Ahn, M.O. Karlsson, A. Dunne, T.M. Ludden. Likelihood based approaches to handling data

below the quantification limit using NONMEM VI. J. Pharmacokinet. Pharmacodyn., 35: 401–21 (2008).

[115] S.L. Beal. Ways to fit a PK model with some data below the quantification limit. J. Pharmacokinet. Pharmacodyn., 28: 481–504 (2001).

[116] W. Byon, C. V. Fletcher, R.C. Brundage. Impact of censoring data below an arbitrary quantification limit on structural model misspecification. J. Pharmacokinet. Pharmacodyn., 35: 101–116 (2008).

[117] X.S. Xu, A. Dunne, H. Kimko, P. Nandy, A. Vermeulen. Impact of low percentage of data below the quantification limit on parameter estimates of pharmacokinetic models. J. Pharmacokinet. Pharmacodyn., 38: 423–432 (2011).

[118] M. Bergstrand, M.O. Karlsson. Handling data below the limit of quantification in mixed effect models. AAPS J., 11: 371–80 (2009).

[119] P.L. Bonate. Pharmacokinetic-Pharmacodynamic Modeling and Simulation [Internet]. Kluwer Academic Publishers, Boston, 1st ed. (2006).

[120] A.C. Hooker, C.E. Staatz, M.O. Karlsson. Conditional weighted residuals (CWRES): a model diagnostic for the FOCE method. Pharm. Res., 24: 2187–97 (2007).

[121] D.R. Mould, R.N. Upton. Basic concepts in population modeling, simulation, and model-based drug development-part 2: introduction to pharmacokinetic modeling methods. CPT pharmacometrics Syst. Pharmacol., 2: 1–14 (2013).

[122] M. Bergstrand, A.C. Hooker, J.E. Wallin, M.O. Karlsson. Prediction-corrected visual predictive checks for diagnosing nonlinear mixed-effects models. AAPS J., 13: 143–51 (2011).

[123] N. Holford, M.O. Karlsson. Model Evaluation Visual Predictive Checks [Internet]. : 1–17 (2008).

[124] L. Lindbom, P. Pihlgren, E.N. Jonsson, N. Jonsson. PsN-Toolkit--a collection of computer intensive statistical methods for non-linear mixed effect modeling using NONMEM. Comput. Methods Programs Biomed., 79: 241–57 (2005).

[125] LLP user guide.

[126] S. Sadray, E.N. Jonsson, M.O. Karlsson. Likelihood-Based Diagnostics for Influential Individuals in Non-Linear Mixed Effects Model Selection. Pharm. Res., 16: 1260–1264 (1999).

[127] P.L. Bonate. Pharmacokinetic-Pharmacodynamic Modeling and Simulation. 2nd ed. (2011).

[128] R.J. Keizer, M.O. Karlsson, A. Hooker. Modeling and Simulation Workbench for NONMEM: Tutorial on Pirana, PsN, and Xpose. CPT pharmacometrics Syst. Pharmacol., 2: 1–9 (2013).

[129] F.B. Zedat. Soroban [Internet]. [cited 2017 Jul 7]

[130] R.C.T. (R F. for S. Computing). R: A Language and Environment for Statistical Computing [Internet]. Vienna, Austria (2016).

[131] H. Wickham. Elegant Graphics for Data Analysis [Internet]. Springer-Verlag New York (2009).

[132] R. Keizer, D. Pastoor, R. Savic. New open source R libraries for simulation and visualization: "PKPDsim" and "vpc" [Internet]. (2015).

[133] J.R. Williams. The Declaration of Helsinki and public health. Bull. World Health Organ., 86: 650–652 (2008).

[134] Association of the British Pharmaceutical Industry. Guidelines for phase 1 clinical trials. Abpi, (2012).

[135] ICH Steering Committee. Guideline for good clinical practice E6(R1). GUIDELINE FOR GOOD CLINICAL PRACTICE. : i–53 (1996).

[136] United Kingdom Government. The Medicines for Human Use (Clinical Trials) Regulations 2004 [Internet]. (2004).

[137] J. Melin, Z.P. Parra-Guillen, N. Hartung, W. Huisinga, R.J. Ross, M.J. Whitaker, C. Kloft. Predicting Cortisol Exposure from Paediatric Hydrocortisone Formulation Using a Semi-Mechanistic Pharmacokinetic Model Established in Healthy Adults. Clin. Pharmacokinet., 57: 515–527 (2018).

[138] R.L. Jones, L.J. Owen, J.E. Adaway, B.G. Keevil. Simultaneous analysis of cortisol and cortisone in saliva using XLC-MS/MS for fully automated online solid phase extraction. J. Chromatogr. B Anal. Technol. Biomed. Life Sci., 881-882: 42–48 (2012).

[139] A. Rohatgi. WebPlotDigitizer [Internet]. 3.10, Austin, Texas, USA (2016).

[140] P.O. Gisleskog, M.O. Karlsson, S.L. Beal. Use of prior information to stabilize a population data analysis. J. Pharmacokinet. Pharmacodyn., 29: 473–505 (2002).

[141] B.J. Anderson, N.H.G. Holford. Tips and traps analyzing pediatric PK data. Paediatr. Anaesth., 21: 222–37 (2011).

[142] J. Venitz. Pharmacokinetic-pharmacodynamic modelling of reversible drug effects. In: .

Derendorf H, Hochhaus G (Eds.). Handbook of Pharmacokinetic/Pharmacodynamic correlation. CRC Press, Boca Raton: 1–34 (1995).

[143] G. Hempel, M. Karlsson, D.I. De Alwis, N. Toublanc. Population pharmacokinetic-pharmacodynamic modeling of moxonidine using 24-hour ambulatory blood pressure measurements. Clin. Pharmacol. Ther., 64: 622–635 (1998).

[144] C.W. Tornøe, H. Agersø, H.A. Nielsen, H. Madsen, E.N. Jonsson. Pharmacokinetic/pharmacodynamic modelling of GnRH antagonist degarelix: A comparison of the non-linear mixed-effects programs NONMEM and NLME. J. Pharmacokinet. Pharmacodyn., 31: 441–461 (2004).

[145] K.C. Carlsson, R.M. Savić, A.C. Hooker, M.O. Karlsson. Modeling subpopulations with the $MIXTURE subroutine in NONMEM: finding the individual probability of belonging to a subpopulation for the use in model analysis and improved decision making. AAPS J., 11: 148–154 (2009).

[146] C.J. Peters, N. Hill, M.T. Dattani, E. Charmandari, D.R. Matthews, P.C. Hindmarsh. Deconvolution analysis of 24-h serum cortisol profiles informs the amount and distribution of hydrocortisone replacement therapy. Clin. Endocrinol. (Oxf)., 78: 347–51 (2013).

[147] F. Schindel. Consideration of endogenous backgrounds in pharmacokinetic analyses: a simulation study. Eur. J. Clin. Pharmacol., 56: 685–688 (2000).

[148] U. Westphal. Steroid-Protein Interactions. Springer-Verlag Berlin Heidelberg New York, New York, 1st ed. (1971).

[149] U. Westphal. Steroid-Protein Interactions XIII. COncentrations and Binding Affinities of Corticosteroid-Binding Globulings in Sera of Man, Monkey, Rat, Rabbit and Guinea pig. Arch. Biochem. Biophys., 118: 556–567 (1967).

[150] J.F. Dunn, B.C. Nisula, D. Rodbard. Transport of Steroid Hormones : Binding of 21 Endogenous Steroids to Both Testosterone-Binding Globulin and Corticosteroid-Binding Globulin in Human Plasma. J. Clin. Endocrinol. Metab., 53: 58–68 (1981).

[151] L.Z. Benet, B. Hoener. Changes in plasma protein binding have little clinical relevance. Clin. Pharmacol. Ther., 71: 115–21 (2002).

[152] World Health Organisation. WHO Child Growth Standards [Internet]. (2006).

[153] E.G.W.M. Lentjes, F.P.T.H.M. Romijn, A.J. Molenaar. Isotope Effect in the Binding of Tritium

and 14C-labelled Cortisol to Corticosteroid-binding-globulin in Serum. J. Steroid Biochem. Mol. Biol., 60: 255–260 (1997).

[154] J.A. Roberts, J. Lipman. Pharmacokinetic issues for antibiotics in the critically ill patient. Crit. Care Med., 37: 840–851 (2009).

[155] M. Ahmed, K. Sarafoglou, M. Al-Kofahi, G.-B. MT, B. RC. A model-based pharmacokinetic/pharmacodynamic analysis of hydrocortisone, 17-hydroxyprogesterone (17OHP), and androstenedione (D4A) in children with congenital adrenal hyperplasia (CAH). J. Pharmacokinet. Pharmacodyn., 43: S89 (2016).

7 Appendix

7.1 Supplementary figures

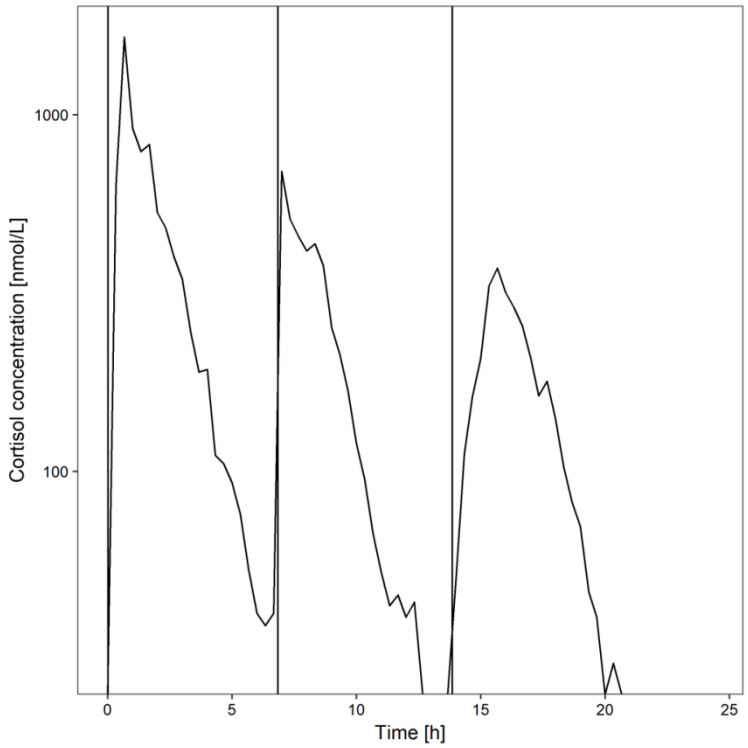

Figure 7.1 Cortisol concentration-time profile including the confirmed dose times (vertical lines) for one patient.

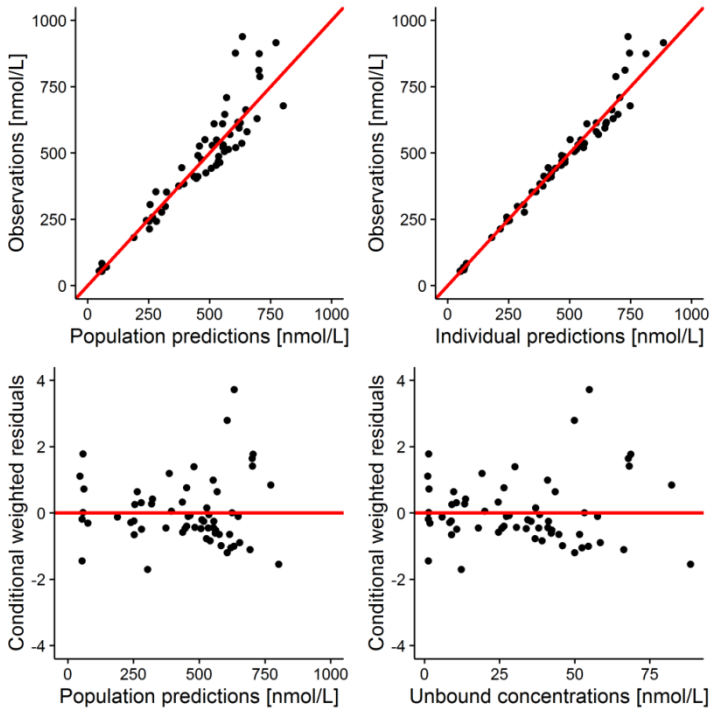

Figure 7.2 Goodness of fit plots for base plasma protein binding model including both a nonlinear and linear component

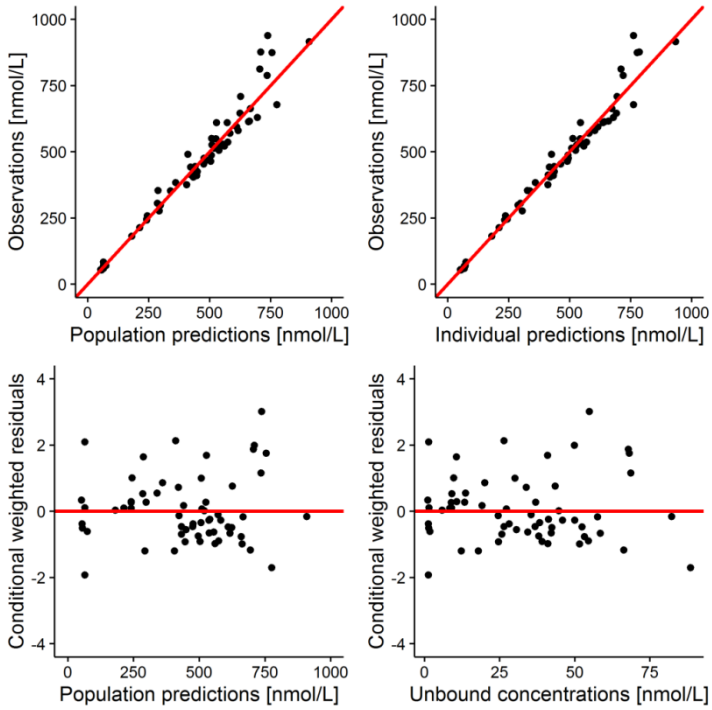

Figure 7.3 Goodness of fit plots for final plasma protein binding model

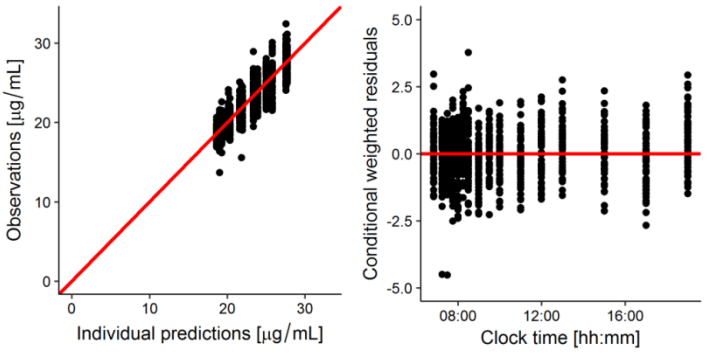

Figure 7.4 Goodness of fit plots for corticosteroid-binding globulin (CBG) model with constant baseline estimated on CBG concentrations during daytime (07:00-19:00).

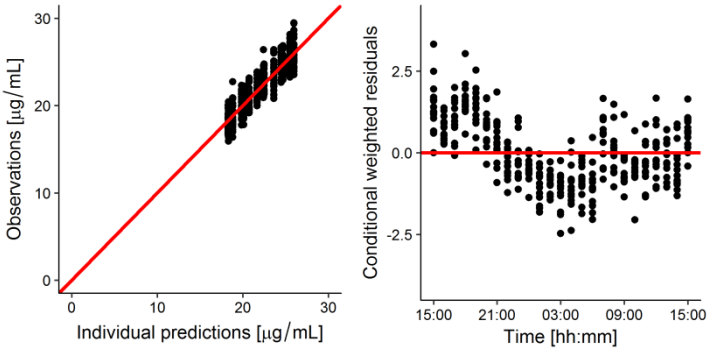

Figure 7.5 Goodness of fit plots for corticosteroid-binding globulin (CBG) model with constant baseline estimated on CBG concentrations during 24 h (15.00-15:00)

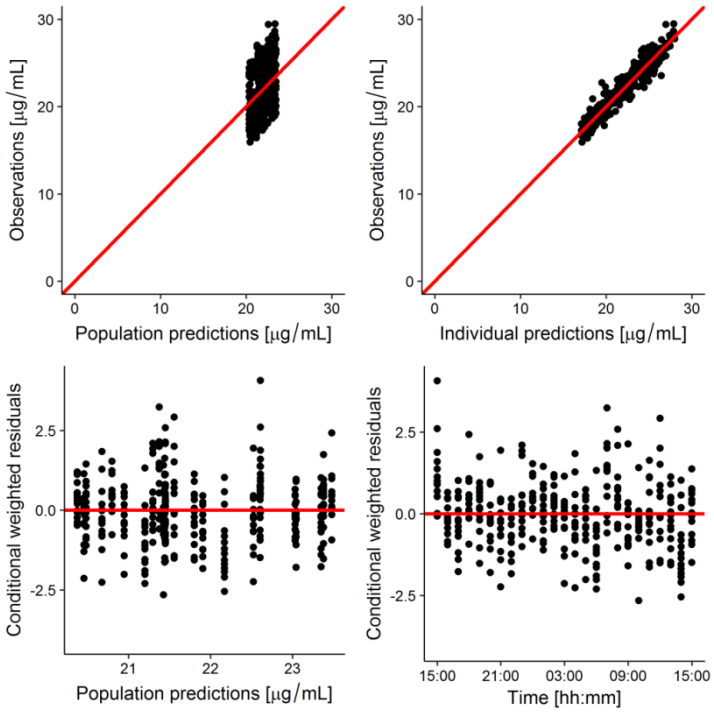

Figure 7.6 Goodness of fit plots for circadian corticosteroid-binding globulin (CBG) model estimated on CBG concentrations during 24 h (15:00 day 1-15:00 day 2).

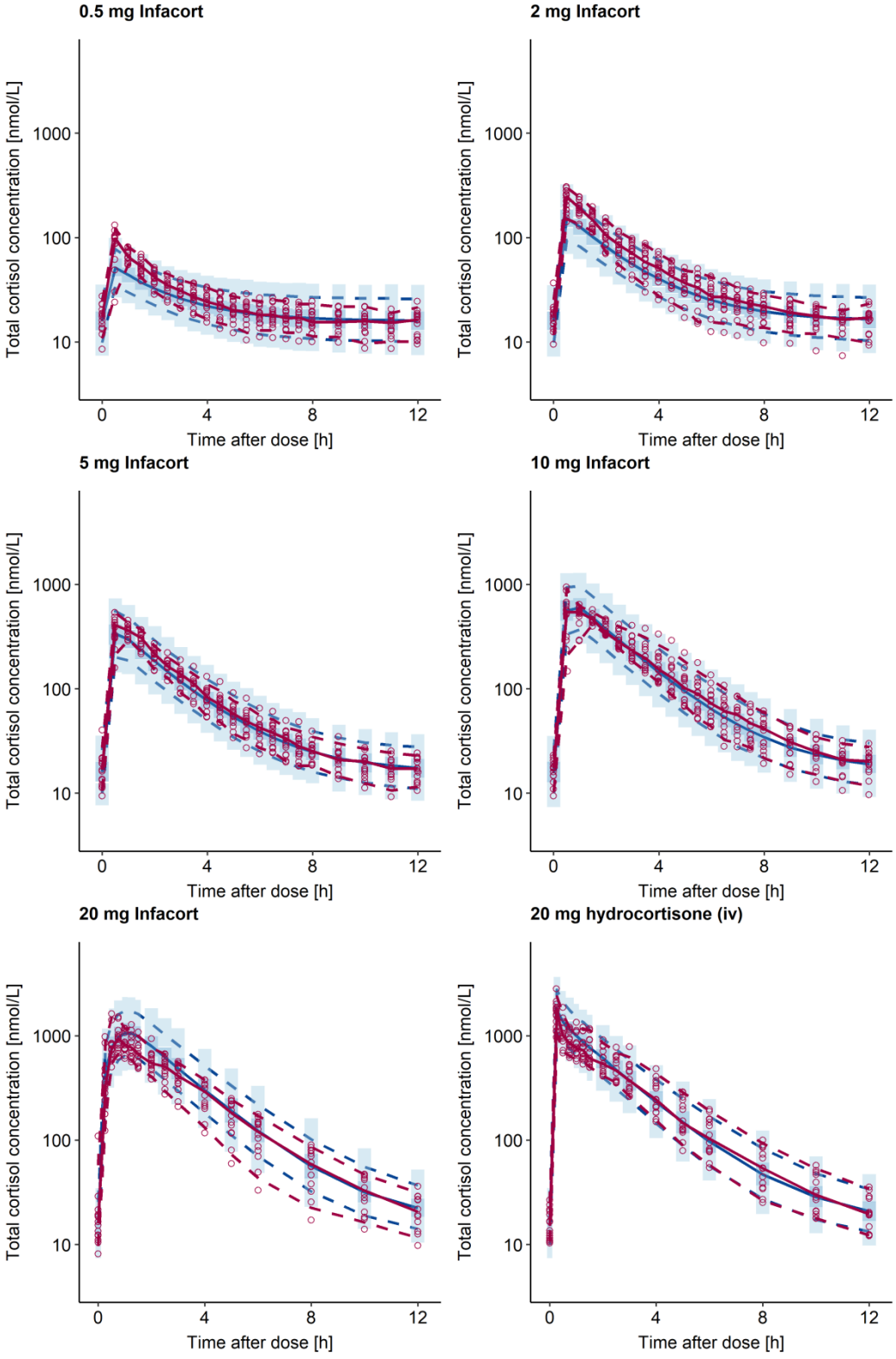

Figure 7.7 Visual predictive check (n=1000) for a two-compartmental pharmacokinetic model including saturable absorption. Lines: the 5th, 50th and 95th percentiles of observed (red) and simulated (blue) data; corresponding areas: 95% confidence interval around the simulated percentiles; circles: observations.

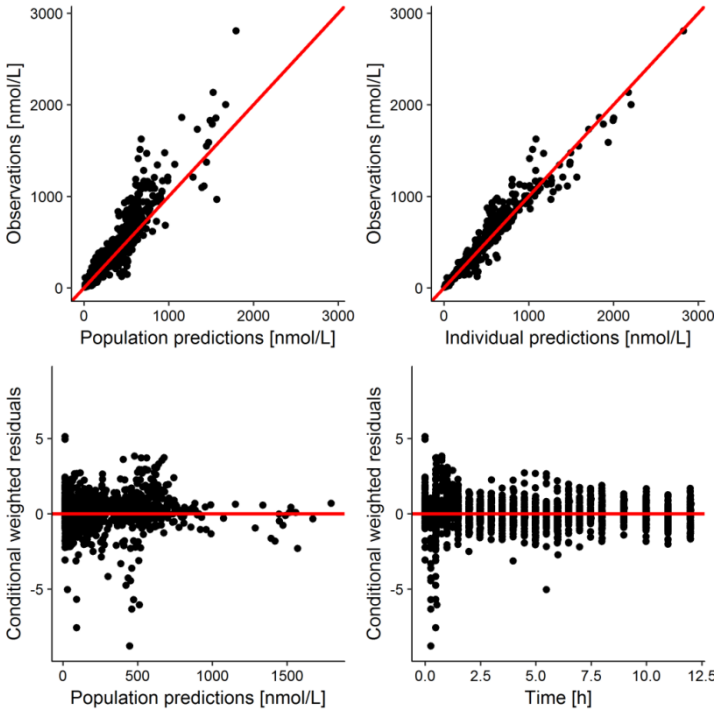

Figure 7.8 Goodness of fit plots for final semi-mechanistic pharmacokinetic model for hydrocortisone.

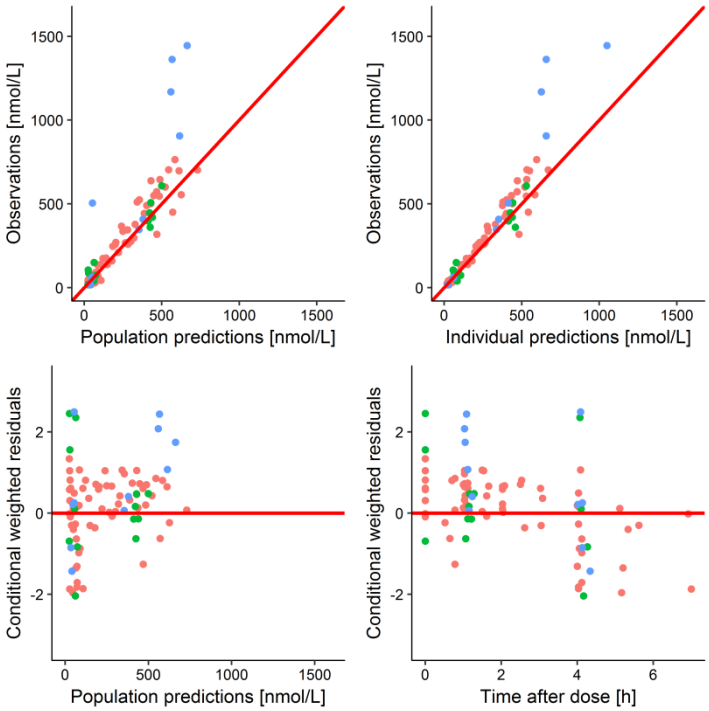

Figure 7.9 Goodness of fit plots for paediatric pharmacokinetic model re-estimating *only* key parameters based on *only* paediatric data and estimating a constant baseline for children (pink), infants (green) and neonates (blue).

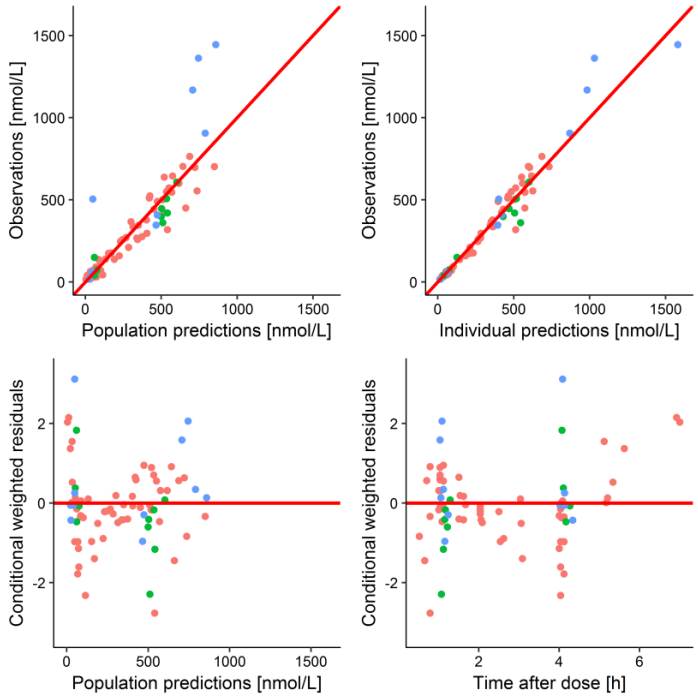

Figure 7.10 Goodness of fit plots for paediatric pharmacokinetic model re-estimating *only* key parameters based on *only* paediatric data and using the *measured* pre-dose concentration to inform the model for children (pink), infants (green) and neonates (blue).

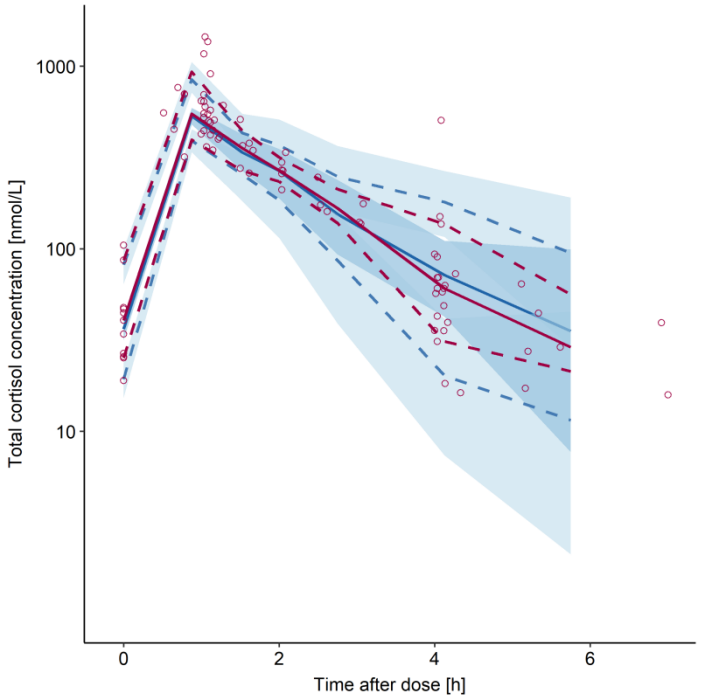

Figure 7.11 Visual predictive check (n=1000) for the reduced paediatric pharmacokinetic model including the maturation model. Lines: the 10th, 50th and 90th percentiles of observed (red) and simulated (blue) data; corresponding areas: 95% confidence interval around the simulated percentiles; circles: observations.

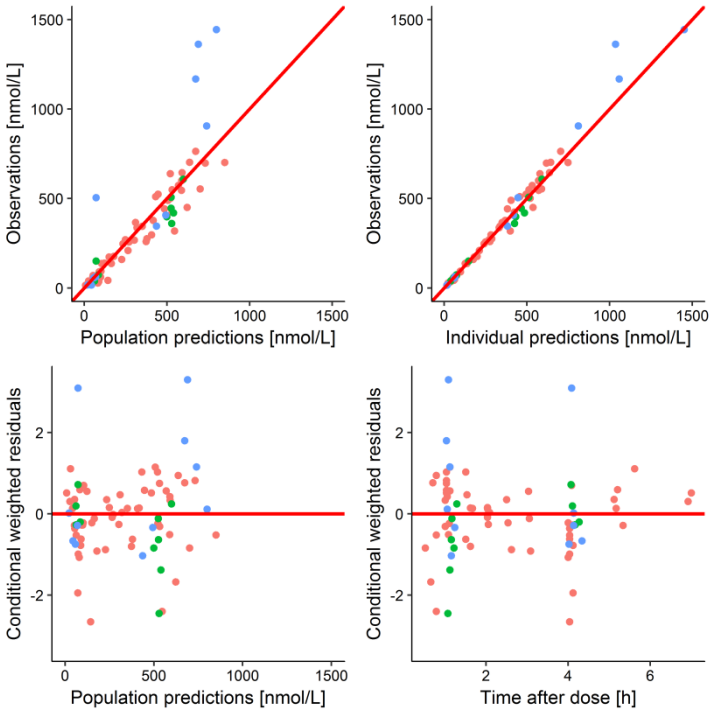

Figure 7.12 Goodness of fit plots for final reduced paediatric pharmacokinetic model for children (pink), infants (green) and neonates (blue).

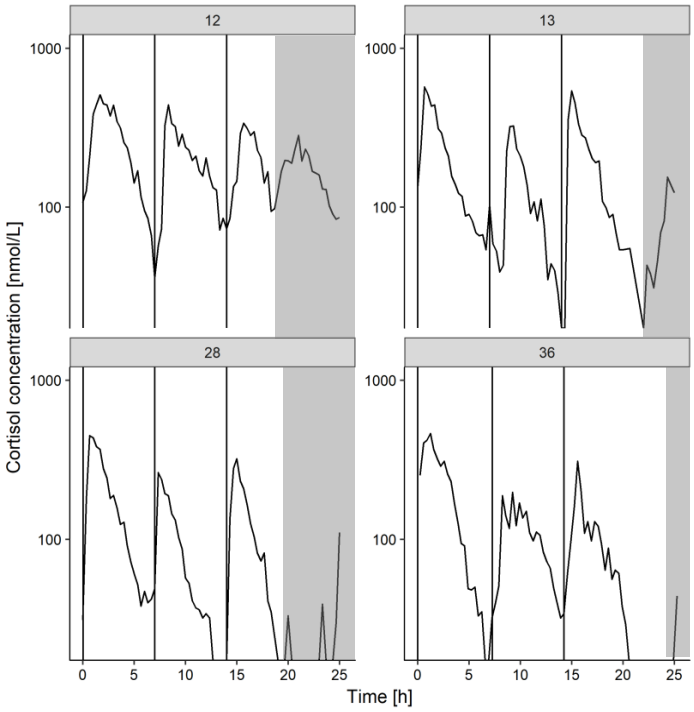

Figure 7.13 Identified patients with spontaneous bursts of cortisol synthesis in project 3. Vertical lines correspond to reported doses. Shaded areas correspond to times which were censored during model development and re-introduced for the key model.

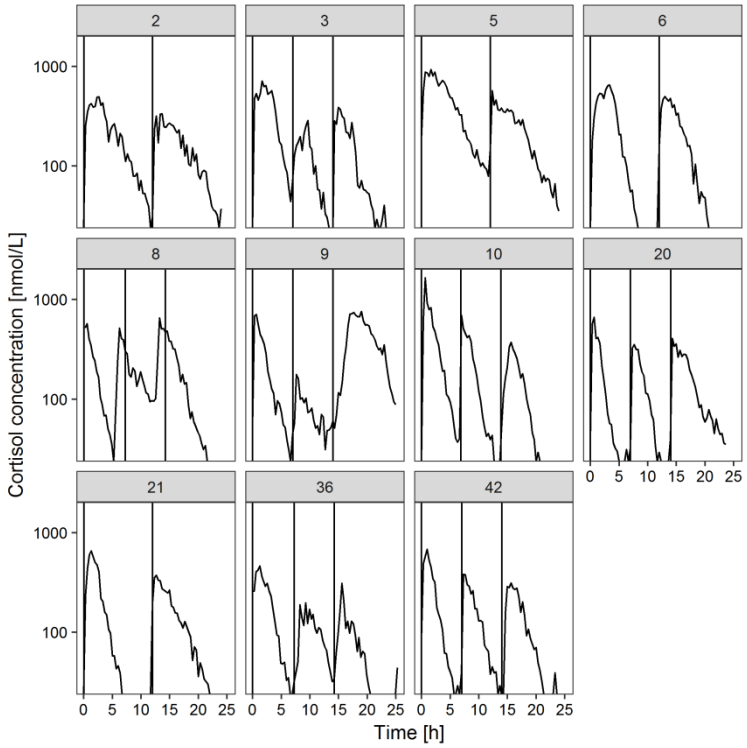

Figure 7.14 Identified patients with a high increase in cortisol concentrations prior to dose.

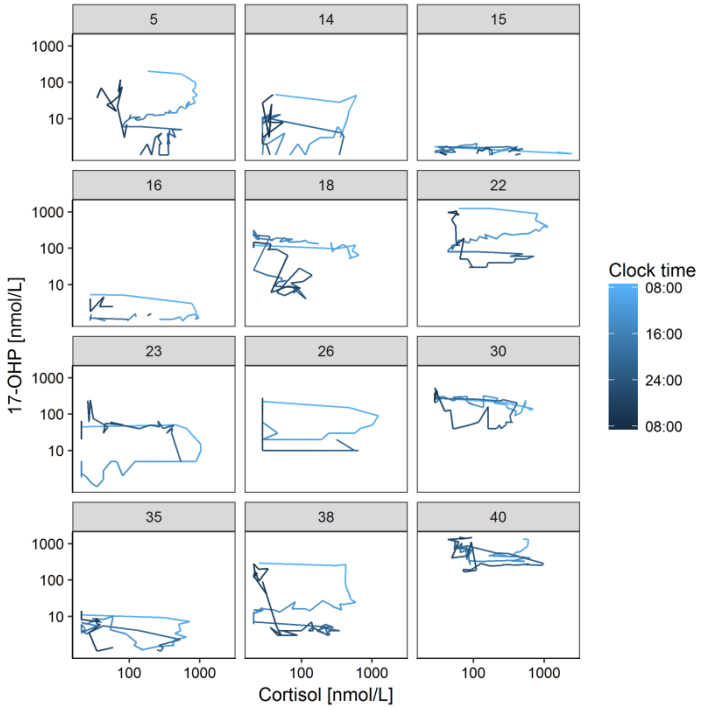

Figure 7.15 17-hydroxyprogesterone (17-OHP) versus cortisol concentrations after two times daily dosing regimen to paediatric patients with congenital adrenal hyperplasia

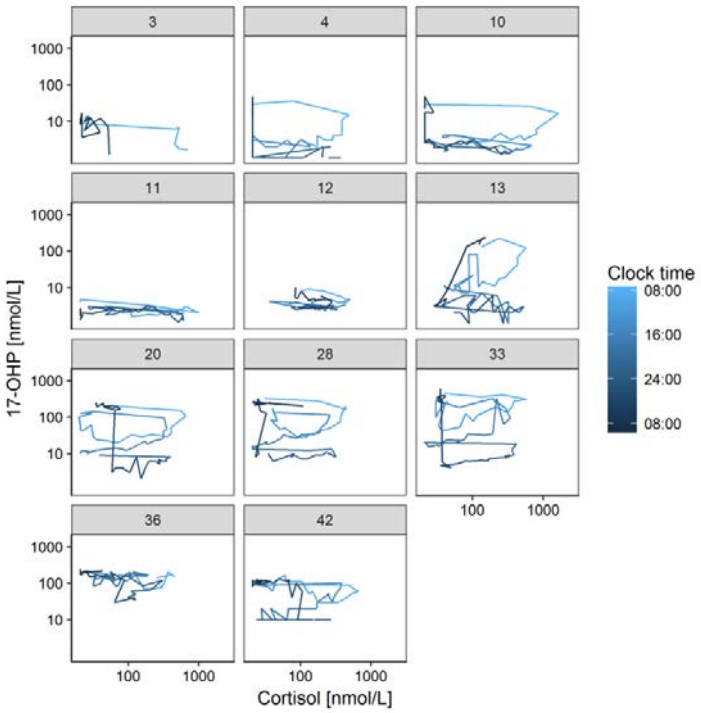

Figure 7.16 17-hydroxyprogesterone (17-OHP) versus cortisol concentrations after three times daily dosing regimen to paediatric patients with congenital adrenal hyperplasia

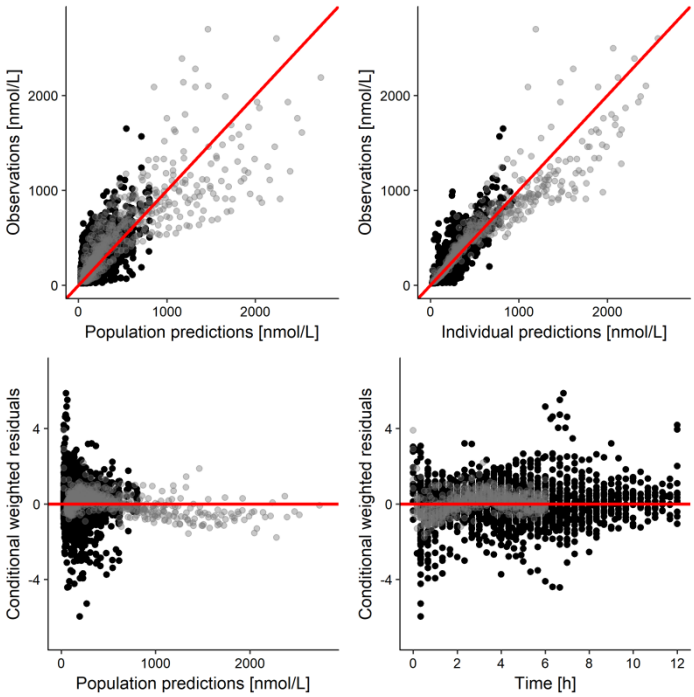

Figure 7.17 Goodness of fit plots for key pharmacokinetic model for hydrocortisone in paediatric patients with congenital adrenal hyperplasia after intravenous (grey) and oral (black) administration of hydrocortisone.

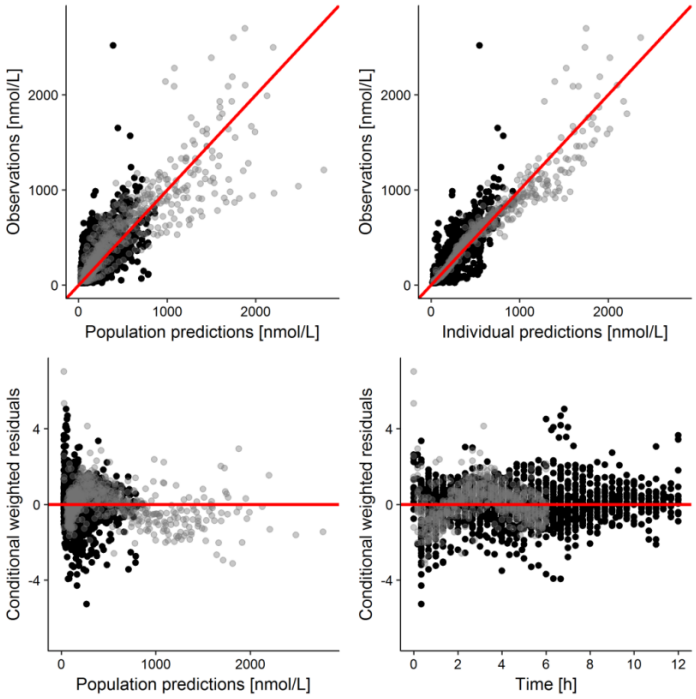

Figure 7.18 Goodness of fit plots for final pharmacokinetic model for hydrocortisone in paediatric patients with congenital adrenal hyperplasia after intravenous (grey) and oral (black) administration of hydrocortisone.

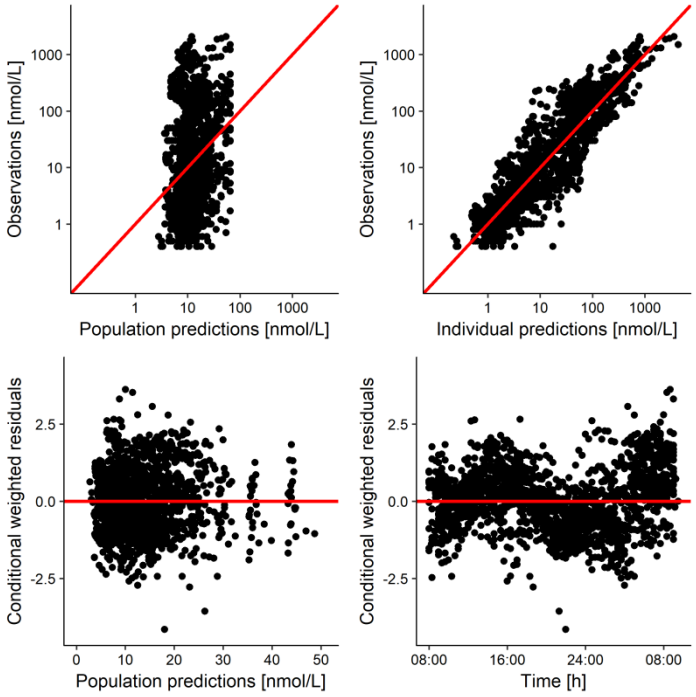

Figure 7.19 Goodness of fit plots for pharmacokinetic/pharmacodynamic model without circadian 17-hydroxyprogesterone synthesis for hydrocortisone in paediatric patients with congenital adrenal hyperplasia

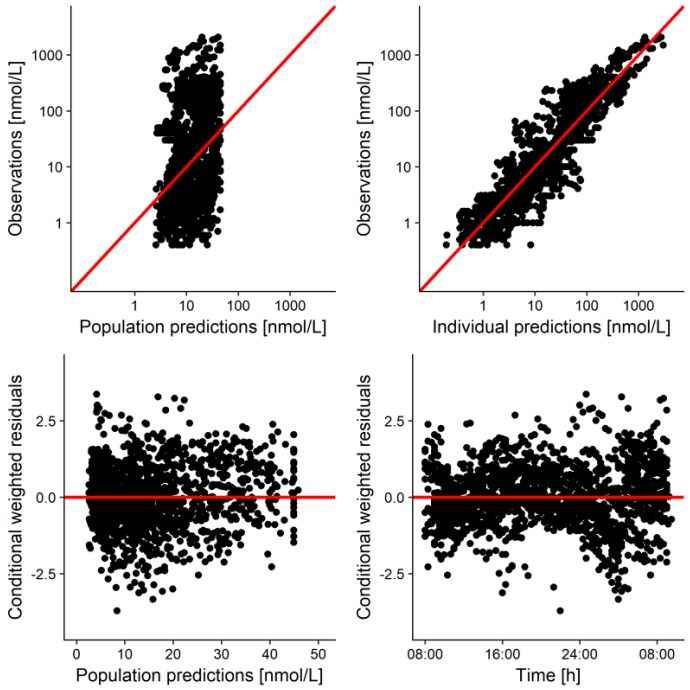

Figure 7.20 Goodness of fit plots for pharmacokinetic/pharmacodynamic model with circadian 17-hydroxyprogesterone synthesis (one cosine function) for hydrocortisone in paediatric patients with congenital adrenal hyperplasia

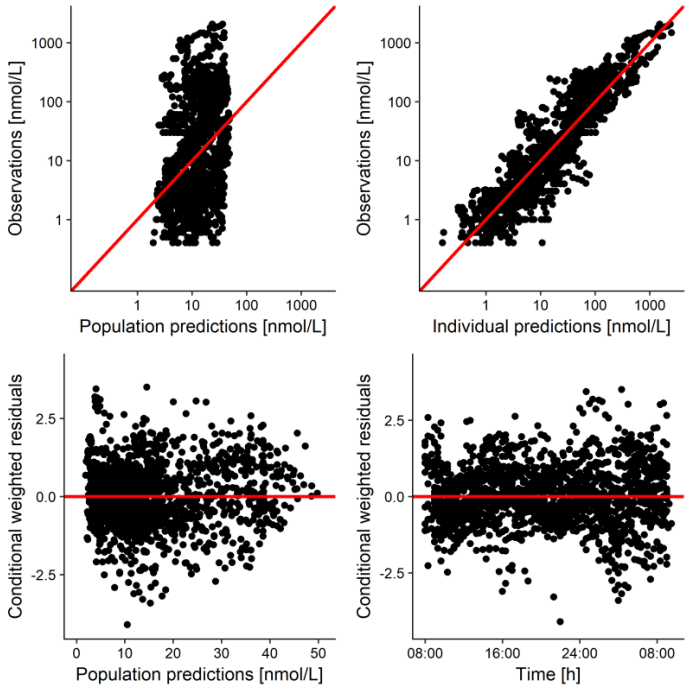

Figure 7.21 Goodness of fit plots for final pharmacokinetic/pharmacodynamic model including circadian 17-hydroxyprogesterone synthesis (two cosine functions) for hydrocortisone in paediatric patients with congenital adrenal hyperplasia

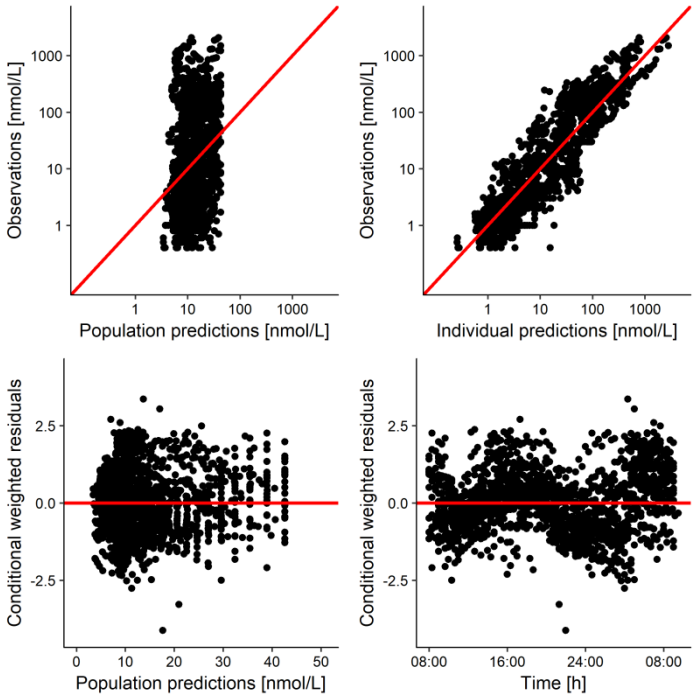

Figure 7.22 Goodness of fit plots for pharmacokinetic/pharmacodynamic model with concentration-dependent rebound model for hydrocortisone in paediatric patients with congenital adrenal hyperplasia

7.2 Supplementary tables

Table 7.1 Base model and covariate model development for plasma protein binding model (Project 1)

Model description	IIV	Number of fixed-effect parameters	OFV
Base model development			
Linear	-	1	-32.4
Nonlinear	-	2	-169.4
Linear and nonlinear	-	3	-181.4
Linear and nonlinear	$\boldsymbol{B_{max}}$	**3**	**-229.5**
Covariate model development			
No covariate	B_{max}	3	-229.5
CBG as linear covariate on B_{max}	B_{max}	4	-246.8
BW as linear covariate on B_{max}	B_{max}	4	-239.3
HT as linear covariate on B_{max}	B_{max}	4	-241.7
Substitution of B_{max}	$\mathbf{N_{CBG}}$	**3**	**-245.7**
Substitution of B_{max}	-	3	-235.3

Interindividual variability (IIV), objective function value (OFV), maximum binding capacity (B_{max}), corticosteroid-binding globulin, number of binding sites at CBG (N_{CBG}), body weight (BW), height (HT)

Table 7.2 Base model development for corticosteroid-binding models in adults (Project 1)

	Model description	IIV	Number of fixed-effect parameters	OFV
During daytime				
	Constant baseline	*Baseline*	2	1628.8
	1 cosine function	*Baseline*	4	1628.6
During 24 hours				
	Constant baseline	*Baseline*	2	595.7
	1 cosine function	*Baseline*	4	394.7
	2 cosine functions	*Baseline*	5	299.4

Interindividual variability (IIV), objective function value (OFV).

Table 7.3 Base model development for semi-mechanistic pharmacokinetic model for hydrocortisone in adults (Project 1)

Est method	Model description	IIV	Number of fixed-effect parameters	OFV	AIC
FOCEI	One-compartmental model	CL, V_c, $Baseline_{cort}$	6	-3717.5	-3697.5
FOCEI	**Two-compartmental model**	$\mathbf{CL}$, $\mathbf{V_c}$, $\mathbf{Baseline_{cort}}$	**8**	**-3814.4**	**-3790.4**
FOCEI	Allometric scaling	CL, V_c, $Baseline_{cort}$	8	-3815.7	-3791.66
FOCEI	Three-compartmental model	CL, V_c, $Baseline_{cort}$	9	-3814.4	-3786.41
Two-compartmental model					
SAEM+IMP	First-order absorption	CL, V_c, $Baseline_{cort}$	8	-3933.9	-4836.3
SAEM+IMP	**Saturable absorption**	$\mathbf{CL}$, $\mathbf{V_c}$, $\mathbf{Baseline_{cort}}$	**9**	**-4104.9**	**-5124.3**
SAEM+IMP	Zero-order absorption into depot compartment, first-order absorption from depot compartment.	CL, V_c, $Baseline_{cort}$	9	-4118.2	-5108.9
SAEM+IMP	Zero-order absorption	CL, V_c, $Baseline_{cort}$	8	-3874.0	-4772.4
Two-compartmental model including saturable absorption					
SAEM+IMP	**Plasma protein binding model (nonlinear + linear)**	$\mathbf{CL}$, $\mathbf{V_c}$, $\mathbf{Baseline_{cort}}$	**9 + 3 FIX**	**-4409.2**	**-6130.5**

Estimation method (Est method), interindividual variability (IIV), objective function value (OFV), first-order conditional estimator with interaction (FOCEI), stochastic approximation expectation maximisation (SAEM), importance sampling (IMP), clearance (CL), central volume of distribution (V_c), individual baseline ($Baseline_{cort}$)

Table 7.4 Simulated impact of circadian corticosteroid-binding globulin (CBG) concentrations on hydrocortisone exposure. ***Scenario 1: The lowest and highest simulated area under cortisol concentration curve ($AUC_{\downarrow}$ & $AUC_{\uparrow}$) and maximum cortisol concentration ($C_{max\downarrow}$ & $C_{max\uparrow}$) after single oral administration of infacort (0.5-20 mg) every hour of the day. The percentage difference for AUC and C_{max} and time of $AUC_{\downarrow}$, $AUC_{\uparrow}$, $C_{max\downarrow}$ and $C_{max\uparrow}$*** **has been summarised.** ***Scenario 2: Summary of simulated AUC and C_{max} assuming constant (AUC_{const}, $C_{max,const}$) or circadian CBG (AUC_{circ}, $C_{max,circ}$)*** **after a three times daily dosing of Infacort (10 mg at 06:00, 5 mg at 14:00 and 5 mg at 22:00).** ***The difference in AUC and C_{max} between groups with constant and circadian profile (% difference AUC_{circ}, % difference $C_{max,circ}$).***

Scenario 1 Dose	$AUC_{\downarrow}$*	$AUC_{\uparrow}$*	% difference $AUC_{\uparrow}$	Time $AUC_{\downarrow}$	Time $AUC_{\uparrow}$	$C_{max\downarrow}$*	$C_{max\uparrow}$*	% difference $C_{max\uparrow}$	Time $C_{max\downarrow}$	Time $C_{max\uparrow}$
0.5 mg	164 (87.6, 311)	183 (97.8, 346)	11.6	01:00	16:00	95.9 (60.5, 156)	100 (62.8, 163)	4.20	02:00	18:00
2 mg	515 (303, 890)	577 (341, 989)	12.2	00:00	16:00	260 (174, 373)	279 (185, 405)	7.42	02:00	18:00
5 mg	962 (608, 1580)	1070 (678, 1730)	11.3	00:00	16:00	412 (288, 557)	449 (313, 602)	9.01	02:00	18:00
10 mg	1510 (991, 2410)	1650 (1100, 2600)	9.60	00:00	15:00	517 (376, 684)	561 (409, 734)	8.42	01:00	17:00
20 mg	2390 (1620, 3740)	2620 (1780, 3980)	9.48	23:00	15:00	605 (442, 818)	652 (479, 871)	7.93	01:00	17:00

Scenario 2 Dose	AUC_{const}*	AUC_{circ}*	% difference AUC_{circ}	$C_{max,\ const}$*	$C_{max,\ circ}$*	% difference $C_{max,\ circ}$
Morning (10 mg)	1660 (1020, 2460)	1530 (992, 2210)	-8.29	574 (395, 721)	532 (395, 676)	-7.31
Afternoon (5 mg)	1080 (641, 1680)	1050 (654, 1590)	-2.79	472 (312, 602)	451 (321, 567)	-4.57
Evening (5 mg)	1080 (639, 1660)	965 (605.0, 1450)	-10.4	471 (311, 598)	439 (313, 555)	-6.70

* Median (95% prediction interval)

Table 7.5 Comparison of pharmacokinetic (PK) parameter estimates for semi-mechanistic adult PK model (iv & po), and PK parameters for paediatric patients with adrenal insufficiency for step i-ii (section 2.3.3.2 in Project 2).

	Only adult data (iv+po)	i) Estimating key parameters paed data	ii) Estimating all parameters adult & paed data
Fixed-effects			
CL [L/h]	131 (111, 148)	110 (92.1, 126)	129 (109, 160)
V_c [L]	3.3 (2.73, 3.78)	2.01 (1.49, 2.35)	3.13 (2.36, 4.09)
Q [L/h]	94.9 (75.6, 118)	94.9 *Fixed*	100 (72.0, 149)
V_p [L]	60 (50.1, 69.5)	60 *Fixed*	60.3 (50.1, 76.8)
$Baseline_{cort}$ [nmol/L]	15.5 (14.0, 17.3)	-	14.9** (11.6, 18.6)
V_{max} [nmol/h]	10100 (7620, 12200)	10100 *Fixed*	10600 (7730, 14100)
K_m [nmol]	2230 (1410, 3090)	2230 *Fixed*	2540 (1570, 3510)
F [-]	0.369 (0.302, 0.423)	0.369 *Fixed*	0.383 (0.318, 0.472)
Interindividual variability			
ωCL [CV%]	25.6 (13.8, 32.2)	37.6 (0, 52.5)	30.7 (17.7, 42.3)
Corr (CL,V_c)	1 (1, 1)	0.996 (-1.00,1.00)	0.845 (0.176,1.00)
ωV_c [CV%]	29.7 (15.7, 37.8)	43.6 (0, 62.0)	54.3 (23.5, 107)
$\omega Baseline_{cort}$ [CV%]	30.8 (21.1, 39.4)		31.2 (21.4, 48.4)
Residual variability			
σexp* [CV%]	14.3 (12.2, 16.3)	19.1 (14.5, 24.6)	14.4 (12.2, 16.8)

Clearance (CL), central volume of distribution (V_c), intercompartmental clearance (Q), peripheral volume of distribution (V_p), endogenous cortisol baseline ($Baseline_{cort}$), maximum absorption rate (V_{max}), amount in depot compartment resulting in half of V_{max} (K_m), scaling factor of amount in depot (F), correlation between CL and V_c (Corr (CL, V_c)). *Estimated as additive error on logarithmic scale.

Table 7.6 Comparison of pharmacokinetic (PK) parameter estimates for semi-mechanistic adult PK model (only po), and PK parameters for paediatric patients with adrenal insufficiency step iii-iv (section 2.3.3.2 in Project 2).

	Only adults (po)	iii) Prior for all parameters paed data)	iv) Prior for all non-key parameters paed data
Fixed-effects			
CL [L/h]	342 (308, 372)	342 (334, 356)	333 (298. 451)
V_c[L]	9.31 (6.85, 11.4)	9.39 (8.26, 10.2)	10.6 (7.77, 14.8)
Q [L/h]	172 (126, 223)	181 (145, 199)	194 (156, 208)
V_p [L]	127 (100, 149)	114 (101, 133)	118 (97.3, 133)
$Baseline_{cort}$ [nmol/L]	15.5 (13.8, 17.9)	-	-
V_{max} [nmol/h]	28100 (22100, 34900)	26900 (24200, 28500)	27300 (23700, 28800)
K_m [nmol]	7670 (4580, 11600)	7040 (6170, 8500)	6470 (5600, 9020)
Interindividual variability			
ωCL [CV%]	23.9 (14.8, 32.0)	43.9 (23.1, 55.3)	38.5 (0, 63.2)
Corr (CL,V_c*)*	0.719 (0.380, 1.00)	0.908 (-0.543, 0.961)	1.00 (-0.999, 1.00)
ωVc [CV%]	43.6 (25.0, 78.5)	93.5 (42.4, 167)	23.6 (0, 56.0)
$\omega Baseline_{cort}$ [CV%]	35.5 (21.0, 51.0)	-	-
Residual variability			
*σexp** [CV%]	14.3 (12.2, 16.3)	14.9 (9.79, 19.2)	19.1 (12.3, 24.7)

Clearance (*CL*), central volume of distribution (V_c), intercompartmental clearance (*Q*), peripheral volume of distribution (V_p), endogenous cortisol baseline ($Baseline_{cort}$), maximum absorption rate (V_{max}), amount in depot compartment resulting in half of V_{max} (K_m), correlation between *CL* and V_c (Corr (*CL,* V_c)). *Estimated as additive error on logarithmic scale.

Table 7.7 Base model development for pharmacokinetic model for hydrocortisone in paediatric patients with congenital adrenal hyperplasia (Project 3)

.	Model description	IIV	Number of fixed-effect parameters	OFV	AIC
Baseline model	*1-CMT model*				
	Using the initial concentration to inform the model	k_a, CL, V_c	5	-741.2	-723.2
	Estimating a constant underlying baseline	k_a, CL, V_c	6	-1491.5	-1471.5
	Estimating a constant underlying baseline	$\boldsymbol{k_a, CL, V_c, Baseline_{cort}}$	**6**	**-1563.7**	**-1541.7**
	Estimating a constant underlying baseline & using the initial concentration to inform the model	k_a, CL, V_c, $Baseline_{cort}$	6	-1574.1	-1552.1
Disposition model	*Constant underlying baseline*				
	1-CMT model	$\boldsymbol{k_a, CL, V_c, Baseline_{cort}}$	**6**	**-1563.7**	**-1541.7**
	2-CMT model	k_a, CL, V_c, $Baseline_{cort}$	8	-1566.9	-1540.9
	3-CMT model	k_a, CL, V_c, $Baseline_{cort}$	9	-1566.8	-1536.8
Absorption model	1-CMT, *constant underlying baseline*				
	First-order absorption	$\boldsymbol{k_a, CL, V_c, Baseline_{cort}}$	**6**	**-1563.741**	**-1541.7**
	Saturable absorption	k_m, CL, V_c, $Baseline_{cort}$	7	-1563.741	-1539.8
	Sequential zero- and first-order absorption	k_a, CL, V_c, $Baseline_{cort}$	7	-1606.196	-1582.2
	Zero-order absorption	D_1, CL, V_c, $Baseline_{cort}$	6	-1359.159	-1488.6
	First-order absorption with lagtime	k_a, CL, V_c, $Baseline_{cort}$	7	-1601.939	-1577.9
RUV	1-CMT, *constant underlying baseline , first-order absorption*				
	Separate RUV for po and iv	k_a, CL, V_c, $Baseline_{cort}$	7	-1961.830	-1937.8
	Separate RUV for po and iv, allometric scaling	$\boldsymbol{k_a, CL, V_c, Baseline_{cort}}$	**7**	**-1978.813**	**-1954.8**

Compartment (CMT), interindividual variability (IIV), objective function value (OFV), Akaike Information Criterion (AIC), first-order absorption rate constant (k_a), clearance (CL), volume of distribution (V_c), individual cortisol baseline ($Baseline_{cort}$), oral (po), intravenous (iv), residual unexplained variability (RUV)

Table 7.8 Base model development for the pharmacokinetic/pharmacodynamic model for hydrocortisone in paediatric patients with congenital adrenal hyperplasia (Project 3)

	Model description	IIV	Number of fixed-effect parameters	OFV	AIC
Baseline model	*Indirect response model with linear concentration-effect*				
	Estimating the baseline	$\boldsymbol{Baseline_{17\text{-}OHP}}$	**4**	**1771.3**	**1781.3**
	Using the initial concentration to inform the model	-	3	2195.3	2201.3
Concentration-effect model	*Indirect response model, estimating the baseline*				
	Slope model	$Baseline_{17\text{-}OHP}$	4	1771.3	1781.3
	I_{max} model	$\boldsymbol{Baseline_{17\text{-}OHP}}$	**5 (1 FIX)**	**1466.4**	**1476.4**
	Sigmoidal I_{max} model	$Baseline_{17\text{-}OHP}$	6 (1 FIX)	1459.7	1471.7
Circadian k_{in}	Indirect response model with I_{max} effect, estimating the baseline				
	No circadian k_{in}	$Baseline_{17\text{-}OHP}$	5 (1 FIX)	1466.4	1476.4
	Circadian k_{in} (one cosine)	$Baseline_{17\text{-}OHP}$	7 (2 FIX)	1119.0	1131.0
	Circadian $\boldsymbol{k_{in}}$ (two cosines)	$\boldsymbol{Baseline_{17\text{-}OHP}}$	**9 (2 FIX)**	**1054.9**	**1070.9**
	Circadian k_{in} (three cosines)	$Baseline_{17\text{-}OHP}$	11 (2 FIX)	1011.1	1031.1
Mixture models	Indirect response model with circadian k_{in} (two cosine functions) and I_{max} effect, estimating the baseline				
	No mixture model	$\boldsymbol{Baseline_{17\text{-}OHP}}$	**7 (2 FIX)**	**1054.9**	**1070.9**
	Mixture model	$Baseline_{low}$, $Baseline_{high}$	7 (2 FIX)	1047.1	1069.1

Interindividual variability (IIV), objective function value (OFV), Akaike Information Criterion, maximum inhibition ($\boldsymbol{I_{max}}$), 17-hydroxyprogesterone (17-OHP), baseline for 17-OHP ($Baseline_{17\text{-}OHP}$), zero-order synthesis rate of 17-OHP (k_{in})

8 Acknowledgements

The current work was carried out at the Department of Clinical Pharmacy and Biochemistry at the Institute of Pharmacy at the Freie Universitaet Berlin, Germany with financial support from the Graduate Research Training Program PharMetrX: Pharmacometrics & Computational Disease Modelling. Project 1 and 2 was carried out under a Cooperation Agreement between Freie Universitaet and Diurnal funded by the European Commission FP7 Grant (No. 281654 TAIN). In addition, scholarships for attending a courses and a conference have been received from the Swedish Pharmacy Society (Apotekarsocieteten).

I would first like to sincerely thank my supervisor *Professor Charlotte Kloft* for the opportunity to write my doctoral thesis in pharmacometrics in your group. Thanks for all fruitful (scientific and sometimes less scientific) discussions usually taking place before 22:00, cups with tea, never-ending enthusiasm, kind support and ability to see everything in a positive way when things were not progressing in the right way. Ett stort tack för allt!

Additionally, I would like to express my gratitude to:

My co-supervisor Professor *Wilhelm Huisinga* for your enthusiasm, ability to see things in a different perspective which contributed to a better overall understanding.

The previous postdoc *Zinnia Parra-Guillén* for always believing I would make it (there, there…), making sure I go in the right direction, reading parts of my thesis and for always laughing at the pre words of my project discussions ☺.

The previous postdoc *Niklas Hartung* for your patience, support, ability to see things in a different way and also for reading parts of my thesis.

My industry mentor *Valerie Nock* for being supportive, taking your time every month to discuss my current problems and future plans and for not being too annoyed when I forgot about the meetings…

Our collaboration partners *Richard Ross*, *Martin Whitaker, Trevor Johnson, Oliver Blankenstein*, *Uta Neumann* and *Peter Hindmarsh* for sharing data from their clinical studies, providing valuable clinical input and fruitful discussions.

All colleagues in Berlin and Potsdam for a superspitzenklasse time together (both socially and scientifically), for having patience with my German skills, and for taking care of each other in good and in bad times.

Iris Minichmayr for being an excellent office mate, for all discussions and support, music influences and for showing me around in Berlin so that I would forget my home sickness. *Helena Edlund* for being like a sister to me, and for all fun times and adventures in Berlin and at conferences. *Christine Weiser* for always being there, being a good listener, for caring about everybody and everything (indcluding me and my glasses) and for introducing me and being part of my extended Berlin family (see below). *Jens Borghardt* for your enthusiasm, interest in discussing research problems and for reading parts of my thesis. *Eva Göbgen* for all laughter and discussions before/during/after nice lunch runs which made the body happy and sometimes eased the problem solving. *Sebastian Wicha* for scientific discussions, your enthusiasm and for always appreciating sarcastic undertones. *Andrea Henrich*, *Lena Klopp Schulze* and *Daniela Burau* for scientific and non-scientific discussions, for nice conferences and for showing me how clothes really should be dried. *Lisa Ehmann*, *Franziska Kluwe* and *Ana-Marija Grisic* for the yoga breaks, for making office 130A the best office(!) and for listening interestingly to my stories about "the old days". Extra thank to *Ana-Marija* for reviewing parts of my thesis.

My master thesis student from the University of Gothenburg, *Thi Truong* for diving into the field of pharmacometrics full with enthusiasm, and for together with *Dan Sebring* contributing to figures 1.2, 1.3 and 1.5 in section 1.3.

JST (Johanna support team: *Ulrika Wählby Hamrén*, *Carl Amilon*, *Susanne Prothon*, *Bo Olsson* and *Ulf Eriksson*) and other colleagues at AstraZeneca for teaching me a lot (again scientific and non-scientific) and taking care of me during my internship and for cheering me up during the last few months of thesis writing.

Ulrika Hjertonsson, *Maria Falkdal*, *Anna Nilsson* and *Mattias Lorentzon* at the Center of Bone and Arthritis research at Mölndals Sjukhus for providing me a nice office to write my thesis in during spring, enjoyable and interesting lunch/fika breaks with nice coffee.

Richard Höglund for highly valuable support throughout the years, all fun times, your nice visit in Berlin and reading parts of the thesis.

Extended Berlin family: *Marco Krebs, Fabian Klüser and Stefanie Bach*, for all dinners, random Berlin activities and for making sure I feel at home in Berlin.

My flatmate *Marlene Busche* for being my Berlin family, providing me a home, improving my Geman and for showing me around in Berlin.

Isabella Hübinette for all your patience, for always being you and always trying to understand what I am working with.

Karin Midgren with family for all nice dinners, adventures, and endless support in any situation.

Emelie Olsson for the never-ending support, hejarop and for understanding how important it is to at least believe that the deadline is very far away ☺. To the rest of the Humphrey family (*Daniel Edlund, Karin Karlsson, Elisabeth Nyström & George Birchenough*) for all nice breakfasts and other nice weekend distractions.

Maria Sundh and *Jeppe Hansen* for all nice gatherings which made me think of something else than working, and for your nice visit to Berlin. Thanks also to *Maria* for reading parts of the thesis. *Johan Sundh* for all beer hang-outs, nice laughs and great visit in Berlin. *Bengt* och *Christina Sundh* for nice trips, valuable support and nice times in Helenedal and Vänersborg.

Anna & *Manne Håkansson*, *Elsy Samuelsson*, *Simon* and *Felix* for your support in times it was needed, support with knitting, Japanese lessons, funny jokes, bike adventures and nice family hang-outs.

Mum and *dad*, for all your support with driving to the airport on sad Sundays and to all our adventures (Vasaloppet, Vätternrundan, Helsingborg marathon etc) the past years. Making sure that we eat properly at all times, all nice visits to Berlin and for making "Spielt keine Rolle" and "Du bist Scheiße" memorable quotes☺. For making me company via mobile phone in the Supermarket or on the bus from work especially late evenings. For taking home my Berlin home, and for always being there in vått och torrt. Lastly for all your patience and for always believing in me and supporting my decisions (even when they include moving abroad…).

My dearest *Daniel Sundh* (aka Lilleman=Kleinmann), for always being there and pushing me to the boundary, but never beyond. For always believing that I can achieve things, when I usually doubt myself (including swimming into a dark ship with a tiny flash light in the Philippines, moving to Berlin or finishing this thesis). For always seeing things in a positive light and keeping reminding me that 3.5 years is not forever. For not getting tired of going to Berlin every month or long homesick-related telephone calls. I'm so much looking forward to all our future adventures together. This thesis would never have been possible without you. Du är min superhjälte ♥

9 Publications

9.1 Original articles

J. Melin, Z.P Parra-Guillen, N. Hartung, W. Huisinga, R.J. Ross, M.J. Whitaker, C. Kloft.
Predicting cortisol exposure from paediatric hydrocortisone formulation using a semi-mechanistic pharmacokinetic model established in healthy adults.
Clin. Pharmacokinet. 57: 515-527 (2018)
doi: 10.1007/s40262-017-0575-8

J. Melin, S. Prothon, C. Kloft, A. Cleton, C. Johansson, C. Jorup, B. Olsson, U. Wählby Hamrén.
Pharmacokinetics of the inhaled selective glucocorticoid receptor modulator AZD5423 following inhalation using different devices.
AAPS J. 19: 865-874 (2017).
doi: 10.1208/s12248-016-0042-8

H. Edlund, **J. Melin**, Z.P. Parra-Guillen, C. Kloft.
Pharmacokinetics and pharmacokinetic–pharmacodynamic relationships of monoclonal antibodies in children.
Clin Pharmacokinet. 54:35-80 (2015).
doi:10.1007/s40262-014-0208-4

G.V. Kalayda, M. Michaelis, J. Cinatl jr., R.M. Mader, H. Fröhlich, N. Sarin, **J. Melin**, F. Engel, W. Jäger, R. Frötschl, U. Jaehde, C. Kloft, C.A. Ritter.
A systems pharmacology approach to improve drug therapy in NSCLC: Establishing a CESAR network.
Int. J. Clin. Pharmacol. Ther., 52:89-91 (2014).
doi: 10.5414/CPXCES13EA07

J. Melin, N. Hartung, Z.P. Parra-Guillen, M.J. Whitaker, R.J. Ross, C. Kloft
The circadian rhythm of corticosteroid-binding globulin has little impact on cortisol exposure after hydrocortisone dosing (Submitted)

J. Melin, U. Neumann, M. J. Whitaker, W. Huisinga, M. Davies, O. Blankenstein, R.J. Ross, C. Kloft
Pediatric population pharmacokinetic model to assess hydrocortisone replacement doses in children (In preparation)

J. Melin, Z.P. Parra-Guillen, T. Truong, N. Hartung, P. Hindmarsh, C. Kloft
Evaluating hydrocortisone therapy in paediatric patients with congenital adrenal hyperplasia, using a population pharmacokinetic/pharmacodynamic model (In preparation)

9.2 Conference abstracts (poster)

J. Melin, T. Truong, P. Hindmarsh, Z.P. Parra-Guillen, C. Kloft.
Pharmacokinetic/pharmacodynamic analysis of hydrocortisone in pediatric patients with congenital adrenal hyperplasia.
7th American Conference on Pharmacometrics (ACoP), Bellevue, Washington, USA, 23-26 October 2016.
J. Pharmacokinet. Pharmacodyn. 43 (Suppl.): S27 (2016).

J. Melin, Z.P. Parra-Guillen, N. Hartung, W. Huisinga, R.J. Ross, M.J. Whitaker, C. Kloft.
Semi-mechanistic modelling of the nonlinear hydrocortisone pharmacokinetics to enable extrapolation into paediatric patients.
25th Population Approach Group Europe (PAGE), Lisbon, Portugal, 07-10 June 2016. PAGE 25: 5764 [www.page-meeting.org/?abstract=5764], (2016).

J. Melin, S. Prothon, C. Kloft, A. Cleton, C. Johansson, C. Jorup, B. Olsson, U. Wählby Hamrén.
Pharmacokinetics of the inhaled selective glucocorticoid receptor modulation AZD5423 following inhalation using different devices.
25th Population Approach Group Europe (PAGE), Lisbon, Portugal, 07-10 June 2016. PAGE 25: 5908 [www.page-meeting.org/?abstract=5908], (2016).

J. Melin, B.L. Olsson, C. Johansson, C. Kloft, U. Wählby Hamrén.
Population pharmacokinetic analysis of AZD4818 in healthy volunteers following three different routes of administration.
24th Population Approach Group Europe (PAGE), Hersonissos, Greece, 02-05 June 2015.
PAGE 24: 3570 [www.page-meeting.org/default.asp?abstract=3570], (2015).

J. Melin, P. Hindmarsh, W. Huisinga, C. Kloft.
Population pharmacokinetic analysis of hydrocortisone in paediatric patients with adrenal insufficiency.
23rd Population Approach Group Europe (PAGE), Alicante, Spain, 10-13 June 2014.
PAGE 23: 3106 [http://www.page-meeting.eu/default.asp?abstract=3106], (2014).